Geology and Geological Structure of Tsuruga Power Station Site
The D-1 Shatter Zone

The Japan Atomic Power Company

April 24, 2013

Comprehensive evaluation of D-1 shutter zone and K fault

◆ K fault is not D-1 shatter zone and does not extend to the reactor building of Unit 2.

(Thin section observation)

- The displacement sense of K fault is different from that of D-1 shatter zone (including G fault)

  K fault: displacement sense of reverse fault
  D-1 shatter zone (including G fault): displacement sense of normal fault

(Additional geologic observation of L-cut pit and western pit)

- K fault reaches to basement rock and the direction of its strike changes from N-S to **NW-SE** in D-1 trench **(confirmed in the basement rock)**. It is suggested that K fault does not extend to the reactor building of Unit 2.

(Additional thin section observation of B14-2 drilling)

- At B14-2, which is located to the south of D-1 trench, three fault gouges are found. However each of them does not have reverse fault sense, which is a characteristic of K fault, but has normal fault sense.
- Accordingly, It is judged that K fault does not extend to southern direction at least beyond B14-2 drilling location.

Blue Colored: Newly obtained data

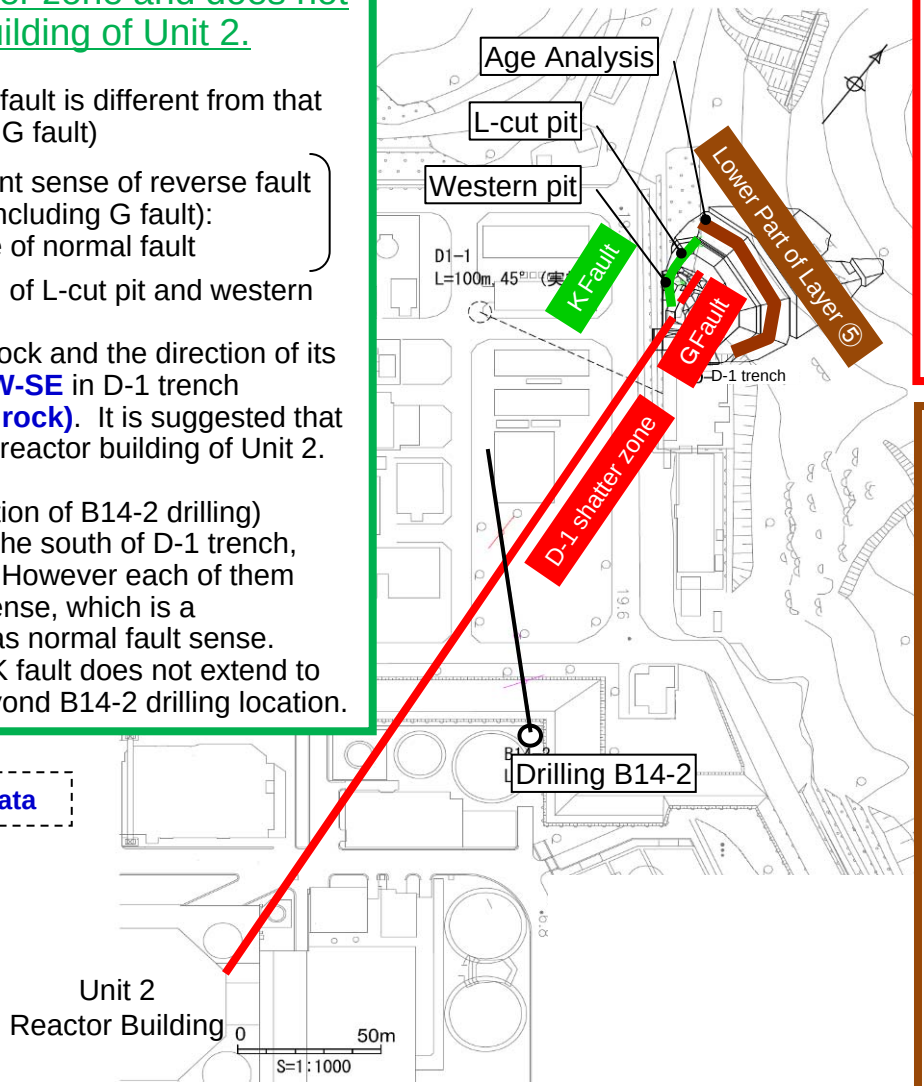

◆ G fault is D-1 shatter zone.

- Strike and dip is similar to each other

(Additional thin section observation)

- Additional thin section observations were performed on the fracture segments that is considered to be D-1 shatter zone (D-1 outcrop, drillings and D-1 trench**, slope behind Unit 2**)
- So both of D-1 shatter zone and G fault have same displacement sense of normal fault that G fault is D-1 shatter zone.

◆ D-1 shatter zone (including G fault) and K fault were not active in and after the Late Pleistocene.

(Additional dating of D-1 trench)

- Both of D-1 shatter zone (including G fault) and K fault is covered by lower part of Layer ⑤. (Both of them have not been active since the deposition of lower part of layer ⑤)
- From the results of additional dating on the lower part of layer ⑤, it is judged that the lower part of layer ⑤ was deposited about 120,000 – 130,000 years ago. (Mihama-tephra was detected. **The tephra was confirmed to be different from DMP. The Hornblende tephra in the layer ③ was confirmed to be different from Mihama-tephra**)
- Accordingly, both of D-1 shatter zone (including G fault) and K fault, which are covered by lower part of Layer ⑤, have not been active since about 120,000 – 130,000 years ago.

D-1 shatter zone and K fault were not active in and after Late Pleistocene. Therefore D-1 shatter zone and K fault are not active faults that should be taken into consideration for the seismic design.

Points of views of the operator and EMS

Evaluation of continuity

The operator's evaluation — We will explain the items written in red today.

EMS's points of views (Basic concepts of evaluation)

Surveys for shatter zone

- The shatter zone was checked by implementing outcrop surveys, boring surveys or trench surveys, etc. (In the D-1 trench, G fault and K fault were checked)

Evaluations for continuity

- The continuity was evaluated based on the similarities in the strikes and the dips.
- D-1 shatter zone, running directly under the reactor building of the unit 2 and G fault are N-S strikes, while K fault extends the rock mass, the direction of its strike changes from N-S to NW-SE.

As strikes and dips of faults could vary in a sedimentary layer in a lot of cases generally, it is not identified that that K fault shouldn't head for the direction of D-1 shutter zone even though it is winding in the layer.

Confirmation of adequacy for evaluations of continuity

- In order to confirm the adequacy for the continuity of D-1 shatter zone and G fault, the displacement senses of the last slips were focused, as well.
- D-1 shutter zone and G fault are considered to be 'normal fault and right-lateral slip', while K fault is 'reverse fault' (currently under survey).

- There is a case that the structure of the last slip cannot be recognized.
- The latest events of each survey point are not necessarily the same period.

The result of evaluation

D-1 shatter zone continues to the G fault but not to K fault.

- In general, faults are not always extended straight but could sometimes be winding or running parallel after being interrupted.
- It is appropriate to consider that D-1 shatter zone continues to G and K faults.

Evaluation of activity

Selection of survey location for activity evaluation

- D-1 trench was selected, because it is located where Urasoko fault affect easily, and it is based on a consideration that the activity should be sufficiently low under the reactor facility if the shatter zone has not been active.

- The sedimentary layers in which the data to be evidence for the evaluation of activity possibly exists were lost by the past construction and excavation activities and there is no decisive evidence to show that the activity of D-1 shatter zone is high.

Evaluation by overlying strata analysis method

- Mihama-tephra (about 120,000 years ago) was identified in the lower part of layer⑤. (currently under survey)
- G fault and K fault are covered by the lower part of layer⑤.

- Only the Mihama-tephra was analyzed and compared but others.
- Only little number of tephras were detected in the lower part of layer⑤, and they were also included in layer③, which provides little credibility.

The result of evaluation

D-1 shatter zone (including G fault) and K fault are not active fault that should be taken into consideration for the seismic design.

It was identified that K fault made slips in the geological strata which was possible to be deposited after the Late Pleistocene.

Our opinions on ‘views against JAPC’s claim’ (1/5)

(Draft) EMS’s views against JAPC’s claim concerning the fault evaluations of Tsuruga PS site, EMS on shatter zones in the site of Tsuruga Power Station		JAPC’s opinion	Reference No.
Main texts	Issues		
<EMS’s view on the claim 1> EMS evaluation report (draft) states that the operator has not give clear evidence on that G fault is D-1 shatter zone. The reasons of EMS’s views are as follows;	–	–	–
1. In EMS, the specialist of geology pointed out; - It is difficult to identify the displacement sense of the last slip surface by thin section observations, because the structure of the last slip cannot always be identified through clearly distinguishing each slip from the others in case of the fault experienced multiple slips. - Even if the displacement senses of the last slip surfaces is identified at each point, it is only the last slip surface at each point but the slip periods of each point cannot be specified. In other words, the last slip surfaces of different points were not necessarily be active in the same period even if their displacement senses are the same. Therefore, the evaluation based on displacement senses cannot be sufficient evidence for the claim that the G fault continues to the D-1 shatter zone.	1. Thin section observations cannot identify displacement senses of the last slip surfaces. 2. There is no sufficient evidence for the claim that the G fault continues to the D-1 shatter zone.	**(Outline of today’s explanation)** **1.Identifications of displacement senses of the last slip surfaces** - Thin section observations have been implemented for identifying the displacement senses of the faults. In order to verify the validity of thin section observations, CT image analyses for the identification of the last slip surface and slickenline observations with stereoscopic microscope for the identification of the displacement senses were implemented for the D-1 shatter zone (at the slope behind the unit 2), the G fault (at D-1 trench) and the K fault (at D-1 trench). - The result shows that there was no problem in the identifications of the last slip surfaces based on the thin section observations which have been implemented so far and the displacement senses were consistent with the ones identified by the slickenline observations. - Therefore, it is possible to identify the displacements sense of the last slip surface by thin section observations. **2. Continuity of D-1 shatter zone** - The strike and the dip of the G fault are similar to the ones of the D-1 shatter zone (N-S strike / high angle west-dipping) and the displacement senses of their last slip surfaces were also the same, which are normal faults. - Meanwhile, the K fault was a reverse fault which is different from the D-1 shatter zone. - Therefore, the K fault is not the D-1 shatter zone but the G fault. **(Point to be clarified by EMS)** - The reasonable reason that EMS claims the active periods of the shatter zones with the same displacement sense are different, and there can be many shatter zones which continue to the D-1 shatter zone.	10-45

Our opinions on ‘views against JAPC’s claim’ (2/5)

(Draft) EMS’s views against JAPC’s claim concerning the fault evaluations of Tsuruga PS site, EMS on shatter zones in the site of Tsuruga Power Station		JAPC’s opinion	Reference No.
Main texts	Issues		
<EMS’s views on the claim 2> The evaluation report states that the K fault is ‘the structure which continues to the D-1 shatter zone’. The reasons are as follows; (1) As stated in the ‘Claim 1’, the specialist of geology pointed out as follows, concerning the thin section observations implemented for the G fault and the D-1 shatter zone; - (Skipped) In this way, EMS considers that the evaluation of displacements are not reliable and provides insufficient evidence for the claim that there is no connection between the K fault and the D-1 shatter zone.	Same as the Claim 1.	Same as our view on the Claim 1 in the EMS.	–
(2) Especially, the point where the strike of the K fault is bent to the NNW – SSE direction* was recognized mainly in the deposits above the bedrock. In general, the strikes and dips of the faults found in deposits are not constant and they could vary from place to place. Therefore, it is not possible to conclude that the K fault does not head for the direction of the D-1 shatter zone just because the fault in the deposit is bent. (3) In addition, faults are not necessarily be extended linearly but turning to the different directions or running parallel after they are once broken, in general. The D-1 shatter zone is considered to have such forms. * In the JAPC’s report dated April 24, 2003, the direction is described as “NW-SE direction.”	1. It has been identified that the K fault was bent in the deposit and the assumption is not credible. 2. Because faults are generally bent or running parallel after they are once broken even if they are bent, the D-1 shatter zone is considered to continue to the K fault.	**(Outline of today’s explanation)** **1. Forms in the K fault bedrock** - In the EMS so far, JAPC has repeatedly said that additional surveys are implemented for extension of the K fault to the bedrock. - Based on the EMS’s comment that the D-1 shatter zone is not necessarily be extended linearly, surveys have continuously been implemented along the strike of the D-1 shatter zone, considering increasing of the survey points as much as possible. - The pit survey in the D-1 trench confirmed that the strike of the K fault changes to the NW-SE direction also in the bedrock (prompt report). **2. Extension of the K fault to the south direction** - According to the thin section observation of the B14-2 drilling between the unit 2 reactor building and the D-1 trench, there was no shatter zone with reverse fault sense which the K fault has at all. Therefore, the K fault is not extended further south than the B14-2 drilling. **(Point to be clarified by EMS)** - EMS’s evidence that ‘the D-1 shatter zone is considered to have such forms’.	46-60

Our opinions on ‘views against JAPC’s claim’ (3/5)

(Draft) EMS’s views against JAPC’s claim concerning the fault evaluations of Tsuruga PS site, EMS on shatter zones in the site of Tsuruga Power Station		JAPC’s opinion	Reference No.
Main texts	Issues		
<EMS’s views on the claim 3> (1) The operator’ s claim that D-1 fault is not the active fault to be taken into consideration. ➢ (Skipped)	–	**(Original thoughts)** - Though the detected amount is small, hornblendes are broadly distributed in the same horizon while Kojaku granites or dolerites which compose the rock mass do not include hornblende. Therefore, it is considered to the amphibolite which originate in the tephra. - Although somewhat re-deposition of layer is indicated by the repeated change of amounts of amphibolite with increasing and decreasing along up and down direction, the lower occurrence limit is present on or above the bottom of layer⑤, therefore it is judged that the bottom of layer⑤ and the lower occurrence limit almost indicate the period in which the tephra was fallen. - From the points above, there is not problem in the identification method.	–
(2) Identification of the tephra by analyzing minerals ➢As for analyzing the minerals contained in tephra, it is general to compare with main components of the several types of tephra to be concerned. However, the operator determined it is the same tephra only by comparing with the tephra, dating back to approx. 120 – 130 thousand years ago (the operator calls it ‘Mihama tephra’) and the identification method is considered to be insufficient. (3) Specification of the deposit which contains the tephra ➢Since the content percentage of the mineral (amphibolite) detected by the lower part of layer⑤ is low frequency which is less than one per 3,000 counts, and small amount of the mineral (amphibolite) are included in layer③ that is lower level, the operator’s claim that the lower part of layer⑤ is deposited with the tephra, dating back to 120 – 130 thousand years ago is not reliable assumption. ➢In order to specify the layer in which the tephra is deposited, it is preferable to recognize volcanic ashes by checking them with eyes. If it is not available with the eye inspection, there is also a way to specify the age, applying the method to count the minerals contained in the tephra in the layer. In that case, it is difficult to specify the layer in which the tephra is deposited unless large amount of minerals are contained in the layer while there is significant difference between the upper and the lower layers.	- The result of main components analysis has only been compared with Mihama tephra. - The contents of the minerals is low frequency, and it cannot be specified as the layer in which the tephra is deposited unless there is a significant difference between the upper and the lower layers. - Amphibolite is also included in layer③.	**(Outline of today’s explanation (new data))** 1. Stratigraphy of D-1 trench => Layer⑤ was deposited in the warm period, while deposit period of layer③ was colder than layer⑤. 2. Regarding hornblendes included in the lower part of layer⑤ and layer③ => Significant difference has been recognized between the hornblende in lower part of layer ⑤ and the one in layer③ in a result of main composition analysis, although mineral products are quite little because they are gravel. => It was identified that the hornblendes produced in the specific layer of the lower part of layer③ was the amphibolite which originated in the tephra. => It was identified that the lower part of layer⑤ was not the re-deposition of layer③ . 3. Hornblendes detected in the lower part of layer⑤ => There is a high possibility that the hornblendes in the lower part of the layer⑤ is Mihama tephra. => Daisen-Hiruzenpara and BT37 are distributed lower than Sanbe-Kisuki (110-115Ka), which are the tephra, deposited in the marine isotope stage 5e. => Therefore, it is considered that the lower part of layer⑤ should be the deposit of the marine isotope stage 5e. => Layer③ is deposit in marine oxygen isotope stage 6 or before, with coonsideration that layer③ is lower and colder than layer⑤. In addition, - additional analyses are implemented by increasing the survey lines in the D-1 trench in order to be progress of the reliability. - the main components are to be identified as for Daisen-Hiruzenbara. - BT 37 is 127.6ka according to the existing literature though it cannot to be confirmed as it is difficult to obtain the sample. **(Points to be clarified by EMS)** - Considering the above, is there still the reason that the lower part of layer⑤ and layer③ are not respectively MIS5e and MIS6? - The EMS confirmed that the geologic layer where the deformation of the K fault ran up did not reach to the silt layer of layer③.	61-78

Our opinions on ‘views against JAPC’s claim’ (4/5)

(Draft) EMS’s views against JAPC’s claim concerning the fault evaluations of Tsuruga PS site, EMS on shatter zones in the site of Tsuruga Power Station		JAPC’s opinion	Reference No.
Main texts	Issues		
<EMS’s views on the claim 4> The evaluation document points out that the D-1 shatter zone could give impacts on the important facilities, by being active working together with the activity of the Urasoko fault near there. This is because the K fault which continues to the D-1 shatter zone is a reverse fault accompanied by left-lateral slip and the possibility it would move, lead by the activity of the Urasoko fault is high as it is extremely close to the Urasoko fault, which is 20 – 30m at the horizontal distance. In addition, the numerical analysis implemented by the operator is the evaluation based on the ‘elasticity theory of dislocation’; however, the specialists of seismic back-check in the former Nuclear and Industrial Safety Agency pointed out that it was difficult to confirm the impacts, applying the ‘elasticity theory of dislocation’ in case it is too close like the case of the Urasoko fault. The EMS inherited the stance.	1. The possibility that the D-1 shatter zone would become active, lead by the activity of the Urasoko fault is high. 2. The EMS inherited the opinion of the specialists of seismic back check in the former Nuclear and Industrial Safety Agency that it is difficult to confirm the impacts, applying the ‘elasticity theory of dislocation’ in case it is too close like the case of the Urasoko fault.	**(Outline of today’s explanation (Original thoughts))** - The operator implemented the evaluation for the simultaneous activities of the D-1 shatter zone and the Urasoko fault based on the activity record and the numerical analysis. <Evaluation based on the activity record> - The latest activity period of the Urasoko fault is after approx. 4000 years ago and the average interval of the activity is 5,000 years ± 2,000 years (AIST, etc 2012); however, the D-1 shatter zone has not been active at least since approx. 120,000 years ago. - Therefore, it is considered that the Urasoko fault has become active 10 – 40 times since approx. 120,000 years ago while the D-1 shatter zone has never been active in that period. - In addition, it is considered that the Urasoko fault and the D-1 shatter zone should not simultaneously become active in future, too, considering the view that the regional stress field has not changed since the Late Pleistocene. <Evaluation based on the numerical analysis> - The bearing capacity of the ground which contains the D-1 shatter zone when being impacted by the activity of the Urasoko fault is evaluated by implementing the numerical analysis. - In the numerical analysis, ‘basic study’ and ‘study to consider uncertainty’ were implemented first in the ground deformation analysis based on the ‘elasticity theory of dislocation’ which assumes the ground as an elastic half-space to extract the evaluation conditions for obtaining the most strict result for the bearing capacity evaluation of the reactor building foundation. - After that, it was analyzed based on the evaluation conditions, applying the FEM model which is made, considering the topography, the ground structure, the ground property and the nonlinearity of the ground, etc for which the ‘elasticity theory of dislocation’ cannot be applied in detail while the stability of the shatter zone was evaluated based on the local safety factor obtained from the FEM analysis result. - Though the result shows shear failures and induction of tensile stresses in the shatter zone near the Urasoko fault, the area is limited while the local safety factor of the shatter zone near the building is sufficiently large. Therefore, it is concluded that the bearing capacity of the ground is sufficiently strong. ・In addition, the purpose of the numeric analysis implemented by the operator is to evaluate ‘if the shatter zone under the reactor building could be broken by the tensile stress in the ground induced due to the activity (displacement) of the Urasoko fault’ and it is the evaluation for the ground stability, in other words. ・Therefore, it is not the evaluation for calculating the displacement magnitude of the shatter zone. ・Such method for the ground stability evaluation is widely applied in the field of geotechnology. **(Points to be clarified by EMS)** ・The operator has been implementing the evaluations for the simultaneous activities of the D-1 shatter zone and the Urasoko fault based on the following process and is that correct? - ‘The regulatory guide for reviewing seismic safety design of nuclear facilities for power generation (approved by Nuclear Safety Commission as of December 20, 2010) instructed that the fault displacements due to earthquakes should be evaluated by calculating the displacements / deformations of the ground where buildings and structures are established due to the fault displacements. Complying with the guideline, the evaluation was implemented by the numeric analysis to identify whether a gap could be made or not due to the activity of the Urasoko fault in the surrounding shatter zone including the D-1 shatter zone. - Being instructed by the former NISA as of November 11, 2011 ‘to show the evaluation method of the geological displacements around the active layers in Tsuruga NPP and implement impact evaluations for the reactor building, etc, applying the concerned method’, we have been implementing the evaluations. - The operator presented the additional survey plan of the site in the opinion hearing meeting of the former NISA regarding earthquakes and tsunamis as of May 14, 2012 and explained that ‘it is evaluated comprehensively based on the results of various geological surveys and the numerical analysis, etc in case it is difficult to evaluate it by overlying strata analysis method’. ・The former NISA discussed that ‘it should take time to review the applicability’ and ‘it is necessary to evaluate more in detail’ as for the elasticity theory of dislocation; however, it only pointed out that the theory should be evaluated carefully but did not mean that it was inapplicable. ・In addition, though the EMS expressed that ‘they would inherited the stance’, the EMS and ‘The study team on the new safety design standards for earthquakes and tsunamis for light water reactors for electric power generation’ have not discussed the application of the elasticity theory of dislocation, at all. We would like to know the process how they reached to the conclusion to inherit the stance. ・Though the possibility that the D-1 shatter zone could move, lead by the activity of the Urasoko fault was pointed out, we would like to know what sort of mechanism was assumed when you meant by ‘lead by the activity’ and how large the impact would be.	79-135

Our opinions on ‘views against JAPC’s claim’ (5/5)

(Draft) EMS’s views against JAPC’s claim concerning the fault evaluations of Tsuruga PS site		JAPC’s opinion	Reference No.
Main texts	Issues		
【EMS views to Claim 5】 The current seismic design policies stipulate that an active fault given consideration in the seismic design is a “fault with signs of activity after the Late Pleistocene that cannot be denied.” It is not stipulated that an active fault is a “fault, of which signs of activity are recognized.” So, to be of concern here is a case with no data relevant to activity available (with no data available proving no activity is found whatsoever). On the occasion that the operator does not present a data accurate enough, like this time, a fault in question is to be judged as an “active fault given consideration in the seismic design.” EMS also considers that <u>the operator is primarily held accountable for proving that a fault is not an active fault</u>. Thus, the operator, which conducted surveys, has a responsibility to present data relevant to fault activity (showing there is no activity whatsoever). In case a new fact emerges, this evaluation might be reviewed, if necessary. Even on that occasion, though, the operator needs to present a set of “objective data” denying any possibility that a fault under survey is not active through further surveys etc.	・Whether the operator is primarily held accountable for having the burden of proof?	From the legal point of view, we consider as inappropriate that the operator is primarily held for having the burden of proof. Generally speaking, under the regulation laws, it is authorities, as an administrator of regulations, that are accountable for proving whether a subject matter in case makes up regulatory requirements. To that end, authorities are entitled to the right of collection of reports and the right to make on-site inspections. Pursuant to new backfitting rules under the Nuclear Reactor Regulation Law, the Nuclear Regulation Authority (or EMS) is authorities found relevant to the case in question and is responsible for having the burden of proof and making final explanations. We already presented to EMS highly accurate and objective facts and data based on surveys to prove that there are “no signs of activity.” If the NRA (or EMS) tries to overturn our position, it will be held accountable for having the burden of proof, or verifying its position, and making explanations on the given data.	136−138

Our opinions on ‘EMS’s evaluation’ (1/2)

(Draft) Evaluation on the faults at Tsuruga PS site (Basic consideration) EMS on shatter zones in the site of Tsuruga Power Station		JAPC's opinion	Reference No.
Main texts	Issues		
① Highly active Urasoko fault is in the extremely close vicinity of Unit 1 and 2 nuclear reactor buildings (about 200-300m apart) within the premises of Tsuruga plant. • In 2008, JAPC reported that Urasoko fault had been active more than once over the past 120,000-130,000 years and that its latest period of activity must have been more recent than around 4,000 years ago from now.	–	**（Points to be clarified by EMS）** ・Urasoko fault is active fault to be taken into account in seismic design. Its affect is evaluated.	–
② A lot of faults are identified in the premises. Around D-1 fault (or around a line extended from the fault), which is directly below Unit 2 reactor building, are several faults, including K fault and G fault, which run in parallel in the same direction.	Expert view to JAPC Same as point of contention in Claim 1	Same as our view to expert views to Claim 1	–
③ Generally speaking, a fault does not necessarily stretch out straight. It sometimes inflects, changes direction, or continues running in parallel to other faults after breaking up once. Because of this, it is considered appropriate that D-1 fault, K fault, G fault are in the associated structures.	Expert view to JAPC Same as point of contention in Claim 2	Same as our view to expert views to Claim 2	–
④ It was confirmed that K fault, considered associated structure with D-1 fault, caused an inconsistency in a layer likely to have been piled up from Late Pleistocene on in D-1 trench. Therefore, to judge D-1 fault inactive (which means it has no need to be take into account in seismic design), it should be proven by highly accurate data that there is no new seismic activity in the structure for sure.	1. Didn’t identify which layers are likely to have piled up from Late Pleistocene on. 2. Didn’t identify which layer caused inconsistency.	**（Points to be clarified by EMS）** ・Please provide a concrete reasoning, based on which experts say that “K fault caused inconsistency in a layer likely to have piled up from the Late Pleistocene on,” while never explaining the relationship between sedimentary layers and faults and the period evaluation of sedimentary layers.	–
⑤ Although the operator presented several data so far, all of these data are not recognized as proven enough to say that D-1 fault is inactive. 【See attachment for examples】 “Specification of active periods of D-1 fault by observing tephra” “Specification of displacement sense by observing fragment samples” etc.	–	**（Points to be clarified by EMS）** ・If there are imperfect parts, further data should be added and confirmed. Thus, EMS experts should clarify what is imperfect.	–
⑥ As most of the layers, on which data was highly likely to have existed and have served as a reasoning for the activity of any fault, were lost in past digging or construction works, it is almost impossible to obtain any decisive evidence for that D-1 fault is highly active. However, the operator says that in the investigation this time it obtained data showing repeated movements of a fault (K fault), of which a certain amount of rationality is recognized in saying that it is associated with D-1 fault.	–	**（Opinions so far expressed）** ・D-1 trench is not necessarily considered as inadequate as a position for investigation. ・The reason for the above, as pointed out in EMS, the objective of the investigation is whether D-1 fault moves in tandem with Urasoko fault. The investigation is underway extremely close to Urasoko fault, because the area under investigation is considered most vulnerable to the fault’s activity. **（Points to be clarified by EMS）** ・At the third meeting, we just said that slickenlines which have several directions are confirmed in L-cut pit. There is no fact that we made any explanation whatsoever suggesting that data was obtained which shows repeated movements in the current stress field.	–

Our opinions on ‘EMS’s evaluation’ (2/2)

(Draft) Evaluation on the faults at Tsuruga PS site (Basic consideration) EMS on shatter zones in the site of Tsuruga Power Station		JAPC’s opinion	Reference No.
Main texts	Issues		
⑦ On data available as of now（including data presented by the operator at Mar. 8 evaluation meeting), EMS defines that D-1 shatter zone is highly likely to be an active fault, which should be taken into account in seismic design and that it is likely to move in sync with Urasoko fault nearby, which means there is a fear to affect important nuclear facilities located immediately above the zone.	–	**(Opinion so far expressed)** ・Based on each of the above discussions ①～⑥, we judge that D-1 shatter zone is not an active fault, which should be taken into account in seismic design.	–
⑧ In case another new fact emerges, it may be possible to review the evaluation. However, even on that occasion, the operator needs to provide objective data, or a result of added surveys, which denies any possibility that this is an active fault.	–	**(Opinion so far expressed)** ・As for evaluation of D-1 shatter zone, we are taking an additional survey to accumulate data.	–
【See attachment】Examples of attested information provided by the operator, which was later found inadequate １． Insistence of the active period of D-1 shatter zone by identifying tephra （１）The operator says that D-1 shatter zone is not an active fault to concern ➢(Same as Claim 2) （２）Identification of tephra through analysis of minerals ➢(Same as Claim 3) （３）Specification of layer, where tephra accumulates ➢(Same as Claim 3)	Expert views to JAPC same as noted as points of contention in Claims 2 and 3	Same as our opinions on the left	–
（Expert comment） The following comment is made by Prof. Takehiko Suzuki of Tokyo Metropolitan University, expert at fourth tephra studies (pyroclastic material). <u>Prof.: Before going into the substance of the matter, please note that this comment may not be accurate without details.</u> “It would be more persuasive, if a string of samples were extracted by 10cm from a 1m-wide loamy layer, that 100 phenocryst minerals were detected out of 3,000 minerals counted in a certain horizon, and that 30 phenocryst minerals were further detected immediate above and below that horizon, as well as that 10 such minerals were further detected immediate above and below that horizon. If there is only less than one phenocryst mineral out of 3,000 minerals in a certain horizon alone in that layer and that no phenocrist mineral was detected immediate above and below that horizon, I should say that credibility is low, however. (extraction)	–	**（Opinions so far expressed）** ・Though the detected amount is small, hornblendes are broadly distributed in the same horizon while Kojaku granites or dolerites which compose the rock mass do not include hornblende. Therefore, it is considered to the amphibolite which originate in the tephra. ・Although somewhat re-deposition of layer is indicated by the repeated change of amounts of amphibolite with increasing and decreasing along up and down direction, the lower occurrence limit is present on or above the bottom of layer ⑤, therefore it is judged that the bottom of layer⑤ and the lower occurrence limit almost indicate the period in which the tephra was fallen. ・From the points above, there is not problem in the identification method.	–
２． Specification of displacement sense by fragment observations (Same as Claims 1 and 2）	Expert views to JAPC are the same as Claims 1 and 2	Same as our opinion on the left	–

(Draft) EMS's views against JAPC's claim concerning the fault evaluations of Tsuruga PS site, EMS on shatter zones in the site of Tsuruga Power Station		JAPC's opinion	Reference No.
Main texts	Issues		
<EMS's view on the claim 1> EMS evaluation report (draft) states that the operator has not give clear evidence on that G fault is D-1 shatter zone. The reasons of EMS's views are as follows;	–	–	–
1. In EMS, the specialist of geology pointed out; - It is difficult to identify the displacement sense of the last slip surface by thin section observations, because the structure of the last slip cannot always be identified through clearly distinguishing each slip from the others in case of the fault experienced multiple slips. - Even if the displacement senses of the last slip surfaces is identified at each point, it is only the last slip surface at each point but the slip periods of each point cannot be specified. In other words, the last slip surfaces of different points were not necessarily be active in the same period even if their displacement senses are the same. Therefore, the evaluation based on displacement senses cannot be sufficient evidence for the claim that the G fault continues to the D-1 shatter zone.	1. Thin section observations cannot identify displacement senses of the last slip surfaces. 2. There is no sufficient evidence for the claim that the G fault continues to the D-1 shatter zone.	**(Outline of today's explanation)** **1.Identifications of displacement senses of the last slip surfaces** - Thin section observations have been implemented for identifying the displacement senses of the faults. In order to verify the validity of thin section observations, CT image analyses for the identification of the last slip surface and slickenline observations with stereoscopic microscope for the identification of the displacement senses were implemented for the D-1 shatter zone (at the slope behind the unit 2), the G fault (at D-1 trench) and the K fault (at D-1 trench). - The result shows that there was no problem in the identifications of the last slip surfaces based on the thin section observations which have been implemented so far and the displacement senses were consistent with the ones identified by the slickenline observations. - Therefore, it is possible to identify the displacements sense of the last slip surface by thin section observations. **2. Continuity of D-1 shatter zone** - The strike and the dip of the G fault are similar to the ones of the D-1 shatter zone (N-S strike / high angle west-dipping) and the displacement senses of their last slip surfaces were also the same, which are normal faults. - Meanwhile, the K fault was a reverse fault which is different from the D-1 shatter zone. - Therefore, the K fault is not the D-1 shatter zone but the G fault. **(Point to be clarified by EMS)** - The reasonable reason that EMS claims the active periods of the shatter zones with the same displacement sense are different, and there can be many shatter zones which continue to the D-1 shatter zone.	10-45

【Displacement sense of D-1 shatter zone】

Survey location：Back slope of Unit 2

D-1 shatter zone, Offscraping of back slope of Unit 2, Survey location

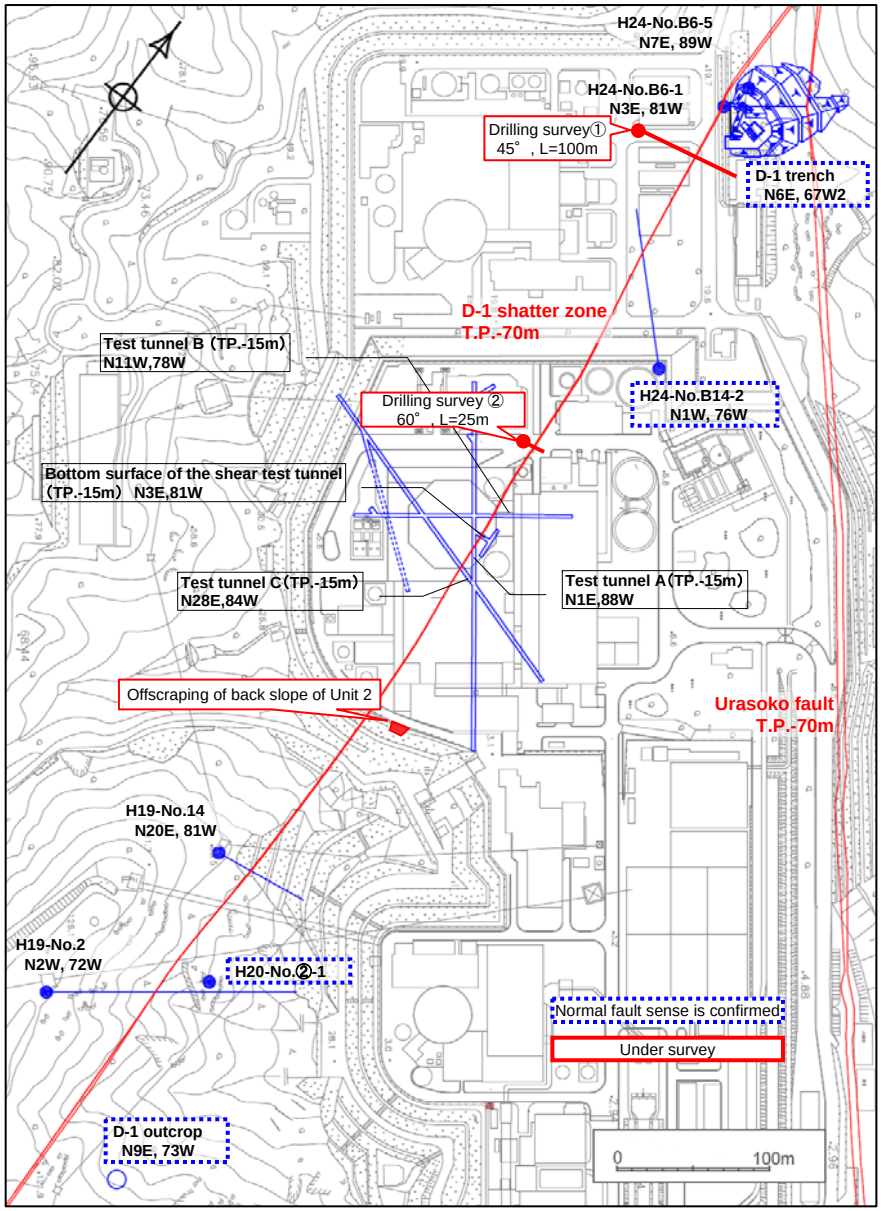

Offscraping of the back slope of Unit 2 was carried out and the data of continuity of D-1 shatter zone was reinforced.

D-1 shatter zone, Offscraping of back slope of Unit 2, Outcrop

E←

→W

Offscraping of slope (full view) 1m

Brown and blackish brown colored fault gouge linearly shears whole of the outcrop.

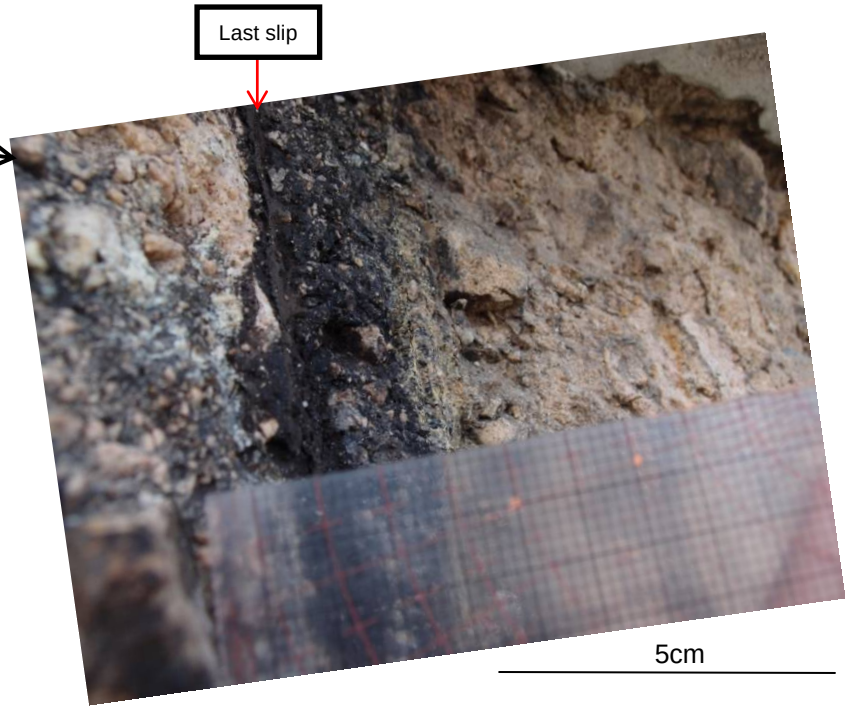

Brownish, thin and soft fault gouge linearly shears other fault gouges around it.

The last slip surface shears whole of the outcrop. That surface is located at the softest portion and has the most rectilinear shape.

D-1 shatter zone, Offscraping of back slope of Unit 2, Polished section

Brownish and thin fault gouge linearly shears whole section.

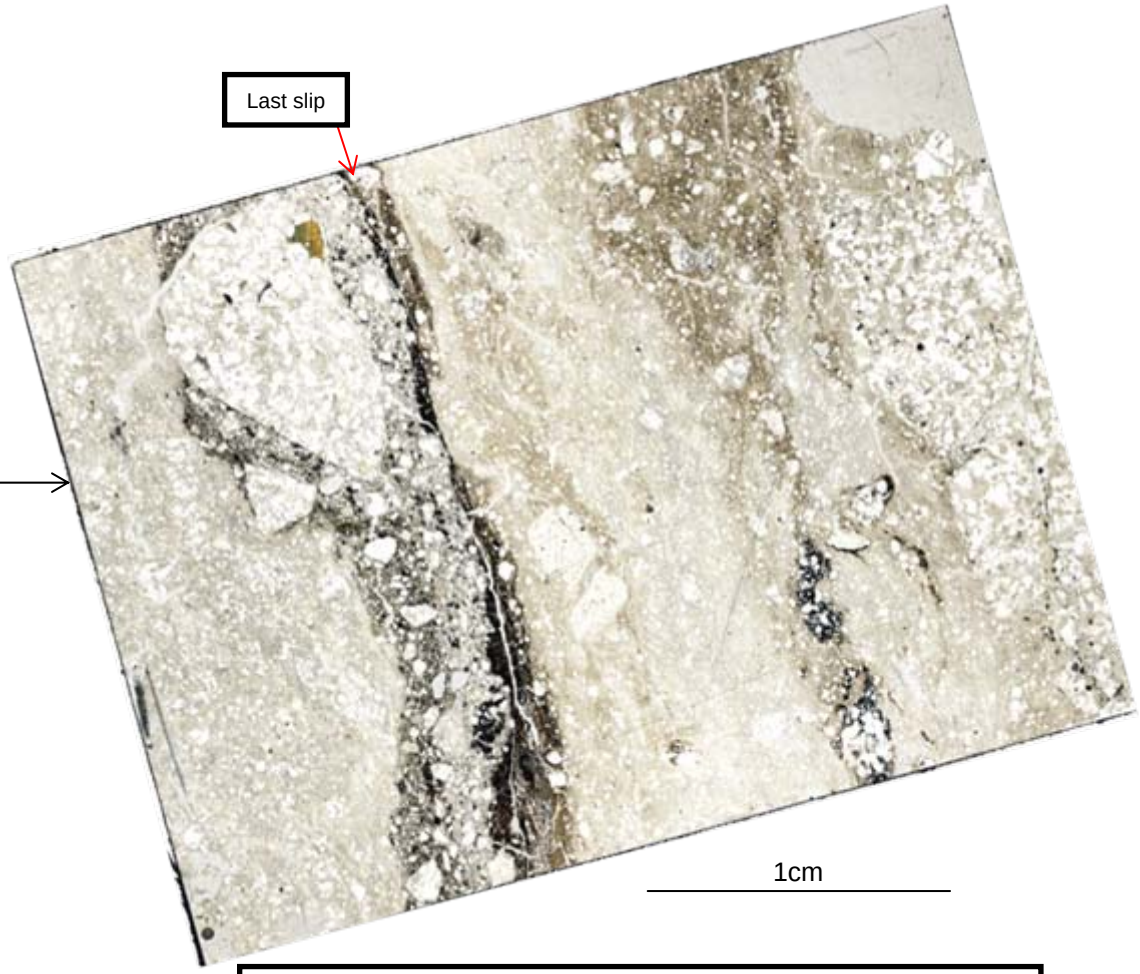

Brownish fault gouge linearly shears whole section.

In the block sample, the last slip surface linearly shears whole of the section. That surface is located at the softest portion and has the most rectilinear shape.

D-1 shatter zone, Offscraping of back slope of Unit 2, Block sample

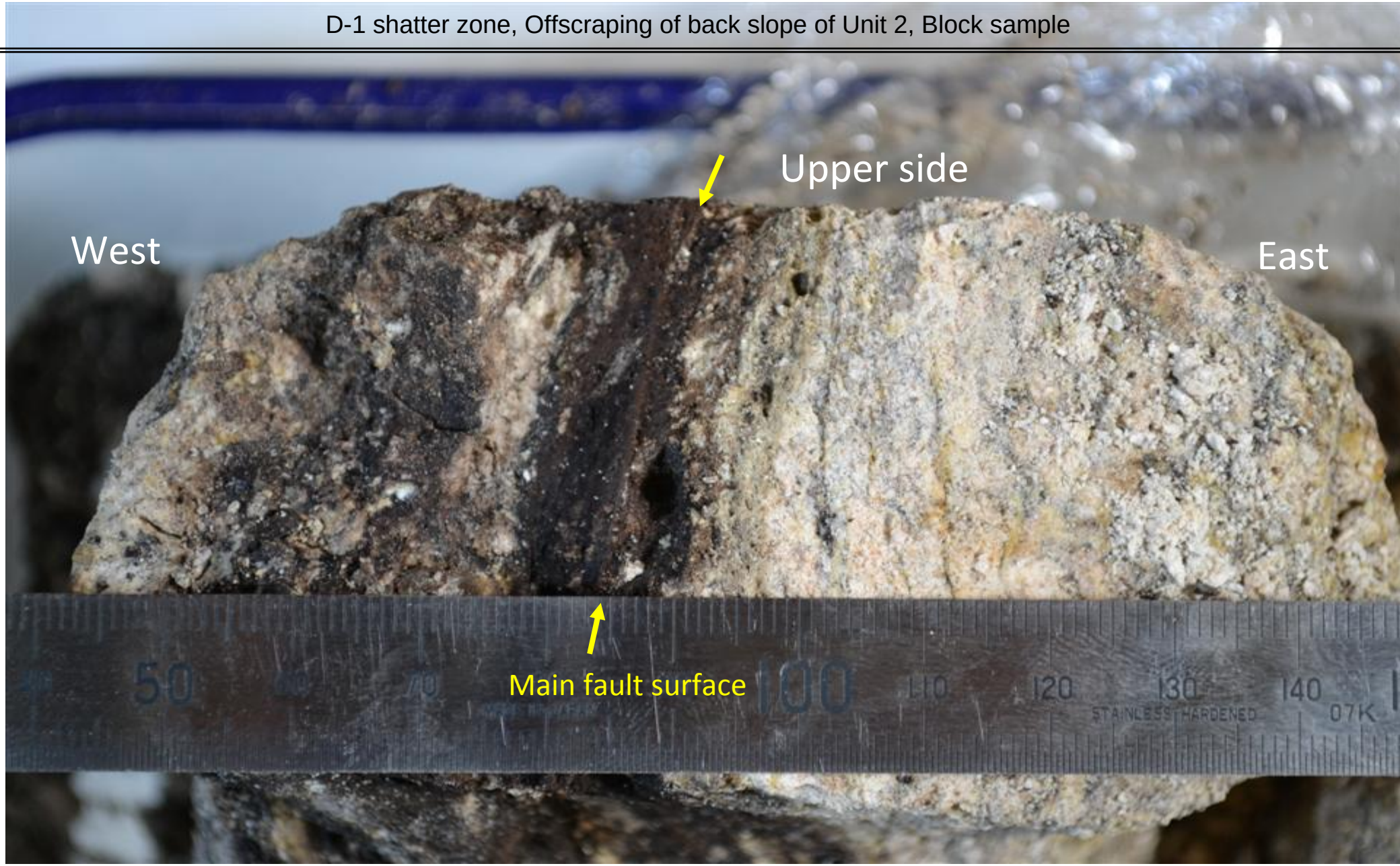

A 2mm thick fault gouge is observed along the main fault surface.

10 mm

CT scan of the block sample (G fault)

Inner structure of the fault rock was analyzed by X-ray CT.

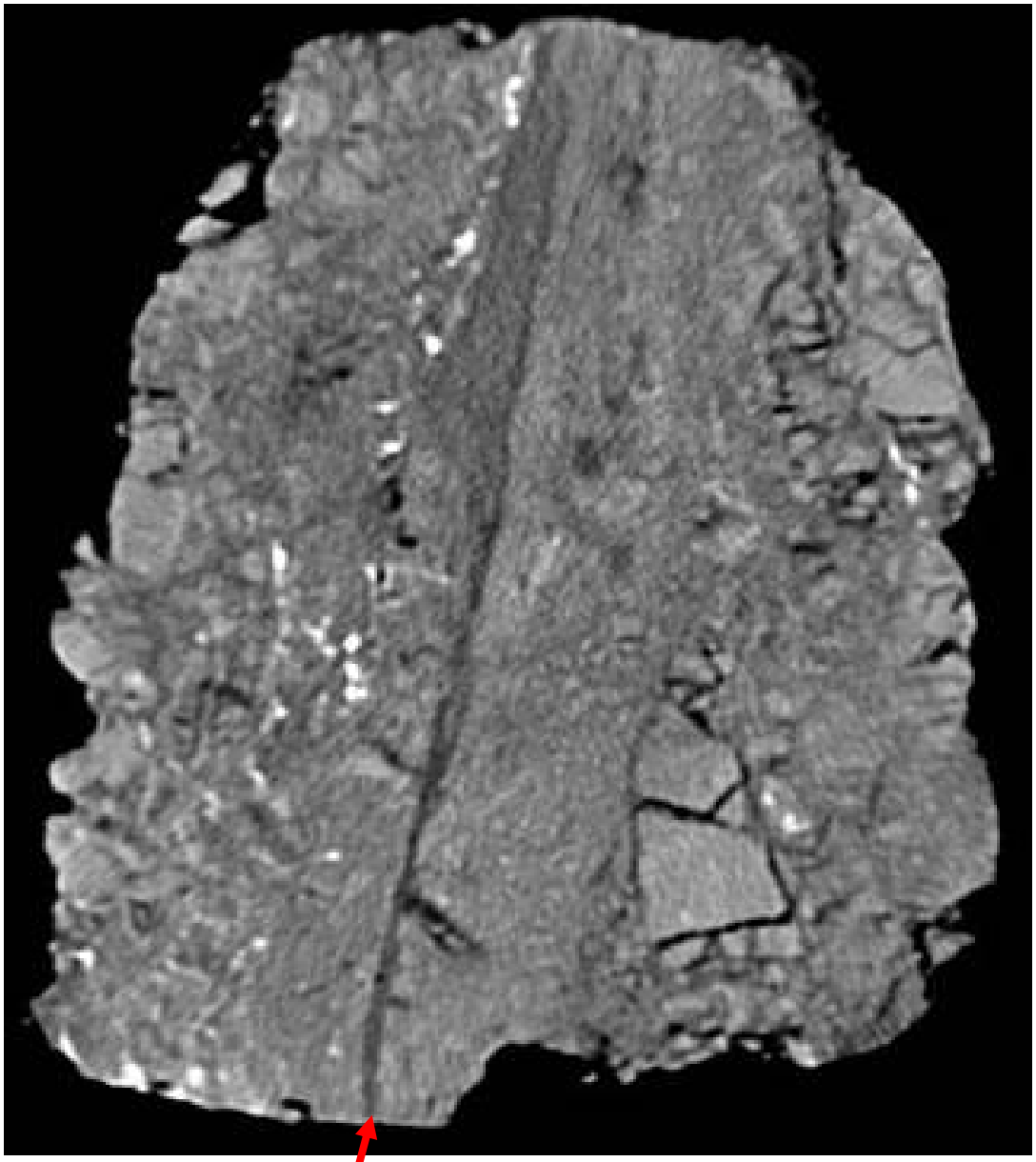

Vertical cross-section

A thin and long fault gouge is observed along the main fault surface (Last slip).

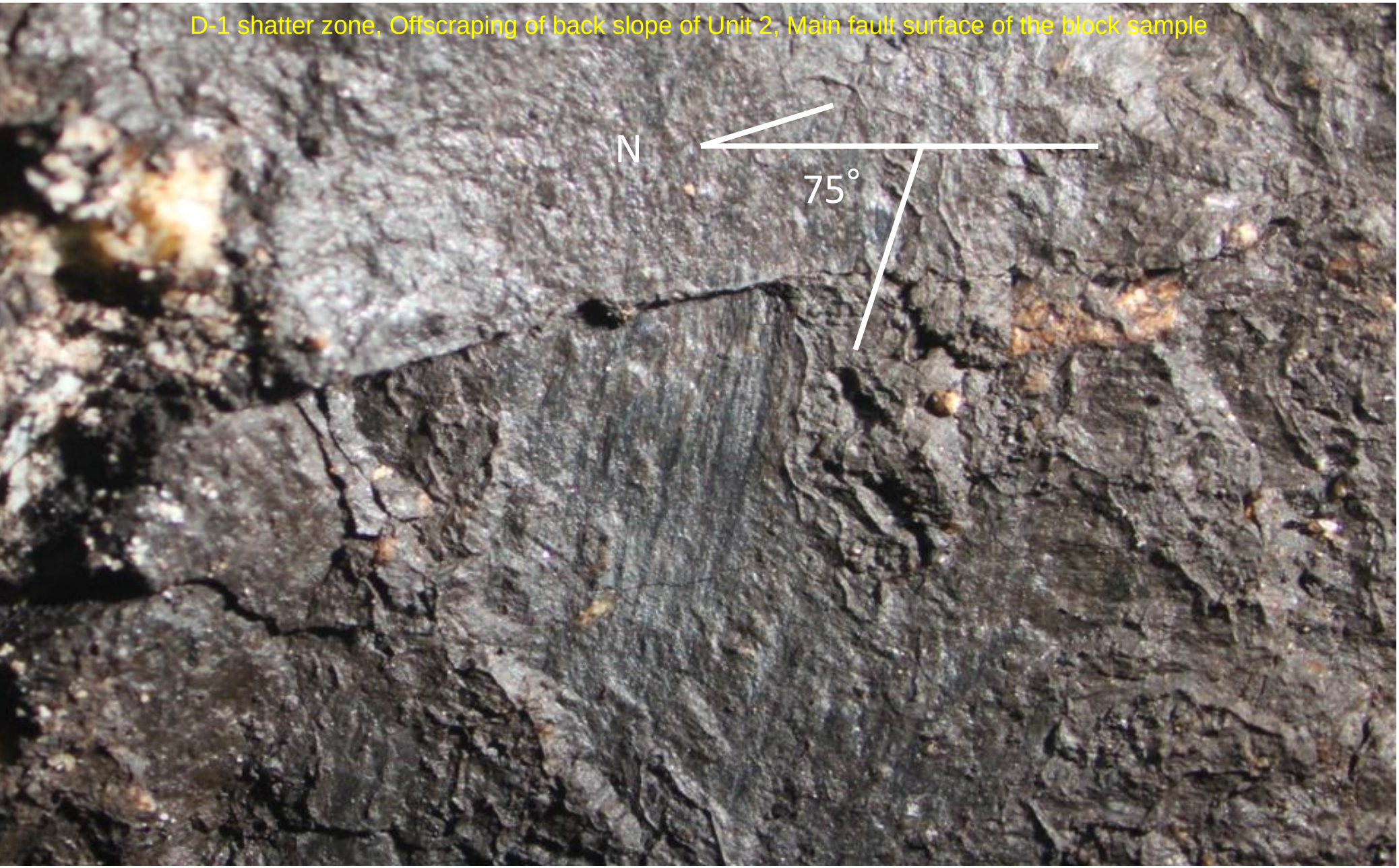

Viewing from the west side of main fault surface on the footwall. Slickenline at a high-angle (75˚) is observed.

N

Upper side

Viewing from the west side of main fault surface on the footwall. Slickenline at a high-angle is observed.

D-1 shatter zone, Offscraping of back slope of Unit 2, Main fault surface of the block sample

Upper side ←

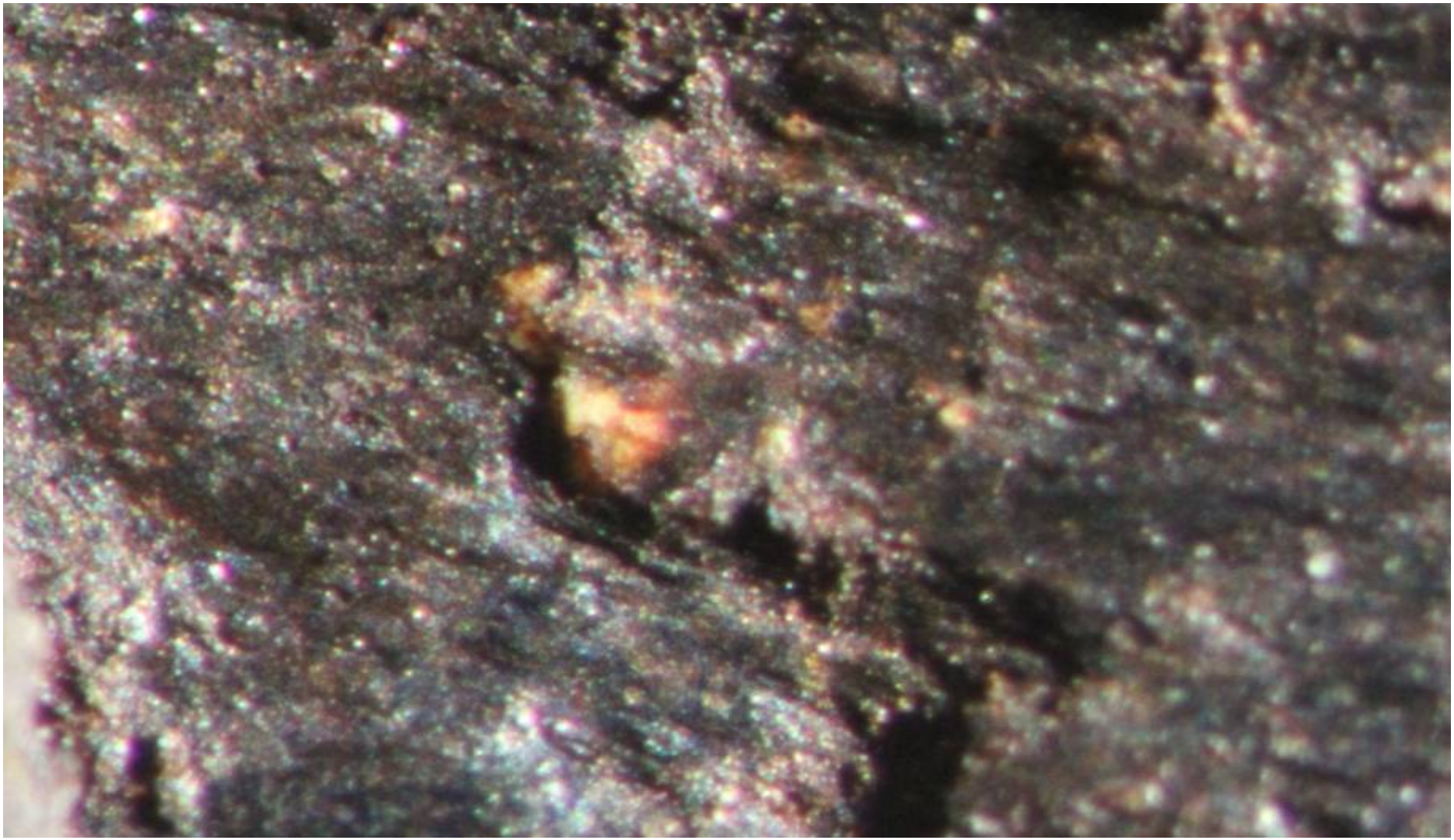

N ↓

Viewing from the west side of main fault surface on the footwall.

D-1 shatter zone, Offscraping of back slope of Unit 2, Thin section (direction of the slickenline) (without auxiliary line of composite surface structures)

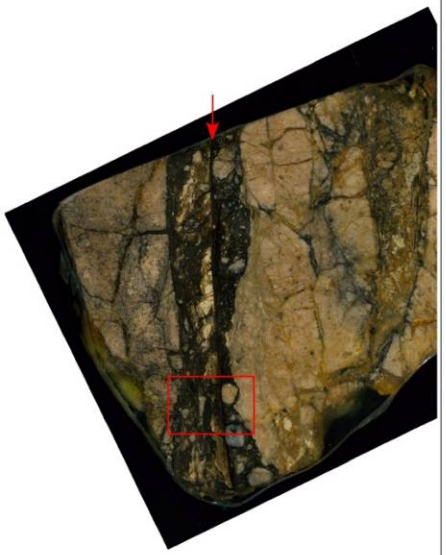

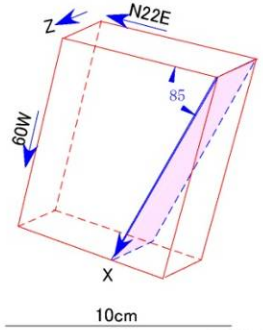

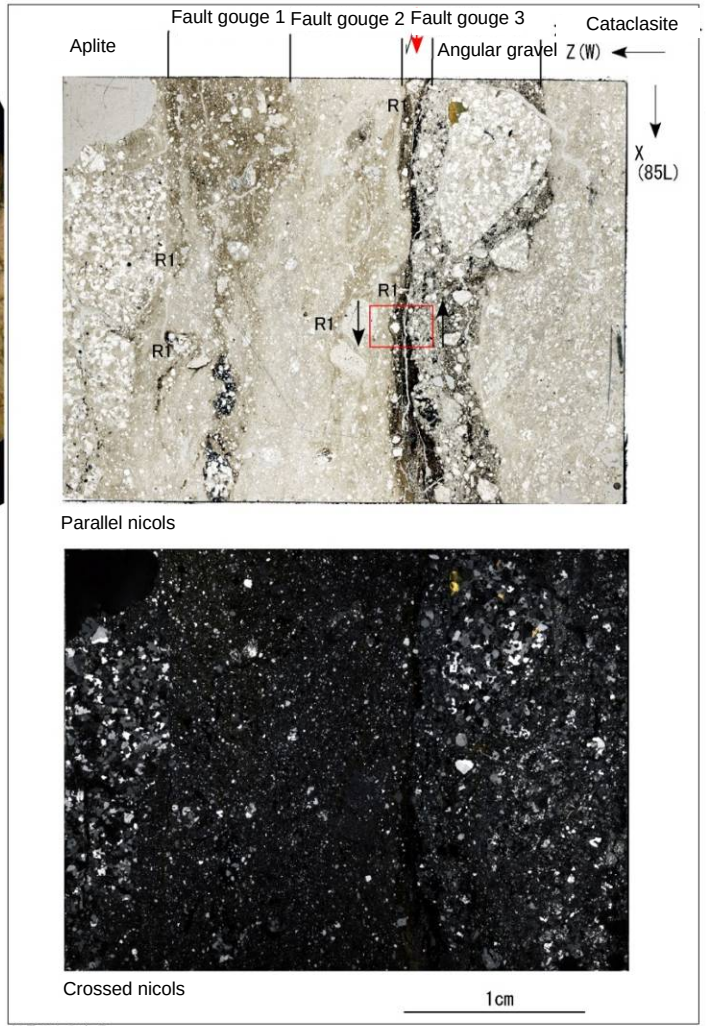

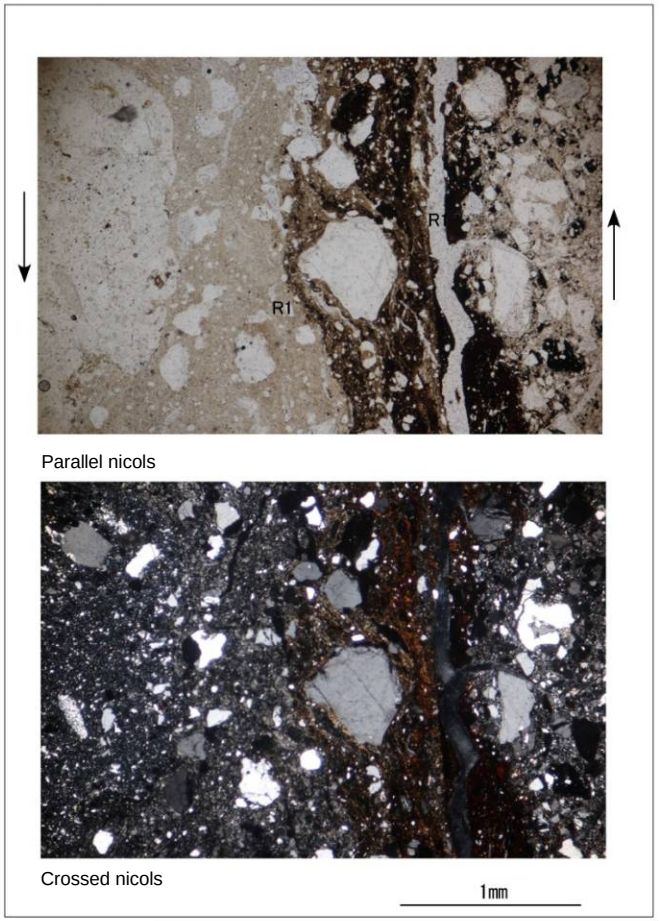

・Aplite
Consists of quartz, potassium feldspar, and plagioclase
・Fault gouge 1
Consists of the brown-gray matrix of fine grain, as well as quartz, feldspar, and cataclasite fragments and that are sub-angular or semi-circular gravels with diameters of 0.01 mm to 6mm. Contains lots of clay minerals. The displacement sense of reverse fault and left-lateral slip can be recognized from R1.
・Fault gouge 2
Consists of the brown-gray matrix of fine grain, as well as quartz, feldspar, and cataclasite fragments and that are semi-circular or sub-angular gravels with diameters of 0.01 mm to 2mm. Contains lots of clay minerals. The displacement sense of normal fault and right-lateral slip can be recognized from R1.
・Fault gouge 3 (last slip)
Consists of the brown matrix of fine grain, as well as quartz, feldspar, and cataclasite fragments and that are semi-circular or sub-angular gravels with diameters of 0.01 mm to 1mm. Contains lots of clay minerals. The displacement sense of normal fault and right-lateral slip can be recognized from R1.
・Cataclasite
Consists of quartz, potassium feldspar, plogioclase, muscovite, and calcite.

D-1 southern slope of Unit 2 direction of XZ(85L)

The displacement sense of normal fault was observed in the thin section along the slickenline of the last slip surface.

D-1 shatter zone, Offscraping of back slope of Unit 2, Thin section (direction of the slickenline) (with auxiliary line of composite surface structures)

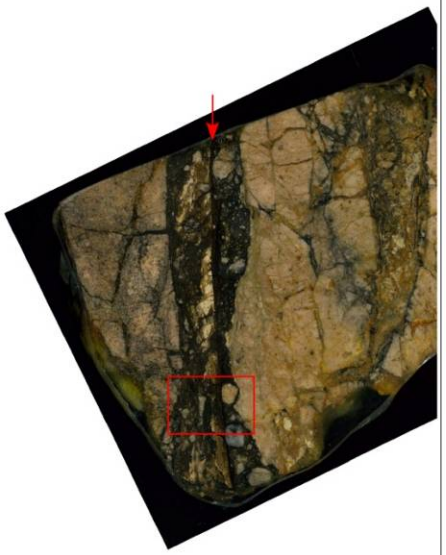

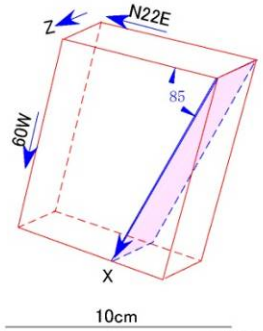

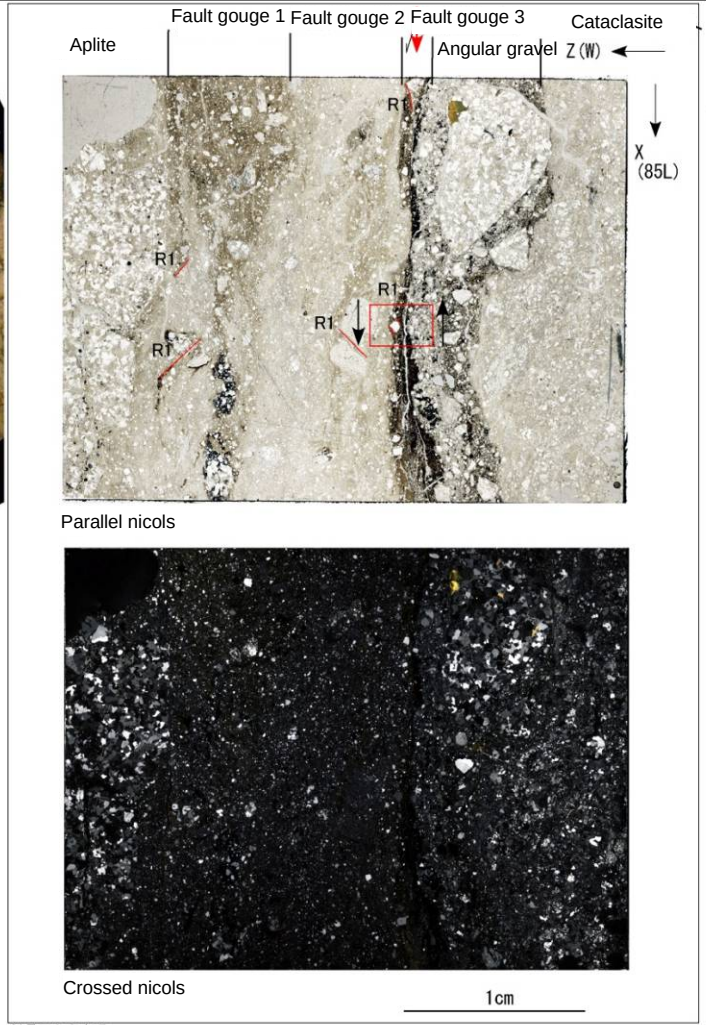

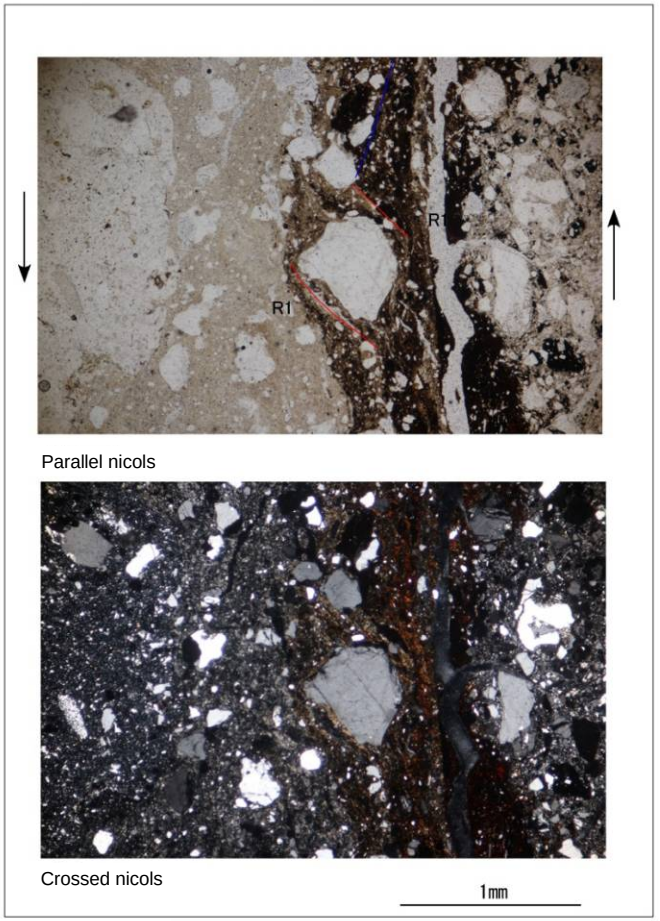

・Aplite
Consists of quartz, potassium feldspar, and plagioclase

・Fault gouge 1
Consists of the brown-gray matrix of fine grain, as well as quartz, feldspar, and cataclasite fragments and that are sub-angular or semi-circular gravels with diameters of 0.01 mm to 6mm. Contains lots of clay minerals. The displacement sense of reverse fault and left-lateral slip can be recognized from R1.

・Fault gauge 2
Consists of the brown-gray matrix of fine grain, as well as quartz, feldspar, and cataclasite fragments and that are semi-circular or sub-angular gravels with diameters of 0.01 mm to 2mm. Contains lots of clay minerals. The displacement sense of normal fault and right-lateral slip can be recognized from R1.

・Fault gauge 3 (last slip)
Consists of the brown matrix of fine grain, as well as quartz, feldspar, and cataclasite fragments and that are semi-circular or sub-angular gravels with diameters of 0.01 mm to 1mm. Contains lots of clay minerals. The displacement sense of normal fault and right-lateral slip can be recognized from R1.

・Cataclasite
Consists of quartz, potassium feldspar, muscovite, and calcite.

D-1 southern slope of Unit 2 direction of XZ(85L)

The displacement sense of normal fault was observed in the thin section along the slickenline of the last slip surface.

【Displacement sense of G fault】

Survey location：D-1 trench

G fault, D-1 trench, Block sample location

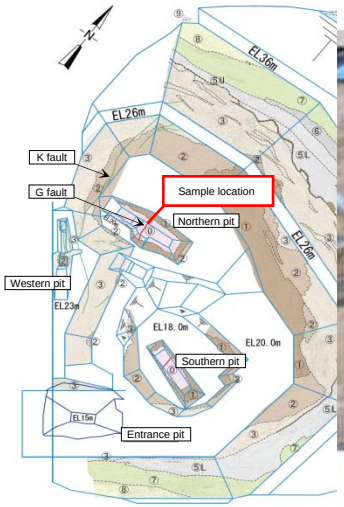

Northern wall surface

Eastern wall surface

Bottom surface

Southern wall surface

The displacement sense of normal fault was observed in the thin section along the slickenline of the last slip surface.

西

上

Two fault surfaces with good continuity were observed and that shear other deformation structures.

CT scan of the block sample (G fault)

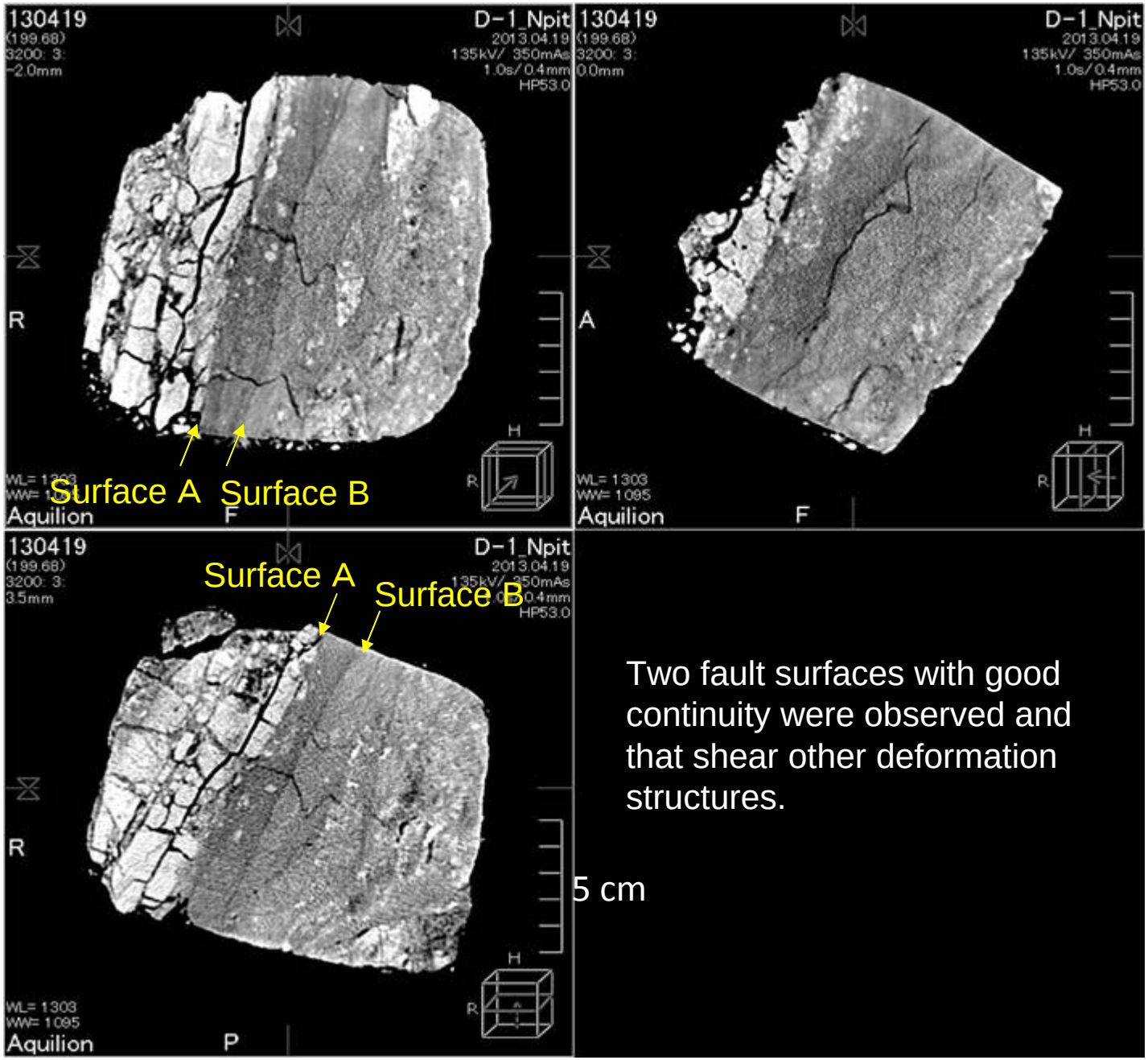
130419
D-1_Npit
2013.04.19
135kV/ 350mAs
1.0s/0.4mm
HP53.0
Surface A
Surface B
Aquilion
F
130419
D-1_Npit
2013.04.19
135kV/ 350mAs
1.0s/0.4mm
HP53.0
WL= 1303
WW= 1095
Aquilion
F
130419
D-1_Npit
Surface A
Surface B
HP53.0
WL= 1303
WW= 1095
Aquilion
P
Two fault surfaces with good continuity were observed and that shear other deformation structures.
5 cm

N ←——— G fault, D-1 trench, Northern pit, Block sample from D-1 shatter zone: Slickenline on the surface A

1 mm

Looking from west side to east side. View of the footwall surface (surface A) with westerly dip. Slickenlines at a high-angle were recognized.

N ←

D-1 trench, Northern pit, Block sample from D-1 shatter zone: Slickenline on the surface A

Looking from west side to east side. View of the footwall surface (surface A) with westerly dip. Slickenlines at a high-angle and small dimples were recognized.

1 mm

D-1 trench, Northern pit, Block sample from D-1 shatter zone: Slickenline on the surface B

N

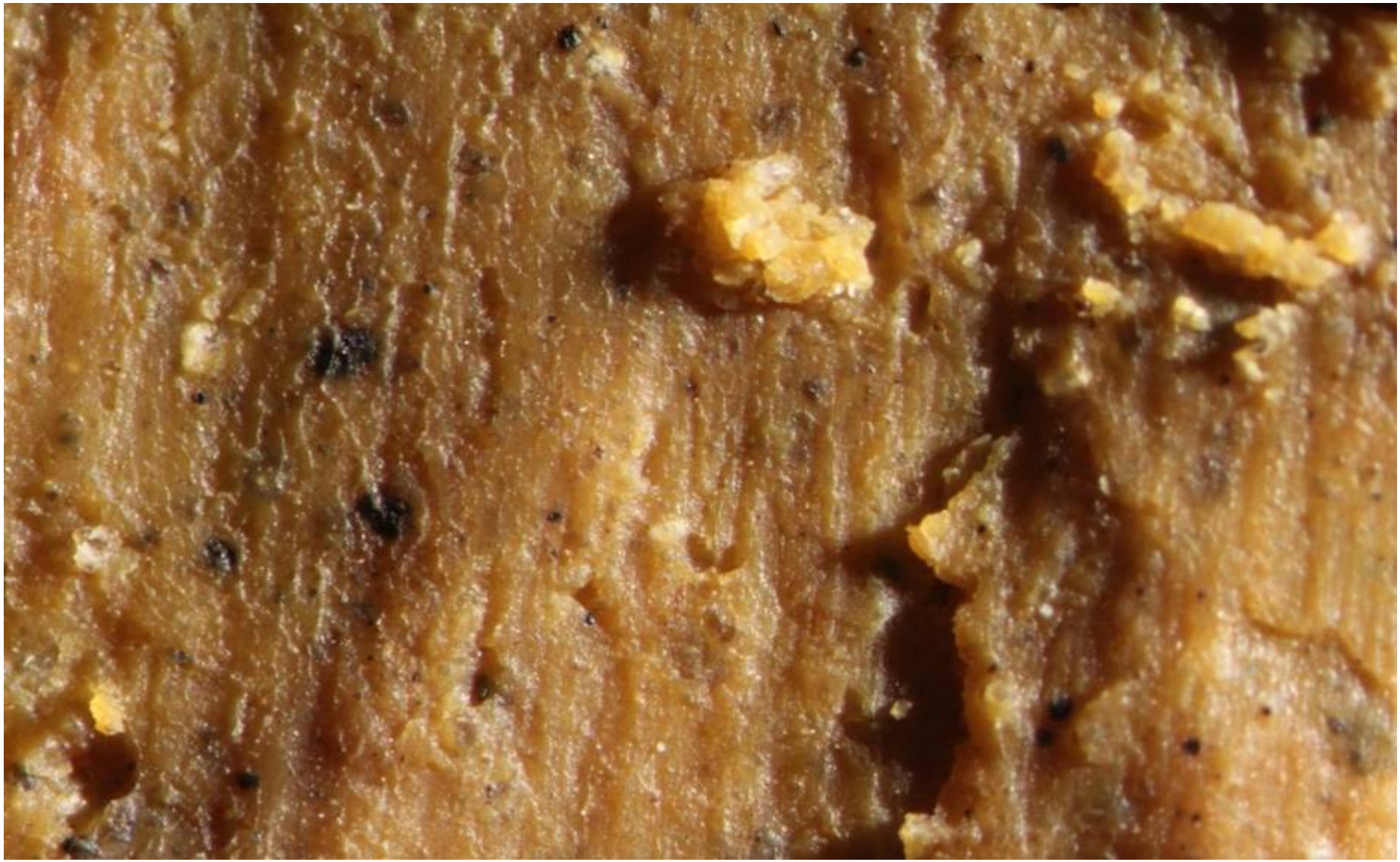

1mm

Looking from west side to east side. View of the footwall surface (surface B) with westerly dip. Slickenlines at a high-angle and small dimples were recognized.

G fault, D-1 trench, Outcrop

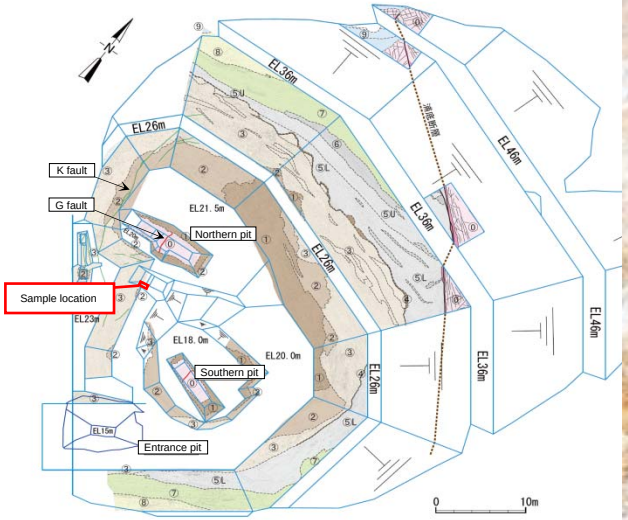

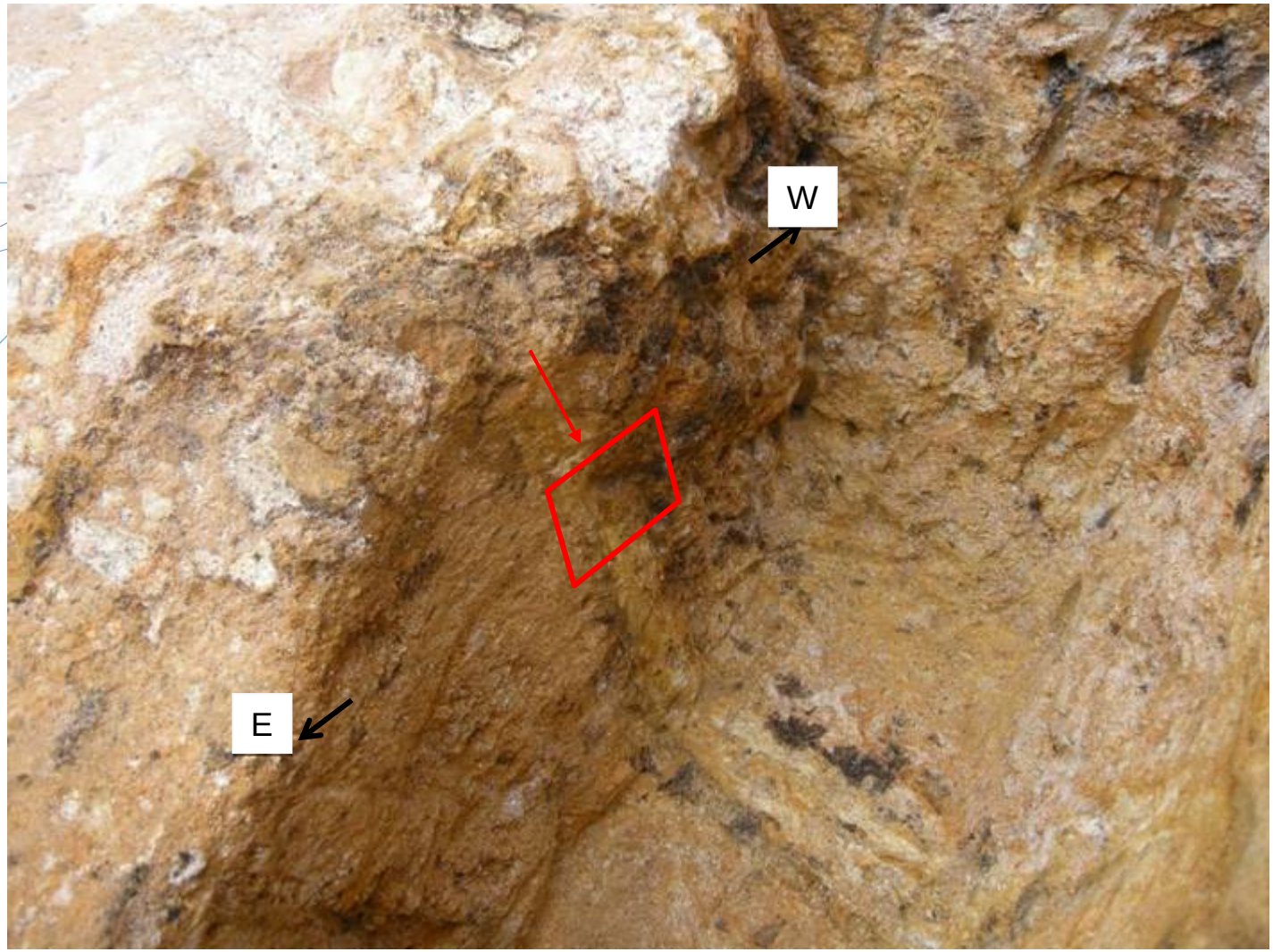

Photograph of sample location

From the hanging side (western side), G fault consists of planate cataclasite, fault gouge, and cataclasite.
The fault gouge linearly shears whole of the outcrop, and its footwall side has the continuous rectilinear shape.

The last slip surface shears whole of the outcrop. That surface is located at the softest portion and has the most rectilinear shape.

G fault, D-1 trench, Polished section

W

E

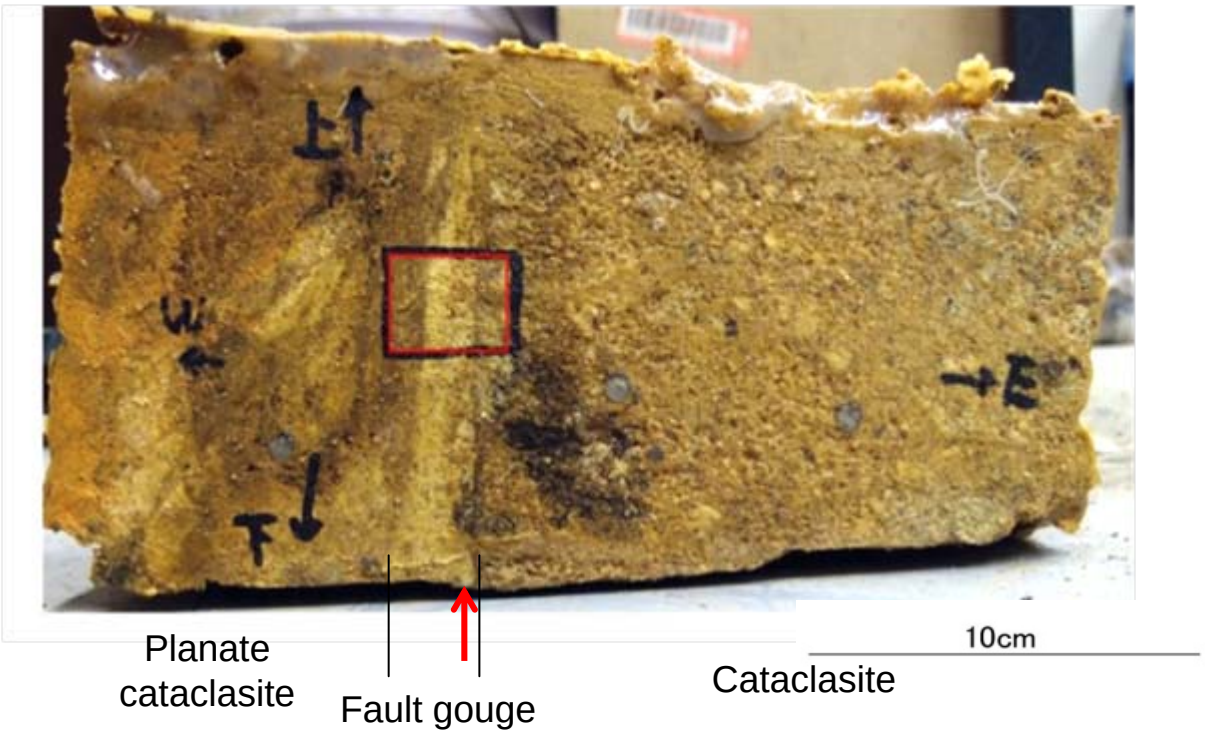

From the hanging side (western side), G fault consists of planate cataclasite, fault gouge, and cataclasite.
The fault gouge linearly shears whole of the outcrop, and its footwall side has the continuous rectilinear shape.

The last slip surface shears whole of the polished section. That surface is located at the softest portion and has the most rectilinear shape.

G fault, D-1 trench, Thin section (Vertical component)

D-1 trench, direction of YZ

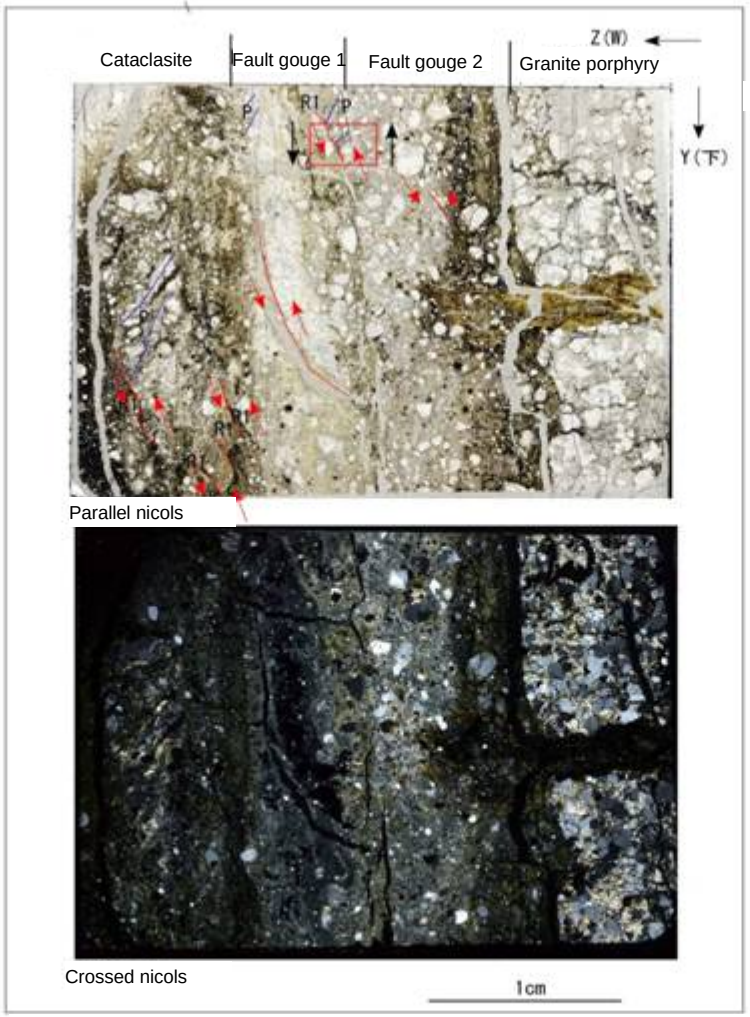

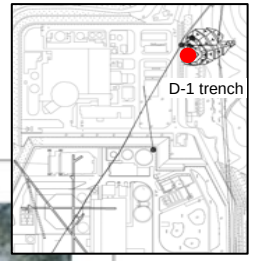

Area within red frame is enlarged

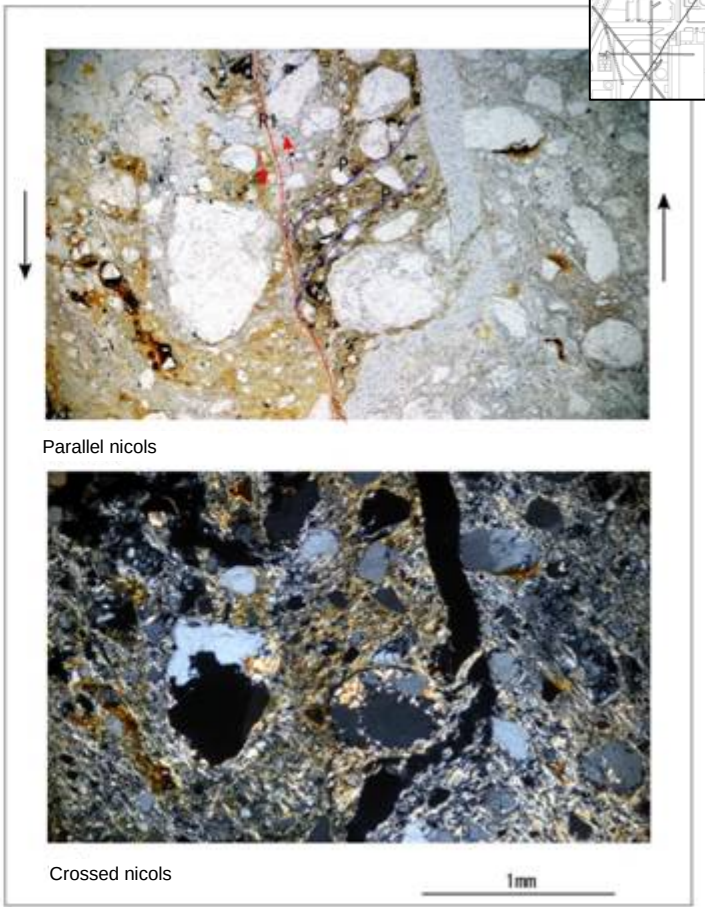

・Cataclasite
Consists of the brown-gray matrix of fine grain, as well as quartz, feldspar, and cataclasite fragments and that are sub-angular or semi-circular gravels with diameters of 0.1mm to 3mm. The matrix contains few clay minerals. The displacement sense of normal fault can be recognized from R1 and P.

・Fault gouge 1 (last slip)
Consists of the brown-gray matrix of fine grain, as well as quartz, feldspar, and cataclasite fragments and that are semi-circular or sub-angular gravels with diameters of 0.1mm to 10mm. The matrix contains lots of clay minerals. The displacement sense of normal fault can be recognized from R1 an P.

・Fault gouge 2
Consists of the brown-gray matrix of fine grain, as well as quartz, feldspar, and cataclasite fragments and that are semi-circular or sub-angular gravels with diameters of 0.1mm to 2mm. The matrix contains lots of clay minerals. The displacement sense of normal fault can be recognized from R1 and P.

・Granite porphyry
Consists of granite porphyry, quartz, and feldspar fragments with diameters of 0.1mm to 2mm.

G fault, D-1 trench, Thin section (Horizontal component)

D-1 trench, direction of XZ

10cm

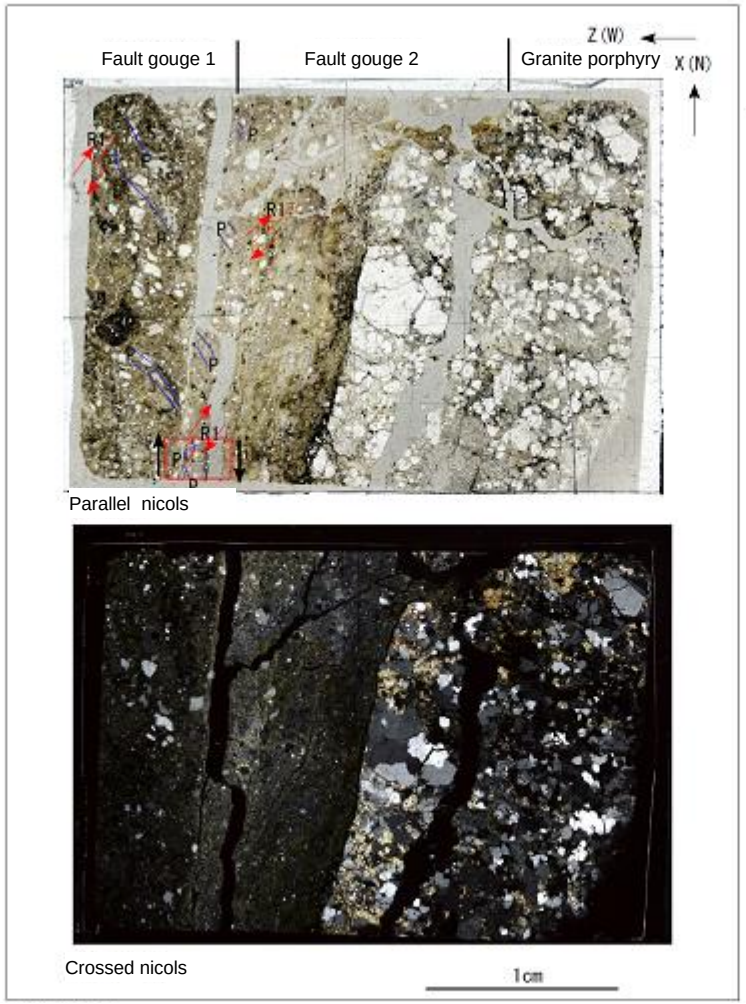

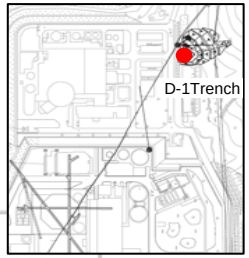

Area within red frame is enlarged

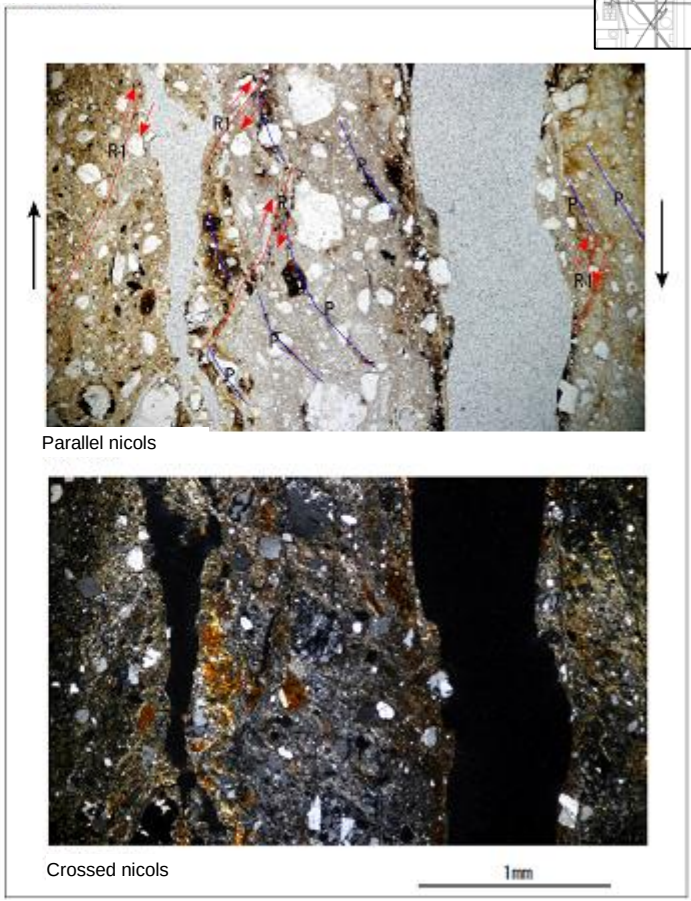

・Fault gouge 1
Consists of the brown-gray matrix of fine grain, as well as quartz, feldspar, and cataclasite fragments and that are sub-angular or semi-circular gravels with diameters of 0.1mm to 3mm. The matrix contains lots of clay minerals. The displacement sense of right-lateral slip can be recognized from R1 an P.

・Fault gouge 2 (last slip)
Consists of the brown-gray matrix of fine grain, as well as quartz, feldspar, and cataclasite fragments and that are semi-circular or sub-angular gravels with diameters of 0.1mm to 2mm. The matrix contains lots of clay minerals. The displacement sense of right-lateral slip can be recognized from R1 and P.

・Granite porphyry
Consists of granite porphyry, quartz, and feldspar fragments with diameters of 0.1mm to 2mm.

【Displacement sense of K fault】

Survey location：D-1 trench L-cut pit

K fault, D-1 trench L-cut pit, Outcrop

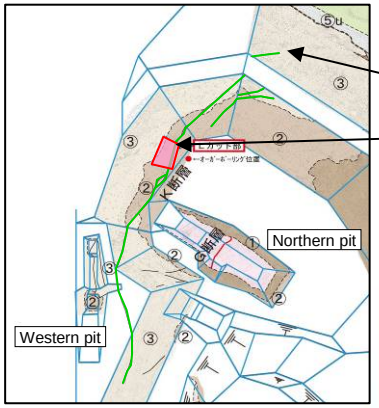

Western wall surface

S←

→N

Layer ③

Layer ②

Decayed granite

Layer ②

Fracture segment

Layer ②

Layer ②

Layer ②

Southern wall surface

Bottom surface

Northern wall surface

The last slip surface shears whole of the outcrop. That surface is located at the softest portion and has the most rectilinear shape.

K fault, D-1 trench L-cut pit, Sample location

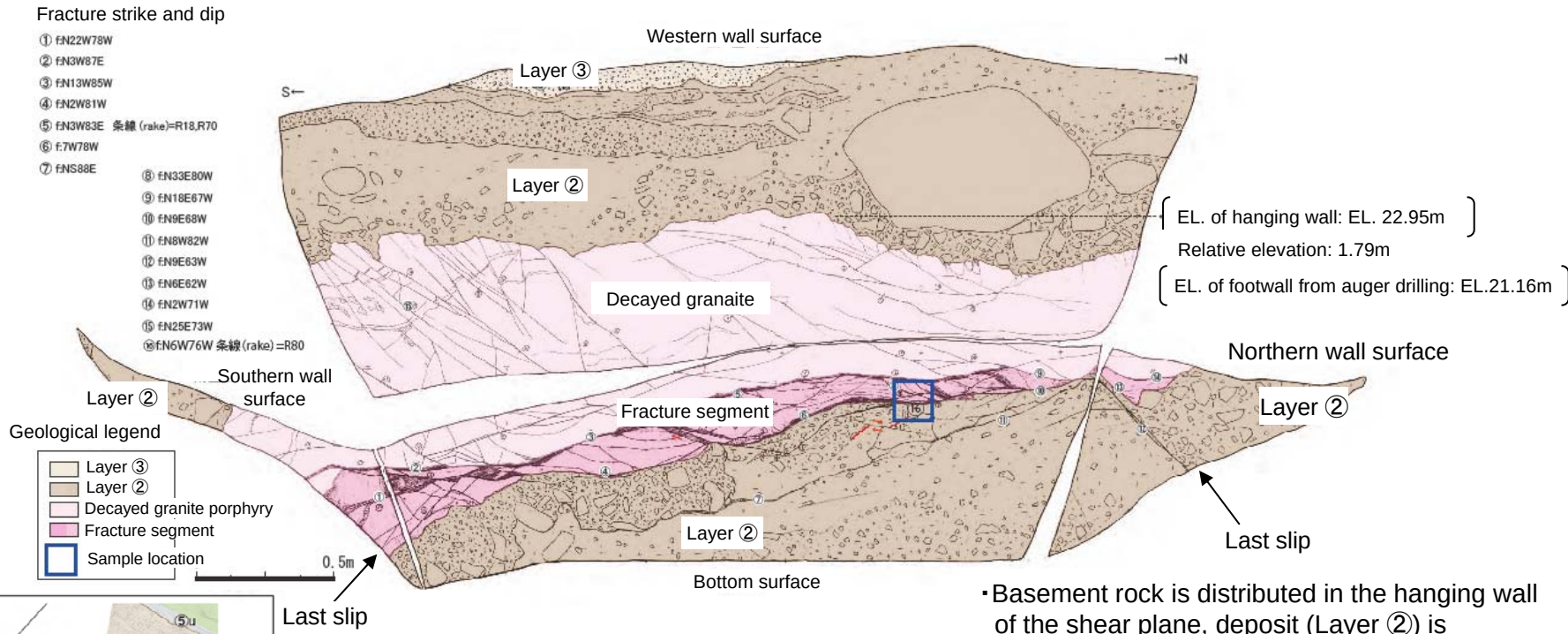

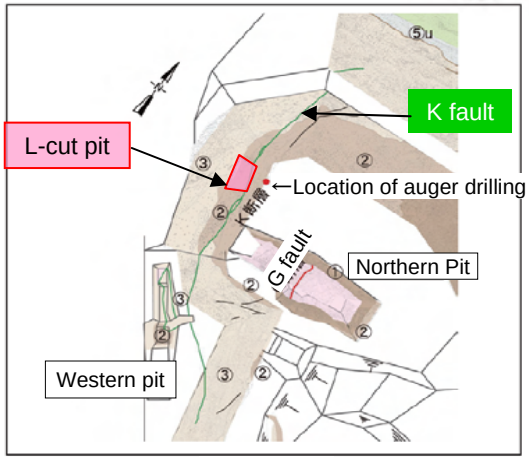

Plain view

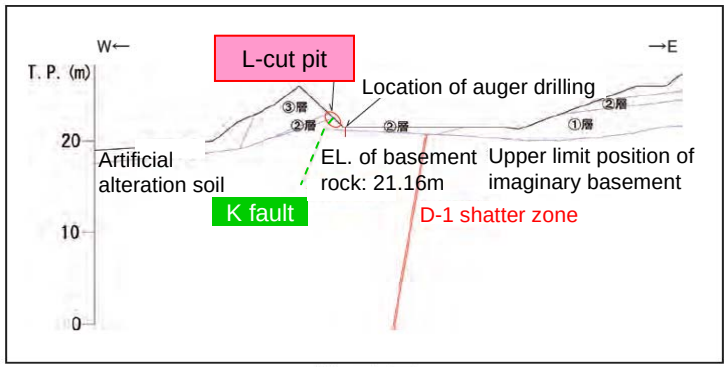

Cross-section view

Fracture segment ⑤ is not a last slip because it has slikenlines with attitude in two directions.

- Basement rock is distributed in the hanging wall of the shear plane, deposit (Layer ②) is distributed in the footwall.
- In the hanging wall above a shear plane, 10-30cm width fracture segment is distributed. In the deposit (Layer ②), fracture and shear structure is developing along the line of a boundary plane with the basement. A linear fault gouge is not recognized. The R1 shear with a few centimeters displacement finely slips the shear planes.
- At the R1 shear in the fracture segment and the deposit (Layer ②), right-lateral slips are observed.
- The relative elevation is 1.79m, that is calculated from the upper limit surface of the hanging wall and auger boring close to the footwall.

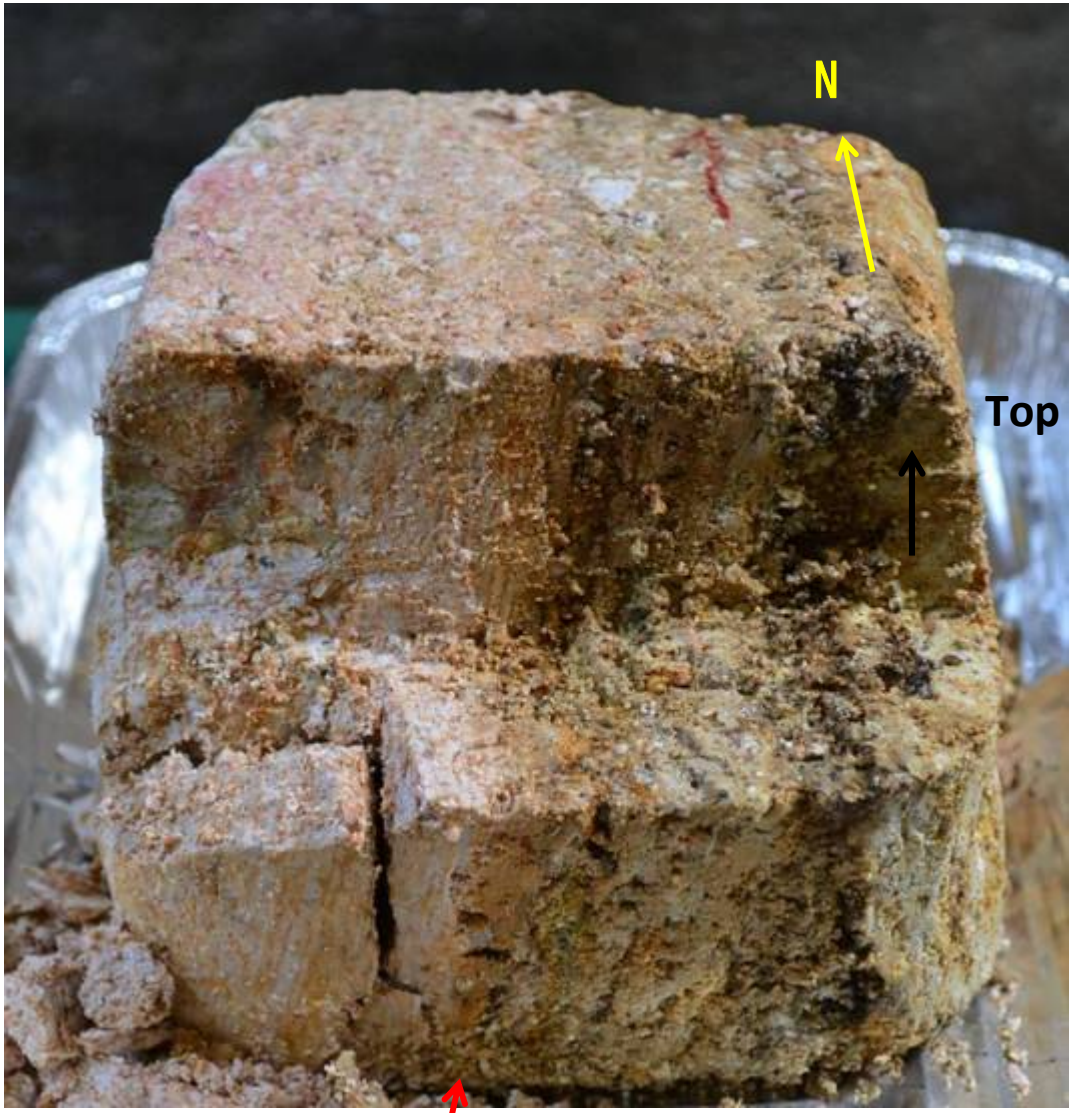
N
Top
50 mm
Last slip N6W76W

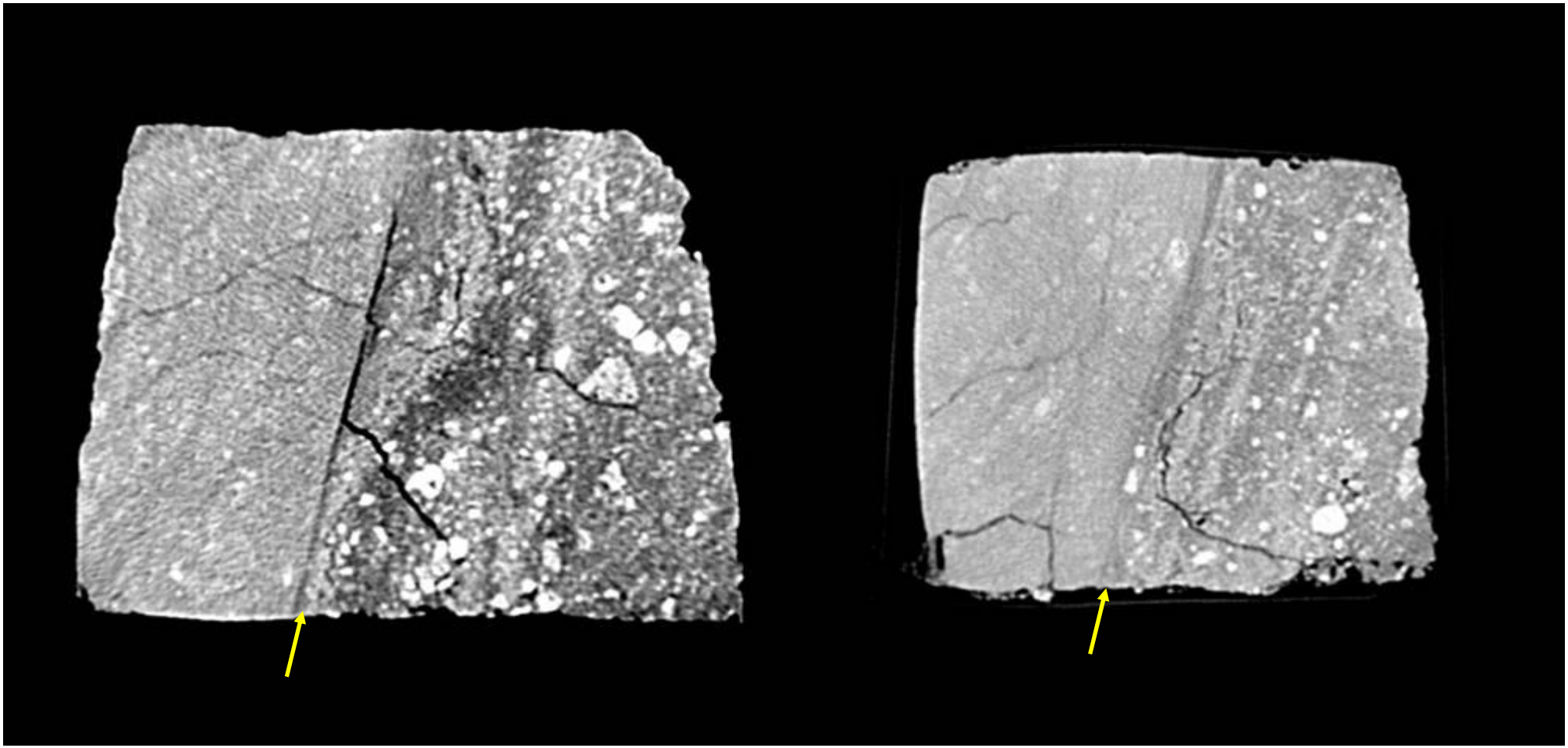

A fault surface with good continuity was observed and that shears other deformation structures.

Fault surface photo from west side

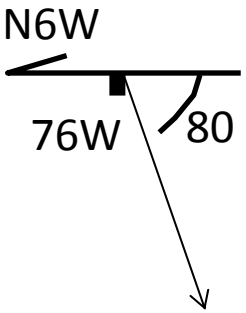

Slikenlines were observed along the main fault surface.

N6W

Fault surface photo from west side

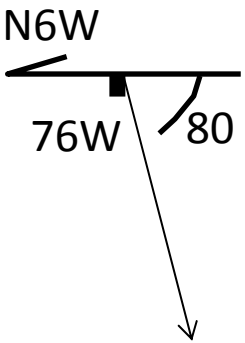

1mm

High-angle slikenlines were observed on the main fault surface.

L-cut trench, K fault, Viewing from west side to east side of the footwall of the last slip

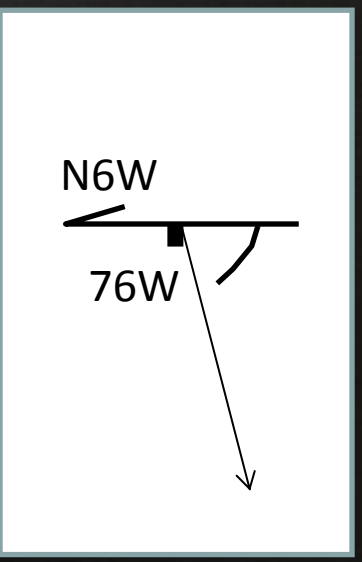

High-angle slikenlines were observed on the main fault surface.

1mm

High-angle slikenlines and uneven surface were observed on the main fault surface.

1mm

K fault, D-1 trench L-cut pit, Thin section (direction of the slickenline)
(without auxiliary line of composite surface structures)

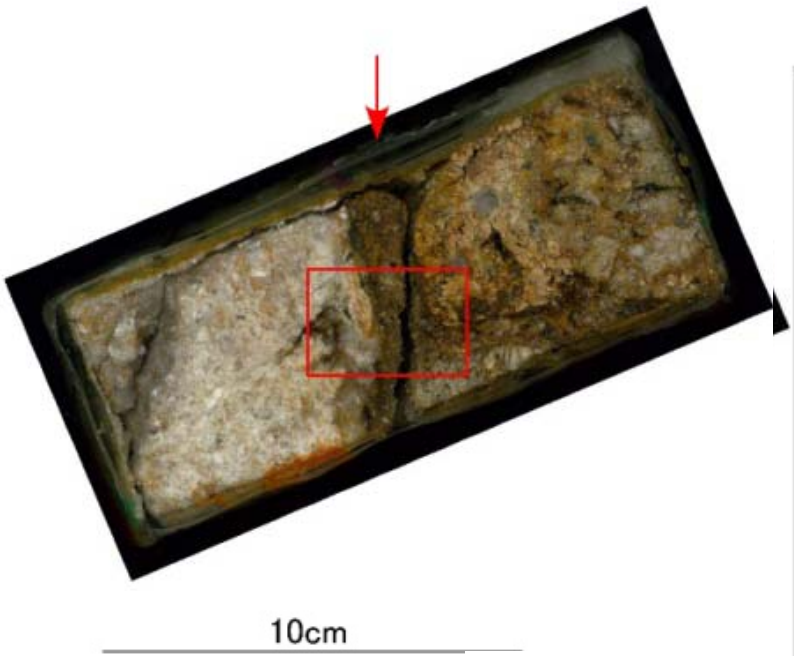

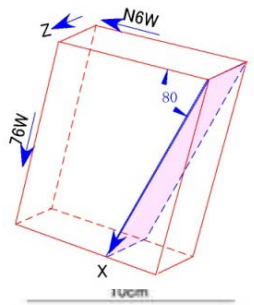

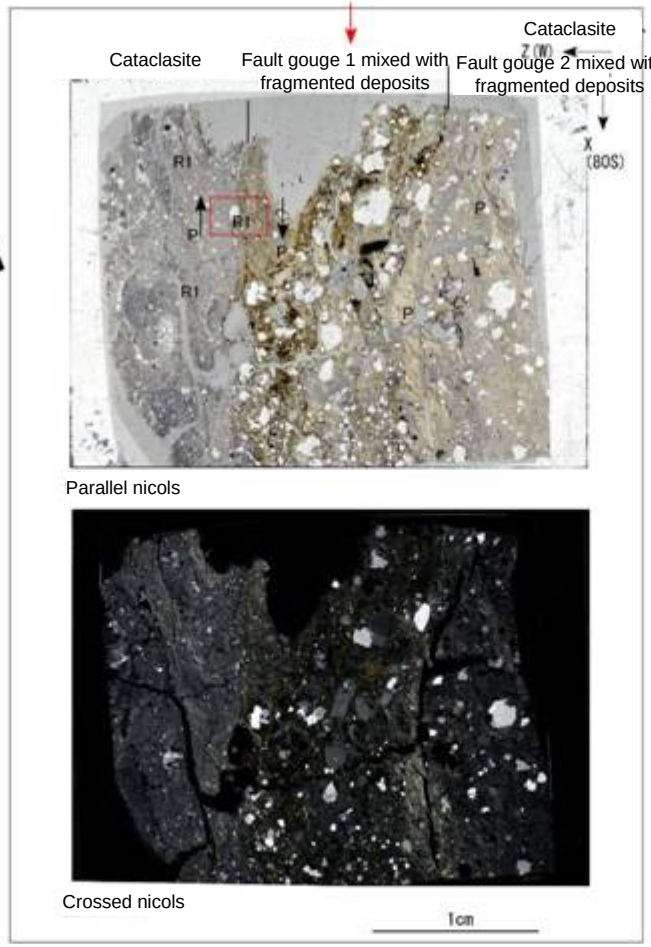

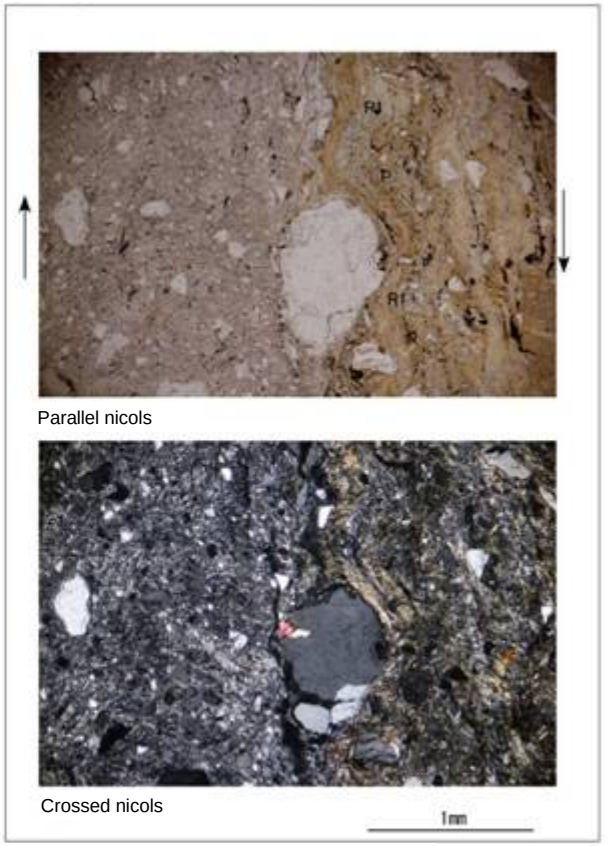

・Cataclasite
Consists of the gray matrix of fine grain, as well as quartz, feldspar, and cataclasite fragments and that are semi-circular or sub-angular gravels with diameters of 0.01 mm to 3mm. Contains some clay minerals. The displacement sense of reverse fault and right-lateral slip can be recognized from R1 and P.

・Fault gouge 1 mixed with fragmented deposits (last slip)
Consists of the brown-gray matrix of fine grain, as well as quartz, plogioclase, potassium feldspar, biotite, and cataclasite fragments and that are angular or sub-angular gravels with diameters of 0.01 mm to 3mm. The Fragments are fresh and sngular originated from deposits. Contains lots of clay minerals. The displacement sense of reverse fault and right-lateral slip can be recognized from R1 and P.

・Fault gouge 2 mixed with fragmented deposits
Consists of the brown-gray matrix of fine grain, as well as quartz, plogioclase, potassium feldspar, biotite, and cataclasite fragments and that are sub-angular gravels with diameters of 0.01 mm to 2mm. The Fragments are fresh and sngular originated from deposits. Contains lots of clay minerals. The displacement sense of reverse fault and right-lateral slip can be recognized from P.

The displacement sense of reverse fault was observed in the thin section along the line of the slickenline.

K fault L-cut pit 80R

K fault, D-1 trench L-cut pit, Thin section (direction of the slickenline) (with auxiliary line of composite surface structures)

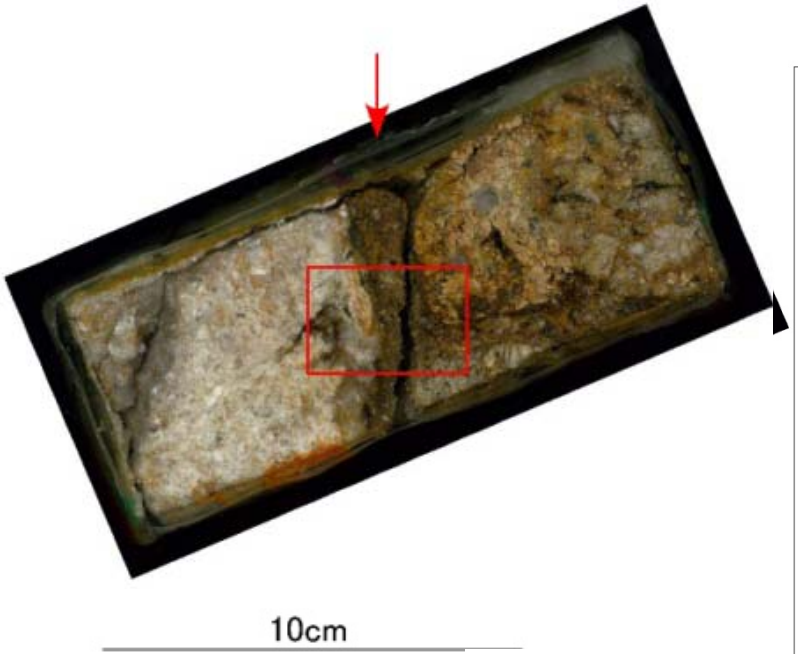

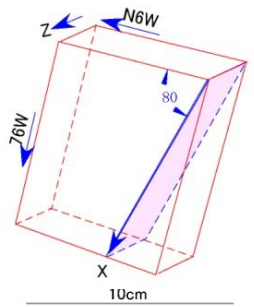

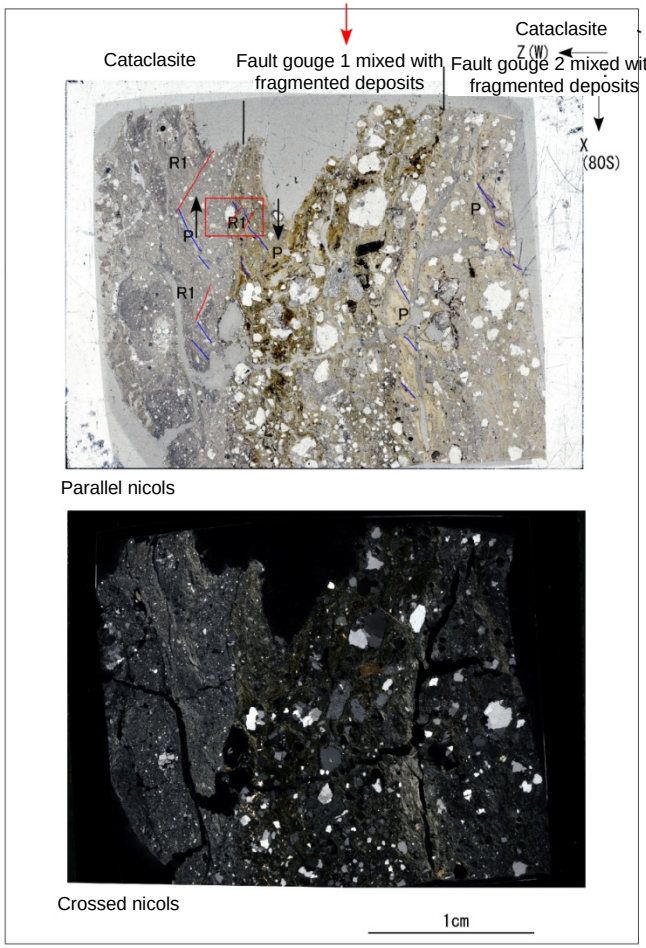

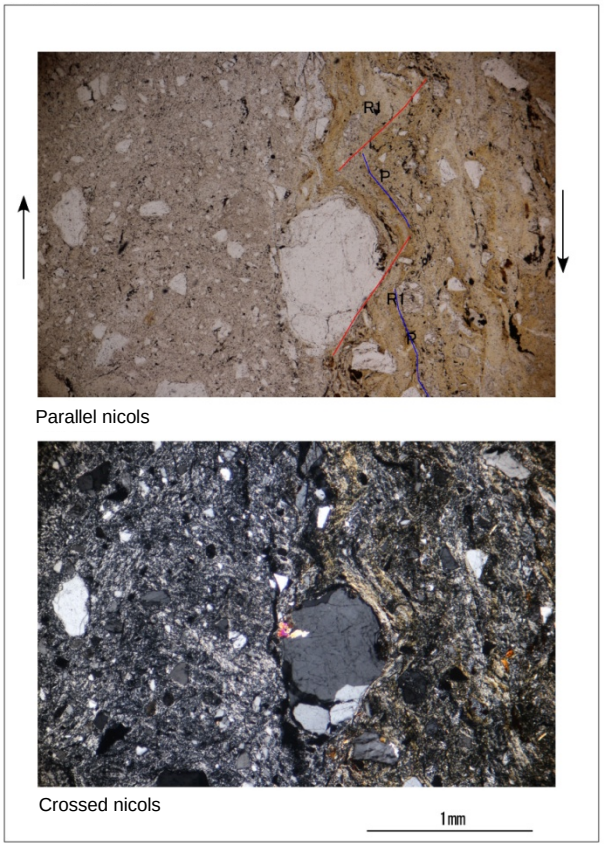

・Cataclasite
Consists of the gray matrix of fine grain, as well as quartz, feldspar, and cataclasite fragments and that are semi-circular or sub-angular gravels with diameters of 0.01 mm to 3mm. Contains some clay minerals. The displacement sense of reverse fault and right-lateral slip can be recognized from R1 and P.

・Fault gouge 1 mixed with fragmented deposits (last slip)
Consists of the brown-gray matrix of fine grain, as well as quartz, plagioclase, potassium feldspar, biotite, and cataclasite fragments and that are angular or sub-angular gravels with diameters of 0.01 mm to 3mm. The Fragments are fresh and angular originated from deposits. Contains lots of clay minerals. The displacement sense of reverse fault and right-lateral slip can be recognized from R1 and P.

・Fault gouge 2 mixed with fragmented deposits
Consists of the brown-gray matrix of fine grain, as well as quartz, plagioclase, potassium feldspar, biotite, and cataclasite fragments and that are sub-angular gravels with diameters of 0.01 mm to 2mm. The Fragments are fresh and angular originated from deposits. Contains lots of clay minerals. The displacement sense of reverse fault and right-lateral slip can be recognized from P.

The displacement sense of reverse fault was observed in the thin section along the line of the slickenline.

K fault L-cut pit 80R

(Draft) EMS's views against JAPC's claim concerning the fault evaluations of Tsuruga PS site, EMS on shatter zones in the site of Tsuruga Power Station		JAPC's opinion	Reference No.
Main texts	Issues		
<EMS's views on the claim 2> The evaluation report states that the K fault is 'the structure which continues to the D-1 shatter zone'. The reasons are as follows; (1) As stated in the 'Claim 1', the specialist of geology pointed out as follows, concerning the thin section observations implemented for the G fault and the D-1 shatter zone; - (Skipped) In this way, EMS considers that the evaluation of displacements are not reliable and provides insufficient evidence for the claim that there is no connection between the K fault and the D-1 shatter zone.	Same as the Claim 1.	Same as our view on the Claim 1 in the EMS.	–
(2) Especially, the point where the strike of the K fault is bent to the NNW – SSE direction* was recognized mainly in the deposits above the bedrock. In general, the strikes and dips of the faults found in deposits are not constant and they could vary from place to place. Therefore, it is not possible to conclude that the K fault does not head for the direction of the D-1 shatter zone just because the fault in the deposit is bent. (3) In addition, faults are not necessarily be extended linearly but turning to the different directions or running parallel after they are once broken, in general. The D-1 shatter zone is considered to have such forms. * In the JAPC's report dated April 24, 2003, the direction is described as "NW-SE direction."	1. It has been identified that the K fault was bent in the deposit and the assumption is not credible. 2. Because faults are generally bent or running parallel after they are once broken even if they are bent, the D-1 shatter zone is considered to continue to the K fault.	**(Outline of today's explanation)** **1. Forms in the K fault bedrock** - In the EMS so far, JAPC has repeatedly said that additional surveys are implemented for extension of the K fault to the bedrock. - Based on the EMS's comment that the D-1 shatter zone is not necessarily be extended linearly, surveys have continuously been implemented along the strike of the D-1 shatter zone, considering increasing of the survey points as much as possible. - The pit survey in the D-1 trench confirmed that the strike of the K fault changes to the NW-SE direction also in the bedrock (prompt report). **2. Extension of the K fault to the south direction** - According to the thin section observation of the B14-2 drilling between the unit 2 reactor building and the D-1 trench, there was no shatter zone with reverse fault sense which the K fault has at all. Therefore, the K fault is not extended further south than the B14-2 drilling. **(Point to be clarified by EMS)** - EMS's evidence that 'the D-1 shatter zone is considered to have such forms'.	46-60

Survey on continuity of K fault　Map of survey locations

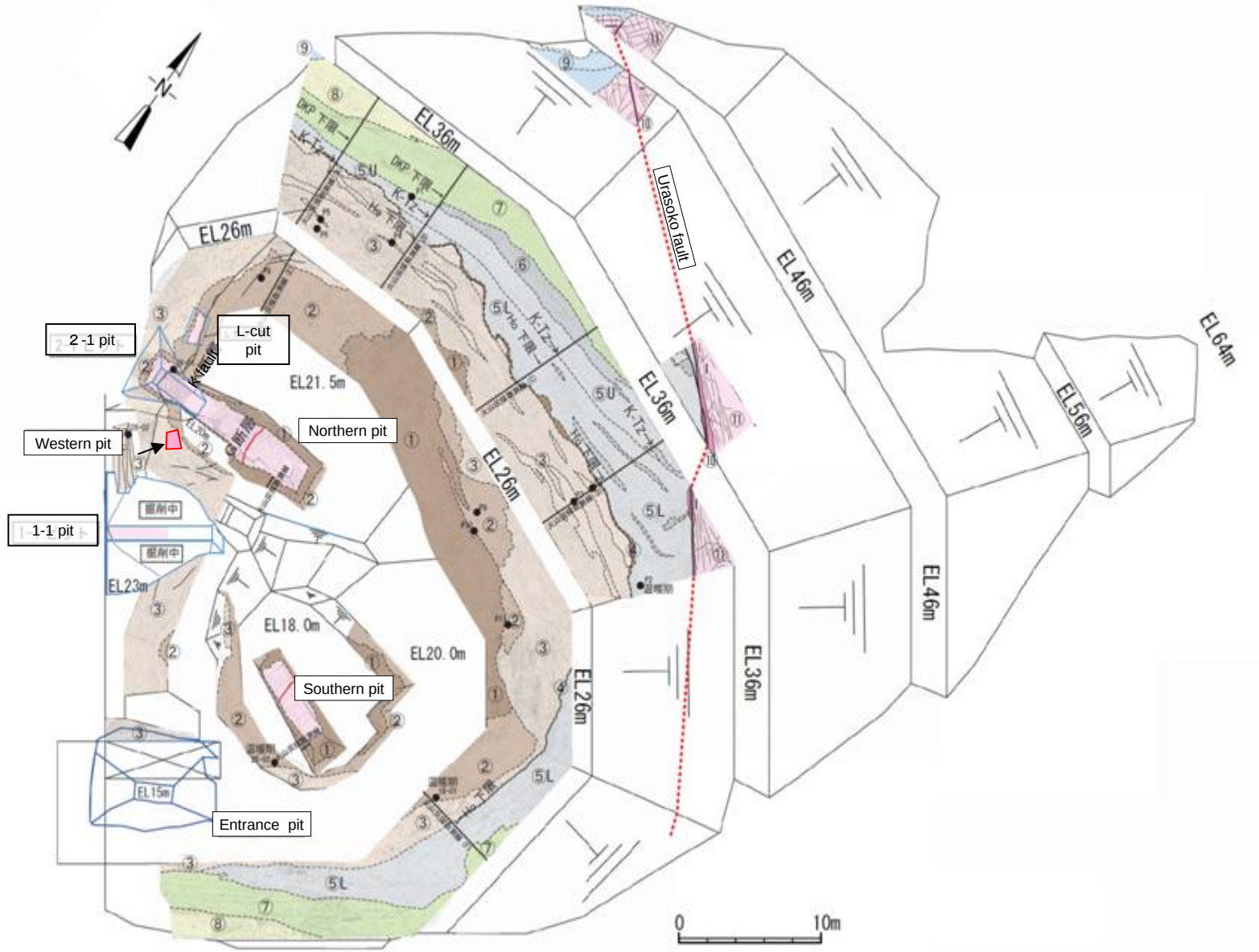

・At D-1 trench, 2-1 and 1-1 pit surveys have been carried out in order to clarify the characteristics, strike, and dip within the basement of the K fault.

Survey on continuity of K fault　2-1 pit

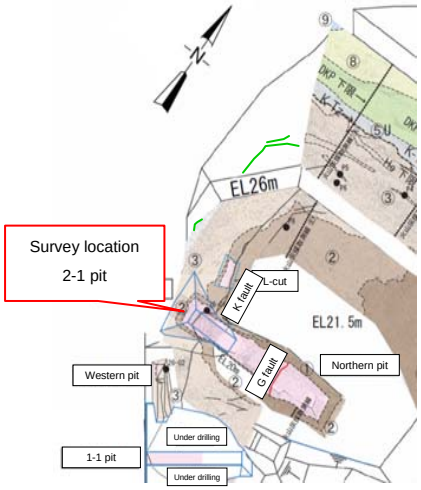

← S　　N →

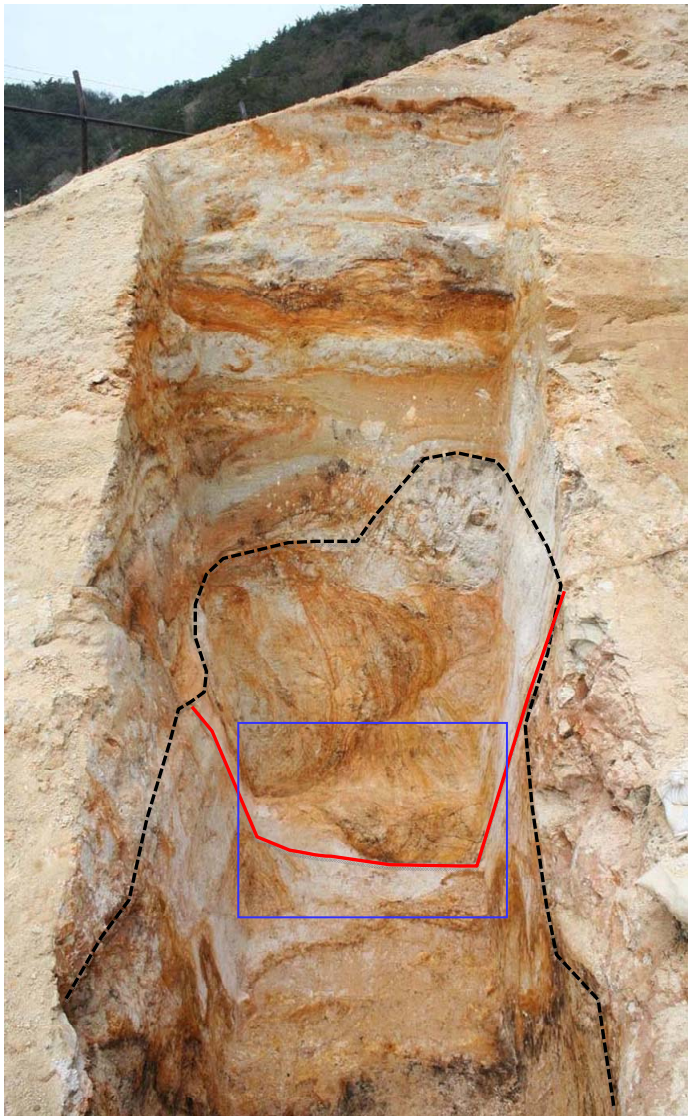

← S　　N →

K fault →

← K fault

・ It is confirmed that the K fault strike is a direction of N-S within the basement based on the result of 2-1pit boring in the side of L-cut pit of D-1 trench.

Survey on continuity of the K fault　Northern widening of western pit

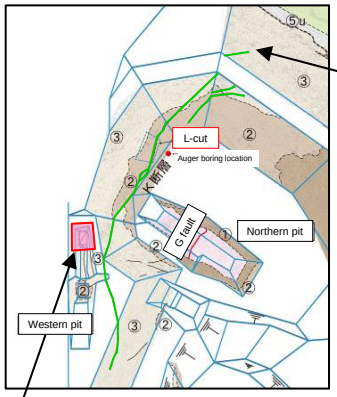

K fault

Northern widening of western pit

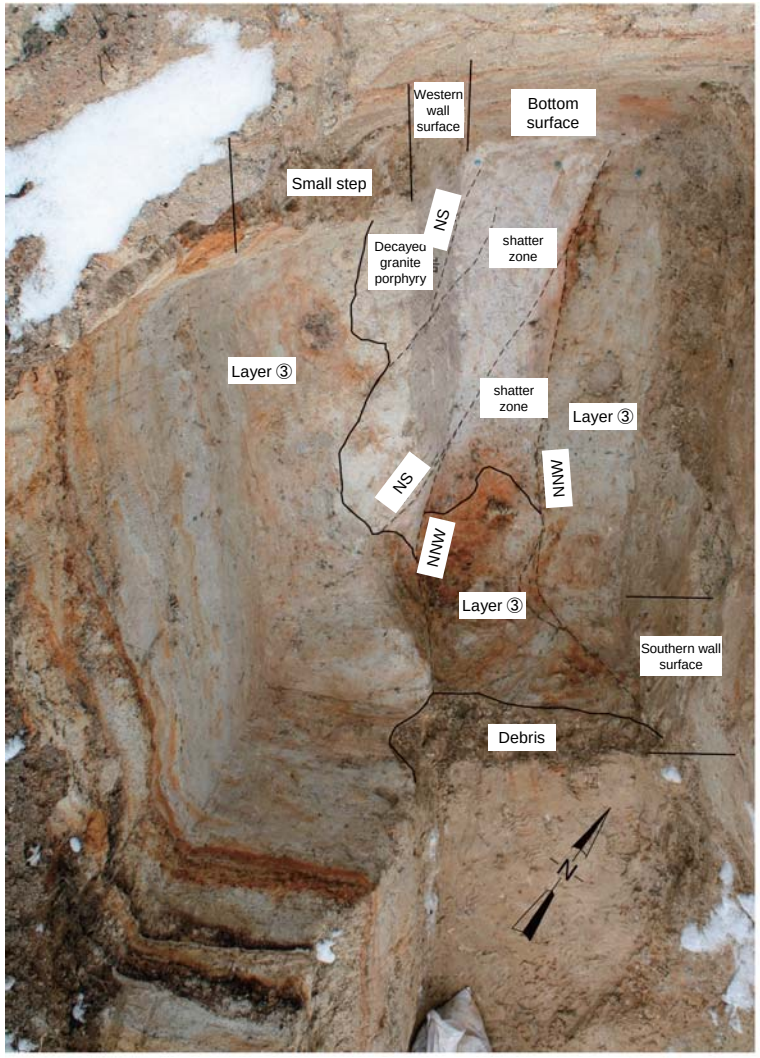

Northern widening of northern pit

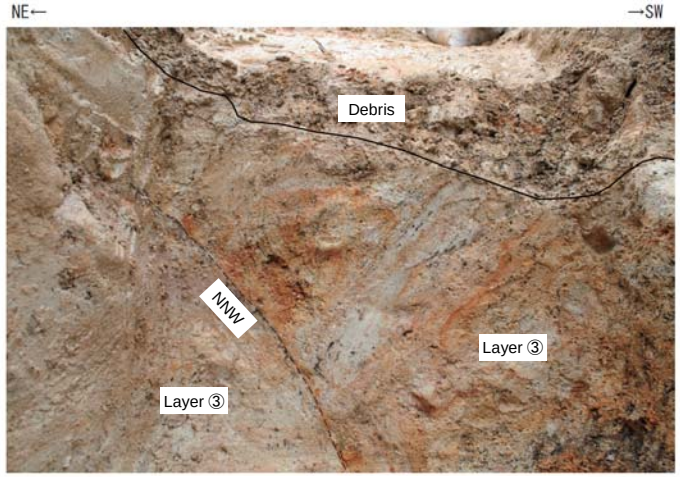

Southern wall surface

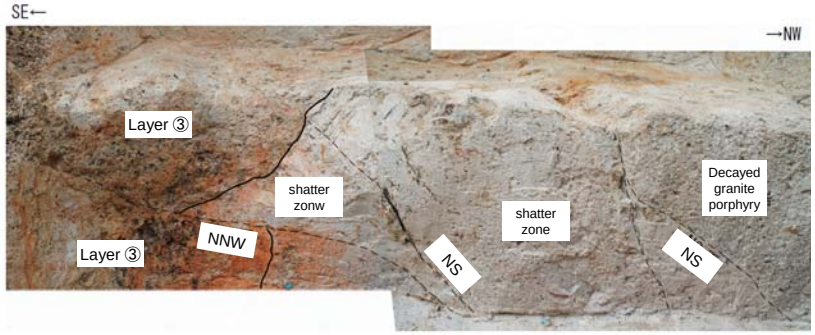

Western wall surface (lower part)

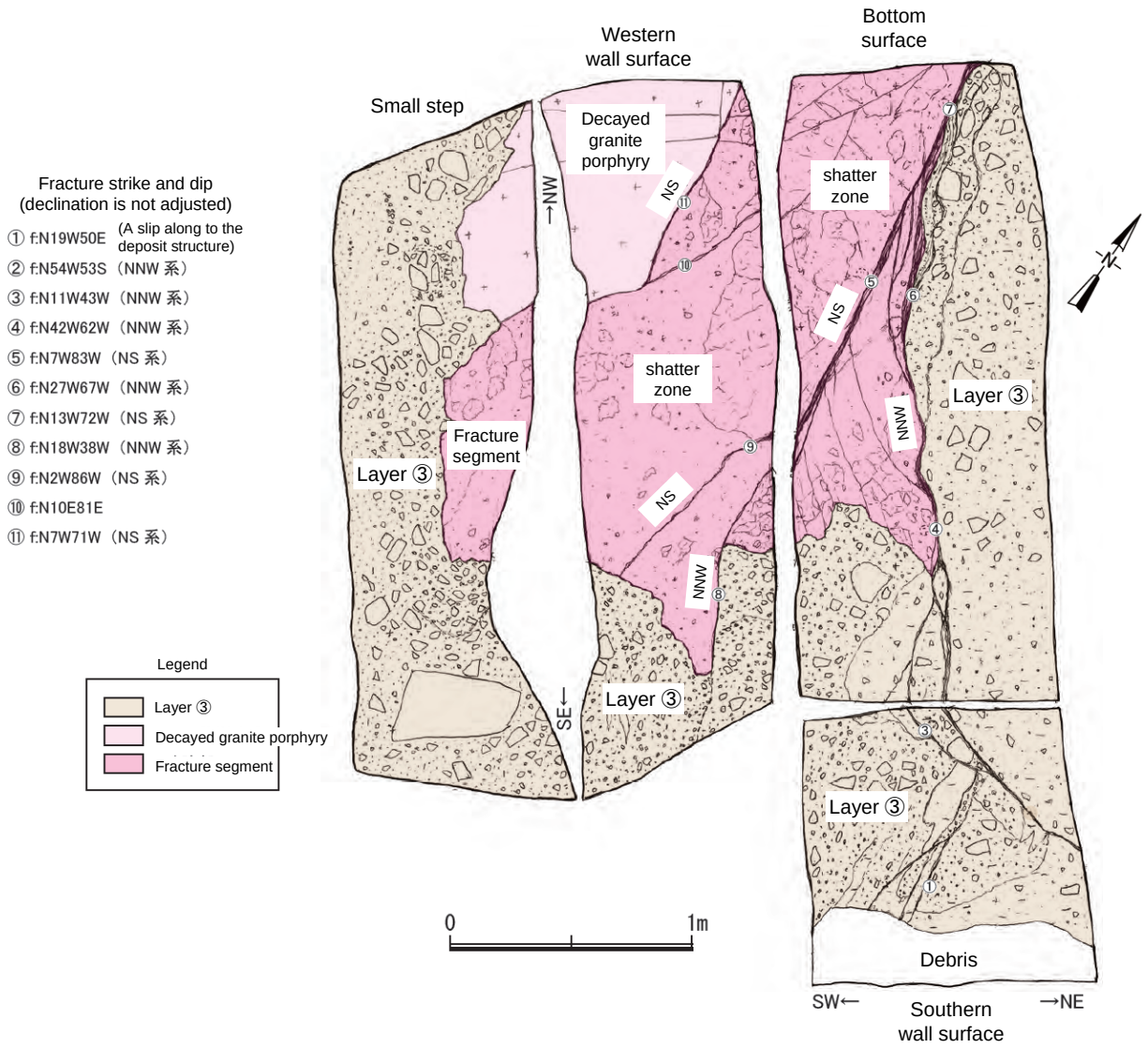

- The shatter zones running to the directions of N-S and NNW-SSW are recognized in the basement rock at the northern widening of western pit.
- The K fault, which displaces and deform layer ③, has changes its strike directions from N-S to NNW-SSW in the western pit.
- The fracture segment with N-S direction strike does not displace and deform layer ③ in the south part from the bend.

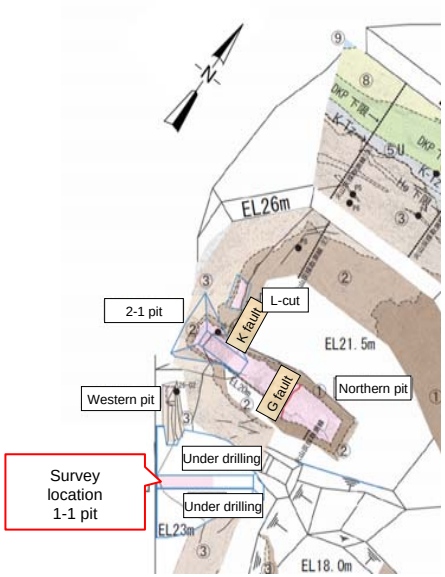

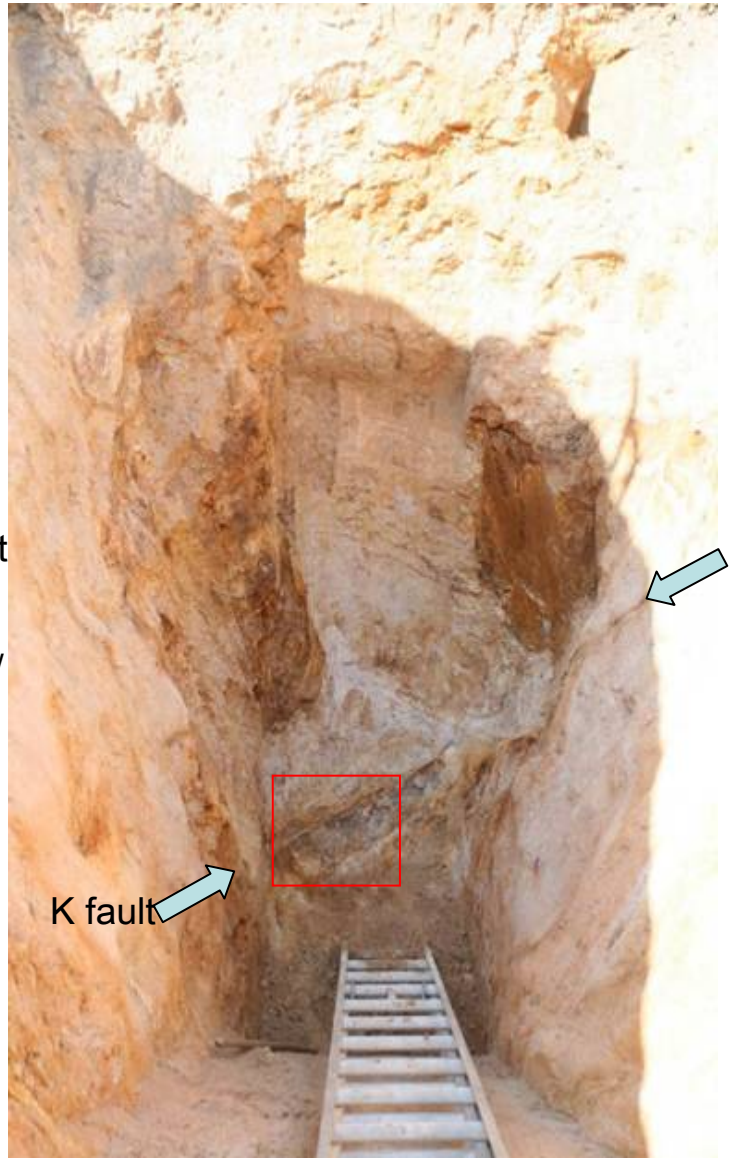

・ In the result of 1-1pit boring in the south of western pit of D-1 trench, K fault indicate NW-SE strike in the basement. It is confirmed that the K fault does not extend to the direction of Unit 2 reactor building.

Pit survey plan regarding continuity of the K fault and activity of the G fault

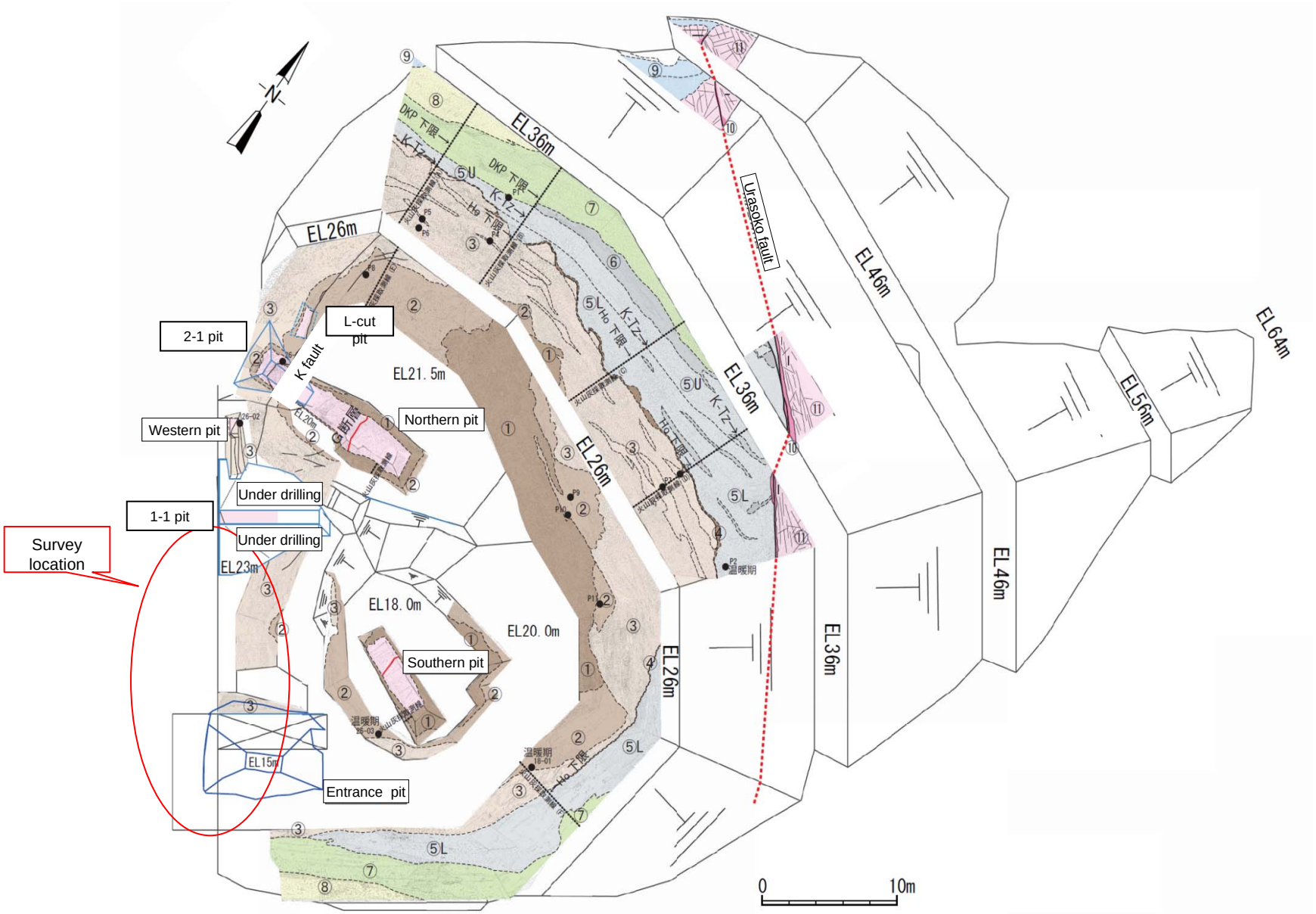

For further clarification of continuity of the K fault, activity of the G fault and so on, additional pit surveys are undergoing now.

Discussion about the K-fault's extension to the southward

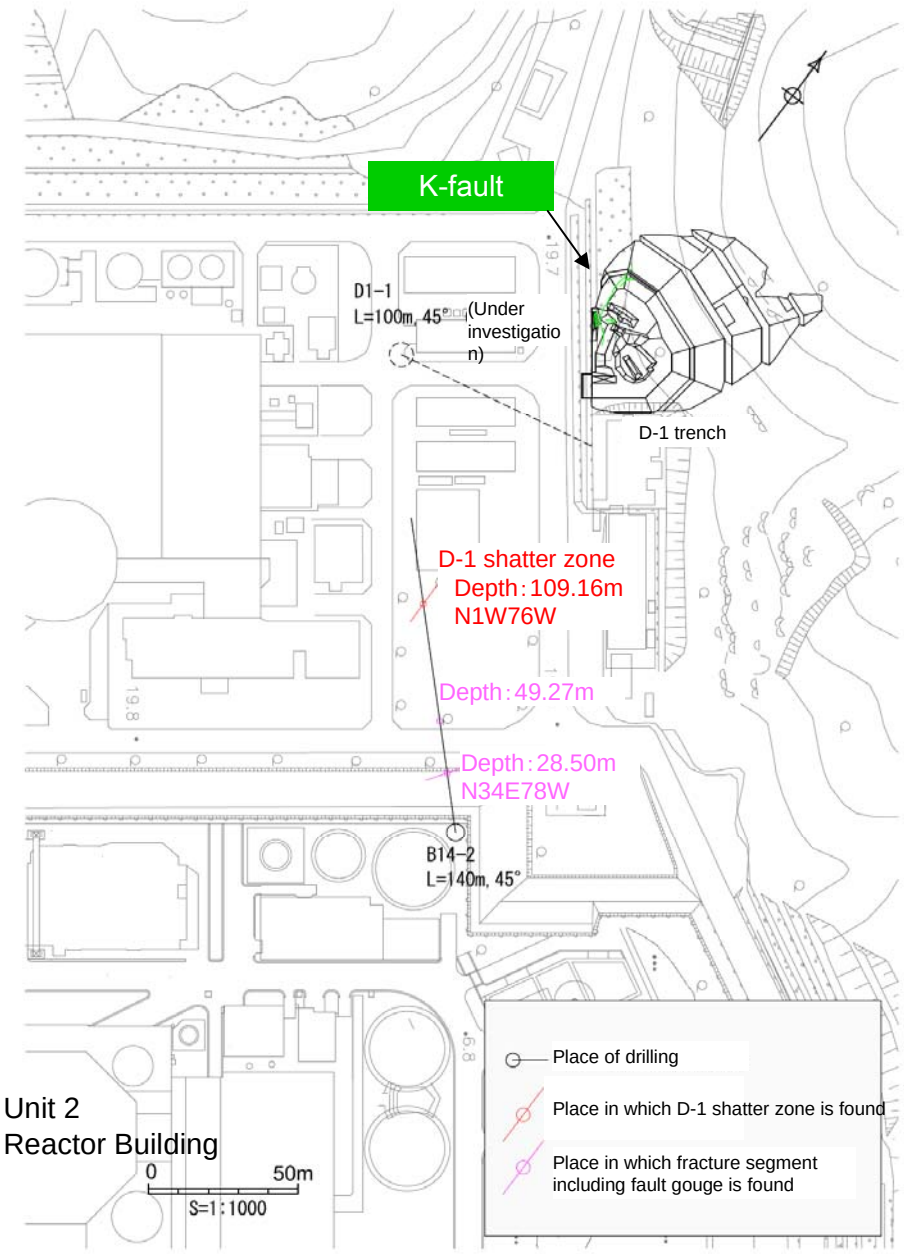

- Three fracture segments with fault gouge have been found at B14-2 drilling, that cross the line between Unit 2 reactor building and K-fault.
- Displacement sense of the last slip has normal fault sense at each fracture segments.

▼

- K-fault, that has reverse fault sense, does not extend to the southward from at least B14-2 drilling place.

※To obtain the additional data, drilling at D1-1 is undergoing.

Displacement sense of fracture segment with fault gouge at B14-2

Place	Name of shatter zone	Depth (m)	Strike and dip	Striation direction	Displacement sense (Observation on striation direction of thin section)
B14-2	—	28.50	N34E78W	50S	Normal fault, left-lateral slip
	—	49.27	N44E80SE ※1	75S ※1	Normal fault ※1
	D-1	109.16	N1W76W	–	Normal fault, right-lateral slip ※2

※1: Fault surface is assumed to be high-angle dip like K-fault, because it was impossible to measure strike and dip by bore-hole TV

※2: Thin section samples are made in the lateral and horizontal direction.

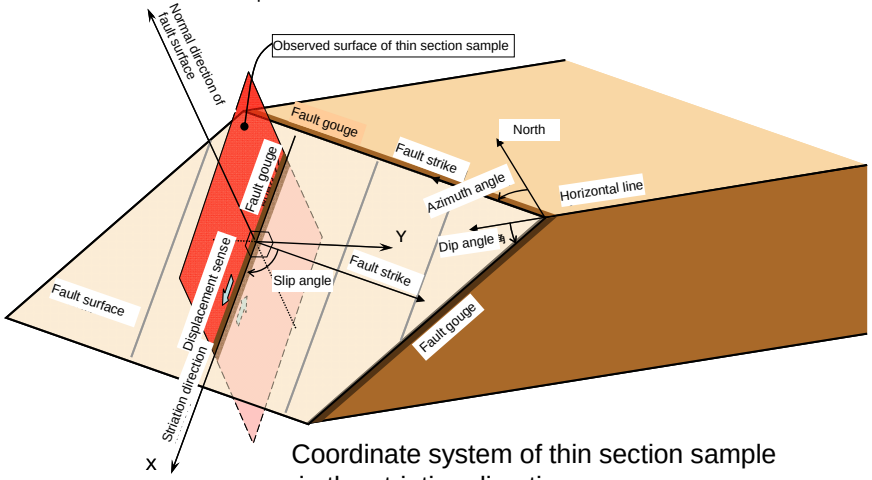

Coordinate system of thin section sample in the striation direction

〔Displacement sense of shatter zone〕 Observation of polished section of B14-2 depth 28.50m (middle-angle southerly dips components)

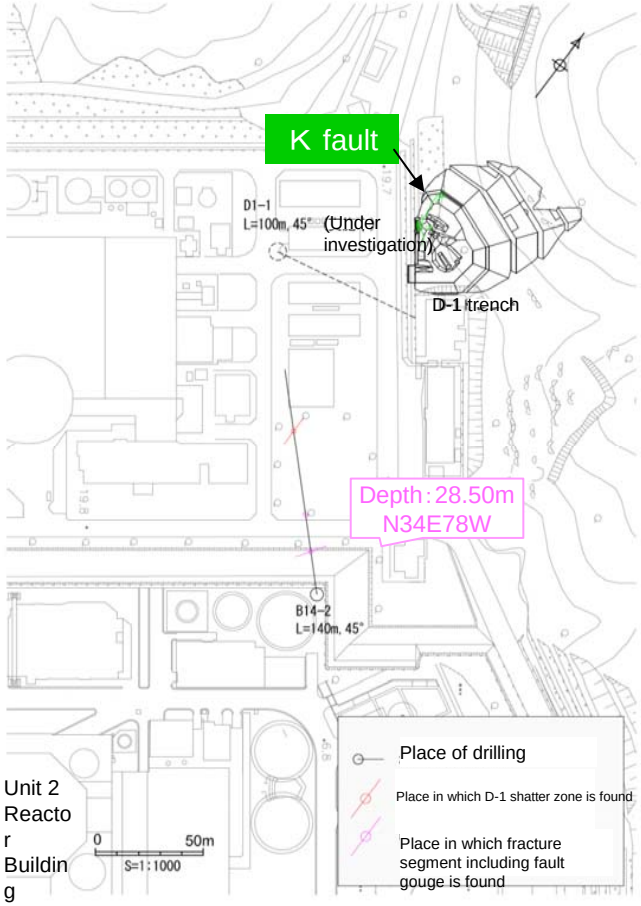

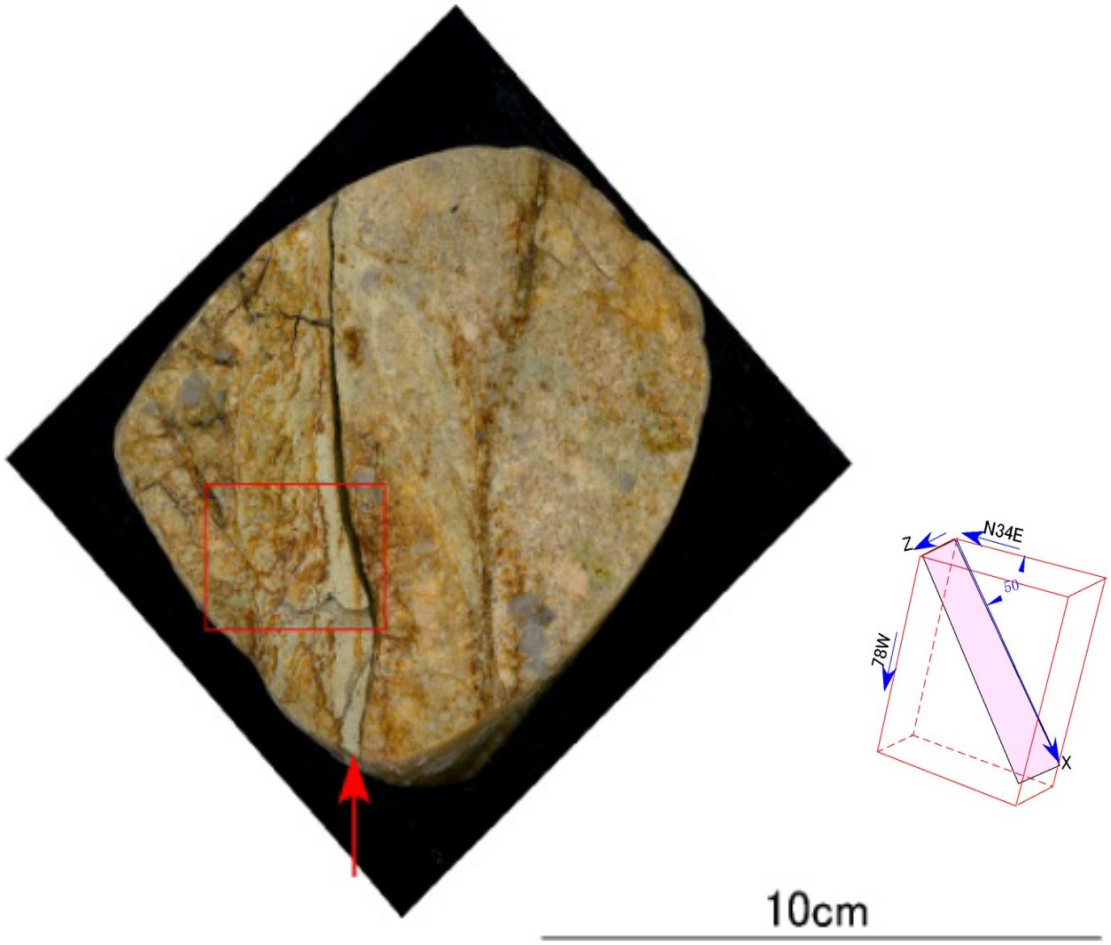

Narrow rectilinear fault gouge has been found in the granite porphyry.

[Displacement sense of shatter zone]
Observation of thin section of B14-2 depth 28.50m (middle-angle southerly dips components)

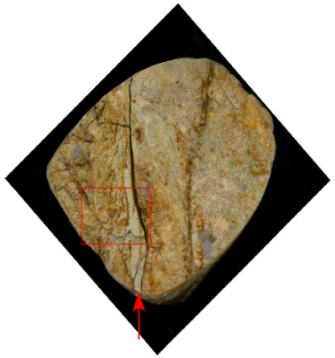

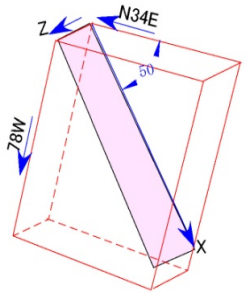

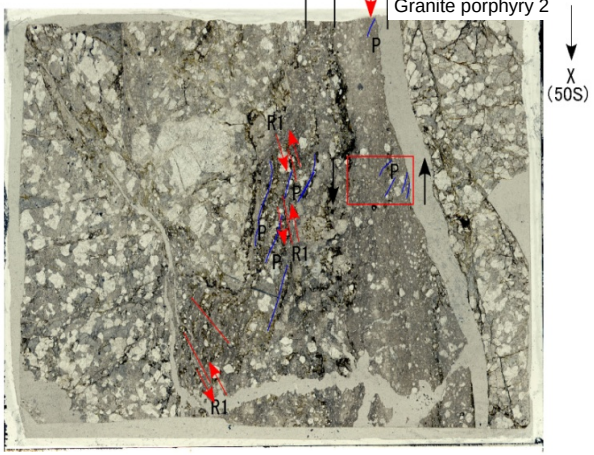

Parallel nicols

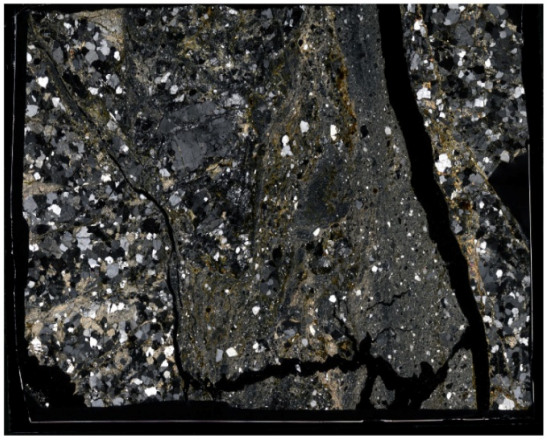

Crossed nicols

1cm

Area within red frame is enlarged

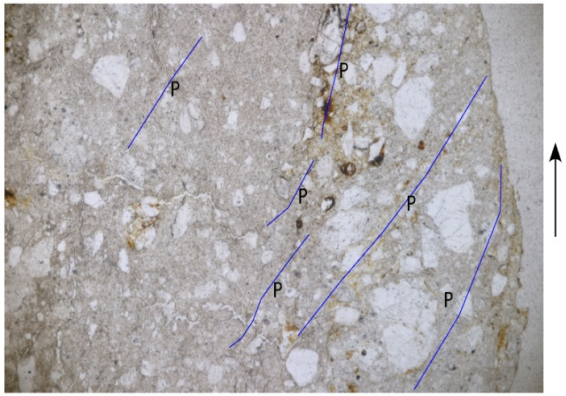

Parallel nicols

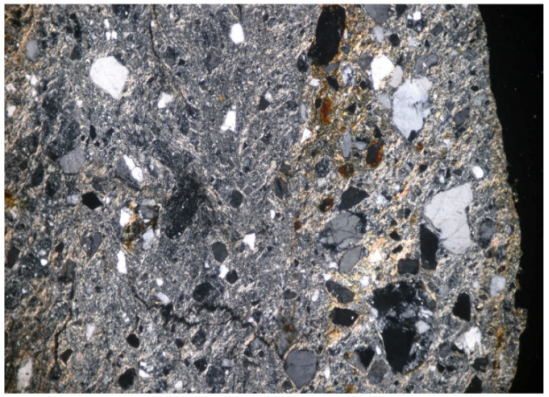

Crossed nicols

1mm

10cm

・Granite porphyry 1
Consist of quarts, potassium feldspar, plagioclase and muscorite with alternation.

・Fault gouge 1
Consists of the brown-gray matrix of fine grain, as well as quartz, feldspar and cataclasite fragments and that are semi-circular or sub-angular gravels with diameters of 0.02 to 3 mm. The matrix contains lots of clay minerals. The displacement sense of westerly dip (normal fault) and left-lateral slip can be recognized from R1 and P.

・Fault gouge 2 (last slip)
Consists of the brown-gray matrix of fine grain, as well as quartz, feldspar, granite porphyry and cataclasite fragments and that are semi-circular or sub-angular gravels with diameters of 0.01 to 1 mm. The matrix contains lots of clay minerals. The displacement sense of westerly dip (normal fault) and left- lateral slip can be recognized from P.

・Granite porphyry 2
Consist of quarts, potassium feldspar, plagioclase and muscorite with alternation.

B14-2_28.50m_8-1_XZ direction

〔Displacement sense of shatter zone〕Observation of polished section of B14-2 depth 49.27m (high-angle southerly dips components)

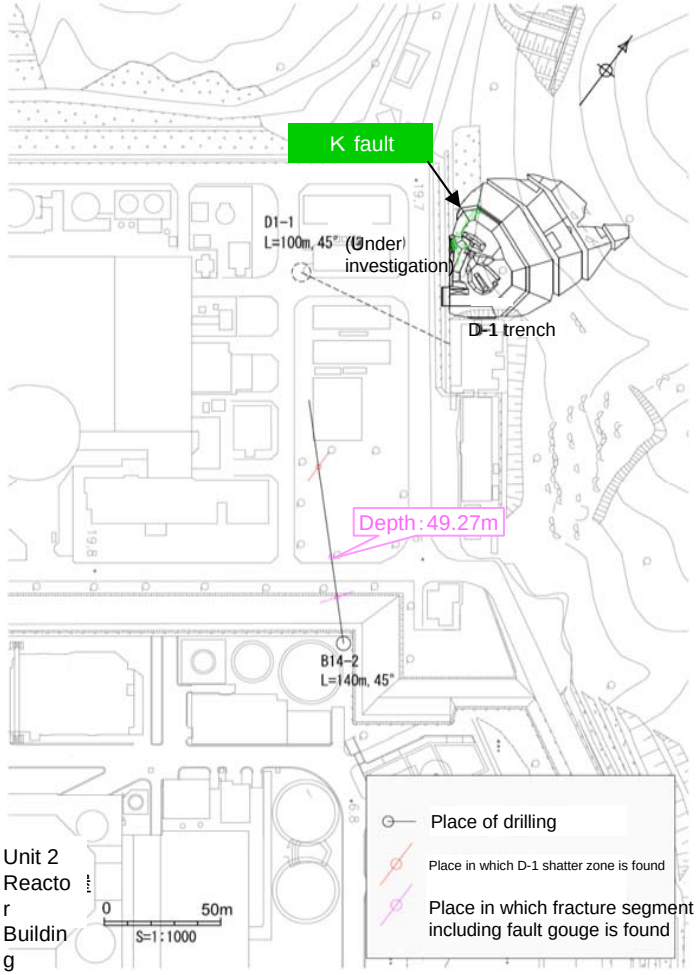

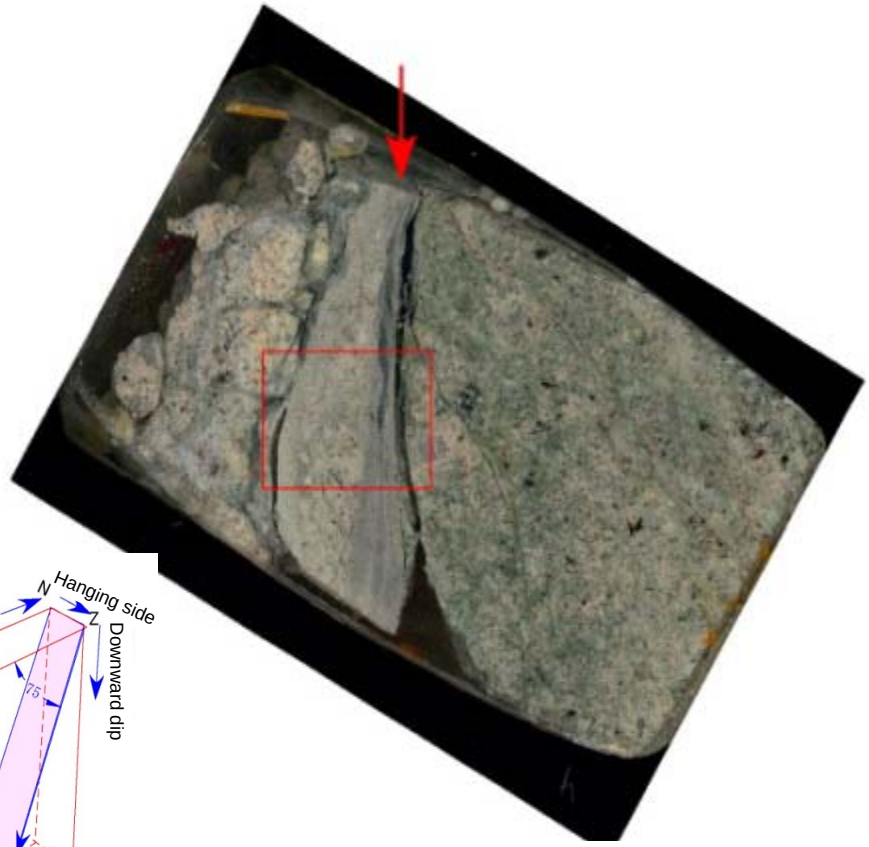

※）Fault surface is assumed to be high-angle dip like K-fault, because it was impossible to measure strike and dip by bore-hole TV

- A few millimeter-breadth of fault gouge has been found in the granite porphyry.
- The fault gouges are segmentalized into two. Foliation is developed in the vicinity of last slip surface.

〔Displacement sense of shatter zone〕Observation of thin section of B14-2 depth 49.27m (high-angle southerly dips components)

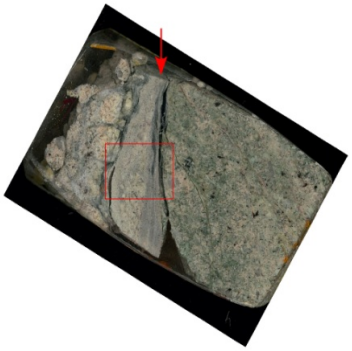

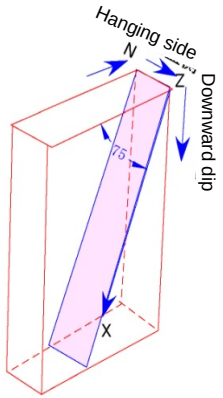

※)Fault surface is assumed to be high-angle dip like K-fault, because it was impossible to measure strike and dip by bore-hole TV

10cm

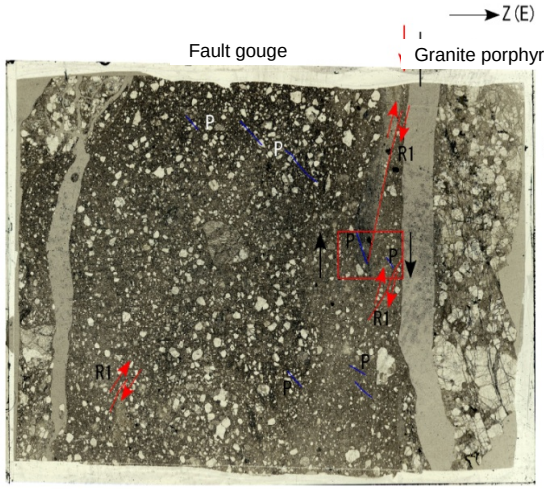

Parallel nicols

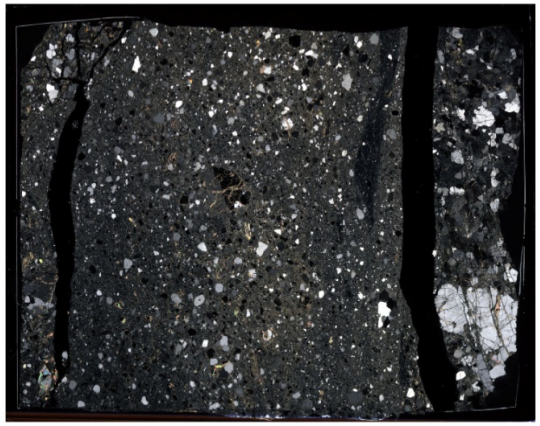

直Crossed nicols

1cm

Area within red frame is enlarged

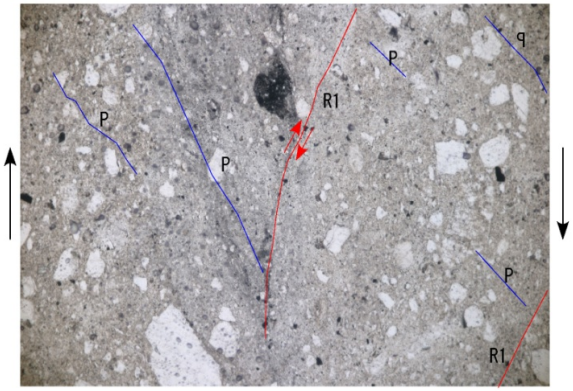

Parallel nicols

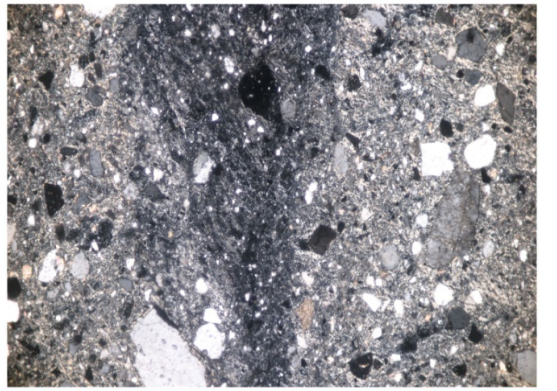

Crossed nicols

1mm

・Fault gouge (last slip)
Consists of the brown matrix of fine grain, as well as quartz, feldspar, cataclasite and granite porphyry fragments and that are semi-circular or sub-angular gravels
with diameters of 0.02 mm to 5mm. The matrix contains lots of clay minerals and calcite. ~~The displacement sense of easterly dip (normal fault) and right-lateral~~
slip can be recognized from R1 and P.
・Granite porphyry
Consist of quarts, potassium feldspar, plagioclase and biotite

B14-2_49.27m_10-1_XZ direction

[Displacement sense of shatter zone]
Observation of polished section of B14-2 depth 109.16m (vertical components)

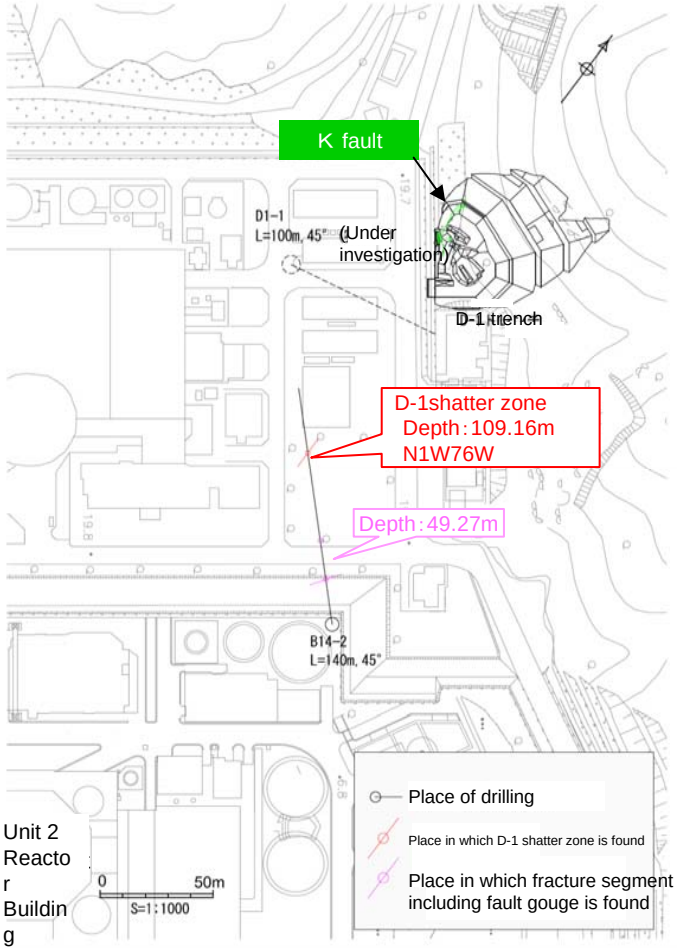

A few millimeter-breadth of fault gouge has been found in the Cataclasite.

[Displacement sense of shatter zone]
Observation of thin section of B14-2 depth 109.16m (vertical components)

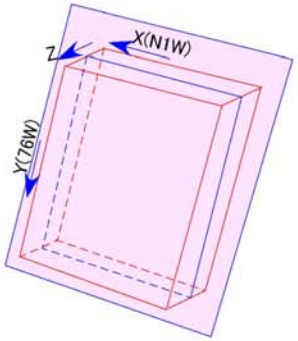

10cm

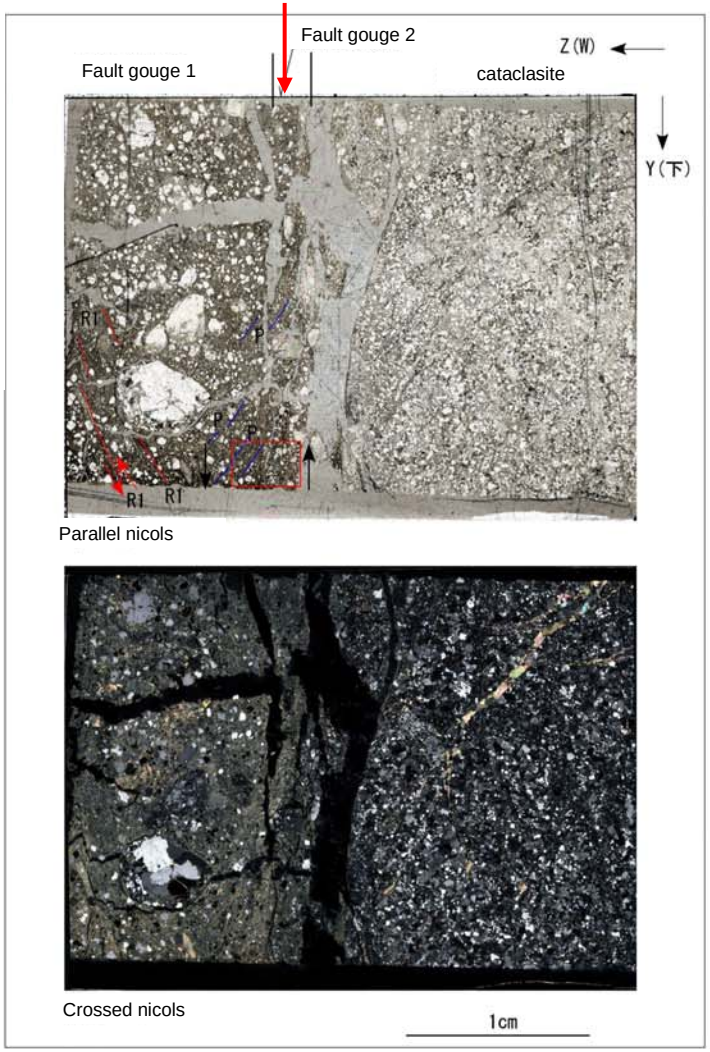

Area within red frame is enlarged

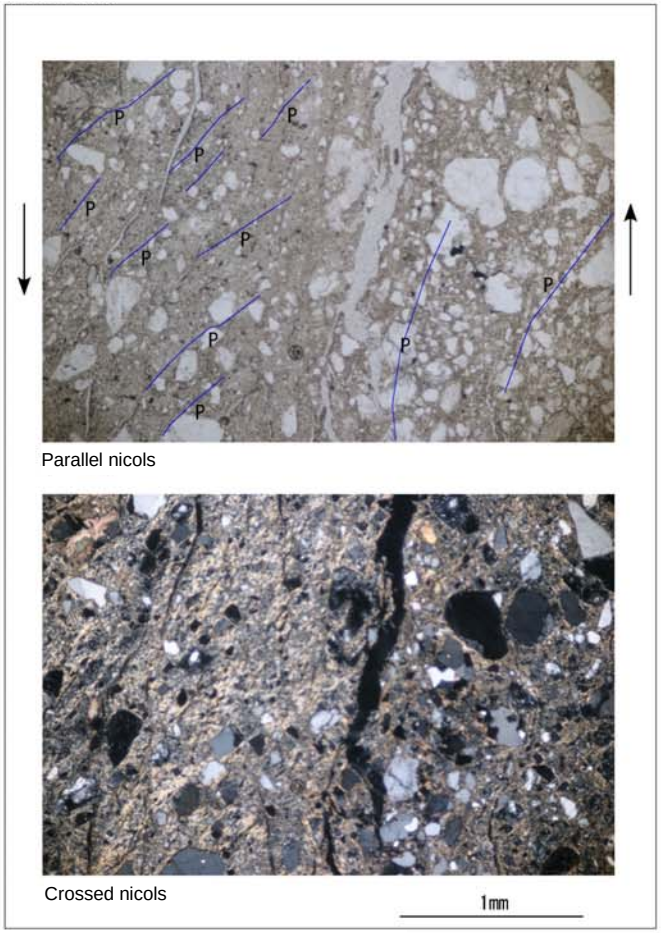

・Fault gouge 1
Consists of the brown matrix of fine grain, as well as quartz, feldspar, granite porphyry and cataclasite fragments and that are semi-circular or
sub- angular gravels with diameters of 0.02 mm to 5mm. The matrix contains lots of clay minerals and calcite. The displacement sense of normal
fault can be recognized from R1 and P.

・Fault gouge 2
Consists of the brown matrix of fine grain, as well as quartz, feldspar, cataclasite fragments and that are semi-circular or sub-angular gravels with
diameters of 0.02 mm to 1mm. The matrix contains lots of clay minerals. The displacement sense of normal fault can be recognized from P.

D-1 B14-2 109.16m_2_YZ direction

[Displacement sense of shatter zone]
Observation of thin section of B14-2 depth 109.16m (horizontal components)

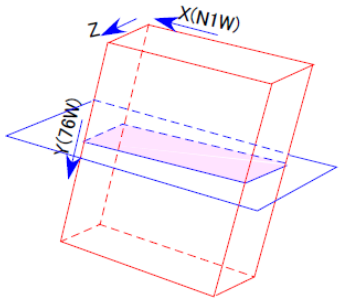

10cm

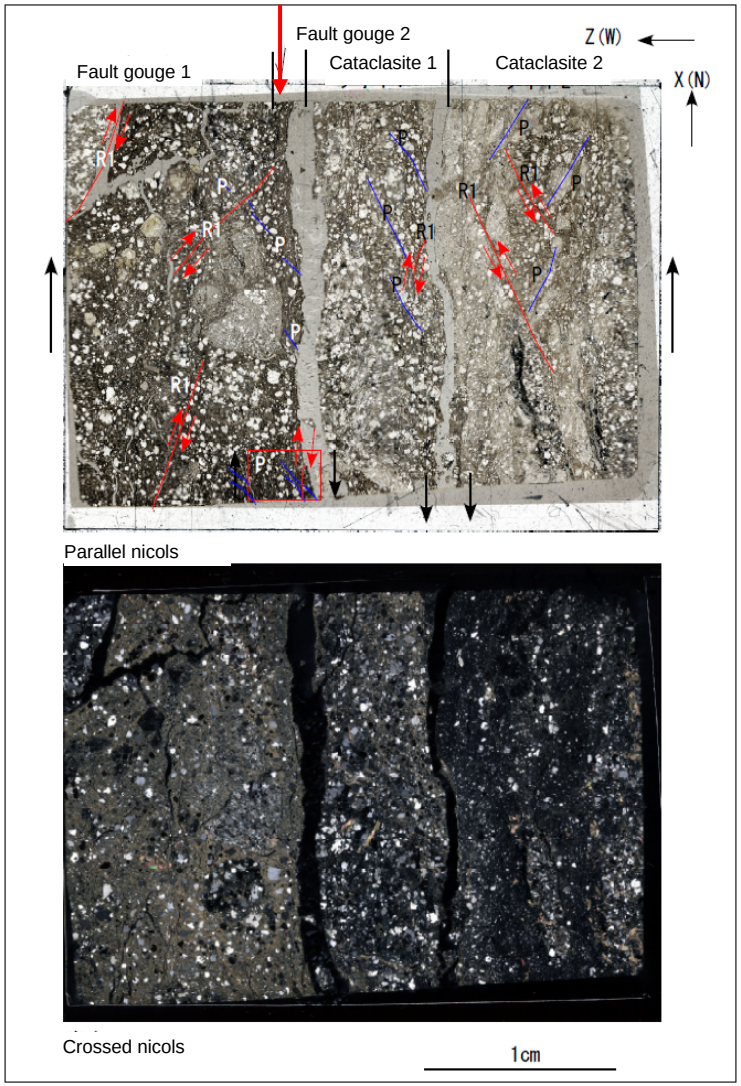

Area within red frame is enlarged

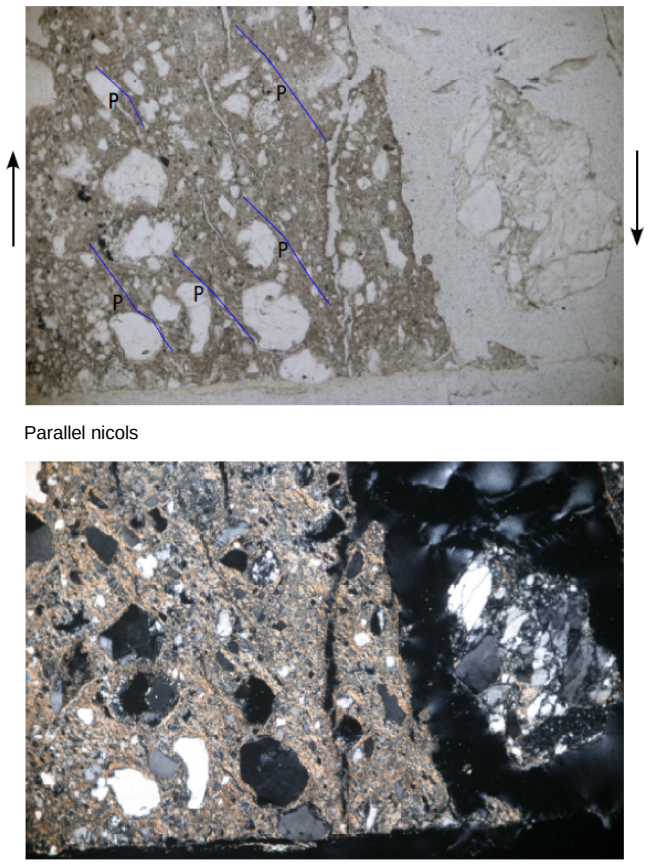

・Fault gouge 1
Consists of the brown matrix of fine grain, as well as quartz, feldspar, aplite and cataclasite fragments and that are semi-circular or sub-angular gravels with diameters of 0.02 mm to
7mm. The matrix contains lots of clay minerals and calcite. The displacement sense of right-lateral slip can be recognized from R1 and P.

・Fault Gauge 2 (last slip)
Consists of the brown matrix of fine grain, as well as quartz, feldspar, cataclasite fragments and that are semi-circular or sub-angular gravels with diameters of 0.02 mm to 1mm. The
matrix contains lots of clay minerals. The displacement sense of right-lateral slip can be recognized from R1 and P.

・Cataclasite 1
Consists of the brown-gray matrix of fine grain, as well as quartz, feldspar, aplite and cataclasite and that are sub-angular or semi-circular gravels with diameters of 0.1 mm to 8mm.
The matrix contains lots of clay minerals and calcite. The displacement sense of right-lateral slip can be recognized from R1 and P.

D-1 B14-2 109.16m_2 XZ directio
n

(Draft) EMS's views against JAPC's claim concerning the fault evaluations of Tsuruga PS site, EMS on shatter zones in the site of Tsuruga Power Station		JAPC's opinion	Reference No.
Main texts	Issues		
<EMS's views on the claim 3> (1) The operator' s claim that D-1 fault is not the active fault to be taken into consideration. ➢ (Skipped)	–	**(Original thoughts)** - Though the detected amount is small, hornblendes are broadly distributed in the same horizon while Kojaku granites or dolerites which compose the rock mass do not include hornblende. Therefore, it is considered to the amphibolite which originate in the tephra. - Although somewhat re-deposition of layer is indicated by the repeated change of amounts of amphibolite with increasing and decreasing along up and down direction, the lower occurrence limit is present on or above the bottom of layer⑤, therefore it is judged that the bottom of layer⑤ and the lower occurrence limit almost indicate the period in which the tephra was fallen. - From the points above, there is not problem in the identification method.	–
(2) Identification of the tephra by analyzing minerals ➢As for analyzing the minerals contained in tephra, it is general to compare with main components of the several types of tephra to be concerned. However, the operator determined it is the same tephra only by comparing with the tephra, dating back to approx. 120 – 130 thousand years ago (the operator calls it 'Mihama tephra') and the identification method is considered to be insufficient. (3) Specification of the deposit which contains the tephra ➢Since the content percentage of the mineral (amphibolite) detected by the lower part of layer⑤ is low frequency which is less than one per 3,000 counts, and small amount of the mineral (amphibolite) are included in layer③ that is lower level, the operator's claim that the lower part of layer⑤ is deposited with the tephra, dating back to 120 – 130 thousand years ago is not reliable assumption. ➢In order to specify the layer in which the tephra is deposited, it is preferable to recognize volcanic ashes by checking them with eyes. If it is not available with the eye inspection, there is also a way to specify the age, applying the method to count the minerals contained in the tephra in the layer. In that case, it is difficult to specify the layer in which the tephra is deposited unless large amount of minerals are contained in the layer while there is significant difference between the upper and the lower layers.	- The result of main components analysis has only been compared with Mihama tephra. - The contents of the minerals is low frequency, and it cannot be specified as the layer in which the tephra is deposited unless there is a significant difference between the upper and the lower layers. - Amphibolite is also included in layer③.	**(Outline of today's explanation (new data))** 1. Stratigraphy of D-1 trench => Layer⑤ was deposited in the warm period, while deposit period of layer③ was colder than layer⑤. 2. Regarding hornblendes included in the lower part of layer⑤ and layer③ => Significant difference has been recognized between the hornblende in lower part of layer ⑤ and the one in layer③ in a result of main composition analysis, although mineral products are quite little because they are gravel. => It was identified that the hornblendes produced in the specific layer of the lower part of layer③ was the amphibolite which originated in the tephra. => It was identified that the lower part of layer⑤ was not the re-deposition of layer③ . 3. Hornblendes detected in the lower part of layer⑤ => There is a high possibility that the hornblendes in the lower part of the layer⑤ is Mihama tephra. => Daisen-Hiruzenpara and BT37 are distributed lower than Sanbe-Kisuki (110-115Ka), which are the tephra, deposited in the marine isotope stage 5e. => Therefore, it is considered that the lower part of layer⑤ should be the deposit of the marine isotope stage 5e. => Layer③ is deposit in marine oxygen isotope stage 6 or before, with coonsideration that layer③ is lower and colder than layer⑤. In addition, - additional analyses are implemented by increasing the survey lines in the D-1 trench in order to be progress of the reliability. - the main components are to be identified as for Daisen-Hiruzenbara. - BT 37 is 127.6ka according to the existing literature though it cannot to be confirmed as it is difficult to obtain the sample. **(Points to be clarified by EMS)** - Considering the above, is there still the reason that the lower part of layer⑤ and layer③ are not respectively MIS5e and MIS6? - The EMS confirmed that the geologic layer where the deformation of the K fault ran up did not reach to the silt layer of layer③.	61-78

Geologic stratigraphy and accumulation era of D-1 trench

1. Regarding geologic stratigraphic sequence of D-1 trench

Investigation for deposits of trench inside
・Dividing stratigraphy into layers as No.①～⑨ based on observation of the slope surface.
→Layer⑤ accumulated with eroding layer③ deeply.
→Layer③ consists of lager particle accumulation comparing with layer⑤.
Sketch, Stratigraphic table
・Pollen analysis
→Only layer② and lower part of layer⑤ include pollen at warm period. It has not been detected in layer③.
Pollen analysis
・Survey of tephra (Continuous 10cm sampling on slope surface)
→Layer⑦ includes DKP, upper part of layer⑤ includes K-Tz.
→Lower part of layer⑤ and layer③ include hornblende, although they are quite little.
Survey of tephra
Photo. of hornblende

⇒Layer⑤ accumulated at warm period, and layer③ accumulated at colder period than layer⑤.

2. Regarding hornblende in lower part of layer⑤ and layer③

Study for the origin of hornblendes detected in lower part of layer⑤ and layer③
・Mineral composition ratio in the basement rock of Tsuruga site.
→It is confirmed that the basement rock doesn't include hornblende.
Mode analysis
・Analysis of reflective index and main component in two layers
→The hornblende of layer③ is confirmed to differ from the one of lower part of layer⑤.
→Lower part of layer⑤ doesn't include the same hornblende to layer③.
→Values of properties are concentrated in the same for every hornblende of lower part of layer⑤
Main components analysis

⇒Significant difference has been recognized between the hornblende in lower part of layer⑤ and the one in layer③ in a result of main composition analysis, although mineral products are quite little because they are gravel.
⇒The hornblende produced from particular lower part of layer⑤ have been found amphibolite which have the origin of tephra.
⇒The lower part of layer⑤ have been found that it didn't re-accumulate from layer③.

3. The origin of hornblende detected in lower part of layer⑤

Study for the origin of hornblendes detected in lower part of layer⑤ and layer③
・Mineral composition ratio in the basement rock of Tsuruga site.
→It is confirmed that the basement rock doesn't include hornblende.
Papers
・Analysis of reflective index and main component in two layers
→The hornblende of layer③ is confirmed to differ from the one of lower part of layer⑤.
→Lower part of layer⑤ doesn't include the same hornblende to layer③.
→Values of properties are concentrated in the same for every hornblende of lower part of layer⑤
Main components analysis

⇒There is a high possibility that the hornblende in lower part of Layer⑤ is Mihama-Tephra
⇒Both Daisen-Hiruzenpara and BT37 are distributing lower than Sanbekisuki(110-115Ka), and these are tephras accumulated at Marine Oxygen Isotope Stage 5e.
⇒Therefore, lower part of layer⑤ has to be an accumulation at Marine Oxygen Isotope Stage 5e.
⇒Layer③ is accumulation at Marine Oxygen Isotope Stage 6 or before, with consideration that layer③ is lower and colder than layer⑤.

【Points to be checked with EMS】
Is there a reason that Layer⑤ and Layer③ are not MIS5e and MIS6 respectively, regardless of above results?

・In order to be progress of reliability, additional surveys are conducted with increasing of analysis line at D-1 trench.
・Main components of Daisen-Hiruzenpara will be investigated.
・BT37 is 127.6ka according to paper, although we couldn't confirm with sampling.

D-1 trench (geologic plan drawing)

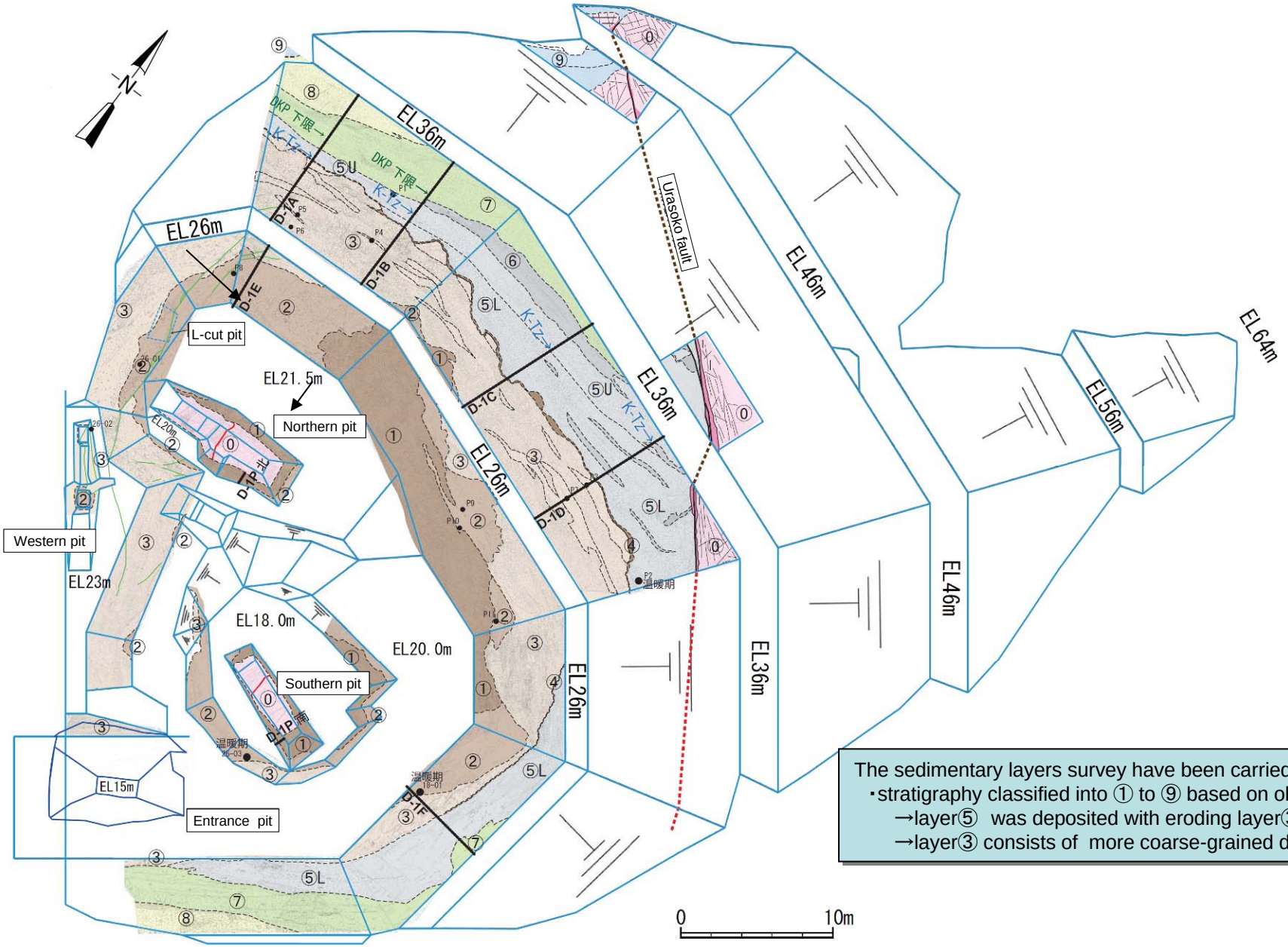

The sedimentary layers survey have been carried out in the trench.

・stratigraphy classified into ① to ⑨ based on observation of slope

→layer⑤ was deposited with eroding layer③ greatly.

→layer③ consists of more coarse-grained deposits compared to layer⑤.

Geologic stratigraphic sequence of D-1 trench

Layer name		Color tone	Facies	Chronometric indicator	
				Tephra	Pollen
Layer ⑨		Brown -darkish yellow brown	Sandy silt with gravel. Contact with lower layer in the horizontal unconformity surface.	–	–
Layer ⑧		Brown -yellow orange	Mainly composed of gravel. Matrix is silty sand. Stratification structure is partly seen. Contact with lower layer in the horizontal unconformity surface.		–
Layer ⑦		Brown -brownish gray	Sandy silt with gravel - Silty sand with gravel. Contact with lower layer in the horizontal unconformity surface.	Including DKP	
Layer ⑥		Gray-dark gray	Humic sandy silt-silty sand Contains lots of wood chips. Contact with lower layer in the horizontal unconformity surface.	–	
Layer ⑤	U (Upper part)	Ash gray -slight yellow orange	Mainly composed of silty gravel.	Including K-Tz	–
	L (Lower part)	Ash gray -slight yellow orange	Mainly composed of silty gravel. Silty gravel layer and silt layer present discontinuous alteration. Erode layer③ and contact with it in the unconformity surface	Including hornblende	Including pollen at warm period
Layer ③	Layer ④※ ※ Oxidized zone of upper end of layer ③ located just beneath unconformity surface.	Brown	Mainly composed of oxidized gravel. Distributed just beneath unconformity surface with undulation and denudation.	Including hornblende	–
		Slight yellow orange -orange	Mainly composed of gravel. Silt layer and sand layer occur in a lenticular and laminae form. Contact with unconformity surface denuding lower layer.		
Layer ②		Darkish orange-ash gray	Sandy silt-silty sand that is massive structure and contains lots of decayed gravel	–	Including pollen at relatively warm period
Layer ①		Darkish red brown -bright brownish yellow	Mainly composed of gravel. Insufficient sorting and very tight	–	–
⓪ Kojaku granite		Ash gray- Brown	Rock mass that constitutes basement. Consist of biotite granite, granite porphyry and aplite.	–	

・layer ⑤ was deposited with widely scraping layer ③.
・layer ③ consists of coarse-grained deposits and contains no orgnics even in relatively/rather fine grain.（environment is estimated to be devoid of vegetation around. Pollens are not detected.）, while layer ⑤ consists of fine grained sediments in addition to coarse-grained deposits containing organics. (environment is estimated to be vegetation around. Pollens of warm interval are detected.)
・layer ③ takes on brown in whole compared to layer ⑤, while layer ⑤ takes on reductive color in whole compared to layer ③.
As above, layer③ and layer⑤ have different depositional environment even in case that both are fan deposits of the same slope.

The results of pollen analysis in D-1 trench (at P1, P2)

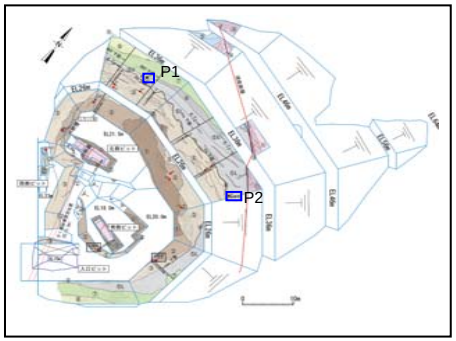

Sampling location

		P1	P2
木本花粉	Arboreal Pollen		
モミ属	*Abies*	–	5
ツガ属	*Tsuga*	78	17
トウヒ属	*Picea*	1	3
マツ属複維管束亜属	*Diploxylon*	–	15
マツ属　不明	*Pinus*	107	65
スギ属	*Cryptomeria*	–	55
イチイ科―イヌガヤ科―ヒノキ科	T.-C.	–	4
ハンノキ属	*Alnus*	12	6
ブナ属	*Fagus*	2	3
コナラ属コナラ亜属	*Lepidobalanus*	–	5
コナラ属アカガシ亜属	*Cyclobalanopsis*	–	30
ニレ属ーケヤキ属	*Ulmus-Zelkova*	–	1
モチノキ属	*Ilex*	–	4
ハイノキ属	*Symplocos*	–	3
草本花粉	Nonarboreal Pollen		
フウロソウ属	*Geranium*	1	–
ヨモギ属	*Artemisia*	1	–
キク亜科	Carduoideae	5	–
不明花粉	Unknown Pollen		
不明花粉	Unknown pollen	1	4
シダ植物胞子	Pteridophyta Spores		
他のシダ植物胞子	other Pteridophyta spores	160	221
合　計	T O T A L		
木本花粉	Arboreal Pollen	200	216
草本花粉	Nonarboreal Pollen	7	0
不明花粉	Unknown Pollen	1	4
シダ植物胞子	Pteridophyta Spores	160	221
総花粉・胞子(不明を除く)	Total Number of Pollen & Spores	367	437
分析後残渣の観察			
有機物残渣量；　VA:Very Abundant(非常に多い)，A:Abundant(多い)，C:Common(普通)，F:Few(少ない)，Tr:Trace(痕跡程度(微量))		Tr	A
花粉・胞子化石の産出傾向；　VA:Very Abundant(非常に多い)，A:Abundant(多い)，C:Common(普通)，R:Rare(稀れ)，VR:Very Rare(極く稀れ)，N:Non(無化石)		R	C
花粉・胞子化石の保存状態；　VG:Very Good(非常に良い)，G:Good(良い)，M:Moderate(普通)，P:Poor(悪い)，VP:Very Poor(非常に悪い)		VP	P

Coniferous

Quercus

Pteridophyta spores

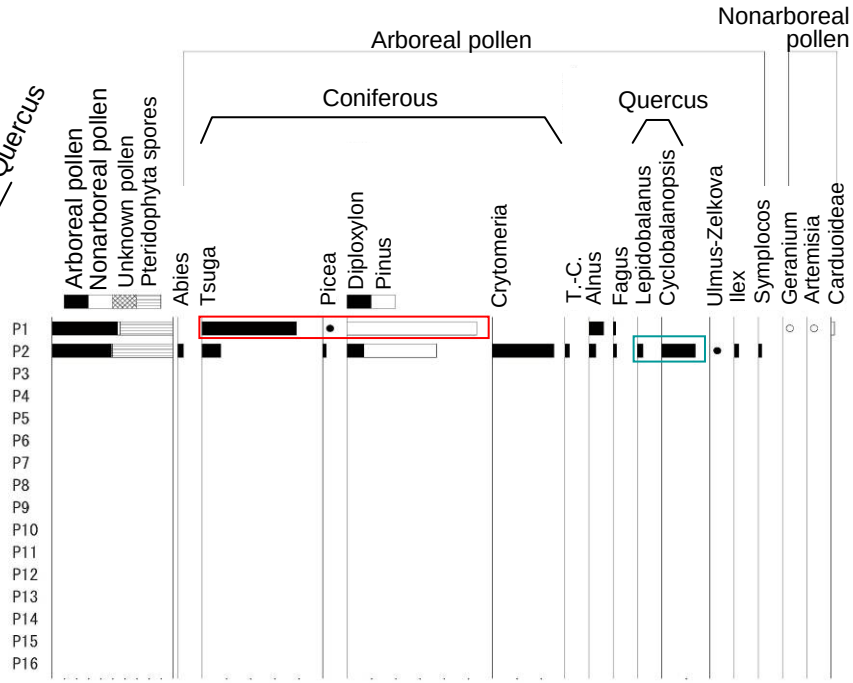

Fig. Fossil pollens list

Appearance rates are represented by percentage with total arboreal as cardinal number in arboreal, and in nonarboreal, with total taken unknown off. And ●○symbols indicate less than 1%.

P1: The top of layer⑤

Paleoclimate is not estimated, because almost all pollen produced is coniferous and pteridophyta spores, and these are not reflected vegetation at that time.

P2: The bottom of layer⑤

As produced pollens are not only coniferous like pinus, cryptomeria and tsuga, but also broadleaved tree like quercus, it is estimated that it was warm period comparatively.

Although lagerstroemia or hemiptelea is observed in the case of Marine Oxygen Isotope stage 5 generally as nationwide feature, they have not been detected in this sample.

The results of pollen analysis in D-1 trench (at 18-01, 26-03)

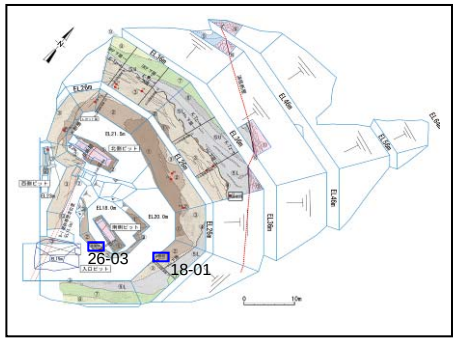

Sampling location

		D1 Po 18-01	D1 Po 26-01	D1 Po 26-02	D1 Po 26-03
木本花粉	Arboreal Pollen				
モミ属	*Abies*	10	–	–	4
ツガ属	*Tsuga*	46	–	–	24
トウヒ属	*Picea*	7	–	–	10
ヒマラヤスギ属	*Cedrus*	7	1	–	–
マツ属単維管束亜属	*Haploxylon*	12	–	–	1
マツ属複維管束亜属	*Diploxylon*	5	–	–	6
マツ属　不明	*Pinus*	77	–	–	20
スギ属	*Cryptomeria*	76	–	–	148
イチイ科―イヌガヤ科―ヒノキ科	T.-C.	1	–	–	–
カバノキ属	*Betula*	1	–	–	2
ハンノキ属	*Alnus*	4	–	–	3
ブナ属	*Fagus*	–	–	–	3
コナラ属コナラ亜属	*Quercus* subgen. *Lepidobalanus*	12	–	–	11
コナラ属アカガシ亜属	*Quercus* subgen. *Cyclobalanopsis*	1	–	–	–
ニレ属－ケヤキ属	*Ulmus-Zelkova*	1	–	1	1
ツゲ属	*Buxus*	–	–	–	2
ウルシ属	*Rhus*	1	–	–	–
カエデ属	*Acer*	1	–	–	–
草本花粉	Nonarboreal Pollen				
カヤツリグサ科	Cyperaceae	3	–	–	1
カラマツソウ属	*Thalictrum*	1	–	–	–
キク亜科	Carduoideae	1	–	–	–
不明花粉	Unknown Pollen				
不明花粉	Unknown pollen	1	–	–	1
シダ植物胞子	Pteridophyta Spores				
他のシダ植物胞子	other Pteridophyta spores	38	–	–	20
合　計	ＴＯＴＡＬ				
木本花粉	Arboreal Pollen	262	1	1	235
草本花粉	Nonarboreal Pollen	5	0	0	1
不明花粉	Unknown Pollen	1	0	0	1
シダ植物胞子	Pteridophyta Spores	38	0	0	20
総花粉・胞子	Total Number of Pollen & Spores	305	1	1	256
分析後残渣の観察					
有機物残渣量；VA:Very Abundant(非常に多い)，A:Abundant(多い)，C:Common(普通)，F:Few(少ない)，Tr:Trace(痕跡程度(微量))		VA	Tr	Tr	VA
有機物形態；am:amorphous主体、mix:混在、wo:woody・coaly・herbaceous主体		wo	wo	wo	wo
花粉・胞子化石の産出傾向；VA:Very Abundant(非常に多い)，A:Abundant(多い)，C:Common(普通)，R:Rare(稀れ)，VR:Very Rare(極く稀れ)，N:Non(無化石)		A	VR	VR	A
花粉・胞子化石の保存状態；VG:Very Good(非常に良い)，G:Good(良い)，M:Moderate(普通)，P:Poor(悪い)，VP:Very Poor(非常に悪い)		M	M	M	M

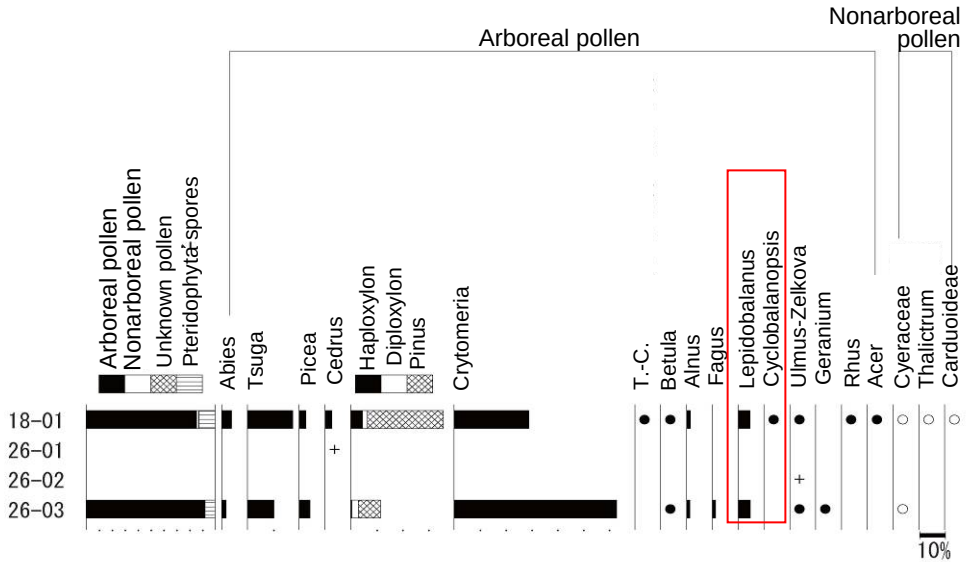

Fig. Fossil pollens list

Appearance rates are represented by percentage with total arboreal as cardinal number in arboreal, and in nonarboreal, with total taken unknown off. And ●○symbols indicate less than 1%.

18-01, 26-03: layer②

As pollens are not only coniferous like pinus, cryptomeria and tsuga, but also broadleaved tree like quercus, it is similar to P2, it is estimated that it was warm comparatively .

D-1 trench (result of tephra analysis)

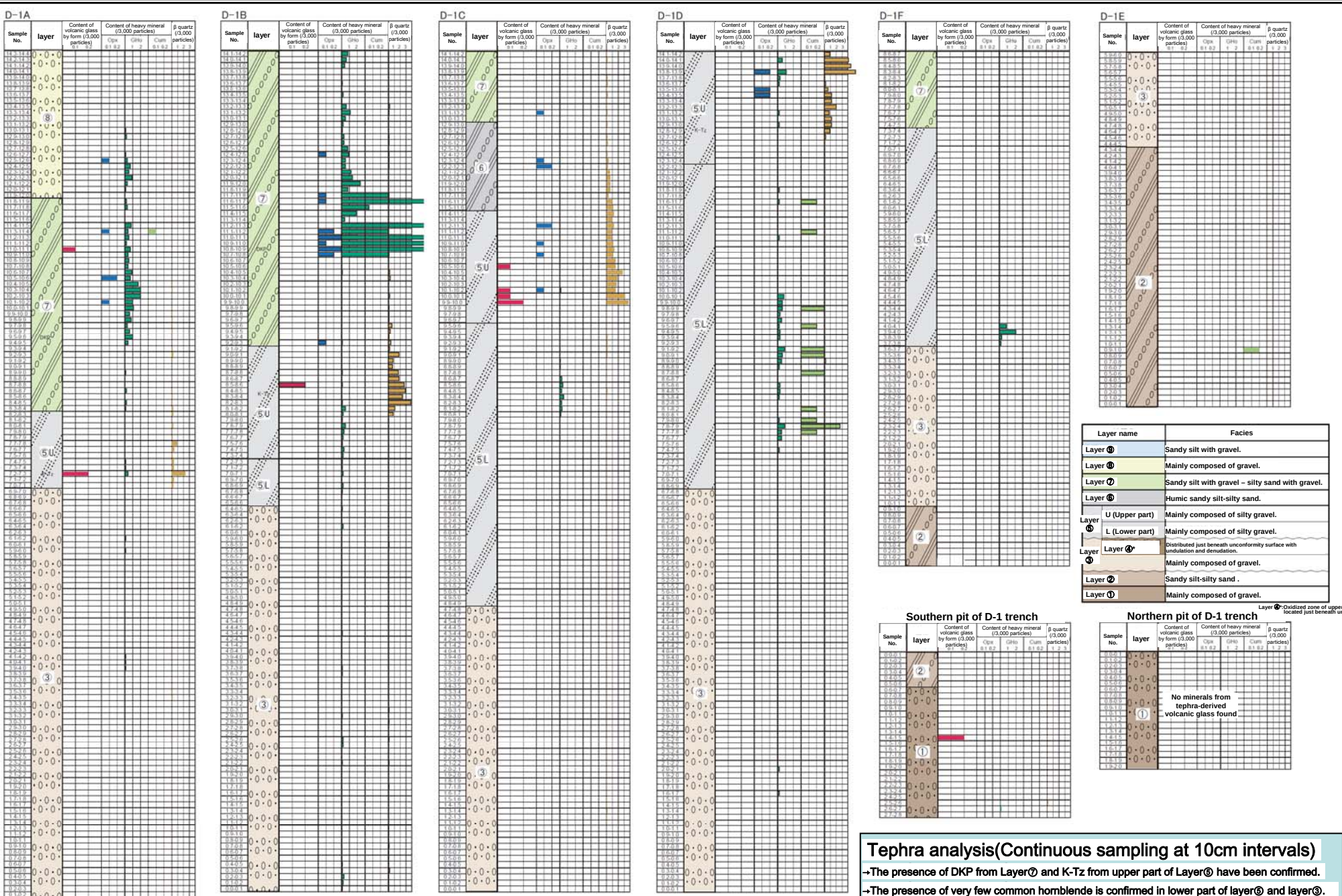

Tephra analysis(Continuous sampling at 10cm intervals)

→The presence of DKP from Layer⑦ and K-Tz from upper part of Layer⑤ have been confirmed.

→The presence of very few common hornblende is confirmed in lower part of layer⑤ and layer③.

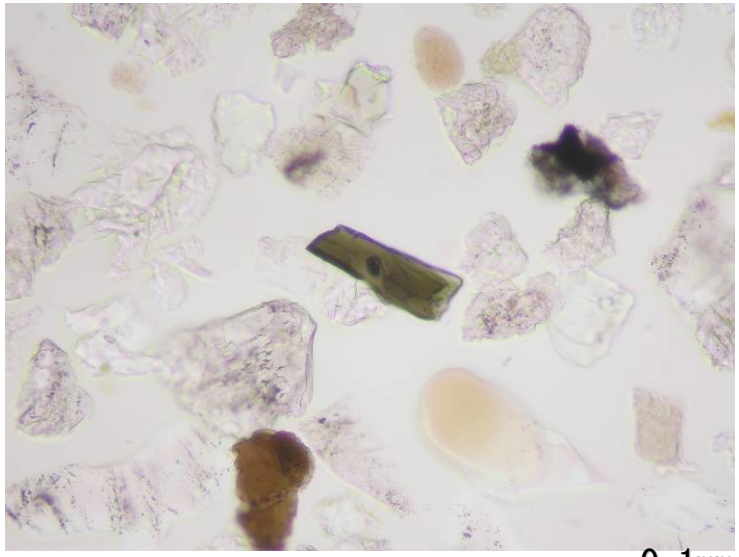

The hornblende included in the layer ③

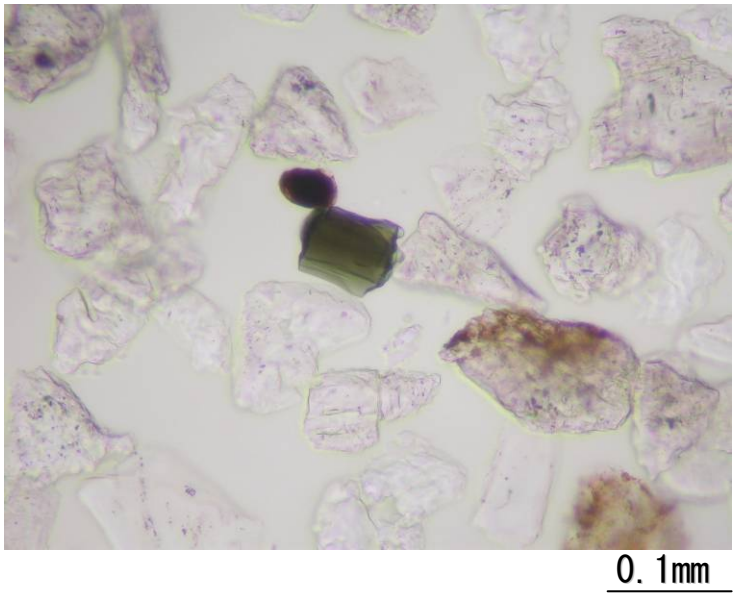

The hornblende included in lower part of the layer ⑤

Idiomorphic hornblendes are included in Layer ③ and lower part of layer ⑤, just like the hornblende in Mihama tephra.

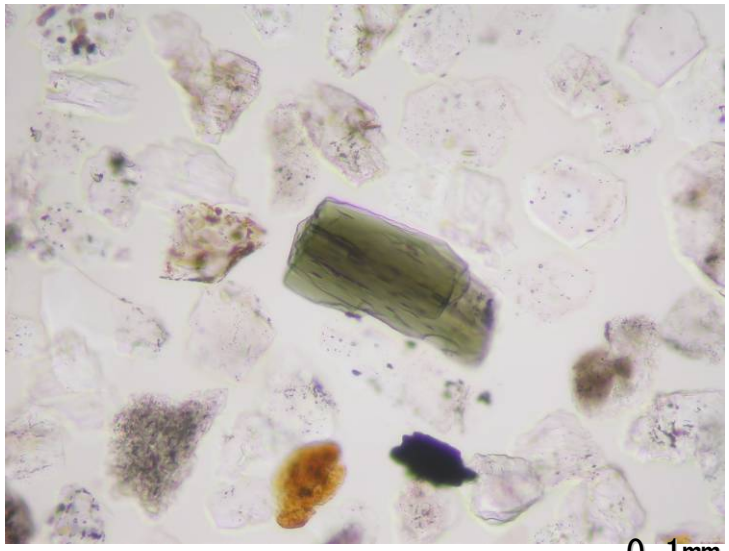

The hornblende of Mihama tephra

Presence or absence of hornblende in the basement rock in the site

Name of rocks	Sample names	items	Name of minerals										total
			Quarts	Plogioclase	Potassium feldspar	Clinopyroxene	Orthopyroxene	Biotite	Muscovite	Opaque mineral	Smectite	Common hornblende	
Biolite granite	Gr-1	Number of counts	1367	891	1315	-	-	12	-	-	-	-	3585
		Content (%)	38.1	24.9	36.7	-	-	0.3	-	-	-	-	100
	Gr-2	Number of counts	906	560	884	-	-	28	-	0	-	-	2378
		Content (%)	38.1	24.8	36.6	-	-	1.2	-	0	-	-	100
Granite porphyry	Gp-1	Number of counts	911	500	719	-	-	53	-	5	-	-	2188
		Content (%)	41.6	22.9	32.9	-	-	2.4	-	0.2	-	-	100
	Gp-2	Number of counts	756	546	728	-	-	39	-	6	-	-	2075
		Content (%)	36.4	26.3	35.1	-	-	1.9	-	0.3	-	-	100
Aplite	Ap-1	Number of counts	1118	675	1264	-	-	24	6	13	-	-	3100
		Content (%)	36.1	21.8	40.8	-	-	0.8	0.2	0.4	-	-	100
	Ap-2	Number of counts	750	500	707	-	-	30	5	8	-	-	2000
		Content (%)	37.5	25.0	35.4	-	-	1.5	0.3	0.4	-	-	100
Dolerite	Do-1	Number of counts	-	1415	-	297	30	-	-	149	861	-	2752
		Content (%)	-	51.4	-	10.8	1.1	-	-	5.4	31.3	-	100
	Do-2	Number of counts	-	1182	-	108	32	-	-	109	569	-	2000
		Content (%)	-	59.1	-	5.4	1.6	-	-	5.5	28.5	-	100

- Mineral composition proportions are found from the observation of thin or polished rock slabs under the microscope regarding samples collected in the site
- Other trace components are granites such as zircon and apatite, and dolerite such as calcite and zeolite.
- As above, no basement rocks in the site include hornblende.

Sampling locations of main component analysis for the hornblende from the Layer③ and Layer⑤L

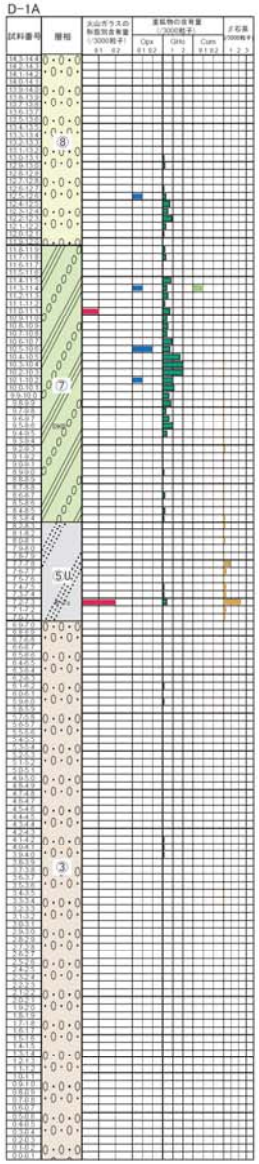

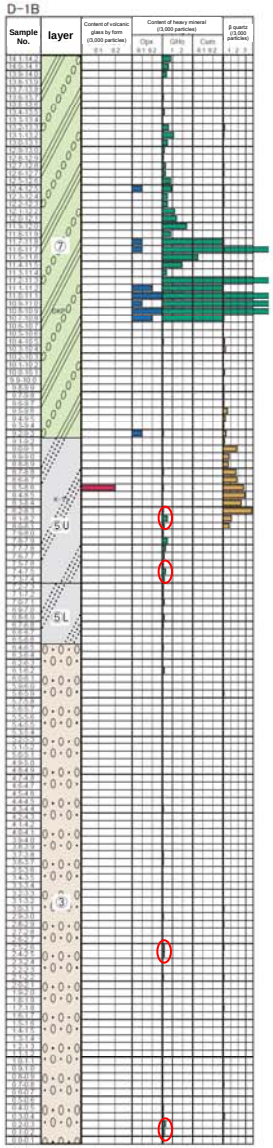

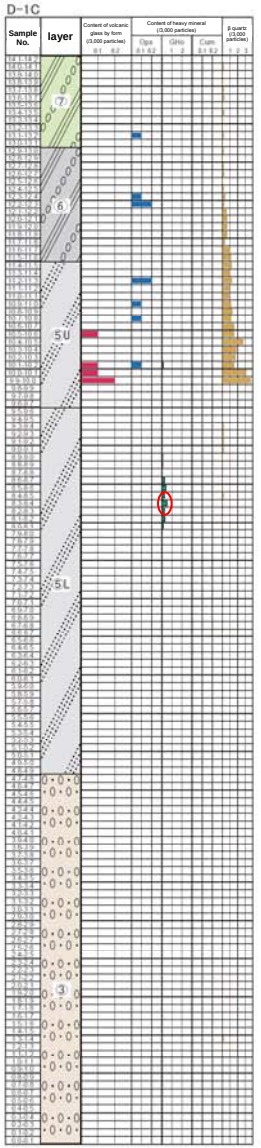

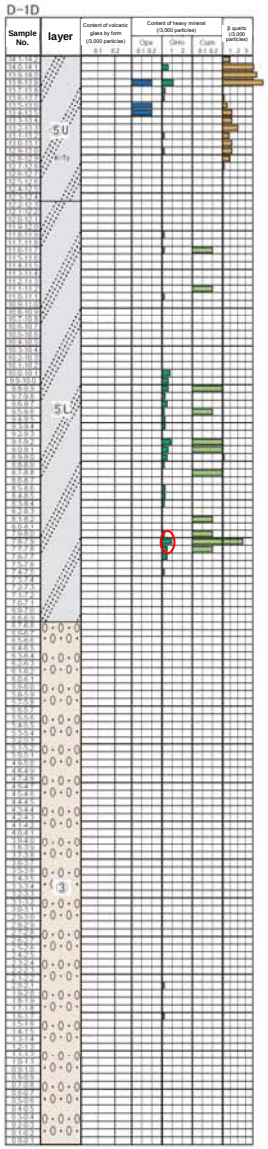

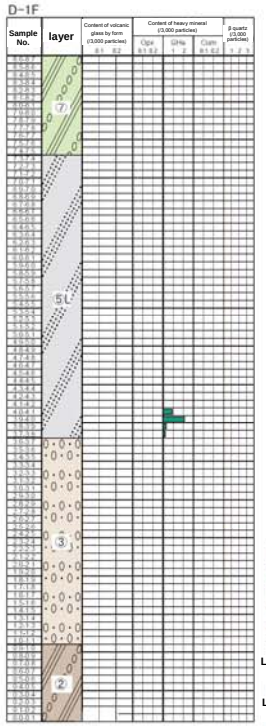

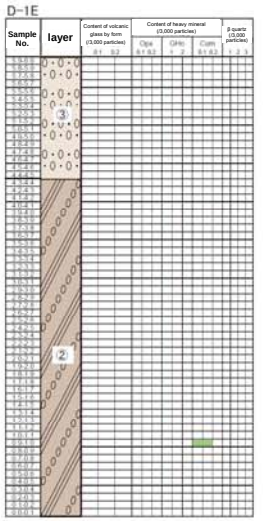

Layer name		Facies
Layer ⑩		Sandy silt with gravel.
Layer ⑧		Mainly composed of gravel.
Layer ⑦		Sandy silt with gravel – silty sand with gravel.
Layer ⑥		Humic sandy silt-silty sand.
Layer ⑤	U (Upper part)	Mainly composed of silty gravel.
	L (Lower part)	Mainly composed of silty gravel.
Layer ④	Layer ④*	Distributed just beneath unconformity surface with undulation and denudation.
Layer ③		Mainly composed of gravel.
Layer ②		Sandy silt-silty sand .
Layer ①		Mainly composed of gravel.

Layer ④*:Oxidized zone of upper end of layer ⑤ located just beneath unconformity surface.

Southern pit of D-1 trench

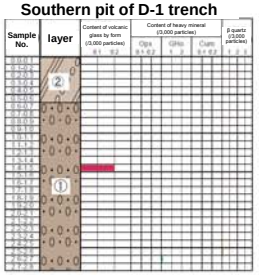

Northern pit of D-1 trench

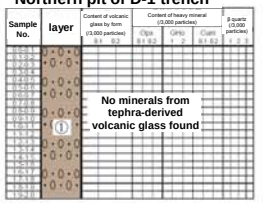

Tephra name; DKP,K-Tz in the table means the position of horizon.

The main component analyses are performed to confirm the difference between the common hornblende from the Layer③ and Layer⑤L.
The sampling locations are circled in red.

The result of main ingredient analysis of hornblende from lower part of layer ⑤ and layer ③

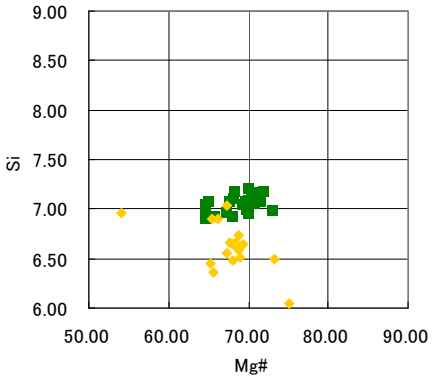

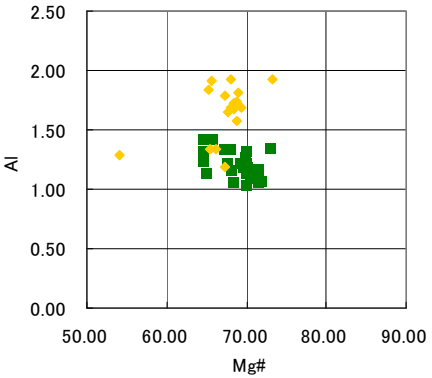

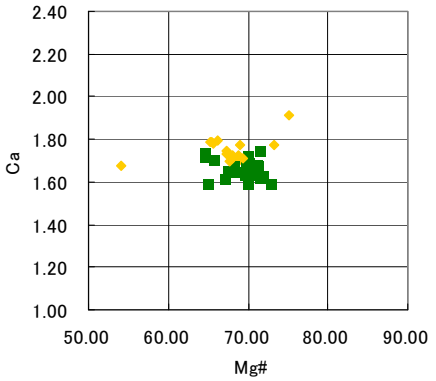

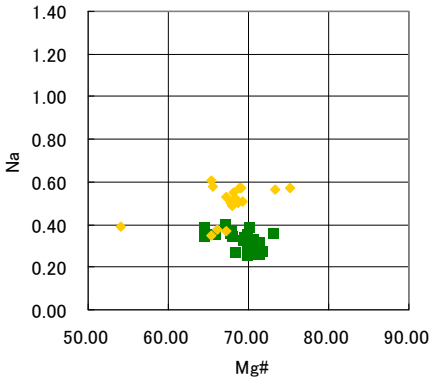

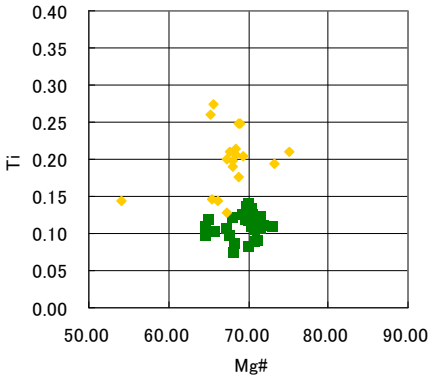

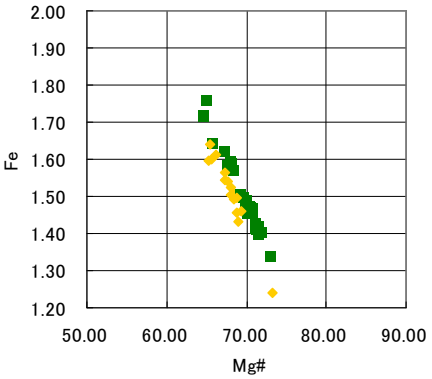

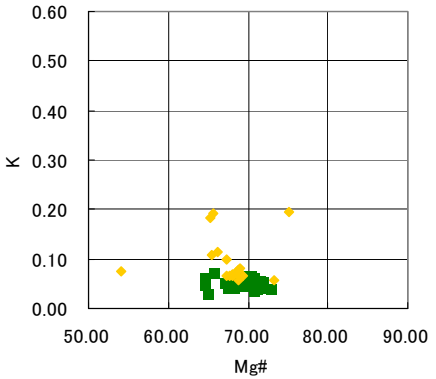

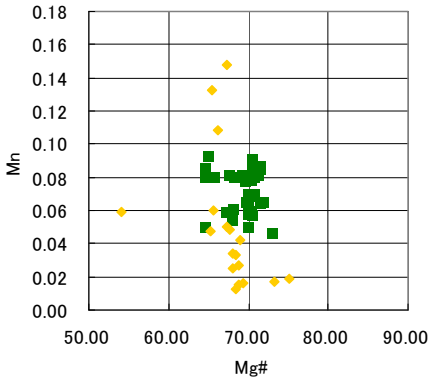

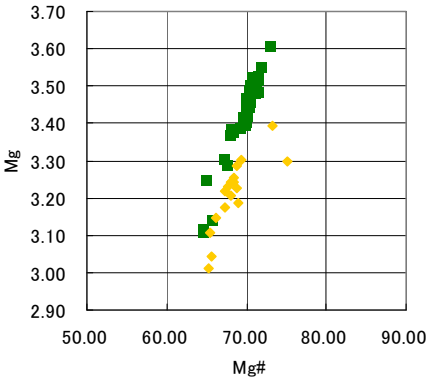

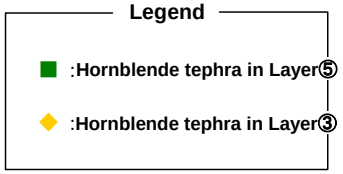

From the result of main component analysis for the hornblende in both layers, it is confirmed that the hornblende in Layer③ have difference from the one in Layer⑤L.

Sampling locations for main component analysis of the hornblende from Layer⑤L.

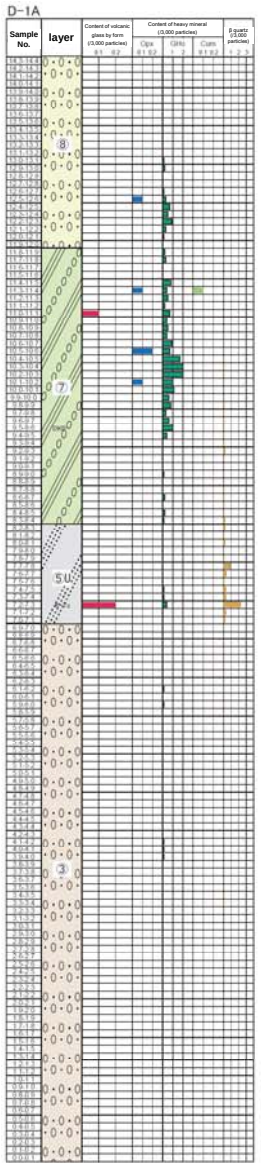

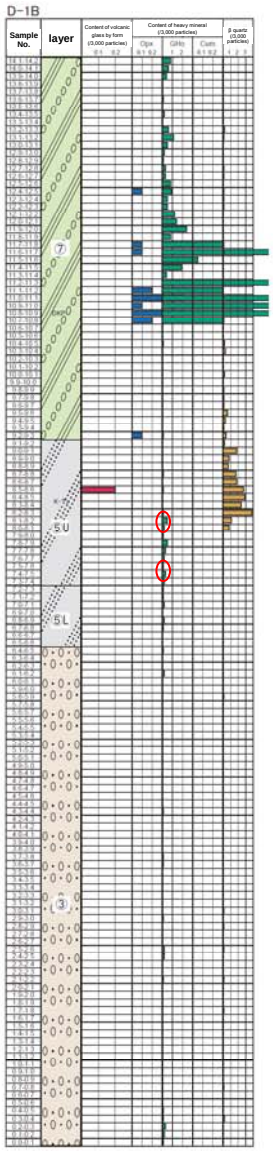

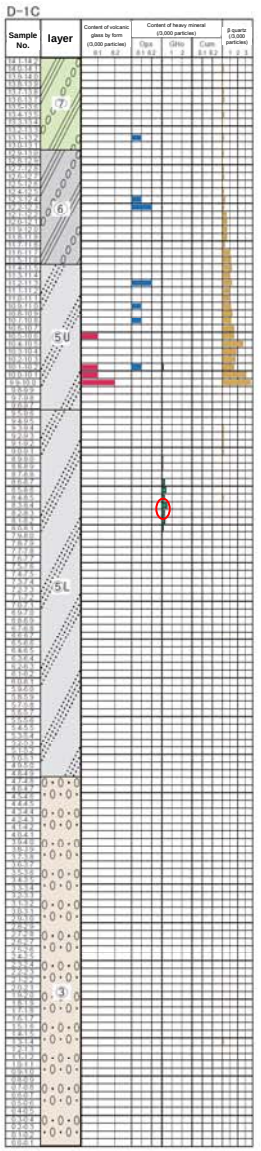

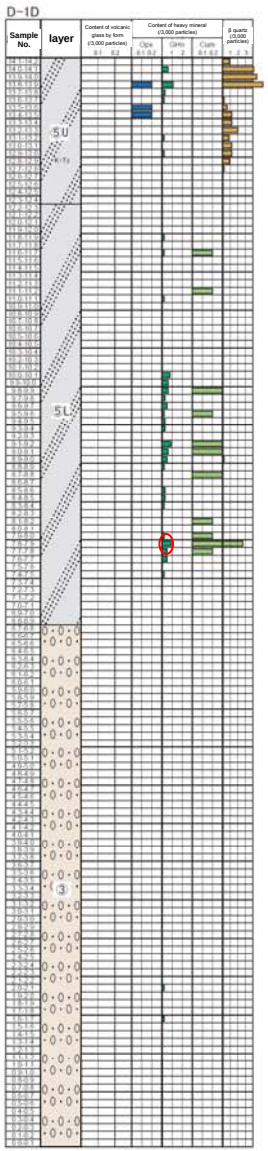

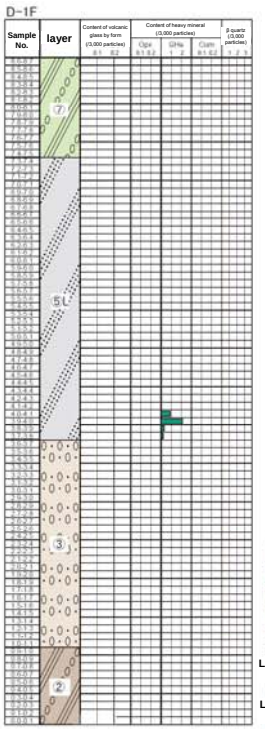

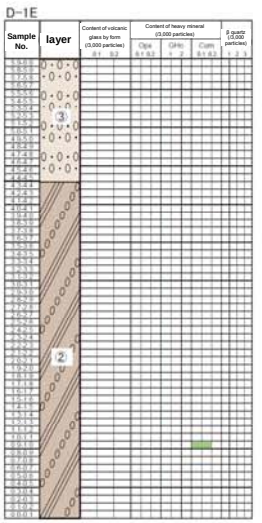

Layer name		Facies
Layer ⑨		Sandy silt with gravel.
Layer ⑧		Mainly composed of gravel.
Layer ⑦		Sandy silt with gravel – silty sand with gravel.
Layer ⑥		Humic sandy silt-silty sand.
Layer ⑤	U (Upper part)	Mainly composed of silty gravel.
	L (Lower part)	Mainly composed of silty gravel.
Layer ④	Layer ④*	Distributed just beneath unconformity surface with undulation and denudation.
Layer ③		Mainly composed of gravel.
Layer ②		Sandy silt-silty sand .
Layer ①		Mainly composed of gravel.

Layer ④*:Oxidized zone of upper end of layer ⑤ located just beneath unconformity surface.

Southern pit of D-1 trench

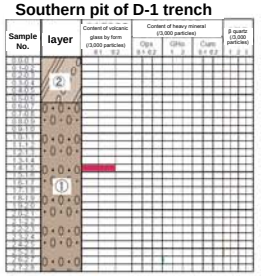

Northern pit of D-1 trench

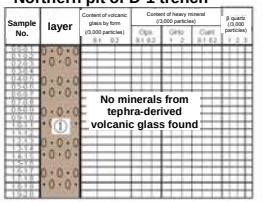

Tephra name; DKP,K-Tz in the table means the position of horizon.

The sampling locations for main component analyses of the hornblende from the Layer⑤L are circled in red.

The result of main component analysis for the hornblende from each survey line of Layer⑤L

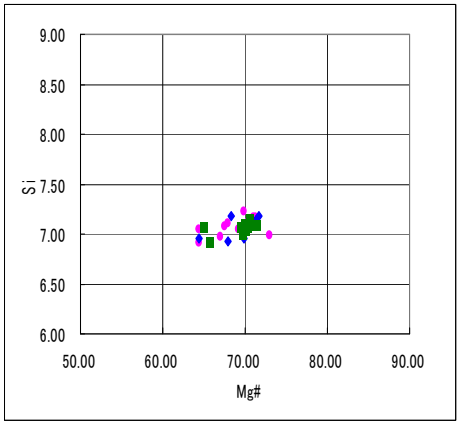

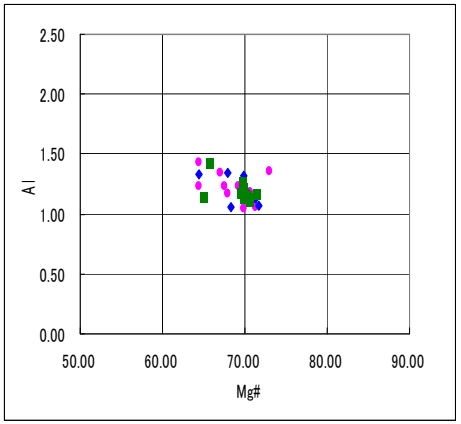

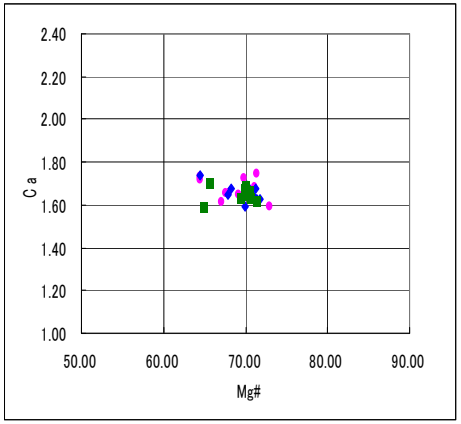

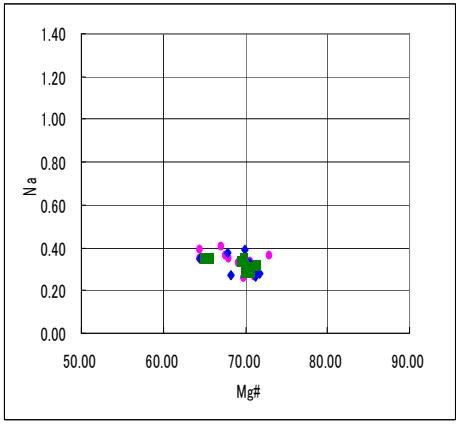

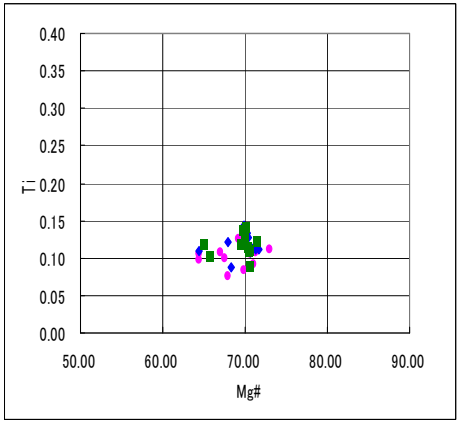

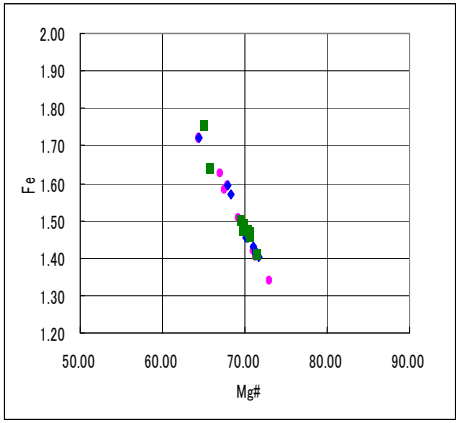

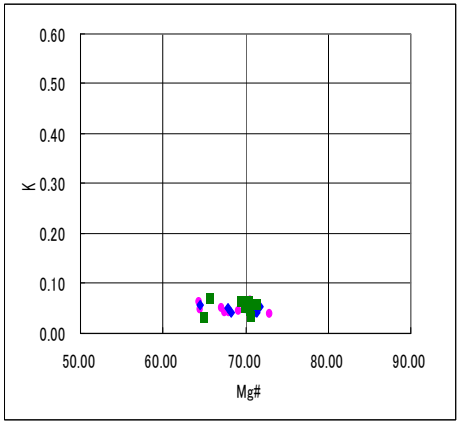

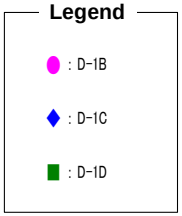

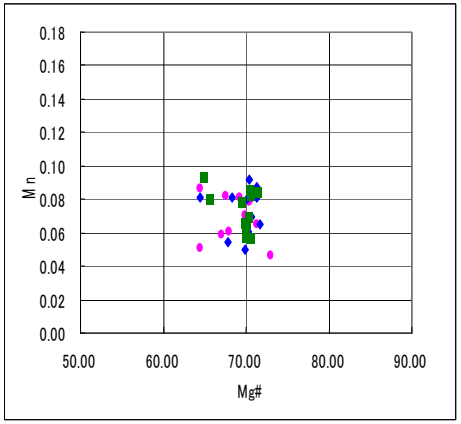

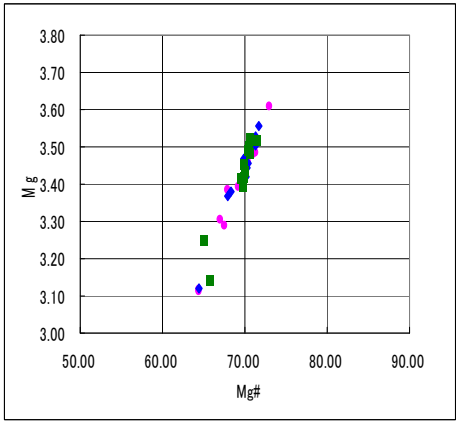

From the result of main component analysis, it is confirmed that the hornblendes in Layer⑤L concentrate in the similar range at each survey line.

[1] Around Sanbensan・Daisen

表 3.2-1

Volcano, Tephra	Symbol	year	Means.	Facies	Distribution Volume	A	V	Note	Symbol	Main mineral	Volcano glass type		opx γ	ho, cum n_2	模式地・その他
大山荒田 I[31,36]	DAP1			pfa	E (S) 50 km	3?	4-5		DAP1	ho, opx, (bi)			1.700-1.706	1.675-1.689	関金町荒田
Kikai-Tozuhara	K-Tz	95		afa(風化)				本文・表 3.1-1 参照.	K-Tz	qt	bw	1.496-1.499			八束村宮城
Ata	Ata	105～110		同上				本文・表 3.1-2 参照.	Ata	(opx)	bw	1.508-1.510	1.706-1.708		同上
Sanbekisuki	SK	110～115	ST	pfl, pfa	ENE 900 km 図 2.2-3	5	6	[古志原][9], 本文参照. 漂着軽石は越前海岸, 能登・男鹿半島に分布[17,18].	SK	bi ; qt	pm	1.494-1.498 (1.497)			木次町寺領, 松江市古志原.
Daisen-Hiruzenpara	DHP			pfa, pfl	E 200 km	4	5-6	pfl は [旧奈和][19].	DHP	ho, bi				1.673-1.679	八束村蒜山高校
Daisen-Matsue	DMP	<130	ST	pfa	W 80 km E 50 km? 図 3.2-1	4	5-6	直下に最終間氷期海成層[7].	DMP	ho, cum, (bi, opx)				1.670-1.676 (1.673) cum 1.656-1.664 (1.659)	米子市岡成上泉, 松江市古志原

1) 松井・井上 (1971), 2) 草野・中山 (1999), 3) 林 (1991), 4) 三浦・林 (1991), 5) 林・三浦 (1987), 6) 服部ほか (1983), 7) 町田・新井 (1976), 8) 津久井 (1984), 9) 堂満ほか (2002), 10) 佐治ほか (1975), 11) 町田・新井 (1976), 12) 蒜山原団研グループ (1973), 13) 林・三浦 (1986), 14) 竹本ほか (1987), 15) 町田ほか (1985), 16) 津久井・柵山 (1981), 17) 豊蔵ほか (1991), 18) 白石ほか (1992), 19) 荒川 (1984), 20) 野村・田中 (1987), 21) 竹村・榎原 (1987), 22) 竹本 (1991), 23) 町田ほか (1991), 24) 福沢・Zolitschka (2000), 25) 吉川ほか (1986), 26) Ooi (1992), 27) 加藤ほか (1996), 28) 佐藤・町田 (1996), 29) 愛媛ローム団研グループ (1969), 30) 宮縁ほか (1999), 31) 石賀 (1997a), 32) 石賀 (1997b), 33) 木村ほか (1999), 34) 福岡・松井 (2002), 35) 野村ほか (1995), 36) 岡田・石賀 (2000).

According to “Atlas of Tephra in and around Japan”, tephras located lower than K-Tz(Kikai-Tozuhara) in this region are Ata, Sanbekisuki, Daisen-Hiruzenpara, Daisen-Matsue in order from upper.

In other papers, Mihama-Tephra(Yasuno1991) and BT37-Tephra(Satoguchi et al.2008, Nagahashi et al.2004) are listed.

（Reference）
・Yasuno. T、1991、Discovery of Molluscan Fossils and a Tephra Layer from the Late Pleistocene Kiyama Formation in West of Fukui Prefecture、Central Japan、Bull.Fukui Mus. Nat.Hist.、No.38:9-14
・Satoguchi. Y、et.al.、2008、The Middle Pleistocene to Holocene tephrostratigraphy of the Takashima-oki core from Lake Biwa、central Japan、Journal of Geosciences、Osaka City University、Vol.51、Art. 6、p.47-58
・Machida. H, Arai. F, 2003, Atlas of Tephra in and around Japan, University of Tokyo Press
・長橋良隆他、2004、近畿地方および八ヶ岳山麓における過去43万年間の広域テフラの層序と編年 ーEDS分析による火山ガラス片の主要成分化学組成ー、第四紀研究、43、15-35

Refractive index and main ingredient analyses of hornblende in the lower part of layer⑤and Mihama and Daisen-Matsue

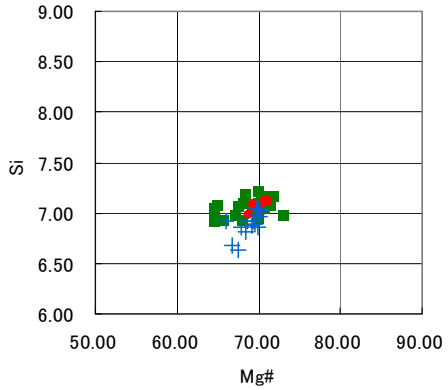

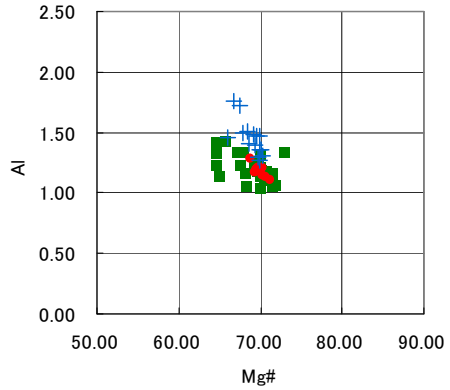

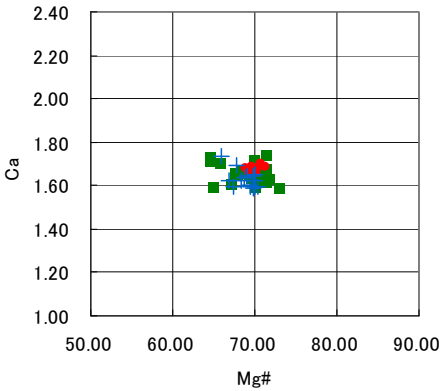

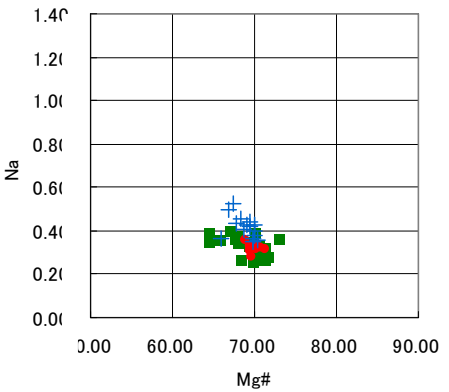

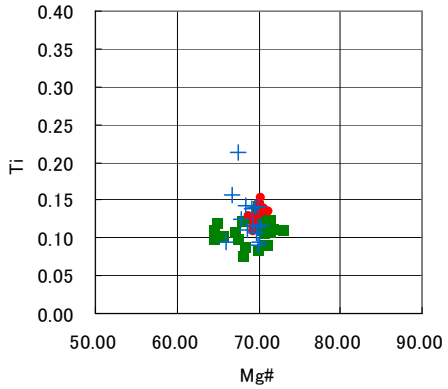

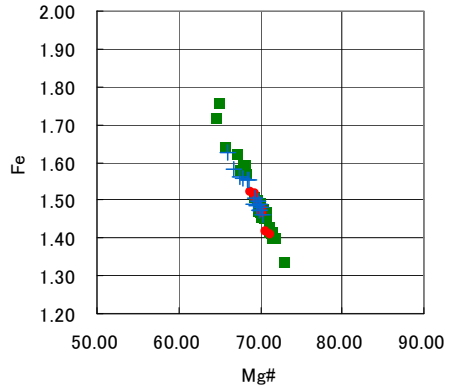

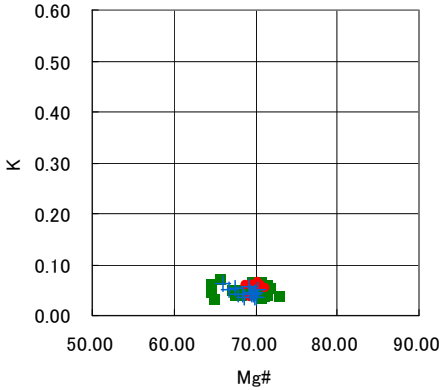

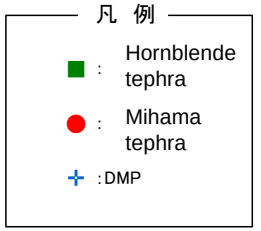

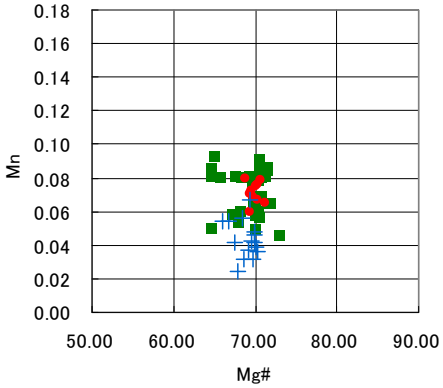

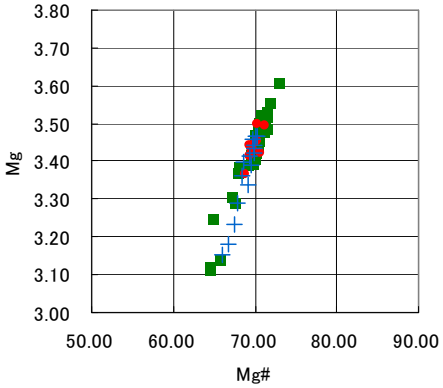

Main ingredient analyses of hornblende in the lower part of layer⑤and Mihama and Daisen-Matsue

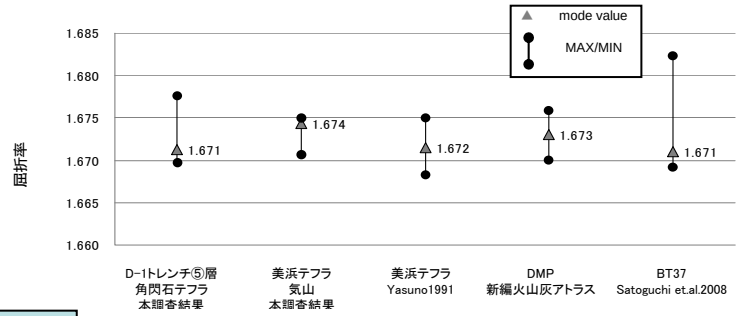

Refractive index of hornblende in the lower part of layer⑤ and Mihama and Daisen-Matsue

Comparing main components analyses of hornblende of layer⑤L with the ones of Daisen-Matsue and Mihama, the hornblendes of the lower part of layer⑤ and Mihama have close remembrances.

D-1 trench geological plan drawing

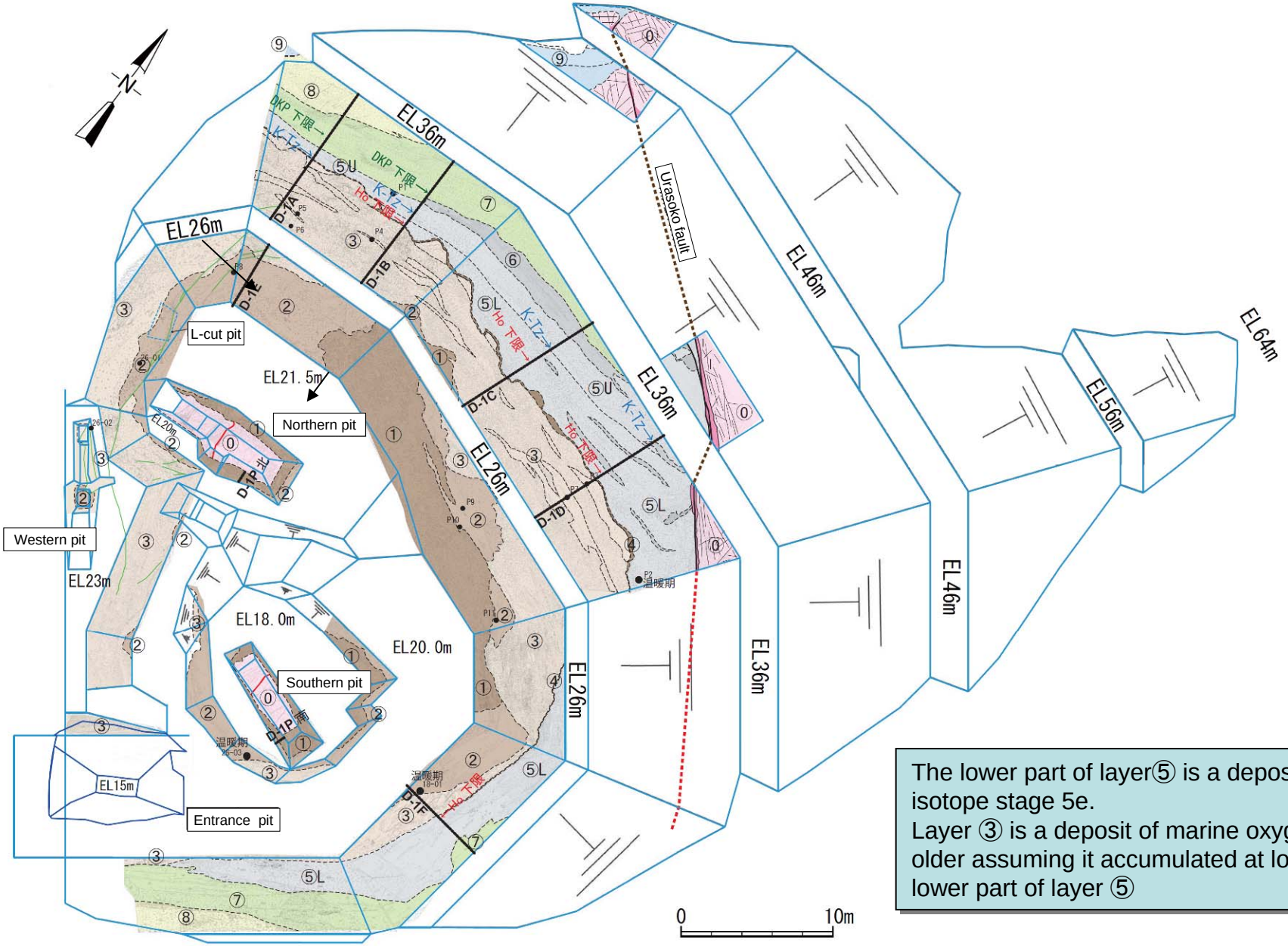

The lower part of layer⑤ is a deposit of marine oxygen-isotope stage 5e.
Layer ③ is a deposit of marine oxygen-isotope stage 6 or older assuming it accumulated at lower colder period than lower part of layer ⑤

Geologic stratigraphic sequence of D-1 trench

Layer name		Color tone	Facies	Chronometric indicator		Deposition al age
				Tephra	Pollen	
Layer ⑨		Brown -darkish yellow brown	Sandy silt with gravel. Contact with lower layer in the horizontal unconformity surface.	–	–	After stage 4
Layer ⑧		Brown -yellow orange	Mainly composed of gravel. Matrix is silty sand. Stratification structure is partly seen. Contact with lower layer in the horizontal unconformity surface.		–	
Layer ⑦		Brown -brownish gray	Sandy silt with gravel - Silty sand with gravel. Contact with lower layer in the horizontal unconformity surface.	Including DKP		
Layer ⑥		Gray-dark gray	Humic sandy silt-silty sand Contains lots of wood chips. Contact with lower layer in the horizontal unconformity surface.	–		stage 5b
Layer ⑤	U (Upper part)	Ash gray -slight yellow orange	Mainly composed of silty gravel.	Including K-Tz	–	stage 5c
	L (Lower part)	Ash gray -slight yellow orange	Mainly composed of silty gravel. Silty gravel layer and silt layer present discontinuous alteration. Erode layer③ and contact with it in the unconformity surface	Including hornblende (highly possibly Mihama)	Including pollen at warm period	stage 5e
Layer ③	Layer ④*	Brown	Mainly composed of oxidized gravel. Distributed just beneath unconformity surface with undulation and denudation.	Including hornblende	–	Stage 6 or earlier
	※ Oxidized zone of upper end of layer ③ located just beneath unconformity surface.	Slight yellow orange -orange	Mainly composed of gravel. Silt layer and sand layer occur in a lenticular and laminae form. Contact with unconformity surface denuding lower layer.			
Layer ②		Darkish orange-ash gray	Sandy silt-silty sand that is massive structure and contains lots of decayed gravel	–	Including pollen at relatively warm interval	
Layer ①		Darkish red brown -bright brownish yellow	Mainly composed of gravel. Insufficient sorting and very tight	–	–	
Kojaku granite		Ash gray- Brown	Rock mass that constitutes basement. Consist of biotite granite, granite porphyry and aplite.	–		Late Cretaceous -Paleogene

Lower part of layer⑤ is a deposit of marine oxygen-isotope stage 5e.
Layer ③ is a deposit of marine oxygen-isotope stage 6 or older assuming it accumulated at lower colder period than lower part of layer ⑤

Survey plan on evaluation of activity of the D-1 shatter zone（including the G fault）and the K fault

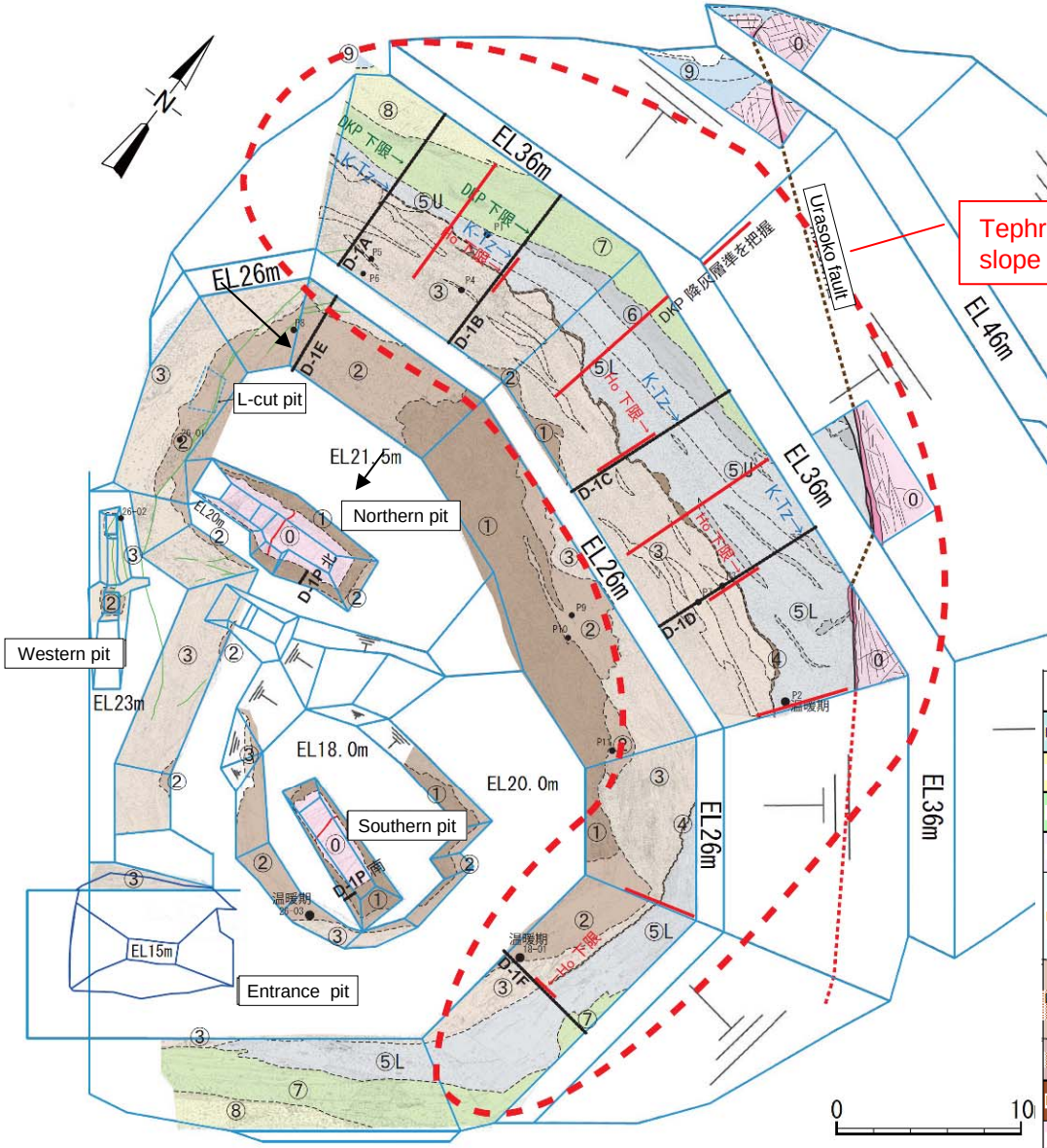

Tephra analyses have been carried out by adding measurement lines in the North slope of D-1trench.

Layer name	Color tone	Facies	Chronometric indicator: Tephra	Chronometric indicator: Pollen	Depositional age
Layer ⑨	Brown -darkish yellow	Sandy silt with gravel. Contact with lower layer in the horizontal unconformity surface.	–	–	After stage 4
Layer ⑧	Brown -yellow	Mainly composed of gravel. Matrix is silty sand. Stratification structure is partly seen. Contact with lower layer in the horizontal unconformity surface.		–	
Layer ⑦	Brown -brownish	Sandy silt with gravel - Silty sand with gravel. Contact with lower layer in the horizontal unconformity surface.	Including DKP		
Layer ⑥	gray Gray-dark gray	Humic sandy silt-silty sand. Contains lots of wood chips. Contact with lower layer in the horizontal unconformity surface.	–		stage 5b
Layer ⑤ U (Upper part)	Ash gray -slight yellow orange	Mainly composed of silty gravel.	Including K-Tz	–	stage 5c
Layer ⑤ L (Lower part)	Ash gray -slight yellow orange	Mainly composed of silty gravel. Silty gravel layer and silt layer present discontinuous alteration. Erode layer③ and contact with it in the unconformity surface	Including hornblende (highly possibly Mihama	Including pollen at warm period	stage 5e
Layer ④ is Oxidized zone of upper part of layer ③ located just beneath unconformity surface.	Brown	Mainly composed of oxidized gravel. Distributed just beneath unconformity surface with undulation and denudation.	Including hornblende	–	Stage 6 or ealier
Layer ③	Slight yellow orange -orange	Mainly composed of gravel. Silt layer and sand layer occur in a lenticular and laminae form. Contact with unconformity surface denuding lower layer.			
Layer ②	Darkish orange-ash gray	Sandy silt-silty sand that is massive structure and contains lots of decayed gravel	–	Including pollen at relatively warm period	
Layer ①	Darkish red brown -bright brownish yellow	Mainly composed of gravel. Insufficient sorting and very tight	–	–	
Kojaku granite	Ash gray- Brown	Rock mass that constitutes basement. Consist of biotite granite, granite porphyry and aplite.	–		Late Cretaceous -Paleogene

For further credibility, additional analyses have been carried out with more survey lines in the D-1 trench

(Draft) EMS's views against JAPC's claim concerning the fault evaluations of Tsuruga PS site, EMS on shatter zones in the site of Tsuruga Power Station		JAPC's opinion	Reference No.
Main texts	Issues		
<EMS's views on the claim 4> The evaluation document points out that the D-1 shatter zone could give impacts on the important facilities, by being active working together with the activity of the Urasoko fault near there. This is because the K fault which continues to the D-1 shatter zone is a reverse fault accompanied by left-lateral slip and the possibility it would move, lead by the activity of the Urasoko fault is high as it is extremely close to the Urasoko fault, which is 20 – 30m at the horizontal distance. In addition, the numerical analysis implemented by the operator is the evaluation based on the 'elasticity theory of dislocation'; however, the specialists of seismic back-check in the former Nuclear and Industrial Safety Agency pointed out that it was difficult to confirm the impacts, applying the 'elasticity theory of dislocation' in case it is too close like the case of the Urasoko fault. The EMS inherited the stance.	1. The possibility that the D-1 shatter zone would become active, lead by the activity of the Urasoko fault is high. 2. The EMS inherited the opinion of the specialists of seismic back check in the former Nuclear and Industrial Safety Agency that it is difficult to confirm the impacts, applying the 'elasticity theory of dislocation' in case it is too close like the case of the Urasoko fault.	**(Outline of today's explanation (Original thoughts))** - The operator implemented the evaluation for the simultaneous activities of the D-1 shatter zone and the Urasoko fault based on the activity record and the numerical analysis. <Evaluation based on the activity record> The latest activity period of the Urasoko fault is after approx. 4000 years ago and the average interval of the activity is 5,000 years ± 2,000 years (AIST, etc 2012); however, the D-1 shatter zone has not been active at least since approx. 120,000 years ago. Therefore, it is considered that the Urasoko fault has become active 10 – 40 times since approx. 120,000 years ago while the D-1 shatter zone has never been active in that period. In addition, it is considered that the Urasoko fault and the D-1 shatter zone should not simultaneously become active in future, too, considering the view that the regional stress field has not changed since the Late Pleistocene. <Evaluation based on the numerical analysis> The bearing capacity of the ground which contains the D-1 shatter zone when being impacted by the activity of the Urasoko fault is evaluated by implementing the numerical analysis. In the numerical analysis, 'basic study' and 'study to consider uncertainty' were implemented first in the ground deformation analysis based on the 'elasticity theory of dislocation' which assumes the ground as an elastic half-space to extract the evaluation conditions for obtaining the most strict result for the bearing capacity evaluation of the reactor building foundation. After that, it was analyzed based on the evaluation conditions, applying the FEM model which is made, considering the topography, the ground structure, the ground property and the nonlinearity of the ground, etc for which the 'elasticity theory of dislocation' cannot be applied in detail while the stability of the shatter zone was evaluated based on the local safety factor obtained from the FEM analysis result. Though the result shows shear failures and induction of tensile stresses in the shatter zone near the Urasoko fault, the area is limited while the local safety factor of the shatter zone near the building is sufficiently large. Therefore, it is concluded that the bearing capacity of the ground is sufficiently strong. ・In addition, the purpose of the numeric analysis implemented by the operator is to evaluate 'if the shatter zone under the reactor building could be broken by the tensile stress in the ground induced due to the activity (displacement) of the Urasoko fault' and it is the evaluation for the ground stability, in other words. ・Therefore, it is not the evaluation for calculating the displacement magnitude of the shatter zone. ・Such method for the ground stability evaluation is widely applied in the field of geotechnology. **(Points to be clarified by EMS)** ・The operator has been implementing the evaluations for the simultaneous activities of the D-1 shatter zone and the Urasoko fault based on the following process and is that correct? 'The regulatory guide for reviewing seismic safety design of nuclear facilities for power generation (approved by Nuclear Safety Commission as of December 20, 2010) instructed that the fault displacements due to earthquakes should be evaluated by calculating the displacements / deformations of the ground where buildings and structures are established due to the fault displacements. Complying with the guideline, the evaluation was implemented by the numeric analysis to identify whether a gap could be made or not due to the activity of the Urasoko fault in the surrounding shatter zone including the D-1 shatter zone. Being instructed by the former NISA as of November 11, 2011 'to show the evaluation method of the geological displacements around the active layers in Tsuruga NPP and implement impact evaluations for the reactor building, etc, applying the concerned method', we have been implementing the evaluations. The operator presented the additional survey plan of the site in the opinion hearing meeting of the former NISA regarding earthquakes and tsunamis as of May 14, 2012 and explained that 'it is evaluated comprehensively based on the results of various geological surveys and the numerical analysis, etc in case it is difficult to evaluate it by overlying strata analysis method'. ・The former NISA discussed that 'it should take time to review the applicability' and 'it is necessary to evaluate more in detail' as for the elasticity theory of dislocation; however, it only pointed out that the theory should be evaluated carefully but did not mean that it was inapplicable. ・In addition, though the EMS expressed that 'they would inherited the stance', the EMS and 'The study team on the new safety design standards for earthquakes and tsunamis for light water reactors for electric power generation' have not discussed the application of the elasticity theory of dislocation, at all. We would like to know the process how they reached to the conclusion to inherit the stance. ・Though the possibility that the D-1 shatter zone could move, lead by the activity of the Urasoko fault was pointed out, we would like to know what sort of mechanism was assumed when you meant by 'lead by the activity' and how large the impact would be.	79-135

Consideration based on the history of activity

Activity of Urasoko fault (Overlying strata analysis method)

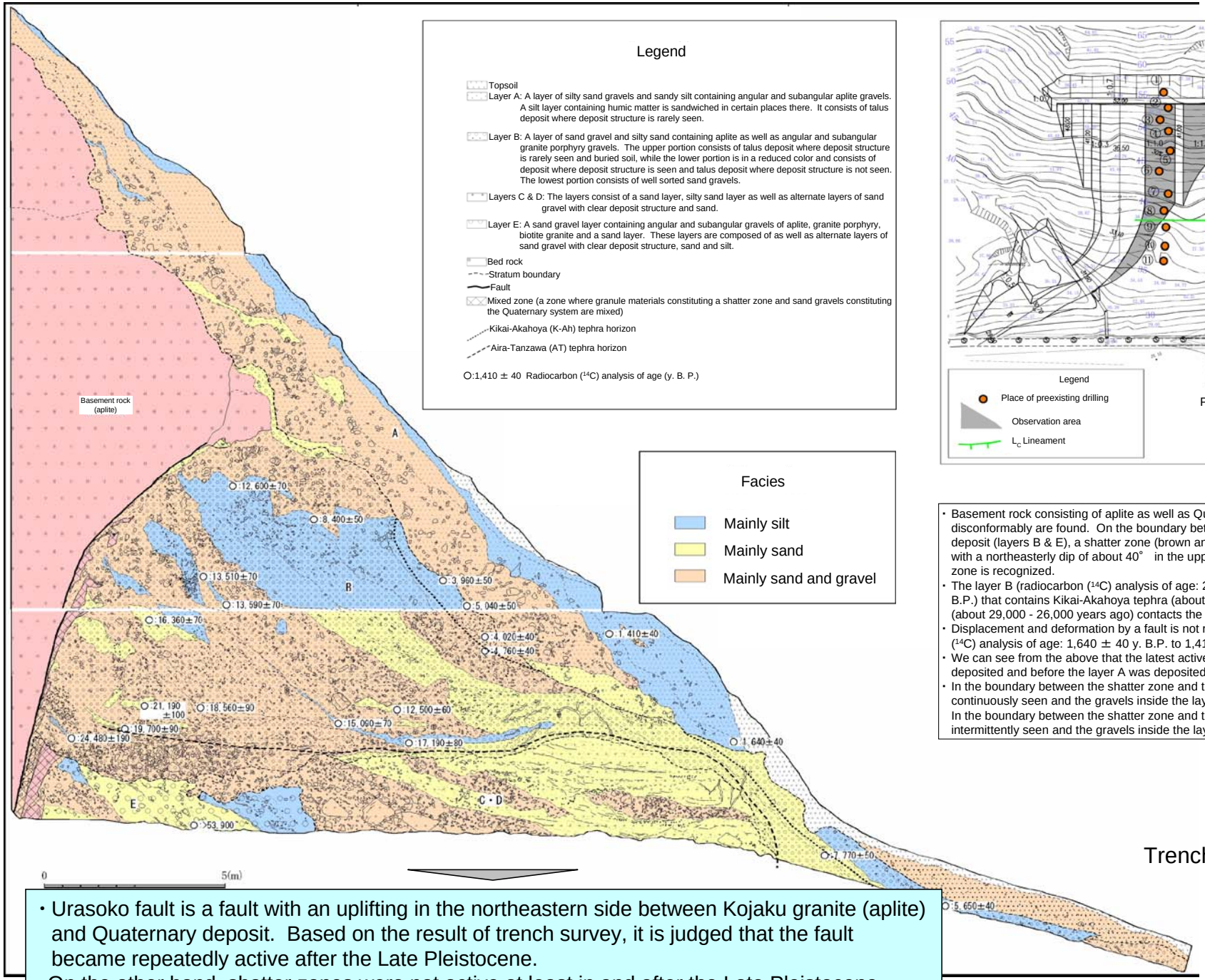

Plane figure of the trench

- Basement rock consisting of aplite as well as Quaternary talus deposit that overlays disconformably are found. On the boundary between aplite as well as Quaternary talus deposit (layers B & E), a shatter zone (brown and ash gray clay of about 10 cm wide) with a northeasterly dip of about 40° in the upper zone and about 70° in the lower zone is recognized.
- The layer B (radiocarbon (14C) analysis of age: 24,480 ± 190 y. B.P. to 3,960 ± 50 y. B.P.) that contains Kikai-Akahoya tephra (about 7,300 years ago) and Aira Tn tephra (about 29,000 - 26,000 years ago) contacts the basement rock in terms of a fault.
- Displacement and deformation by a fault is not recognized in the layer A (radiocarbon (14C) analysis of age: 1,640 ± 40 y. B.P. to 1,410 ± 40 y. B.P.)
- We can see from the above that the latest active period was after the layer B was deposited and before the layer A was deposited.
- In the boundary between the shatter zone and the layer E, a mixed zone is continuously seen and the gravels inside the layer E show strong preferred orientation. In the boundary between the shatter zone and the layer B, a mixed zone is intermittently seen and the gravels inside the layer B show poor preferred orientation.

Trench survey（place B）

- Urasoko fault is a fault with an uplifting in the northeastern side between Kojaku granite (aplite) and Quaternary deposit. Based on the result of trench survey, it is judged that the fault became repeatedly active after the Late Pleistocene.
- On the other hand, shatter zones were not active at least in and after the Late Pleistocene. According to this reason, it is judged that shatter zones and Urasoko fault were not active simultaneously in and after the Late Pleistocene.

Evaluation of simultaneous activities based on history of activity

Contents	Urasoko fault	D-1 Shatter zone
Latest activity	After about 4,000 years ago	No activity in and after the Late Pleistocene *D-1trench*
Average activity interval	5,000 years ±2,000 years※	–
Activity times for the past about 120,000 years	Over 10 ～ 40 *120,000years÷average activation interval* In the trench at place B, there are signs which indicate moving more than one time after 60,000 years ago. (DKP ash fall)	No activity

※ Survey on active faults in coastal zones; Yanagase and Sekigahara fault zones; Urasoko-Yanagase fault belt; Report of Results; May 2012; the National Institute of Advanced Industrial Science and Technology & Tokai University; p33

Evaluation based on the numerical analysis

Table of Contents

1. Introduction

・The Nuclear and Industrial Safety Agency requested “Clarification of the assessment method for heterotaxis in the vicinity of the active fault at Tsuruga PS site and impact assessment of heterotaxis on the reactor buildings or other facilities based on the method” .*

＊”Regarding Implementation of Safety Assessment Concerning the Impact of Seismic Ground Motion and Tsunami on the Nuclear Facilities Based on the Knowledge of the 2011 Off the Pacific Coast of Tohoku Earthquake “ 11th Nov. 2011, NISA

・In accordance with the direction, the assessment methods for displacement and deformation of the ground caused by activity of Urasoko-Uchiikemi fault was organized, and impact assessment on the reactor buildings was considered.

2. Outline of Urasoko-Uchiikemi fault

・Survey results of geography and geology indicate that Urasoko fault runs in a direction of NW-SE and is vertical to easterly dip.
・Because the fault has signs for activities after the Late Pleistocene, the fault is an active fault that should be taken into account in the seismic design, the length is estimated 18km.
・The sea part of the fault is located western edge of higher level surface of C layer（Middle Pleistocene） in Tsuruga bay, the displacement sense is left-lateral slip sense including constituent of uplifting in northwestern side.
・The offset distance between Urasoko fault and centers of unit 1＆2 reactor buildings is approximately 250m.

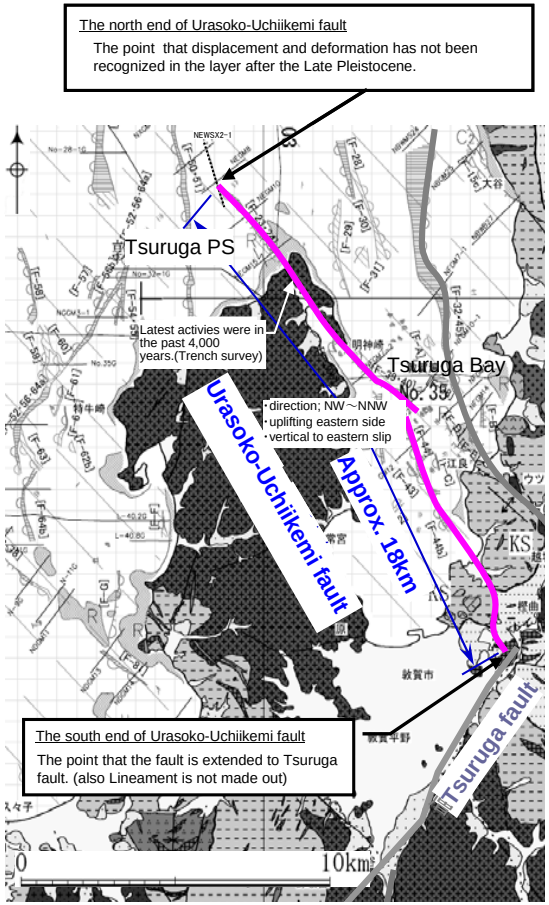

Fig. Urasoko-Uchiikemi fault

Table Properties list of Urasoko-Uchiikemi fault

Contents	Properties	Main Survey
Direction	・NW－SE	Geography Surface geology Sea surface sonic
Fault dip angle	・generally vertical to easterly dip	Geography Boring Trench Sea surface sonic
History of activity	・active in the past 4,000 years	Trench
Fault length	・18km	Surface geology Sea surface sonic
Displacement sense	・Left-lateral slip including constituent of uplifting in northwestern side	Geography Boring Trench Sea surface sonic

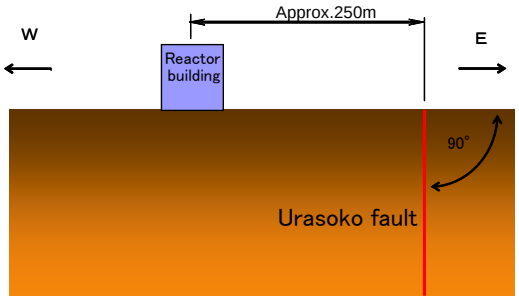

Fig. Offset distance between Urasoko fault and the reactor building（Concept map）

3. Flow of evaluations (1)

1. Evaluation contents
・Using numerical analysis in accordance with “Regulatory Guide for Reviewing Seismic Design of Nuclear Power Reactor Facilities” and “Guidelines for Reviewing safety related Seismic Safety of Nuclear Power Reactor Facilities” , JAPC evaluated bearing capacity of the basement ground of reactor building against the displacement caused by activity of Urasoko-Uchiikemi fault.
・”Influence of displacement of the ground in vertical cross section to the facility” and “Influence of horizontal deformation to the facility in the case which a fault displacement has constituent of lateral slip” were evaluated, referring to ” Guidelines for Reviewing safety related Seismic Safety of Nuclear Power Reactor Facilities“
2. Selection of a numerical analysis method
・Taking into account the situation that the fault is near to the reactor facility and properties of Urasoko-Uchiikemi fault, elasticity theory of dislocation and FEM were selected.

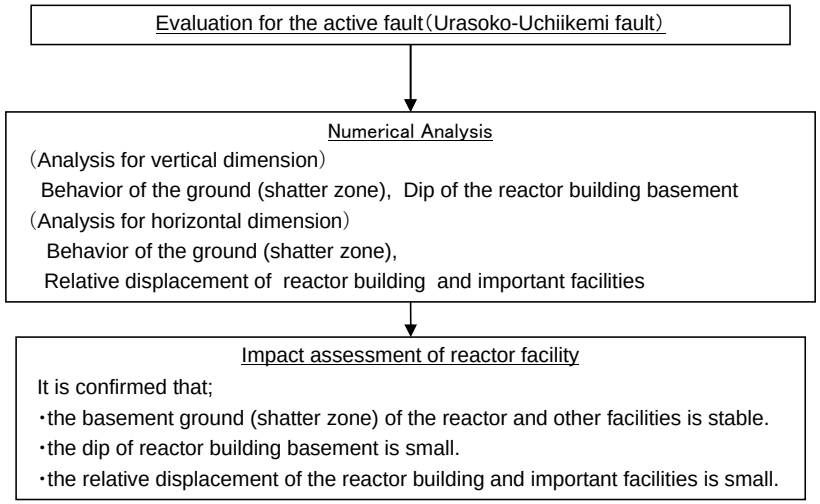

Fig. Evaluation contents

Table Selection of numerical analysis method

Contents	Policies, Supplements	Selection criteria	Main methods
Understanding of the ground behavior affected with displacement caused by Urasoko fault① activity, and influence to the reactor building and other facilities. Evaluation has to be due to numerical analysis②.	①Urasoko fault actived repeatedly after at least the Late Pleistocene, and the distribution of fault is understood by geological survey.	Methods inputting slip into advance fault surfaces.	・Elasticity theory of dislocation ・FEM（Finite Element Method） ・BEM（Boundary Element Method）
	②Methods having accomplishments or inspection examples for displacement and deformation of ground are preferable.	Methods used at organizations like Geospatial Information Authority of Japan, or National Research Institute for Earth Science and Disaster Prevention, or U.S. Geological Survey.	・Elasticity theory of dislocation ・FEM（ Finite Element Method ）
Cases took into consideration uncertainties of broken area in a fault, slip, model.③	③Because of many cases, comparatively easy methods are preferable.	Methods obtaining analysis solutions during short time.	・Elasticity theory of dislocation
And, careful consideration for the fact that Urasoko-Uchiikemi fault is distributed nearby reactor facilities.④	④The actual conditions of ground around the fault should be considered in order to analyze the case that the ground of facilities have large displacement or deformation. facilities	Methods that could represent non-homogeneity and others of the geography and ground.	・FEM（Finite Element Method）

・The Elasticity theory of dislocation is selected to evaluate because of its many accomplishments in principle, and a lot of evaluations take into account uncertainties.

・In addition, FEM(Finite Element Method) analysis is selected, which is able to represents more detailed behavior of the ground of the fault that is near the reactor facilities.

3. Flow of evaluations (2)

3. Procedure of numerical analysis
・In the numerical analysis, “basic study” and “ study taking uncertainties into account ” have been examined.
・By using the severest conditions, which are drawn up from the evaluation of bearing capacity of the foundation ground, a FEM analysis has been examined based on the elasticity theory of dislocation.

【Analysis conditions】＊Basic parameters and uncertainties have been surveyed
・Geometric shape of the fault (length, width, dip angle, depth)
・Slip of the fault（slip angle, slip quantity）
・Model of the fault（structures, poason’s ratio）

The Elasticity theory of dislocation

・First of all, deformation analysis of the ground at “basic study” and “study taking uncertainties into account” have been examined based on “the elasticity theory of dislocation” with assuming that the ground is semi-infinite elastic medium, and analysis conditions have been drawn up which would produce the severest results in evaluation of bearing capacity of the foundation ground of the reactor building.

Drawing up the severest analysis conditions for the reactor facilities

FEM

・Stability of the shatter zone has been evaluated from local safety factors calculated with detail modeled FEM in which geography/ground structure and physical properties/non-linearity of the geography and others taken into account, and using conditions that would produce the severest results based on the elasticity theory of dislocation.

・Forced displacement has been inputted on the boundary of FEM, which was examined with the elasticity theory of dislocation at the boundary.

・Vertical two-dimensional FEM analysis was used for the examination of vertical slip, and horizontal two-dimensional FEM was used for lateral slip.

Fig. Procedure of the numerical analysis

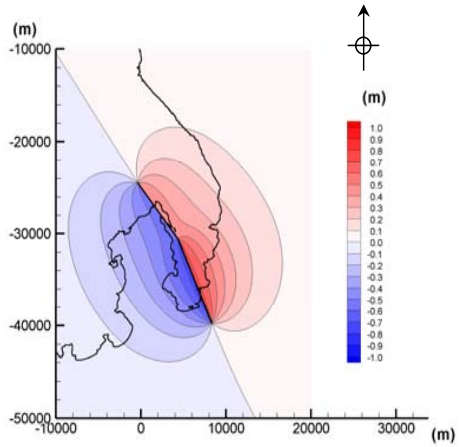

Fig. The elasticity theory of dislocation (distribution of vertical displacement)

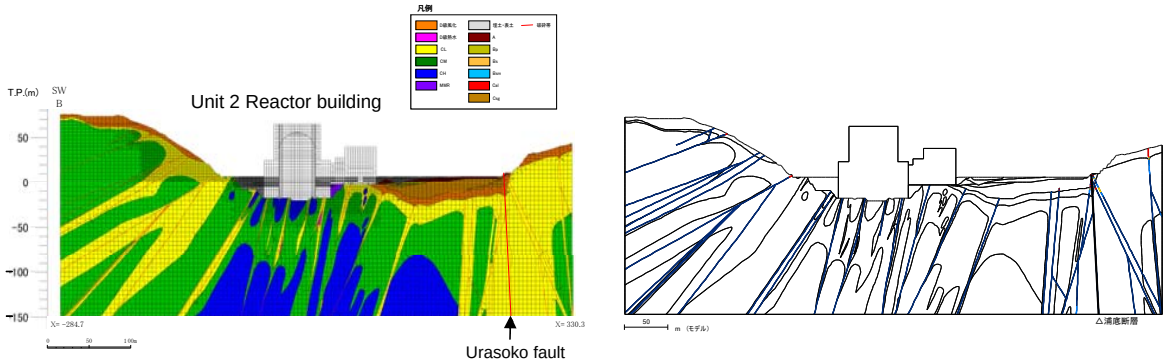

Fig. Vertical two-dimensional FEM analysis (analysis model, distribution of local safety factors)

4. Survey for Urasoko fault and around facilities (1) Survey locations

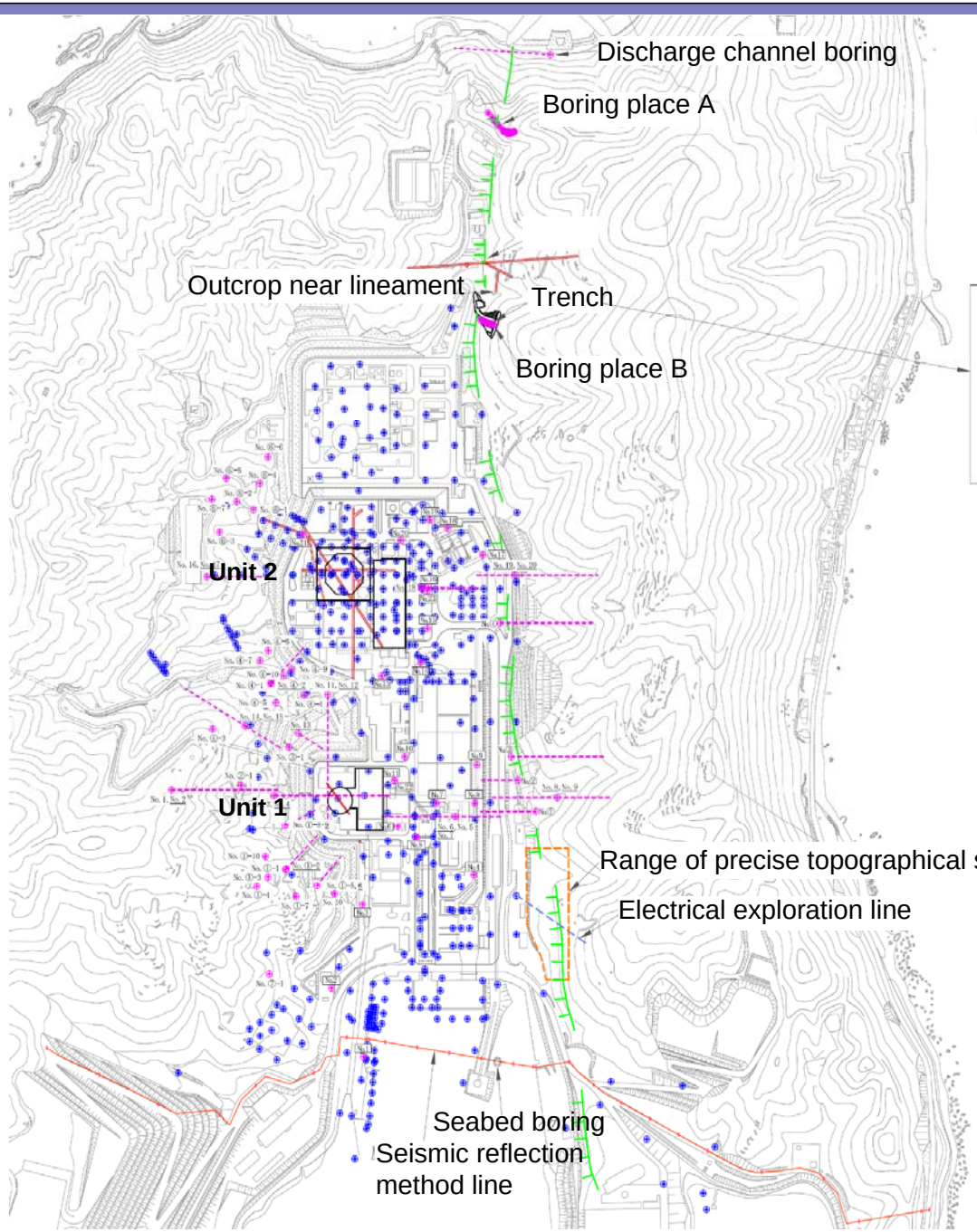

For Urasoko fault, location and angle and others have been confirmed from surveys in boring or trench or trial pit (when unit 2 was constructed).

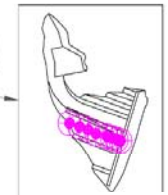

Enlarged illustration of the trench

Legend

- : Lineament
- : Place of preexisting drilling around units 1&2
- (vertical)(dip) : Place of drilling implemented for seismic back-check of units 1&2
- : Test pit, trial pit
- : Electrical exploration line
- : Seismic reflection method line
- : Range of precise topographical surveying
- : Trench

4. Survey for Urasoko fault and around facilities (2) Results ① Horizontal geological section (Units 1&2)

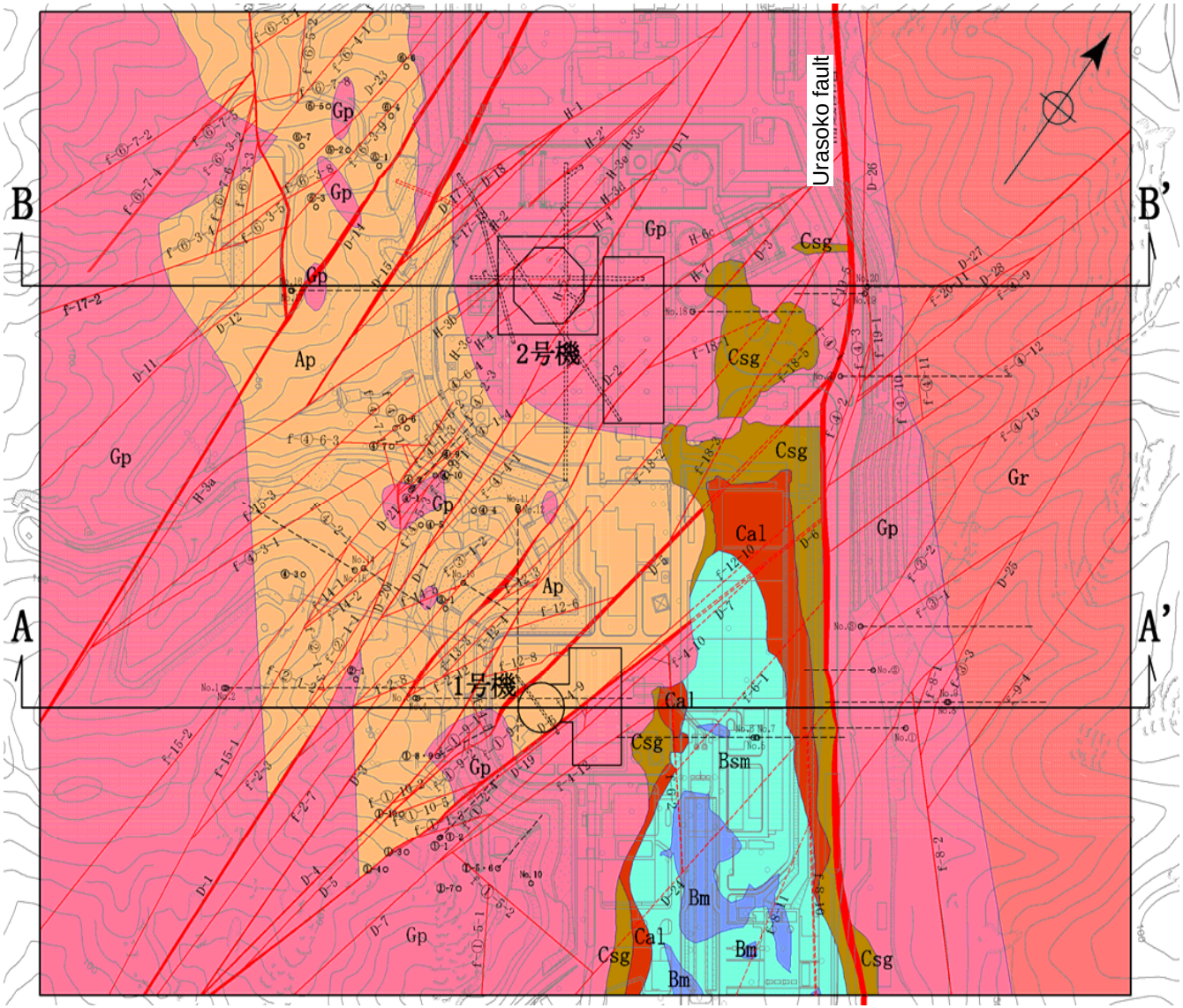

- Urasoko fault is distributed NW-SE direction.
- Shatter zones are predominant with directions between N-S and NE-SW.

Geological classification legend

- Bm — Bm layer : Enclosed bay deposits (that contains silt, fine sand and shell)
- Bsm — Bsm layer : Enclosed bay deposits (that contains medium sand, coarse sand, granule, silt and shell)
- Cal — Cal layer : Lowland deposits (that contains a large volume of fine sand, medium sand and humus)
- Csg — Csg layer : Fan deposits (that mainly contain gravel, coarse sand, medium sand and humus)

Quaternary system

- Ap — Aplite
- Gp — Granite porphyry
- Gr — Biotite granite

Kojaku Granite

H-3a — Shatter zone and its number

Fig. Horizontal cross section（ T.P.-15m ）

4. Survey for Urasoko fault and around facilities (2) Results ② Vertical geological section (Unit 1)

- Urasoko fault is a fault with an uplifting in the northeastern, bordered with bedrock and the Quaternary system in the shallows.
- As for dips, middle-angle easterly in the shallows, vertical mainly in the deeps.
- A lot of Shatter zones are high-angle westerly dips, and these have displaced the boundary between rocks types (Gp/Ap boundary).

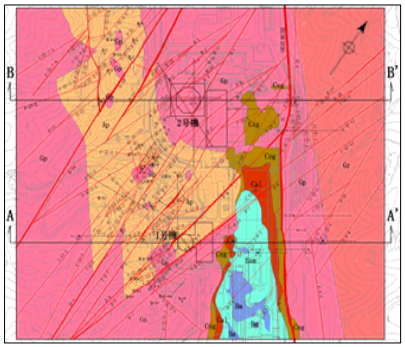

Location of this section

Geological classification legend

- bk: Surface soil and filling soil
- A: A layer : Alluvial plain deposits and talus deposits (that contain sand, gravel, silt, humus and humic matters)
- Bs: Bs layer : Deltaic deposits (that contains coarse sand, medium sand and shell)
- Bsm: Bsm layer: Enclosed bay deposits (that contains medium sand, coarse sand, granule, silt and shell)
- Cal: Cal layer : Lowland deposits (that contains a large volume of fine sand, medium sand and humus)
- Csg: Csg layer: Fan deposits (that may contain gravel, coarse sand, medium sand and humus)

Quaternary system

- Ap: Aplite
- Gp: Granite porphyry
- Gr: Biotite granite

Kojaku granite

- Boring
- H-3a: Shatter zone and its number
- Geological boundary

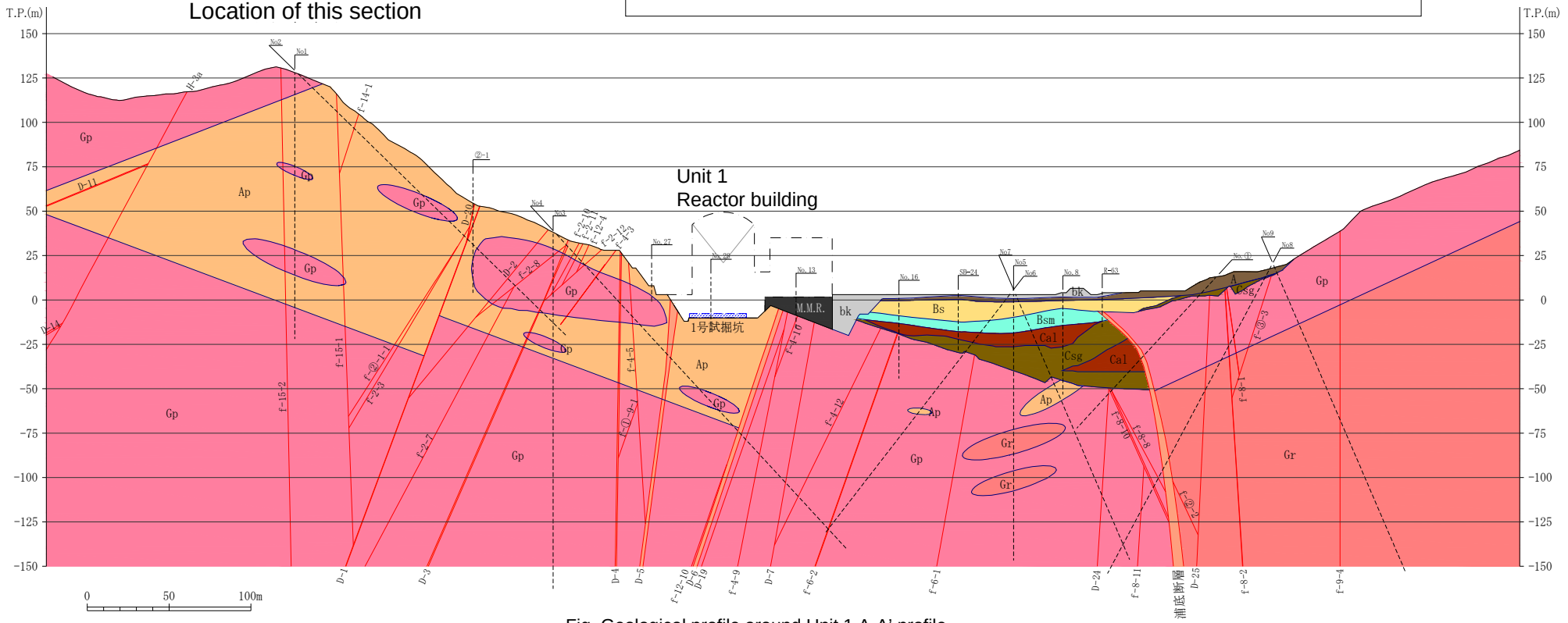

Fig. Geological profile around Unit 1 A-A' profile

4. Survey for Urasoko fault and around facilities (2) Results ③ Vertical geological section（Unit 2）

- Urasoko fault is a fault with an uplifting in the northeastern, bordered with bedrock and the Quaternary system in the shallows. And these have vertical dips mainly.
- A lot of Shatter zones are high-angle westerly dips, and these have displaced the boundary between rocks types (Gp/Ap boundary).

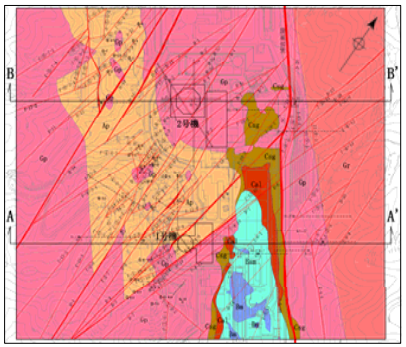

Location of this section

Geological classification legend

- bk — Surface soil and filling soil
- A — A layer : Alluvial plain deposits, fan deposits and talus deposits (that may contain sand, gravel, silt, humus and humic matters)
- Bp — Bp layer : Marsh deposits (that contains humic soil and fine sand and partly coarse sand and granule)
- Csg — Csg layer : Fan deposits (that may contain gravelk, coarse sand, medium sand and humus)

Quaternary system

- Ap — Aplite
- Gp — Granite porphyry
- Gr — Biotite granite

Kojaku granite

- Boring
- H-3a — Shatter zone and its number
- Geological boundary

SW B — NE B'

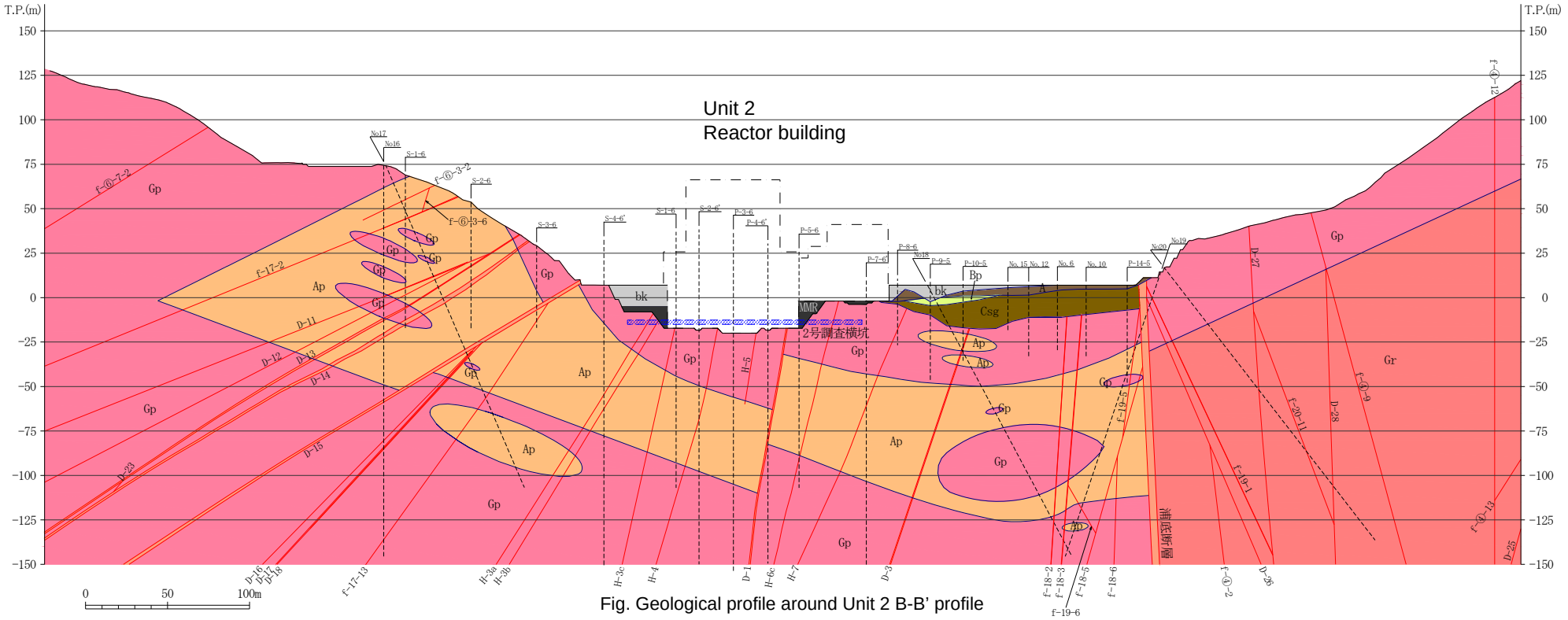

Fig. Geological profile around Unit 2 B-B' profile

5. Examination based on the elasticity theory of dislocation (1) Policy of analysis

・Based on the elasticity theory of dislocation, we studied vertical displacement (inclination) and horizontal deformation (shearing strain) of the foundation for reactor building to be caused by the activity of Urasoko-Uchiikemi fault.
・We set the conditions of study with using the concept of Tsunami Evaluation Method* as a reference, which is based on geological survey and the elasticity theory of dislocation.
・In conducting study, we also took into consideration the uncertainties of parameters (length of fault, angle of dip, width of fault, etc.) that are used in analysis.

＊Tsunami Evaluation Subcommittee, Nuclear Civil Engineering Committee, Japan Society of Civil Engineers (2002)

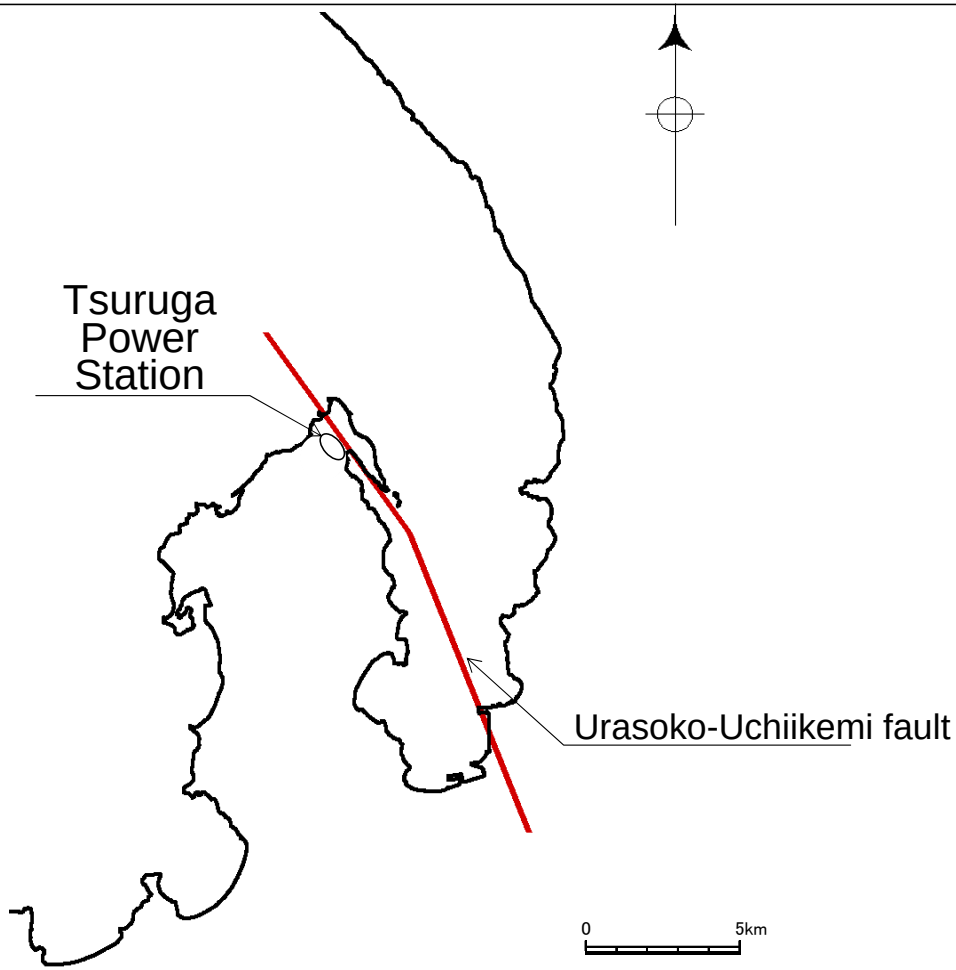

Fig. Modeled fault to be analyzed

5. Examination based on the elasticity theory of dislocation
(2) Analysis conditions

・Parameters using in examination based on the elasticity theory of dislocation is organized below.
・Basic values of each parameters and uncertainties and its reason are listed.

Table Analysis conditions of basic study and study taking uncertainties into account

Urasoko-Uchiikemi fault		Geometric shape of the fault				Slip of the fault		Ground model	
		Length of the fault	Width of the fault	Angle of dip	Depth of the fault	Slip angle (direction of P-axis)	Slip quantity	Structure	Poisson's ratio
Basic	Basic study (Case ①)	18km (20km equivalently with a width and slip)	13.3km	90°	0km	Calculated from the relation between the fault plate and the direction of compression axis in regional stress field (90° ～120°)*1	1.66m	Single-layer model*3 (homogeneous semi-infinite medium)	0.25
	Reason	・18km：length of the active fault ・20km：length set as Ss	" Tsunami Evaluation Technique for Nuclear Power Station"*2	Results of geological survey indicates it almost vertical, it is estimated that the fault has lateral-slip because of its geography and direction and dip, etc.	The fault plate is confirmed to be reached for ground surface from geography.	"Tsunami Evaluation Technique for Nuclear Power Station"*2	"Tsunami Evaluation Technique for Nuclear Power Station"*2	There is a reproduce example using single-layer model.	Ground model in seismic evaluation
Study taking uncertainties into account	Length of the fault (Case ②)	・14.6km～13.0km (Fixed south end) ・Study for influence of the fault end location. ・As Tsuruga PS is located north of Urasoko-Uchiikemi fault, movement of north end could affect to length of the fault (Slip) lager than south end. ・Movement range is set to observe peaks of dip angle and horizontal deformation. ・Urasoko-ikekawauchi (25km) ・As it is one of the uncertainty in seismic evaluation.	13.3km	90°	0km	The slip angle that indicated maximum dip or maximum horizontal deformation in basic study.	Slip quantity due to fault length	Basic study	Basic study
	Width of the fault (Case ③)	18km	5/6 times 4/6 times 3/6 times ・The width is set to be less than a half of the length.	90°	0km	The slip angle that indicated maximum dip or maximum horizontal deformation in basic study.	1.66m	Basic study	Basic study
	Angle of dip (Case ④)	18km	13.3km	85° E 80° E 75° E 70° E ・As the uncertainty in seismic evaluation is set to 70° E.	0km	The slip angle that indicated maximum dip or maximum horizontal deformation in basic study.	1.66m (85°) 1.64m (80°) 1.61m (75°) 1.56m (70°) (slip ange)	Basic study	Basic study
	Slip quantity (Case ⑤)	18km	13.3km	90°	0km	The slip angle that indicated maximum dip or maximum horizontal deformation in basic study.	Calculated from formulas ・Comparing with the Matsuda formula to calculate displacement of ground surface, etc.	Basic study	Basic study
	Ground model (Case ⑥)	18km	13.3km	90°	0km	The slip angle that indicated maximum dip or maximum horizontal deformation in basic study.	1.66m	Ground model using in seismic evaluation Multi-layer model*3	Value due to each density ρ , Vs, Vp of layers
	Fault model (Case ⑦)	The fault model using in seismic evaluation (upper：Basic factor of seismic center, downward ：Considered depth uncertainty)						Single-layer model	0.25
		20km	16km	90°	4km	0° (Left-lateral slip)	Considering asperity		
		20km	17km	90°	3km				

＊1 Direction of the compression axis (P-axis) in regional stress field is represented angle from north with clockwise.

＊2 This analysis refers to a concept of "Tsunami Evaluation Technique for Nuclear Power Station" (Tsunami Evaluation Subcommittee, Nuclear Civil Engineering Committee, Japan Society of Civil Engineers (2002)) , as tsunami evaluation is need to calculate initial seabed movement.

＊3 Single-layer model due to Okada(1992I), Multi-layer model due to Wang et al.(2003)

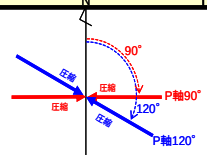

5. Examination based on the elasticity theory of dislocation (3) Dip of Reactor building (basic study) Case① depend on P-axis variable

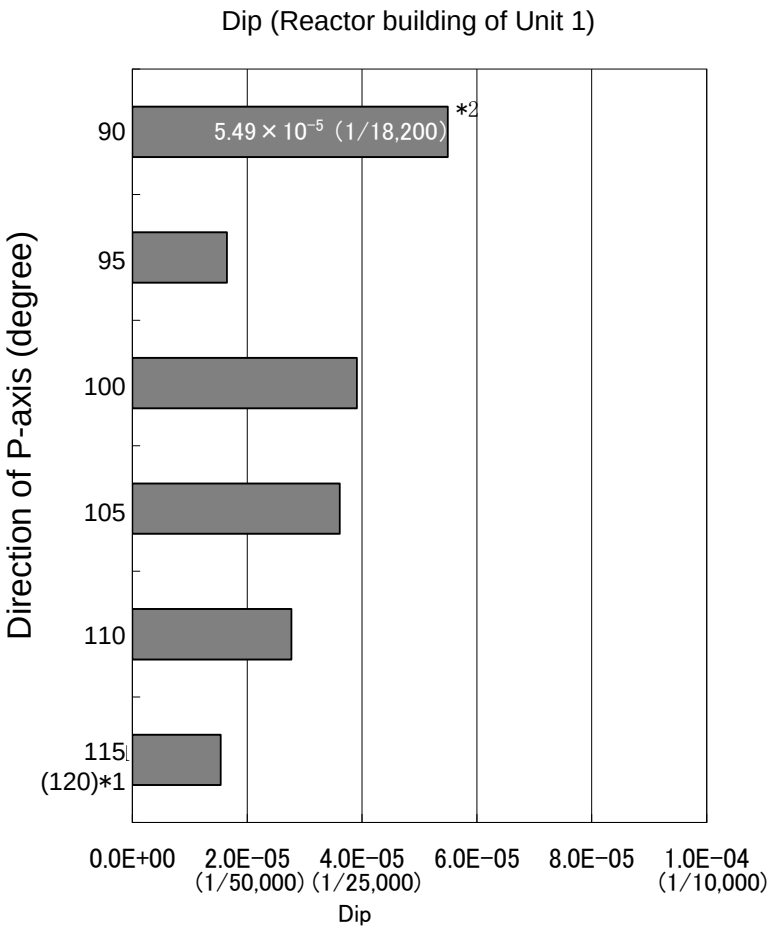

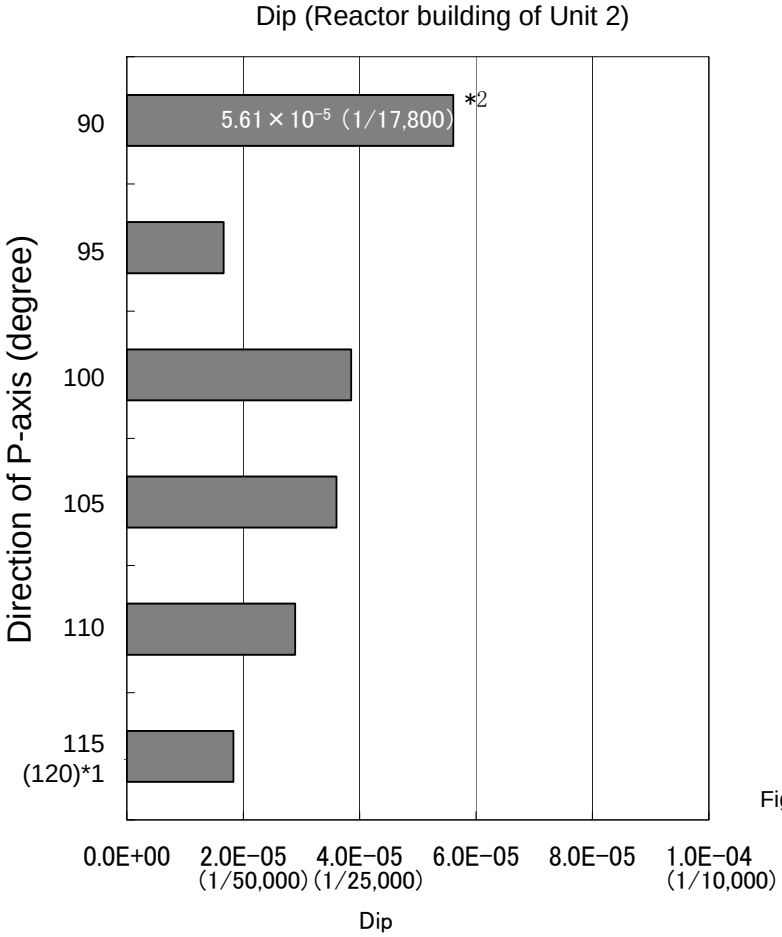

Fig. Dips of reactor buildings

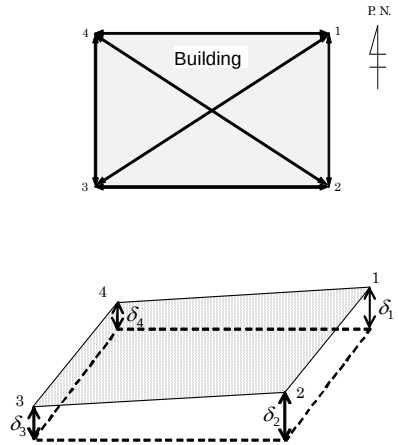

Vertical displacement is maximum value of δ_1, δ_2, δ_3, δ_4

Dip is maximum value of six directions calculated from below equation.

$$Dip_{ij} = |\delta_i - \delta_j| / L_{ij}$$

L: distance between two points

Fig. Calculation of vertical displacement and dip of building

・In this basic study, the P-axis direction which make dip maximum have been defined.
・As for dips of reactor buildings, six dips are calculated from vertical displacement at 4 corners as illustration.
・Maximum dips is indicated when P-axis is 90 degree in both Unit 1 and Unit 2.
・In later study taking uncertainties into account, P-axis direction is set to 90 degree.

∗1 In the P-axis 120° , only lateral slip occurred as the P-axis 115° .
∗2 Maximum dips are 1/18,200 at Unit 1, and 1/17,800 at Unit 2。

5. Examination based on the elasticity theory of dislocation (3) Dip of the site (basic study) Case① basic study (P-axis 90°)

	Vertical displacement [m]	Dip
Unit1 Reactor Building	-0.55（P-axis 90°）	5.49×10^{-5}（1/18,200）
Unit2 Reactor Building	-0.55（P-axis 90°）	5.61×10^{-5}（1/17,800）

Vertical displacement and dip is showed below in the case using P-axis 90° that indicated maximum dip at Unit 1&2.

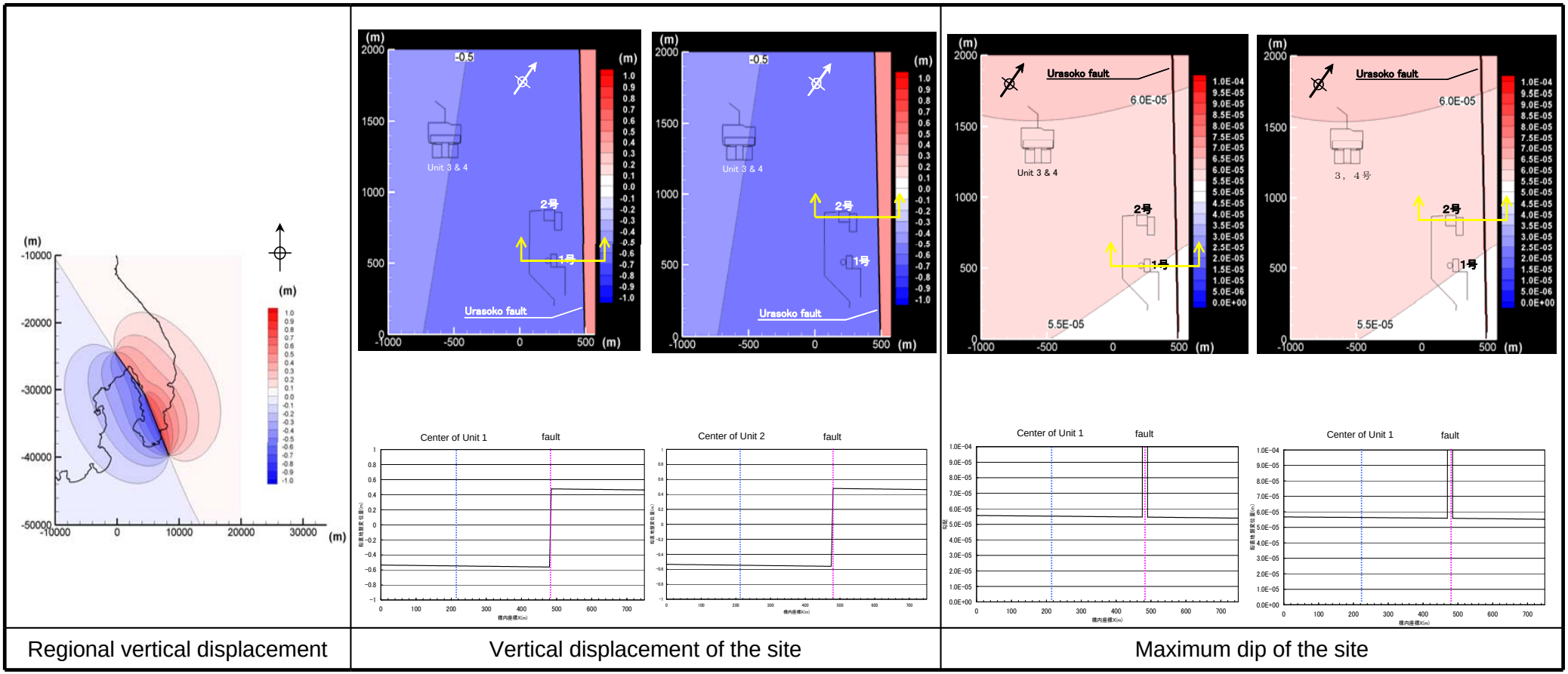

Regional vertical displacement | Vertical displacement of the site | Maximum dip of the site

Fig. Vertical displacement and maximum dip of the site

Result with P-axis 90° is illustrated.

5. Examination based on the elasticity theory of dislocation (4) Dip of reactor building (taking account of uncertainty) Case②～④ Length and angle and width of the fault（Unit 1 Reactor Building）

・The case is examined with uncertainties of fault length and angle and width for P-axis90° that indicated maximum dip in the basic study.
・Result of examinations, the case indicates maximum dip, in which assuming that the fault length (north end of the fault) is around the reactor building. The value of Unit 1 Reactor building is 1/2,100.

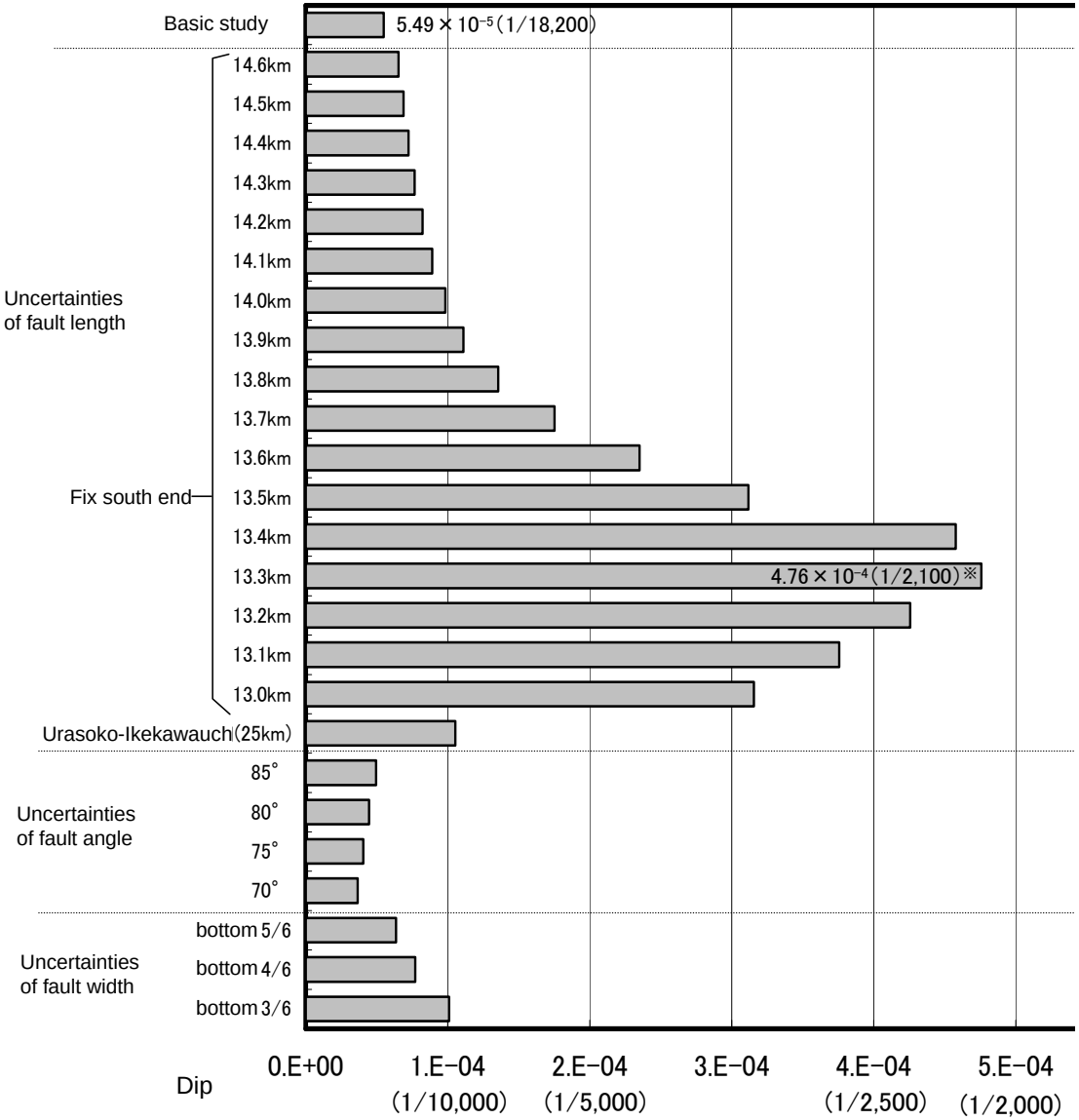

※ Maximum value of dip 4.76×10⁻⁴(1/2,100)

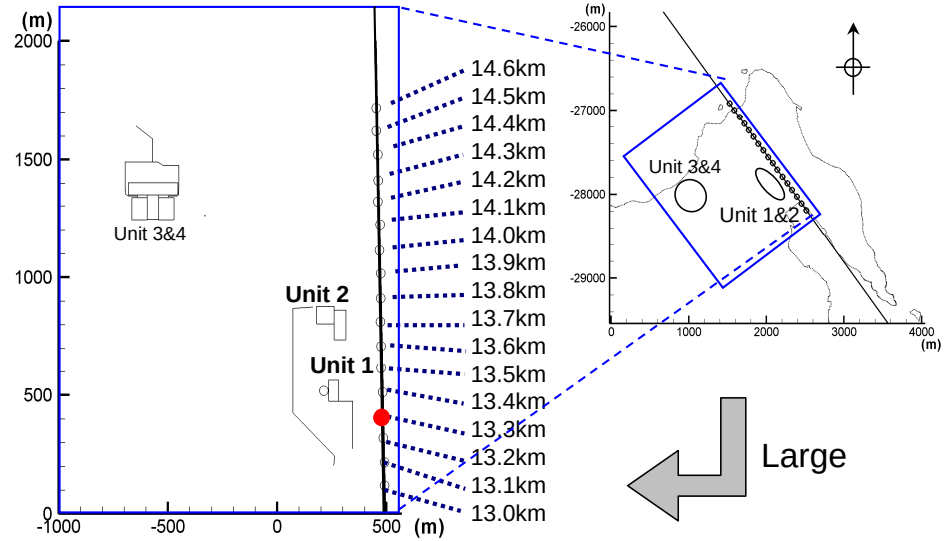

As Tsuruga PS is located north of Urasoko-Uchiikemi fault, movement of north end could affect to length of the fault (Slip) larger than south end, therefore south end of the fault is set to be fixed.

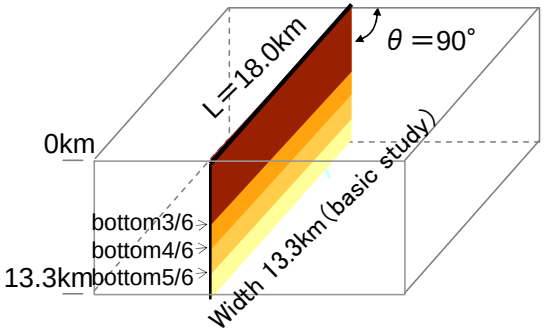

Fault width W 13.3km
(basic study)
① 5/6 W = 11.1km
② 4/6 W = 8.9km
③ 3/6 W = 6.7km

Fig. Dip studied with uncertainties (Unit 1 Reactor Building)

5. Examination based on the elasticity theory of dislocation (4) Dip of reactor building (taking account of uncertainty) Case②～④ Length and angle and width of the fault（Unit 2 Reactor Building）

・The case is examined with uncertainties of fault length and angle and width for P-axis90° that indicated maximum dip in the basic study.
・Result of examinations, the case indicates maximum dip, in which assuming that the fault length (north end of the fault) is around the reactor building. The value of Unit 2 Reactor building is 1/1,800.

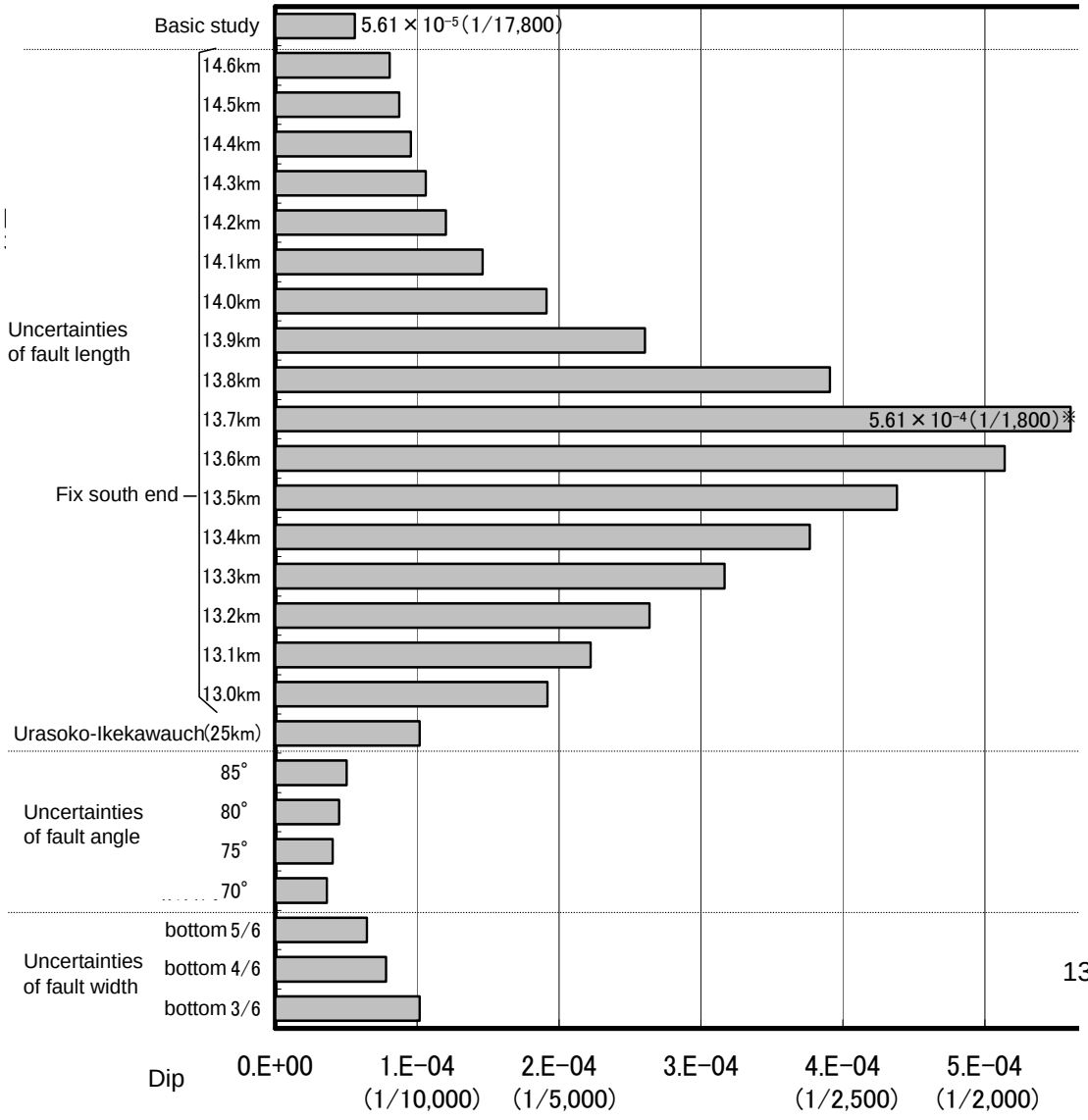

※ Maximum value of dip 5.61×10⁻⁴(1/1,800)

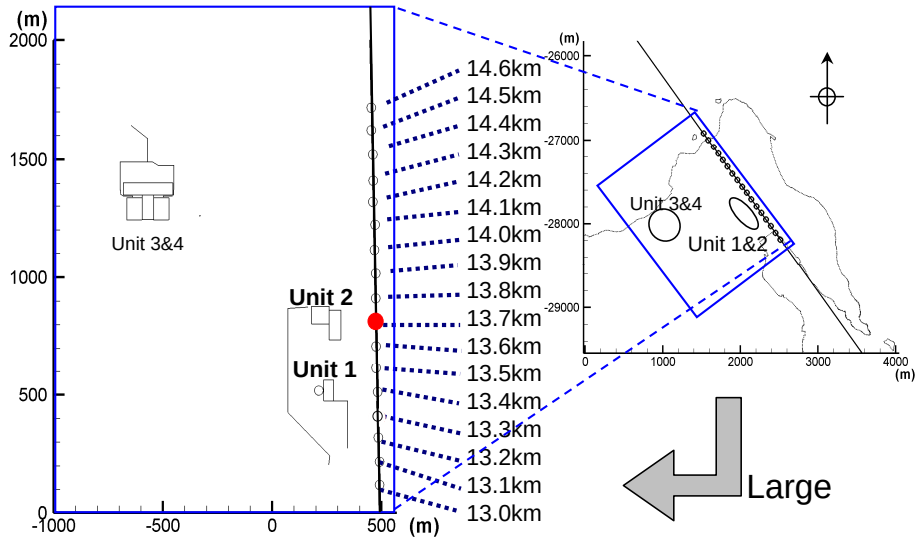

As Tsuruga PS is located north of Urasoko-Uchiikemi fault, movement of north end could affect to length of the fault (Slip) lager than south end, therefore south end of the fault is set to be fixed.

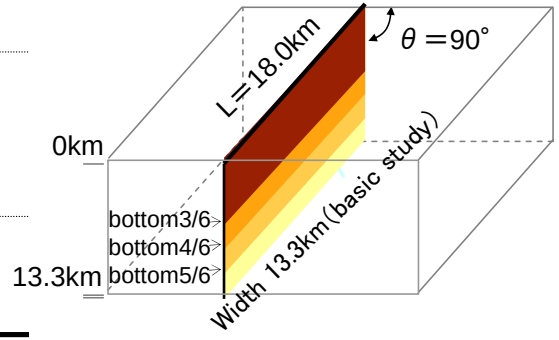

Fault width W 13.3km
(basic study)
① 5/6 W = 11.1km
② 4/6 W = 8.9km
③ 3/6 W = 6.7km

Fig. Dip studied with uncertainties (Unit 2 Reactor Building)

5. Examination based on the elasticity theory of dislocation (4) Dip of the site (taking account of uncertainty) Case②～④ with maximum dip of reactor building

Vertical displacement and dip of the site are showed below, in the case when reactor buildings indicated maximum dips with examination of uncertainties and P-axis90°.

	Vertical displacement [m]	Dip	Uncertainty
Unit 1 Reactor Building	- 0.23	4.76×10^{-4}（1/2,100）	Fault length 13.3km（P-axis90°）
Unit 2 Reactor Building	- 0.28	5.61×10^{-4}（1/1,800）	Fault length 13.7km（P-axis90°）

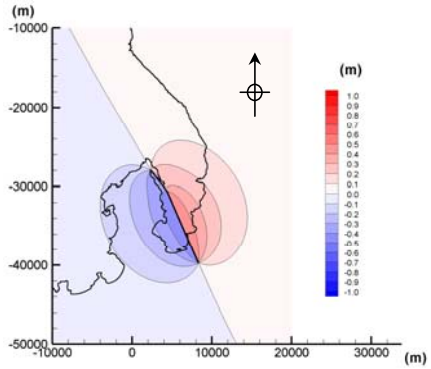

【with maximum dip of Unit 1】

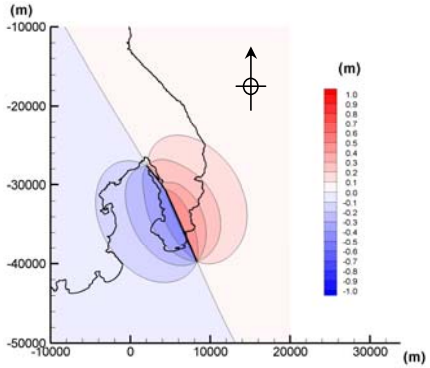

【with maximu dip of Unit 2】

Regional vertical displacement

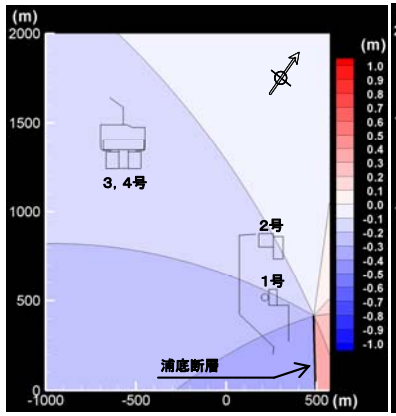

【with maximum dip of Unit 1】

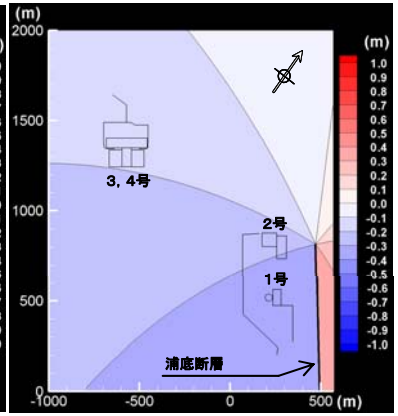

【with maximum dip of Unit 2】

Vertical displacement of the site

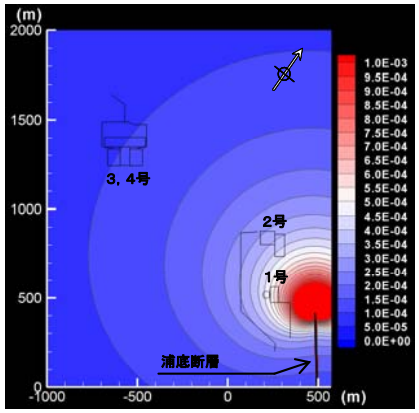

【with maximum dip of Unit 1】

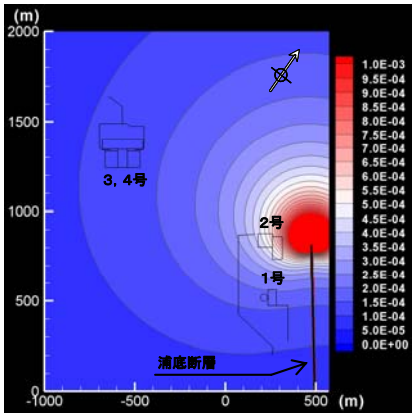

【with maximum dip of Unit 1】

Maximum dip of the site

Result with P-axis 90° is illustrated.

Fig. Vertical displacement and maximum dip of the site

5. Examination based on the elasticity theory of dislocation (4) Dip (taking account of uncertainty) Case⑤ Comparison of slips

・Slip of the fault is set based on the concept of Tsunami Evaluation Technique(2002) in principle.
・In order to make sure that set slip quantity has validity, we have compared with value from other formulas which were related to slip.
・As a result, values based on Tsunami Evaluation Technique(2002) have been larger than others
・The method in which slip is set based on Tsunami Evaluation Technique(2002) has been conservative results, because vertical displacement and dip are becoming larger in proportion to slip In the elasticity theory of dislocation.

Table Comparison of slip in Urasoko-Uchiikemi faut

	Fault length	Fault width	Fault slope	Slip	
Tsunami Evaluation Technique (2002)	20km	13.3km	90°	1.66m	
Matsuda (1975) ※1	f20km	No examination	No examination	1.59m	
Sato (1989) ※2	20km	10.0km	No examination	0.60m	
Model for seismic evaluation	20km	16.0km	90°	0.509m (Average slip D)	(information) 1.022m (Asperity) 0.398m (Background field)

Basic study

Tsunami Evaluation Technique (2002)

$D = M_0/(\mu \cdot S)$
D : Slip
M_0 : Seismic Moment
μ : Modulus of Rigidity ※3
S : Section of Fault

(Calculate M_0 from Takemura(1998)※4 and kanamori(1997)※5)

Matsuda (1975)

$\log L = 0.6M - 2.9$
$\log D = 0.6M - 4.0$
D : Slip (m)
M : Seismic Scale (Magnitude M)
L : Length of Fault (km)

Sato (1989)

$\log L = 0.5M - 1.88$
$\log D = 0.5M - 3.40$
D : Slip (m)
M : Seismic Scale (Magnitude M)
L : Length of Fault (km)

Model for seismic evaluation

$D = M_0/(\mu \cdot S)$
D : Average Slip
M_0 : Seismic Moment
μ : Modulus of Regidity
S : Section of Fault

※1 Matsuda Tokihiko, Seismic scale and cycle of earthquake caused by active fault, Jishin 2nd vol.28(1975), pp.269-283.
※2 Sato Ryosuke, The handbook of seismic fault in Japan(1989)
※3 Using 3.5×10^{10}N/m^2 based on Tsunami Evaluation Technique(2002)
※4 Takemura Masayuki, Scaling rule of distrophism earthquake in Japan –A influence of fault and relation to damage-, Jishin 2nd, vol.51(1998), pp.211-228
※5 Kanamori,H(1997) : The energy release in great earthquakes, Journal of Geophysical Research, Vol.82, No.20, pp.2981-2987

5. Examination based on the elasticity theory of dislocation (4) Dip (taking account of uncertainty)
Case⑥ Uncertainties of ground model

・In order to study for uncertainties of ground model, the result using basic study (Single-layer model) have been compared with the result using Multi-layer model in the ground structure.
・Physical properties of the ground in Multi-layer model have been similar to the analysis model in seismic evaluation using fault model, and the elasticity theory of dislocation (Multi-layer model) *Wang et al*. have been examined.
・The result of Single-layer model have not been different from the Multi-layer model hardly.
・In studies of uncertainties, therefore, Single-layer model is determined to apply for ground structure in principle.

Table Ground Model for deciding of basic seismic ground motion in Tsuruga Power Station

E.L. (m)	layer	thickness (m)	density ρ (t/m^3)	Vs (m/s)	Vp (m/s)	Poisson's ratio
-9						
-44	1	34	2.6	1,450	3,700	0.41
-130	2	86	2.6	1,760	4,300	0.40
-200	3	70	2.6	2,200	4,600	0.35
-630	3'	430	2.6	2,200	4,600	0.35
-1400	4	770	2.6	2,800	5,130	0.29
-4000	5	2600	2.6	3,100	5,310	0.24
	6	—	2.7	3,600	6,270	0.25

$$V_p / V_s = \sqrt{\frac{2(1-\sigma)}{1-2\sigma}}$$

σ : Poisson's ratio

Table Dips of building (Unit 1) with Single-layer and Multi-layer model

Case	Vertical dislocation (m)	Dip
Single-layer (basic study)	-0.55	5.49×10^{-5} (1/18,200)
Multi-layer	-0.55	5.65×10^{-5} (1/17,700)

Table Dips of building (Unit 2) with Single layer and Multi-layer model

Case	Vertical dislocation (m)	Dip
Single-layer (basic study)	-0.55	5.61×10^{-5} (1/17,800)
Multi-layer	-0.55	5.73×10^{-5} (1/17,500)

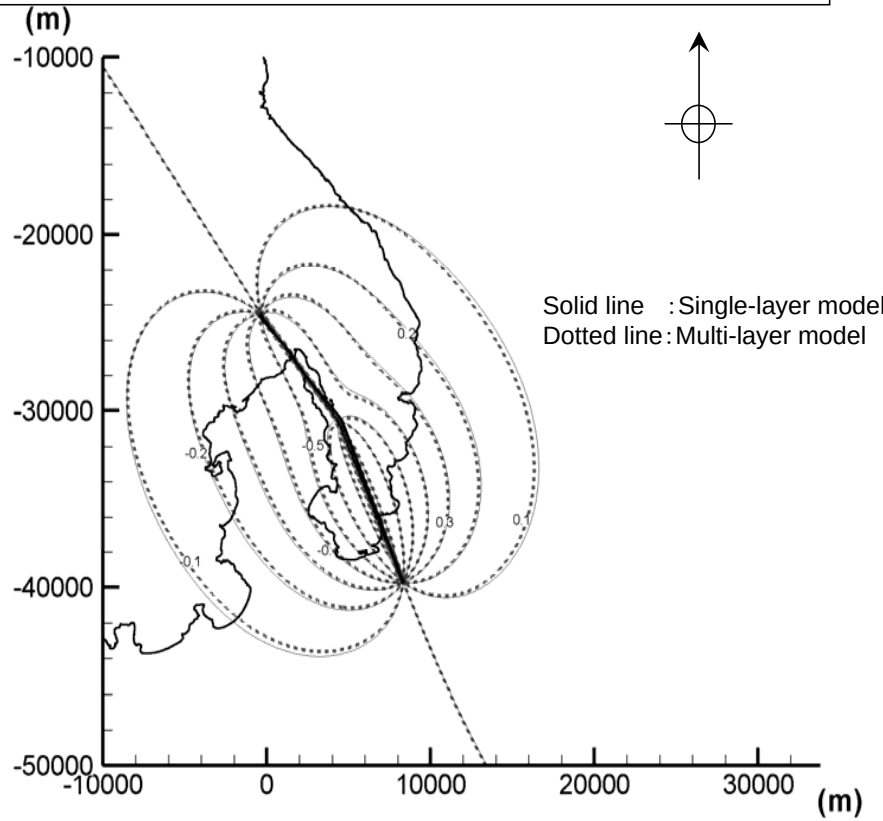

Fig. Comparison between Single-layer with Multi-layer model in distribution of vertical ground dislocation

Single-layer model : Okada(1992)
Multi-layer model : Wang et al. (2003)

5. Examination based on the elasticity theory of dislocation (4) Dip (taking account of uncertainty)
Case⑦ Uncertainties of ground model（Depth 4km) No.1(1)

・The fault model in seismic evaluation have been examined to study for uncertainties of fault model.
・The case No.1 is depth of fault top 4km, and No.2 is 3km in fault models respectively, these are similar to the concept of seismic evaluation.
・As a result, both vertical dislocation and dip was smaller than results of basic study.

Depth of the fault top 4km

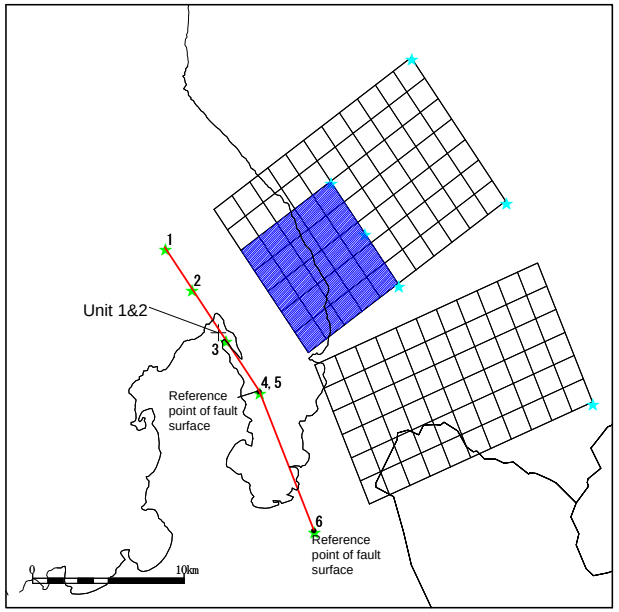

※ Drawing dip 90° as dip 0°

★ : Starting point of destruction

i）Fault location

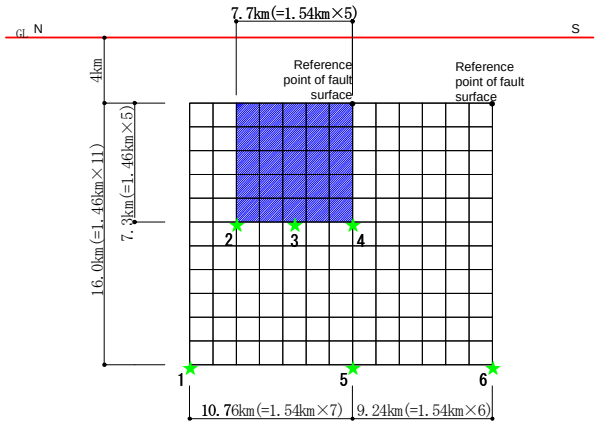

ii）Cross section

Fig. Schematic view of the fault model using to seismic evaluation in Tsuruga Power Station (Depth of fault top 4km)

Table Parameters of the fault model using to seismic evaluation in Tsuruga Power Station (Depth of fault top 4km)

Parameters of fault	Values	Means
Fault length L（km）	20 (18)	Extending fault location
Fault angle（° ）	90 (90)	The result of survey
Depth of the fault top（km） Depth of the fault bottom（km）	4 (0) 20 (13.3)	Setting with reference to occurrence of minute earthquake and underground structure in order to keep scale
Fault width W（km）	16 (13.3)	The same as above
Section of fault S（km^2）	320 (239.4)	Calculation from fault surface
Crack propagation pattern	Concentric circular	—
Seismic moment M_0（Nm）	5.70×10^{18}	$M_0=\{S/(4.24\times10^{-11})\}^{2.0}$
Modulus of rigidity (N/m^2)	3.5×10^{10}	$\mu=\rho\beta^2$、ρ=2.7g/cm^3、β=3.6km/s
Average slip D（cm）	50.9	$D=M_0/(\mu S)$
Average stress drop $\Delta\sigma$（MPa）	2.4	$\Delta\sigma=(7\pi^{1.5}/16)(M_0/S^{1.5})$
Crack propagation velocity Vr（km/s）	2.59	$Vr=0.72\beta$
Startup time Tr (sec)	0.78	$Tr=2.03\times10^{-9}M_0^{1/3}$
Cutoff frequency fmax（Hz）	8.3	Kagawa et al.(2003)
Short-period level A（Nm/s^2）	9.47×10^{18}	$A=2.46\times10^{17}\times M_0^{1/3}$
Value of Q	$50f^{1.1}$	Sato et al.(2007)

	Parameters of fault	Values	Means
Total asperity	Section S_a（km^2）	56.71 (not consider)	$Sa=\pi r^2$ $r=(7\pi M_0\beta^2)/(4AaR)$,$R=(S/\pi)^{0.5}$
	Average slip D_a（cm）	102.2（166）	$D_a=\gamma_D D$、γ_D=2.01
	Seismic moment M_{0a}（Nm）	2.03×10^{18}	$M_{0a}=\mu S_a D_a$
	Stress drop $\Delta\sigma_a$（MPa）	13.7	$\Delta\sigma_a=(S/S_a)\Delta\sigma$
Background field	Section S_b（km^2）	263.29 (not consider)	$S_b=S-S_a$
	Average slip D_b（cm）	39.8 (166)	$D_b=M_{0b}/(\mu S_b)$
	Seismic moment M_{0b}（Nm）	3.67×10^{18}	$M_{0b}=M_0-M_{0a}$
	Effective stress $\Delta\sigma_b$（MPa）	2.7	$\sigma_b=0.2\Delta\sigma_a$

（Note） Single-layer mode based on Okada's formula, and physical properties of ground was similar to basic study.

Parameters using to calculation based on the elasticity theory of dislocation
Inside ( ) represents parameters on basic study

5. Examination based on the elasticity theory of dislocation (4) Dip (taking account of uncertainty)
Case⑦ Uncertainties of ground model（Depth 4km) No.1(2)

Table Vertical dislocations and dips of reactor buildings in seismic evaluation models (Depth of fault top 4km)

	Vertical dislocation [m]	Dip
Unit 1 Reactor Building	-0.01	4.41×10^{-6}（1/227,000）
Unit 2 Reactor Building	-0.01	5.74×10^{-6}（1/174,300）

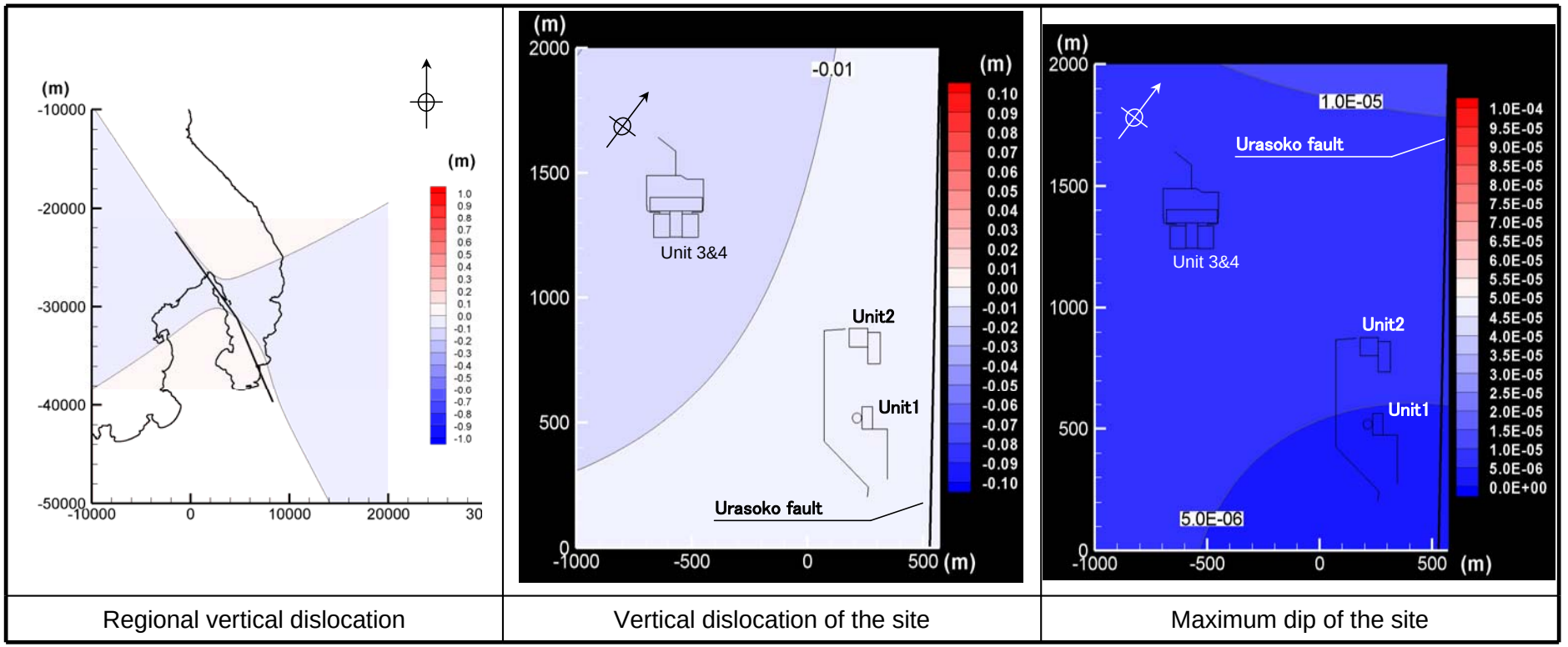

Regional vertical dislocation	Vertical dislocation of the site	Maximum dip of the site

Fig. Distribution of vertical dislocation and dip (Depth of fault top 4km)

5. Examination based on the elasticity theory of dislocation (4) Dip (taking account of uncertainty)
Case⑦ Uncertainties of ground model（Depth 3km) No.2(1)

Depth of fault top 3km

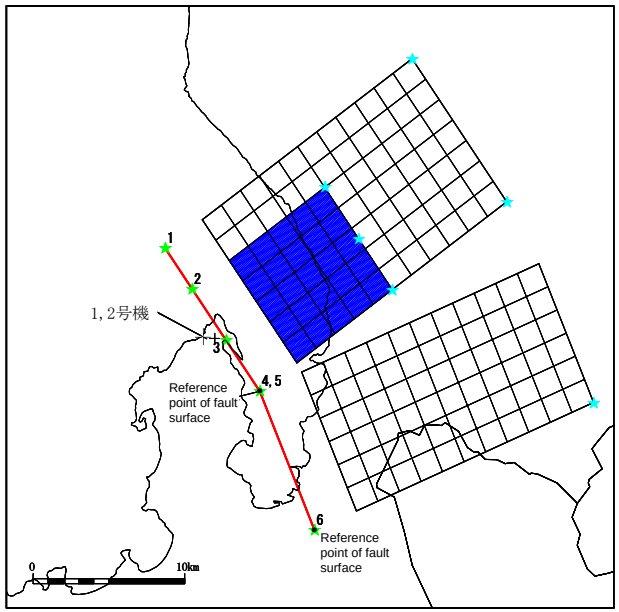

※ Drawing dip 90° as dip 0°

★ : Starting point of destruction

ⅰ) Fault location

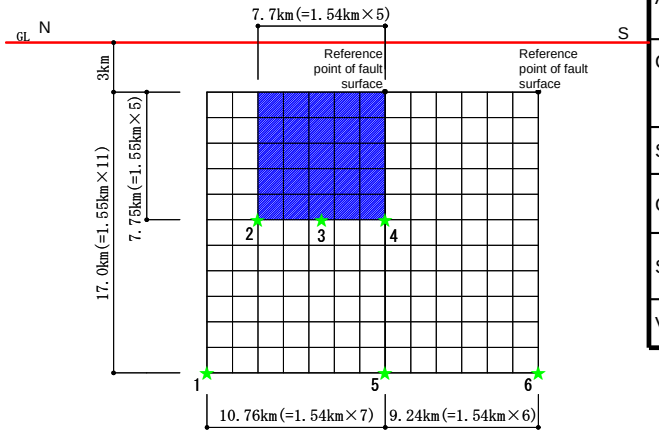

ⅱ) Cross section

Table Parameters of the fault model using to seismic evaluation in Tsuruga Power Station (Depth of fault top 3km)

Parameters of fault	Values	Means
Fault length L（km）	20（18）	Extending fault location
Fault angle（° ）	90（90）	The result of survey
Depth of the fault top（km） Depth of the fault bottom（km）	3（0） 20（13.3）	Setting with reference to occurrence of minute earthquake and underground structure in order to keep scale
Fault width W（km）	17（13.3）	The same as above
Section of fault S（km^2）	340（239.4）	Calculation from fault surface
Crack propagation pattern	Concentric circular	—
Seismic moment M_0（Nm）	6.43×10^{18}	$M_0=\{S/(4.24\times10^{-11})\}^{2.0}$
Modulus of rigidity（N/m^2）	3.5×10^{10}	$\mu=\rho\beta^2$、ρ=2.7g/cm^3、β=3.6km/s
Average slip D（cm）	54.0	$D=M_0/(\mu S)$
Average stress drop $\Delta\sigma$	2.5	$\Delta\sigma=(7\pi^{1.5}/16)(M_0/S^{1.5})$
Crack propagation velocity Vr（km/s）	2.59	$Vr=0.72\beta$
Startup time Tr (sec)	0.81	$Tr=2.03\times10^{-9}M_0^{1/3}$
Cutoff frequency fmax（Hz）	8.3	Kagawa et al.(2003)
Short-period level A（Nm/s^2）	9.86×10^{18}	$A=2.46\times10^{17}\times M_0^{1/3}$
Value of Q	$50f^{1.1}$	Sato et al.(2007)

	Parameters of fault	Values	Means
Total asperity	Section S_a（km^2）	62.73（not consider）	$Sa=\pi r^2$ $r=(7\pi M_0\beta^2)/(4AaR)$、$R=(S/\pi)^{0.5}$
	Average slip D_a（cm）	108.6（166）	$D_a=\gamma_D D$、γ_D=2.01
	Seismic moment M_{0a}（Nm）	2.38×10^{18}	$M_{0a}=\mu S_a D_a$
	Stress drop $\Delta\sigma_a$（MPa）	13.5	$\Delta\sigma_a=(S/S_a)\Delta\sigma$
Background field	Section S_b（km^2）	277.27（not consider）	$S_b=S-S_a$
	Average slip D_b（cm）	41.7（166）	$D_b=M_{0b}/(\mu S_b)$
	Seismic moment M_{0b}（Nm）	4.05×10^{18}	$M_{0b}=M_0-M_{0a}$
	Effective stress $\Delta\sigma_b$（MPa）	2.7	$\sigma_b=0.2\Delta\sigma_a$

（Note）Single-layer mode based on Okada's formula, and physical properties of ground was similar to basic study.

Parameters using to calculation based on the elasticity theory of dislocation
Inside ( ) represents parameters oon basic study

Fig. Schematic view of the fault model using to seismic evaluation in Tsuruga Power Statrion (Depth of fault top 3km)

5. Examination based on the elasticity theory of dislocation (4) Dip (taking account of uncertainty)
Case⑦ Uncertainties of ground model（Depth 3km) No.2(2)

Table Vertical dislocations and dips of reactor buildings in seismic evaluation models (Depth of fault top 3km)

	Vertical dislocation [m]	Dip
Unit 1 Reactor Building	-0.01	5.60×10^{-6}（1/178,700）
Unit 2 Reactor Building	-0.01	7.59×10^{-6}（1/131,800）

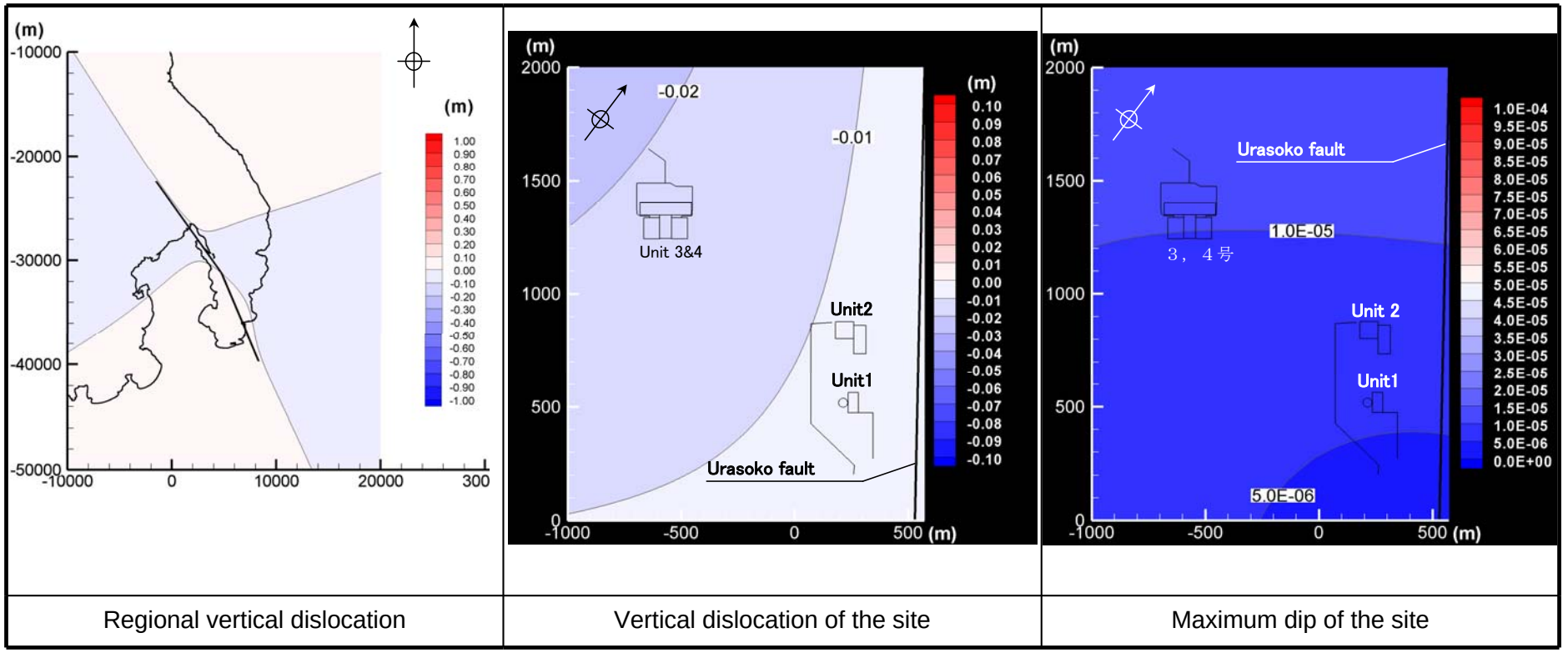

Regional vertical dislocation	Vertical dislocation of the site	Maximum dip of the site

Fig. Distribution of vertical dislocation and dip (Depth of fault top 3km)

5. Examination based on the elasticity theory of dislocation, (5) Horizontal deformation of the structure (basic case)
Study ① Parameter study on compressional axis (P-axis) in wide-area stress field

・In the basic study, parameter study on compressional axis (P-axis) in wide-area stress field was curried out. A direction of the P-axis, which maximize the deformation of the basement of rector building, was determined.
・As a parameter of the deformation, shearing strain was selected.
・The shearing strain was calculated from the horizontal displacements of the rector building corners.
・In the both cases of Unit 1 and Unit 2, P-axis at a 115 degrees angle maximized the shearing strain.
・Therefore in the study taking account of uncertainty, the angle of P-axis was defined as 115 degrees.

・"Regulatory Guide for Seismic Design of Nuclear Power Reactor Facilities" requests to evaluate "effect of a horizontal deformation against facilities if a fault have a lateral slip component".
・Urasoko fault has a left-lateral slip component. Therefore study on the deformation of the horizontal plane was carried out.

Horizontal shearing strain of reactor building of Unit 1 ※1, 2

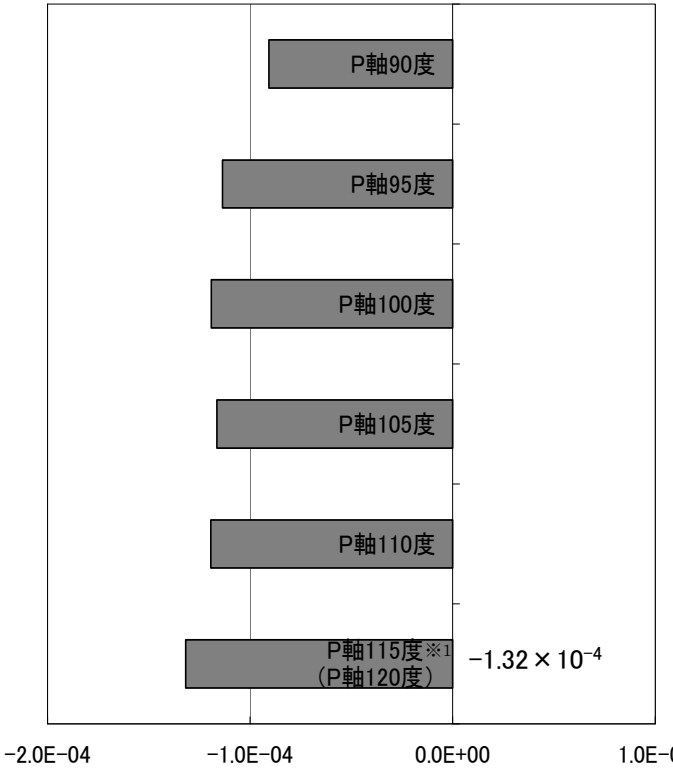

Horizontal shearing strain of reactor building of Unit 2 ※1, 2

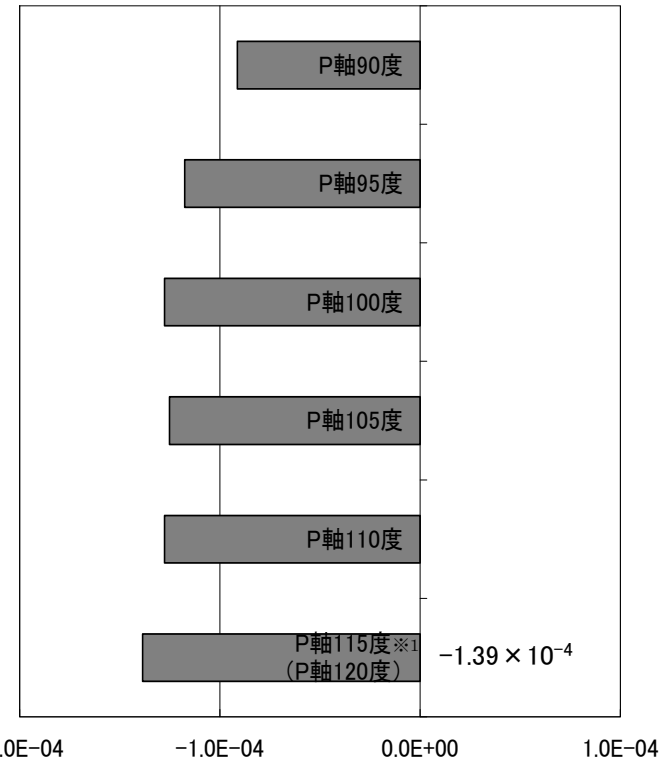

Fig. Horizontal shearing strain of reactor buildings of Unit 1 and Unit 2 (Base case)

※1 A case of P-axis at a angle of 120 degrees has only lateral slip as well as it of P-axis at a angle of 115 degrees.
※2 Scale of reactor building: Unit 1 42mx42m, Unit 2 80mx75m

Horizontal shearing strain is the maximum shearing strains of rector building calculated from the following formula.

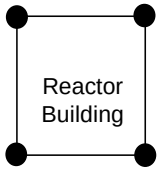

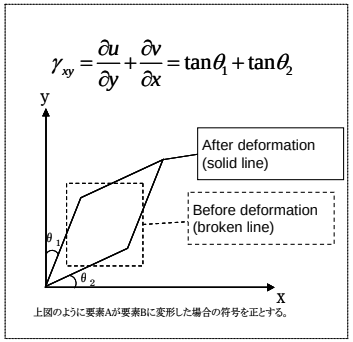

Fig. Calculation method of horizontal shearing strain of a building.

5. Examination based on the elasticity theory of dislocation, (5) Horizontal deformation of the structure (basic case)
Study ① Fundamental study (P-axis at an angle of 115 degrees)

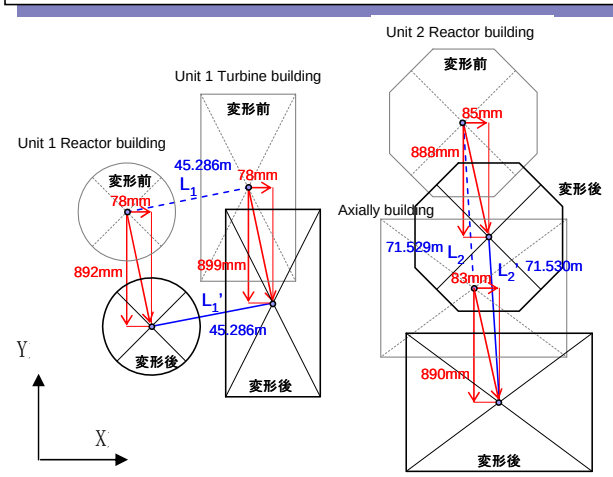

【Image of relative displacement】

・Horizontal displacement and horizontal shearing strain of the basement of Unit 1 and Unit 2 are shown in the following table in the case of P-axis at an angle of 115 degrees.
・Maximum shearing strain is -1.32×10^{-4} at Unit 1 reactor building and -1.39×10^{-4} at Unit 2 reactor building.
・The locations of rector building and surrounding ground move into a same direction with a same displacement, and the relative displacement between them is small. (For example, relative displacement between the center of reactor building and axially building is about 1mm)

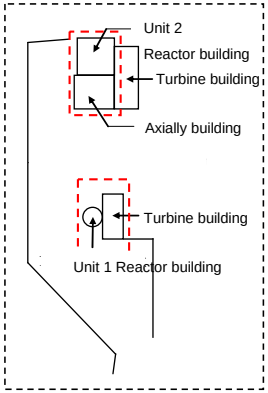

Table. Horizontal shearing strain and relative displacement with 115° P-axis

Horizontal shearing strain ※1	Relative displacement between the center of reactor building and turbine building or axially building※2
Unit 1 Rector building: -1.32×10^{-4}	-0.2mm（L_1'-L_1）
Unit 2 Rector building: -1.39×10^{-4}	1mm（L_2'-L_2）

※1 Scale of reactor building: Unit 1 42mx42m, Unit 2 80mx75m
※2 Direction away from each other is positive.

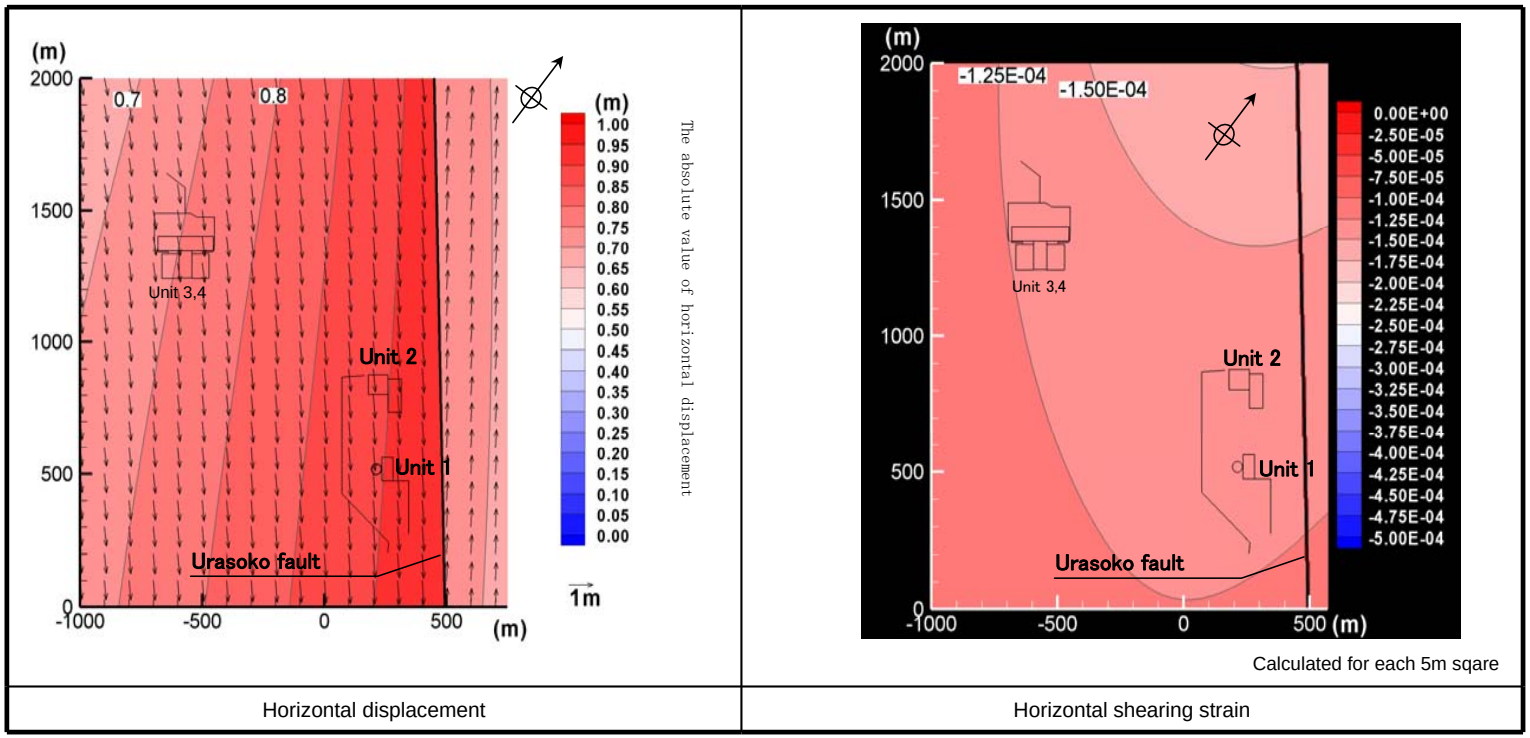

Horizontal displacement | Horizontal shearing strain

Fig. Distribution of horizontal displacement and horizontal shearing strain in the case of 115° P-axis

5. Examination based on the elasticity theory of dislocation, (6) Horizontal deformation of the structure (taking account of uncertainty)
Study ①～③ Fault length, dip angle, fault width (Unit 1 reactor building)

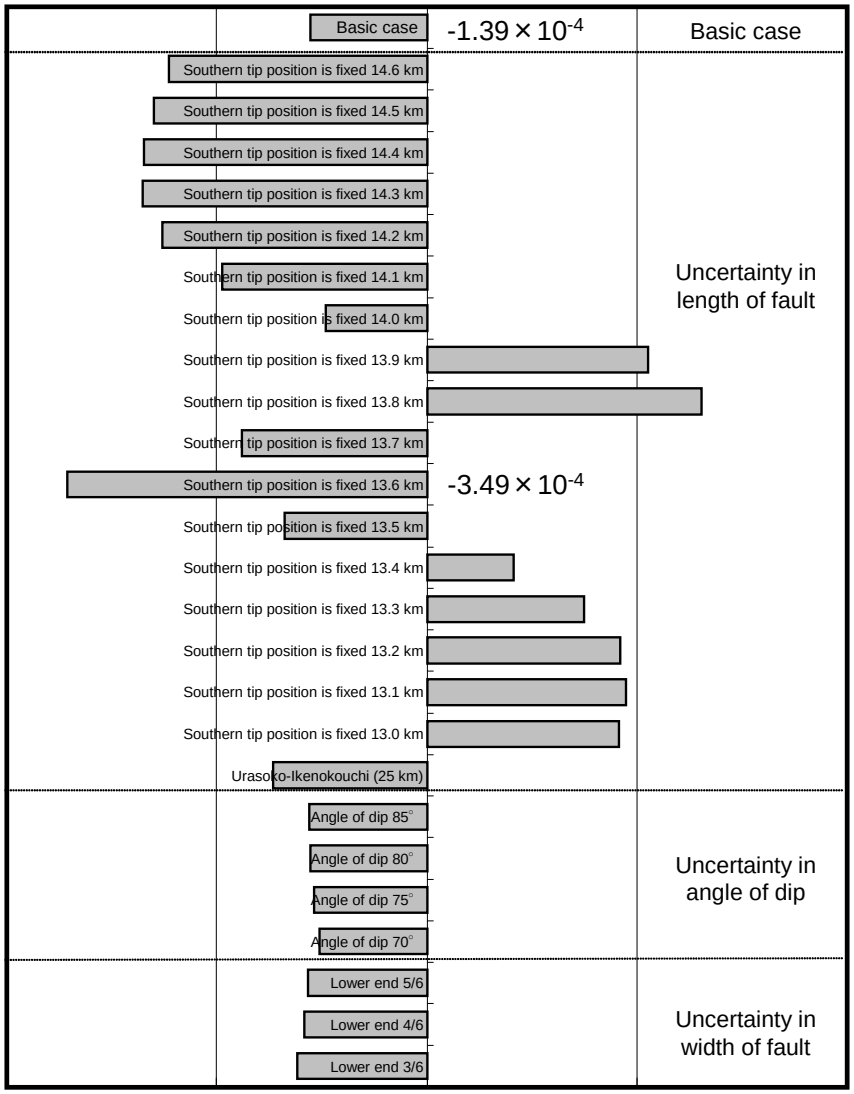

* Horizontal shearing strain acquired with a reactor building scale (Unit1: about 42 m x about 42 m)

・In basic study, as for the case of p-axis = 115° that represents the maximum shearing strain, we carried out the study with taking into account uncertainties of length of fault, angle of dip and width of fault.
・As a result, a shearing strain becomes maximum in the case of 13.3 km (the southern tip position is fixed), and is -3.49 x 10-4 at Unit 1 reactor building.

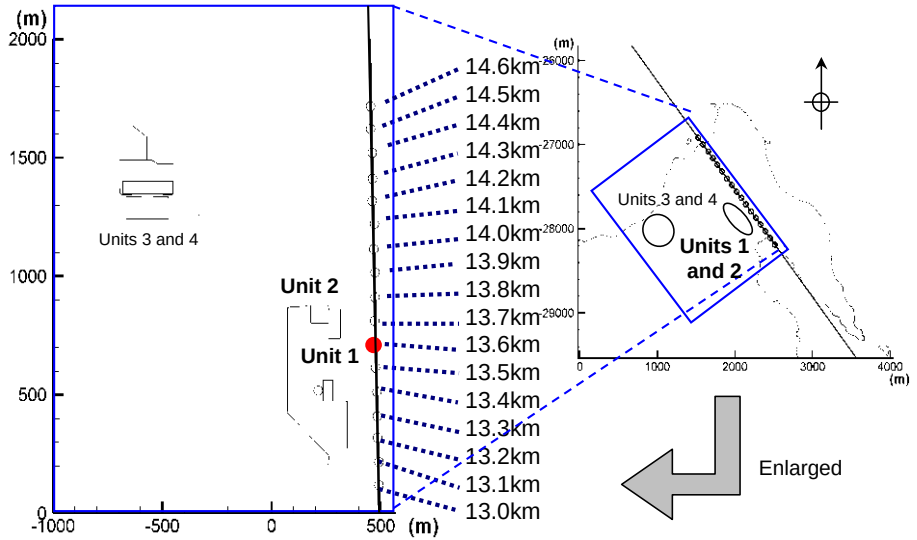

As Tsuruga Power Station is located in the north of Urasoko-Uchiikemi fault, study was done with fixing the location of the southern end of the fault with changing the location of the northern end.

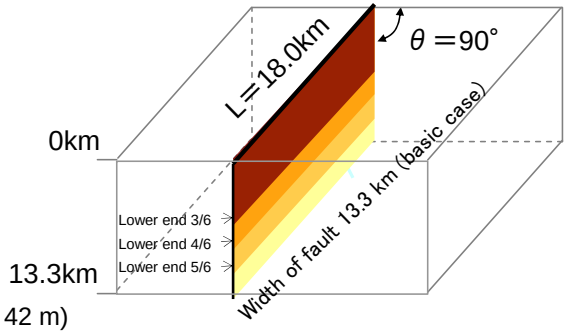

Width of fault W 13.3 km (basic case)
① 5/6 W = 11.1 km
② 4/6 W = 8.9 km
③ 3/6 W = 6.7 km

Fig. Horizontal shearing strain with taking uncertainty into account (Unit 1 reactor building)

5. Examination based on the elasticity theory of dislocation, (6) Horizontal deformation of the structure taking account of uncertainty)
Study ①～③ Fault length, dip angle, fault width (Unit 2 reactor building)

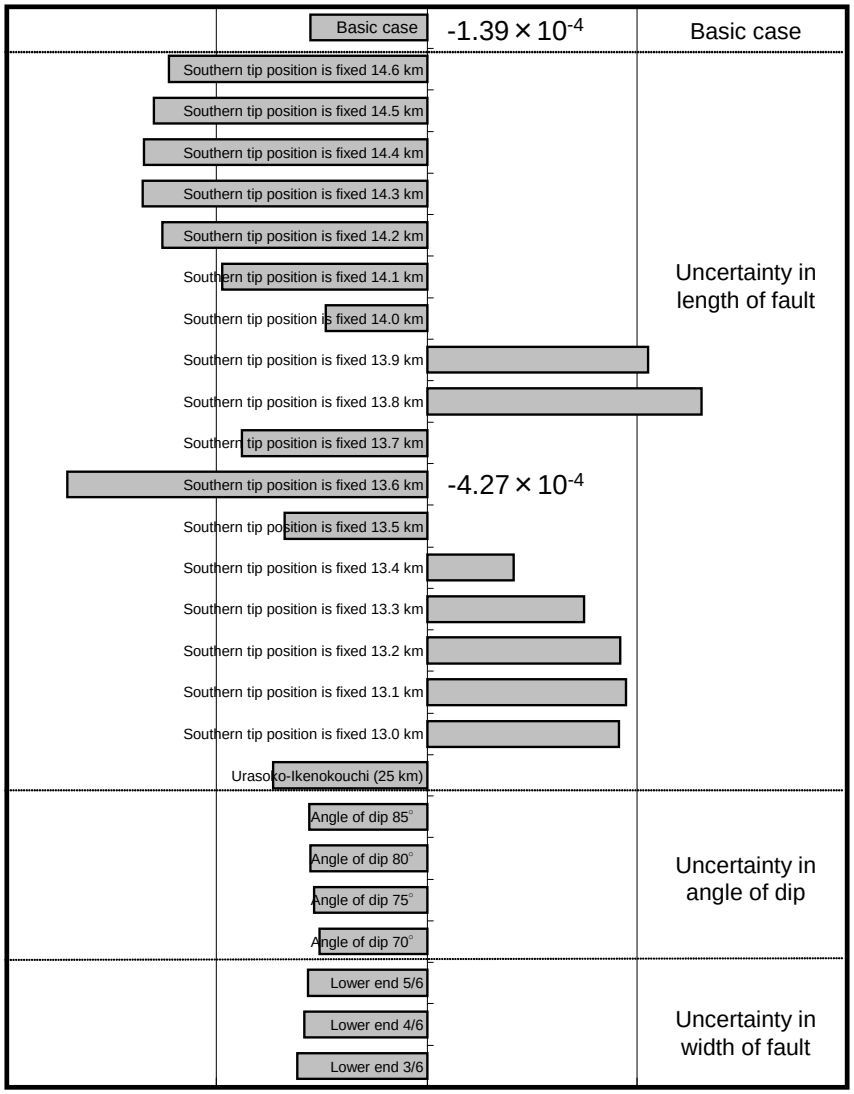

* Horizontal shearing strain acquired with a reactor building scale (Unit 2: about 80 m x about 75 m)

- In basic study, as for the case of p-axis = 115° that represents the maximum shearing strain, we carried out the study with taking into account uncertainties of length of fault, angle of dip and width of fault.
- As a result, a shearing strain becomes maximum in the case of 13.6 km (the southern tip position is fixed), and is -4.27 x 10^{-4} at Unit 2 reactor building.

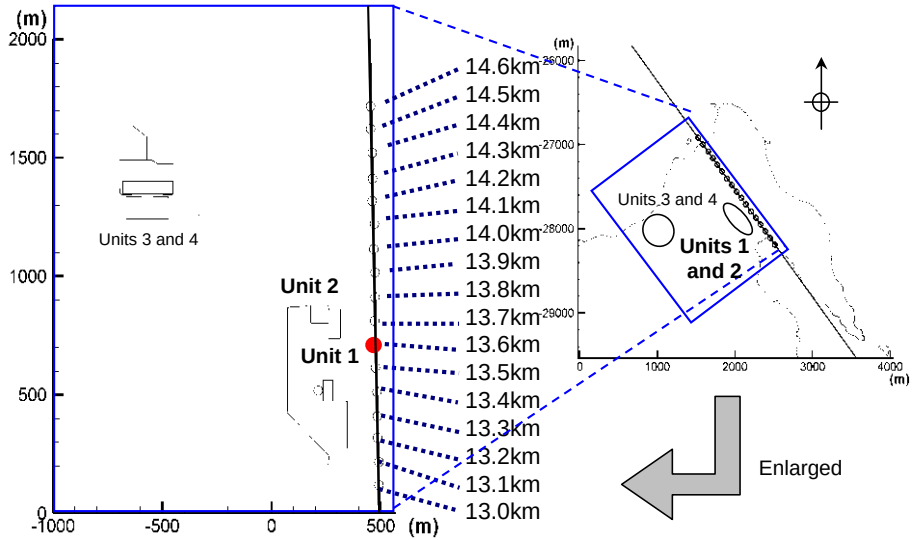

As Tsuruga Power Station is located in the north of Urasoko-Uchiikemi fault, study was done with fixing the location of the southern end of the fault with changing the location of the northern end.

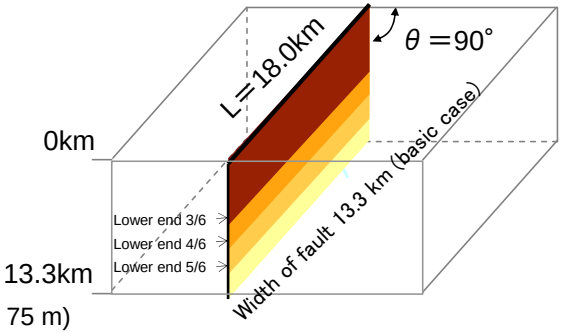

Width of fault W 13.3 km (basic case)
① 5/6 W = 11.1 km
② 4/6 W = 8.9 km
③ 3/6 W = 6.7 km

Fig. Horizontal shearing strain with taking uncertainty into account (Unit 2 reactor building)

5. Examination based on the elasticity theory of dislocation, (6) Horizontal deformation of the structure (taking uncertainty into account)
Study ②-④ Fault length, dip angle, fault width

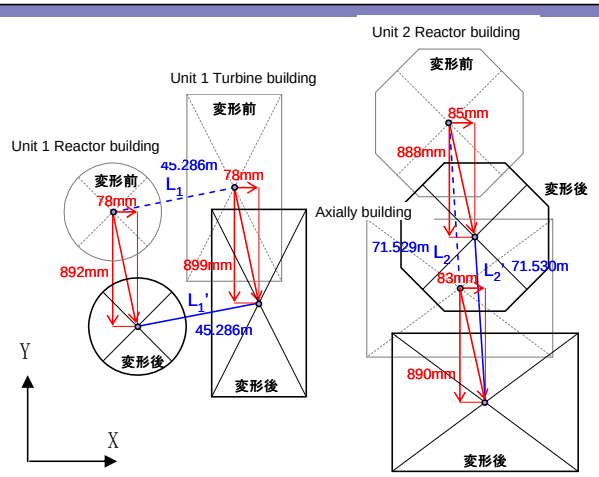

【Image of relative displacement】

・Maximum shearing strain is -3.49×10-4 at Unit 1 reactor building and -4.27×10-4 at Unit 2 reactor building.
・The locations of rector building and surrounding ground move into a same direction with a same displacement, and the relative displacement between them is small. (For example, relative displacement between the center of reactor building and axially building is about 19mm)

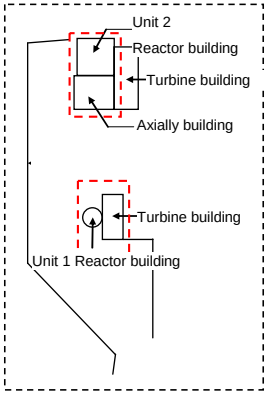

Table. Maximum horizontal shearing strain and relative displacement

Horizontal shearing strain ※1	Relative displacement between the center of reactor building and turbine building or axially building※2
Unit 1 Rector building: -3.49×10^{-4}	-0.1mm（L_1'-L_1）
Unit 2 Rector building: -4.27×10^{-4}	19mm（L_2'-L_2）

※1 Scale of reactor building: Unit 1 42mx42m, Unit 2 80mx75m
※2 Direction away from each other is positive.

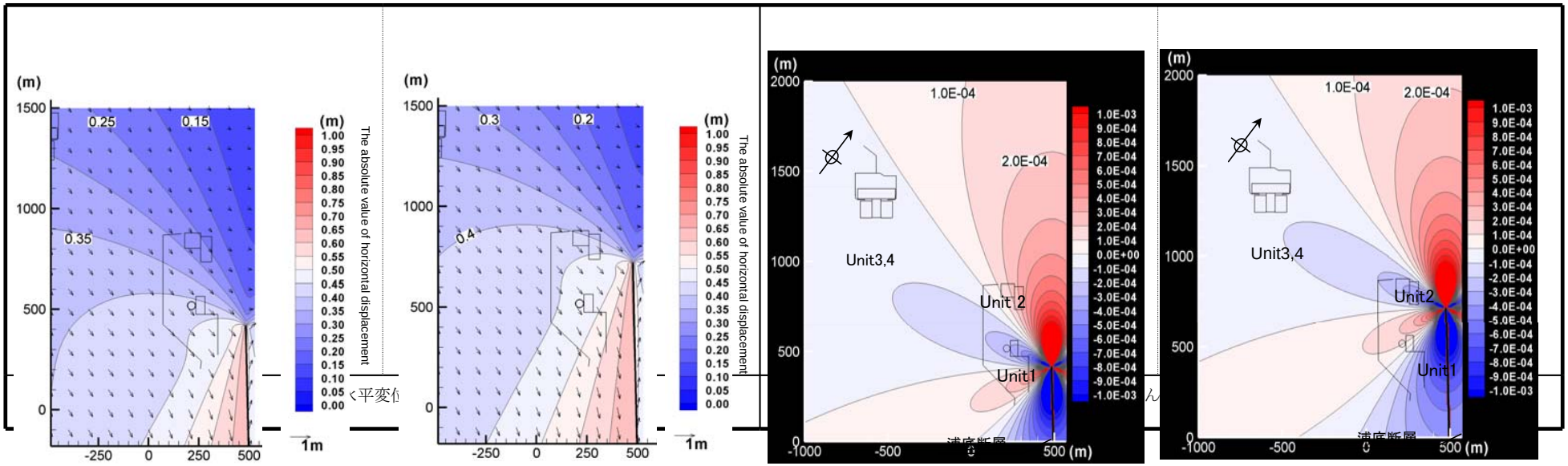

【Unit 1 R/B max. case】 【 Unit 1 R/B max. case 】 【Unit 2 R/B max. case】 【 Unit 2 R/B max. case 】

Horizontal displacement Horizontal shearing strain

Calculated for each 5m sqare

Fig. Distribution of horizontal displacement and horizontal shearing strain of Unit 1 and Unit 2 in the case of maximum horizontal strain

6. Vertical two-dimensional FEM analysis, (1) Flow of the study

【Details to be studied】

For the detail study on vertical displacement, vertical two-dimensional FEM was carried out on the case that maximize dipping of the ground at a reactor building.

【Flow of the study】

1. Creating an analytical model
   - ・Vertical two-dimensional model
2. FEM analysis
   - ・Maximum dipping case at reactor building
3. Result

Fig. Flow of the study

【Max. dipping case at Unit 1 reactor building】
P-axis: 90 degrees, Fault length: 13.3 km

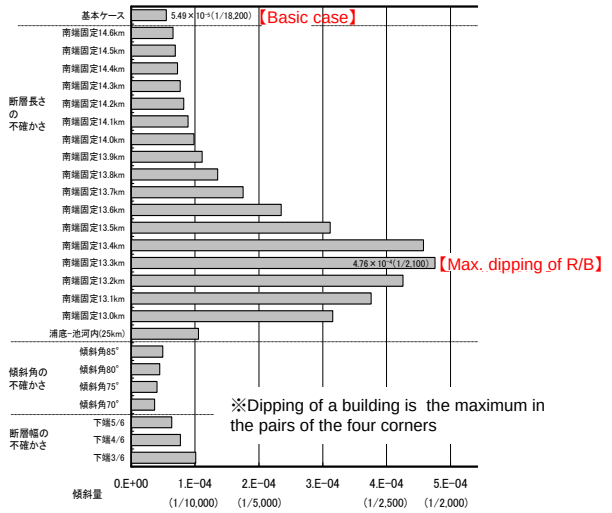

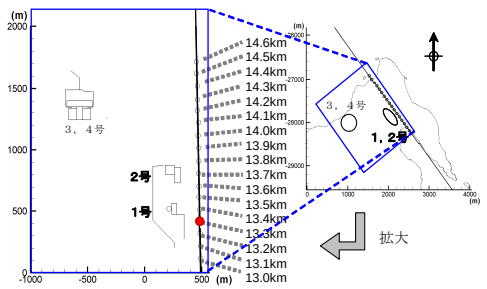

【Location of northern end of the fault】

【Max. dipping case at Unit 2 reactor building】
P-axis: 90 degrees, Fault length: 13.7 km

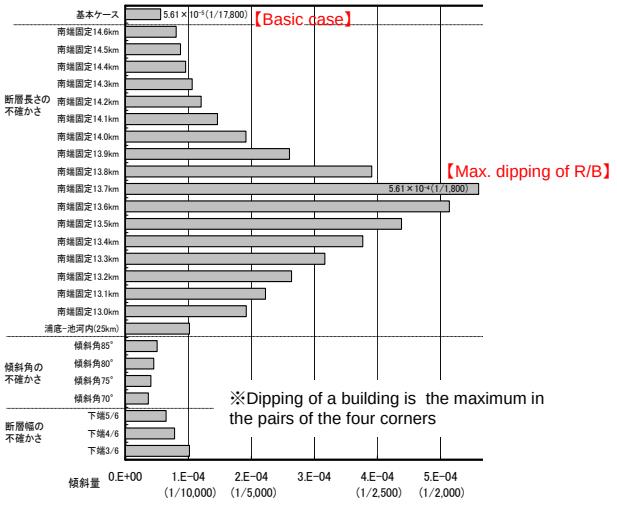

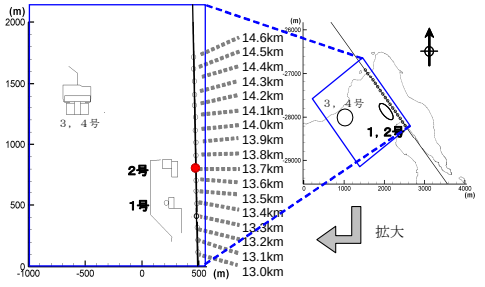

【 Location of northern end of the fault 】

Fig. Dipping of a reactor building taking account of uncertainty
(left: Unit 1 reactor building, right: Unit 2 reactor building)

6. Vertical two-dimensional FEM analysis, (2) Analysis condition, ① Location of the cross section

Cross sections at reactor buildings perpendicular to Urasko-fault are selected to be studied.（Unit 1: A-A', Unit 2: B-B'）

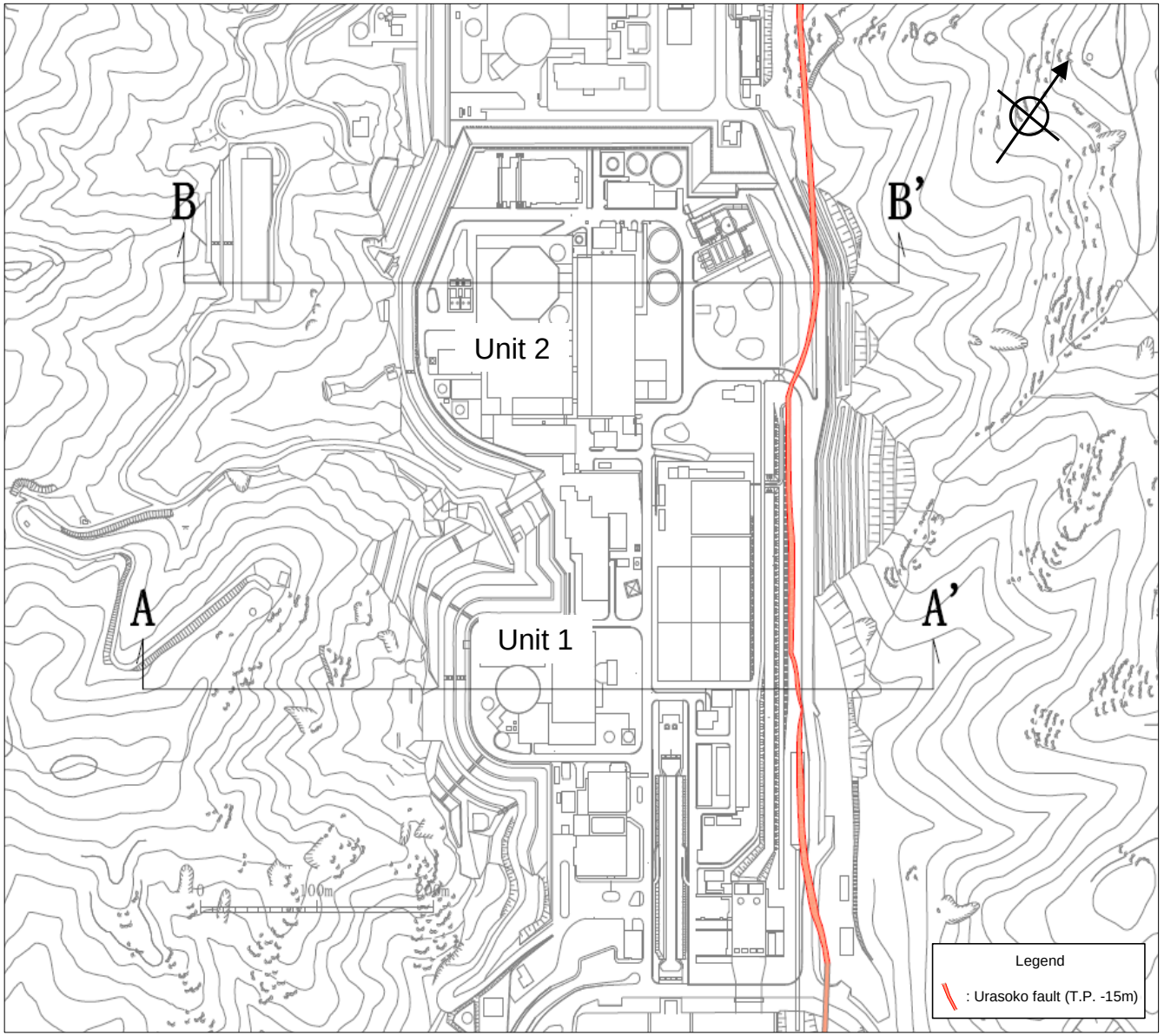

Fig. Location of the cross section

6. Vertical two-dimensional FEM analysis, (2) Analysis condition, ② Figure of vertical rock distribution (Cross section at Unit 1: A-A' cross section)

Location of cross section

・Figure of rock distribution was made based on the geological profile of each cross sections.
・Rock distribution in depth direction is D-class rock at the earth's surface, C_L-class rock, and over C_M-class hard rock.

Legend of rocks

- bk: Surface soil, Filling soil
- A: Layer A: Alluvial lowland deposit, Alluvial fan deposit, Talus deposit (might include sand, gravel, silt, humus and plant root)
- Bs: Layer Bs: Delta deposit (including coarse sand, medium sand and shell)
- Bsm: Layer Bsm: Inside bay deposit (including medium sand, coarse sand, fine sand, silt and shell)
- Ca1: Layer Ca1: Lowland deposit (including a lot of fine sand, medium sand, sand, and humus)
- Csg: Layer Csg: Alluvial fan deposit (might include gravel, coarse sand, medium sand and humus)

Quaternary

Granite
- D: [D] class
- CL: [C_L] class
- CM: [C_M] class
- CH: [C_H] class

Shatter zones (H-3a)

Drilling

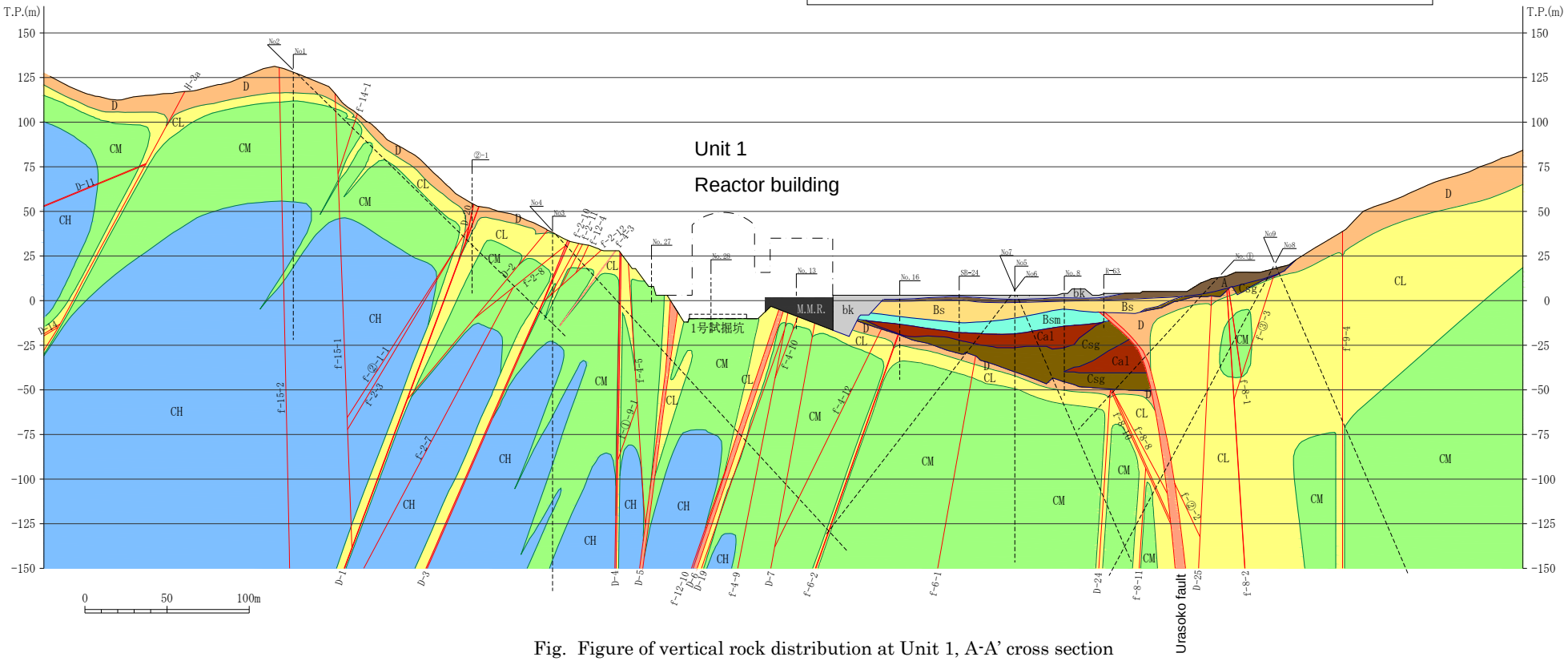

Fig. Figure of vertical rock distribution at Unit 1, A-A' cross section

6. Vertical two-dimensional FEM analysis, (2) Analysis condition, ③ Figure of vertical rock distribution (Cross section at Unit 2: B-B' cross section)

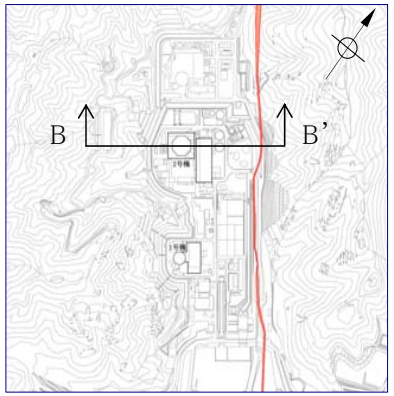

Location of cross section

・Figure of rock distribution was made based on the geological profile of each cross sections.
・Rock distribution in depth direction is D-class rock at the earth's surface, C_L-class rock, and over C_M-class hard rock.

Legend of rocks

- bk — Surface soil, Filling soil
- A — Layer A: Alluvial lowland deposit, Alluvial fan deposit, Talus deposit (might include sand, gravel, silt, humus and plant root)
- Bp — Layer Bp: Swamp deposit (including humic soil, fine sand, and partially including coarse sand, fine gravel)
- Csg — Layer Csg: Alluvial fan deposit (might include gravel, coarse sand, medium sand and humus)

第四系

- D — [D] class (weathering)
- D(熱) — [D] class (hydrothermally-alteration)
- CL — [C_L] class
- CM — [C_M] class
- CH — [C_H] class

Granite

Drilling

H-3a — Shatter zones

SW B — NE B'

T.P.(m)

Unit 2

Reactor building

Urasoko fault

0 50 100m

Fig. Figure of vertical rock distribution at Unit 2, B-B' cross section

Table. Setting of physical properties for analysis

Classification \ Item		Physical characteristics	Deformational characteristics		Strength characteristics		
		Wet density ρt (g/cm^3)	Elastic modulus E_S (N/mm^2)	Static Poisson's ratio ν_S	Shear strength τ_0 (N/mm^2)	Angle of internal friction ϕ (°)	Residual strength τr (N/mm^2)
Granite	CH class	Density test	Secant modulus of Plate load test	Uniaxial compression test	Same as CM class		
	CM class				Rock shear test		
	CL class						
	D class (weathering)				Rock shear test		
	D class (Hydro-thermal alteration)				Rock shear test		
Shatter zone					Rock shear test		N/A
Quaternary	A		E50 of Triaxial compression test	Same as Bs class	Triaxial compression test		N/A
	Bp						
	Bs			Triaxial compression test			
	Bsm						
	Cal						
	Csg						
Filling soil				Same as Bs class			N/A
Man made rock (MMR)		Same as CL class			Same as CL class		

Note) Physical properties of CL class are conservatively substituted for that of MMR to decrease constraint effect for shatter zone, because NMR is just located around the buildings and has a limited depth.

Table. Physical properties for analysis

Classification \ Item		Physical characteristics	Deformational characteristics		Strength characteristics		
		Wet density ρt (g/cm^3)	Elastic modulus E_S (N/mm^2)	Static Poisson's ratio ν_S	Shear strength τ_0 (N/mm^2)	Angle of internal friction ϕ (°)	Residual strength τr (N/mm^2)
Granite	CH class	2.6	7,160	0.25	0.499	44	$1.31\sigma^{0.602}$
	CM class	2.5	1,180	0.27	0.499	44	$1.31\sigma^{0.602}$
	CL class	2.4	152	0.30	0.266	36	$0.813\sigma^{0.554}$
	D class (weathering)	2.06	140	0.35	0.169	36	$0.792\sigma^{0.630}$
	D class (Hydro-thermal alteration)	2.0	44	0.35	0.0697	33	$0.386\sigma^{0.484}$
Shatter zone		2.0	44	0.35	0.0257	32	0
Quaternary	A	1.90	13.1	0.47	0.0113	25.0	0
	Bp	1.82	11.6	0.47	0.0453	23.6	
	Bs	1.94	23.4	0.47	0.0718	34.2	
	Bsm	1.97	20.8	0.47	0.0416	29.9	
	Cal	2.04	41.9	0.48	0.158	31.5	
	Csg	2.08	31.2	0.47	0.110	34.5	
Filling soil		2.07	27.0	0.47	0.156	21.5	0

Note) Physical properties of granite are based on the application for permission for establishment of Tsuruga PS

σ : normal stress (N/mm^2)

Tree significant digits are basically applied.

6. Vertical two-dimensional FEM analysis, (3) Analytical model (Cross section at Unit 1)

・The ground model is made based on the figure of rock distribution.
(bedrock: plane strain element, shatter zone: joint element)
・Non-linearity of each element is taken account of by decreasing stiffness depending on the generated stress.

Location of the cross section

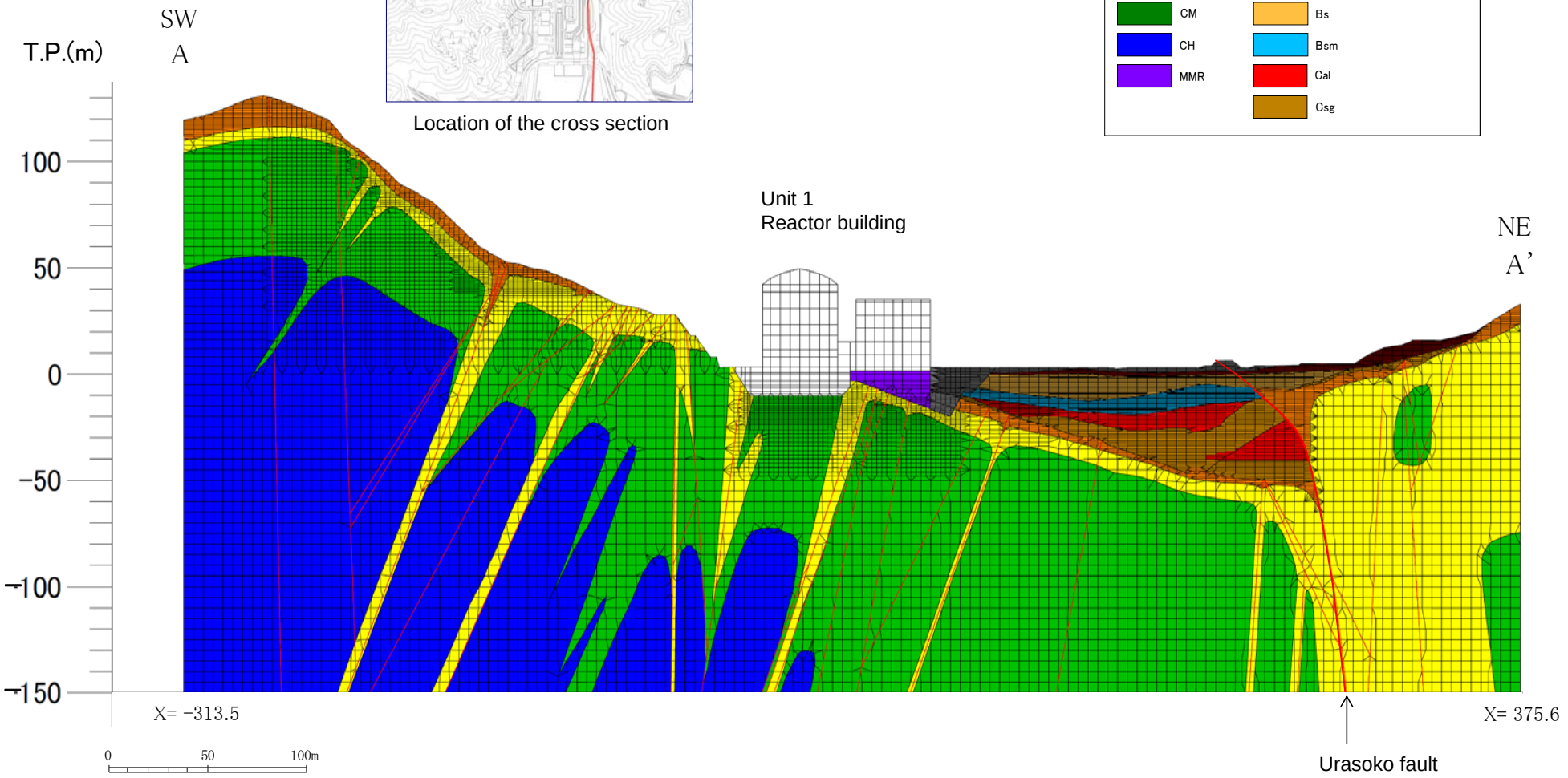

Fig. Analytical model (Unit 1 cross section)

6. Vertical two-dimensional FEM analysis, (3) Analytical model (Cross section at Unit 2)

・The ground model is made based on the figure of rock distribution.
(bedrock: plane strain element, shatter zone: joint element)
・Non-linearity of each element is taken account of by decreasing stiffness depending on the generated stress.

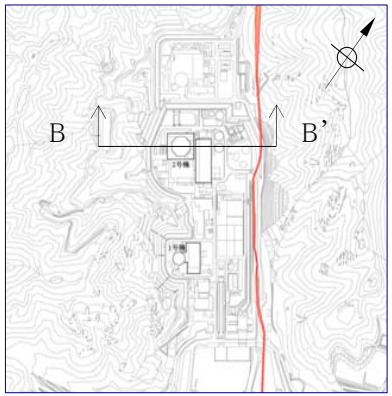

Location of the cross section

Legend

D-class (Weathering)
Filling soil, Surface soil
Shatter zone
D-class (hydro-thermal)
A
CL
Bp
CM
Bs
CH
Bsm
MMR
Cal
Csg

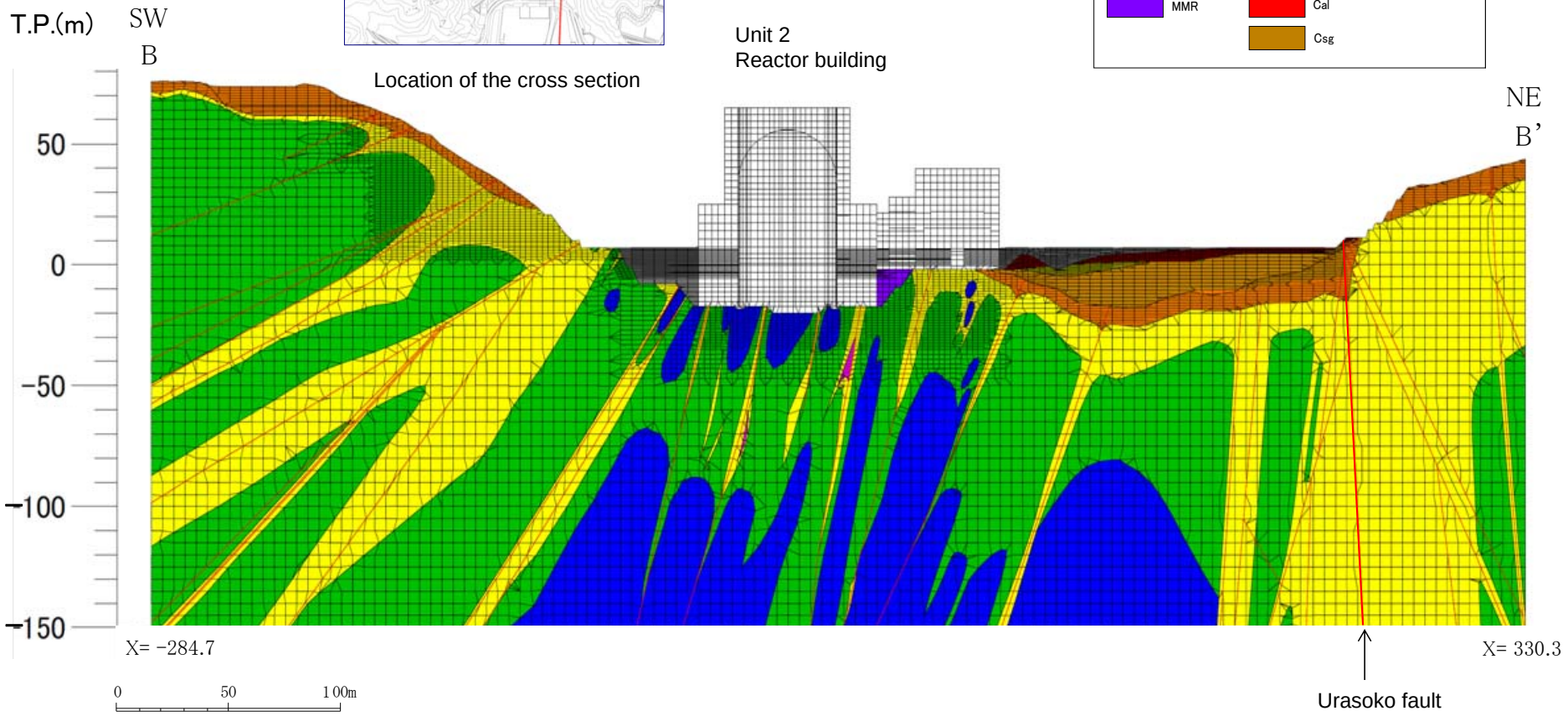

Fig. Analytical model (Unit 2 cross section)

6. Vertical two-dimensional FEM analysis, (4) Input of displacement (Unit 1 cross section)

・FEM analysis is conducted on the case that maximize the dipping of rector building basement in the elasticity theory of dislocation.

・Displacements at boundary of the analytical model is calculated by the elasticity theory of dislocation, and that displacement data is used as enforced displacements of the boundary condition of FEM model.

【Max. dipping case at Unit 1 reactor building】
P-axis: 90 degrees, Fault length: 13.3 km

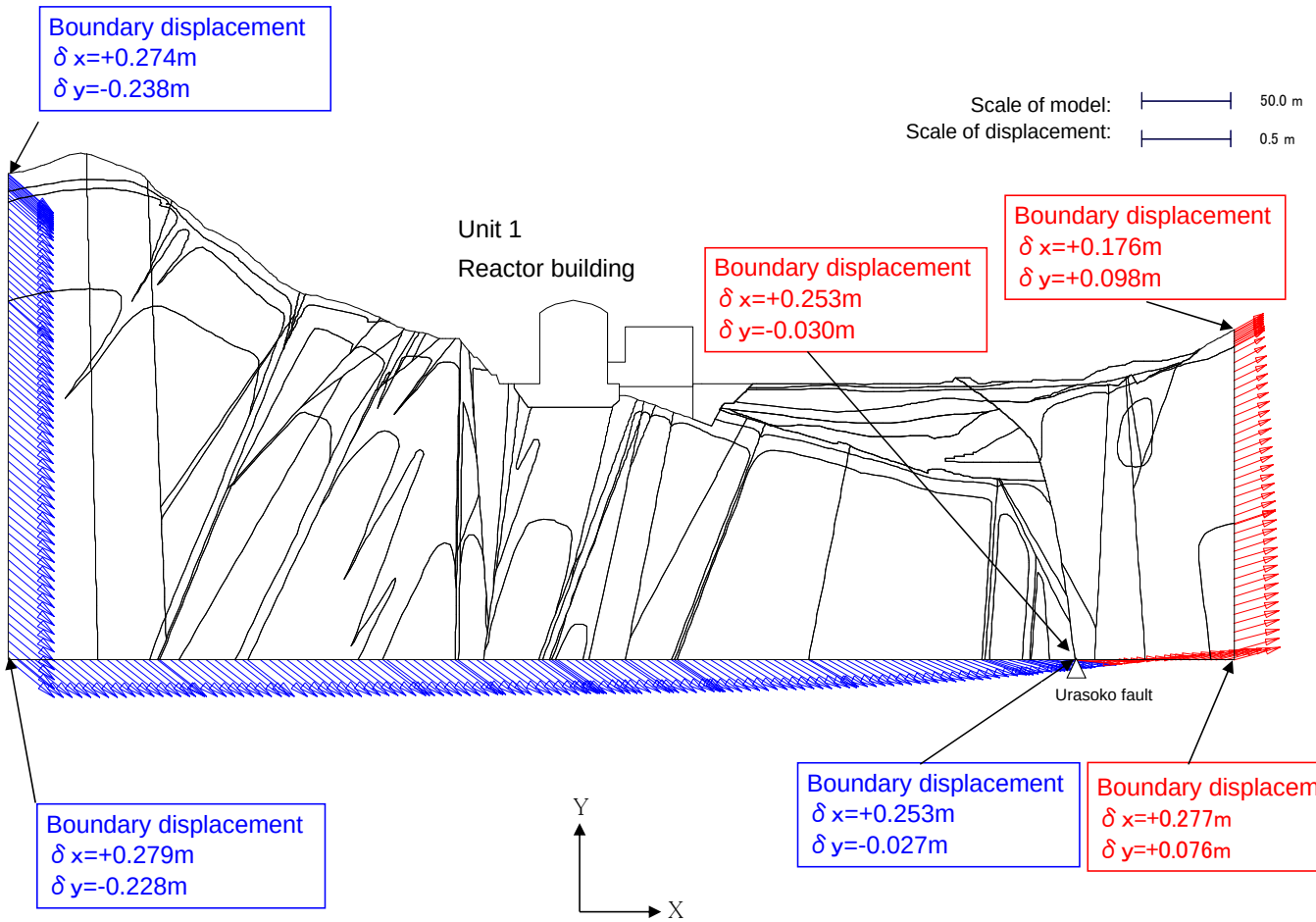

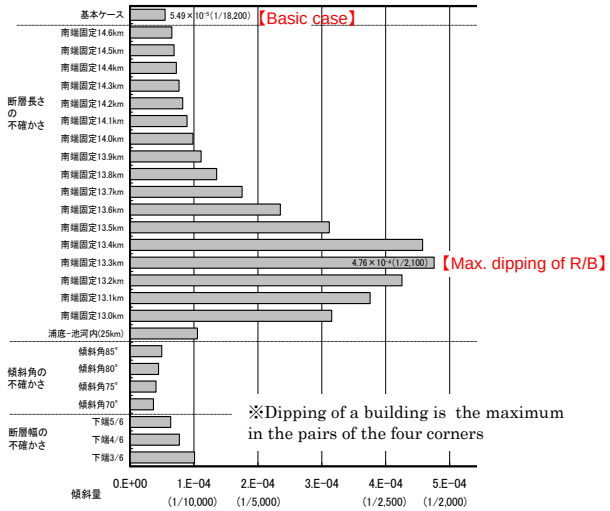

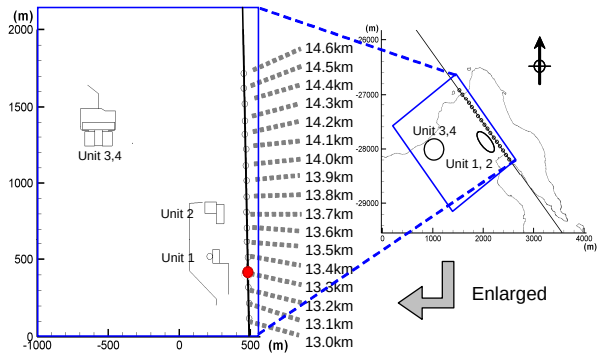

【 Location of northern end of the fault 】

Fig. Input of displacement (Unit 1 cross section)

6. Vertical two-dimensional FEM analysis, (4) Input of displacement (Unit 2 cross section)

・FEM analysis is conducted on the case that maximize the dipping of rector building basement in the elasticity theory of dislocation.

・Displacements at boundary of the analytical model is calculated by the elasticity theory of dislocation, and that displacement data is used as enforced displacements of the boundary condition of FEM model.

【Max. dipping case at Unit 2 reactor building】
P-axis: 90 degrees, Fault length: 13.7 km

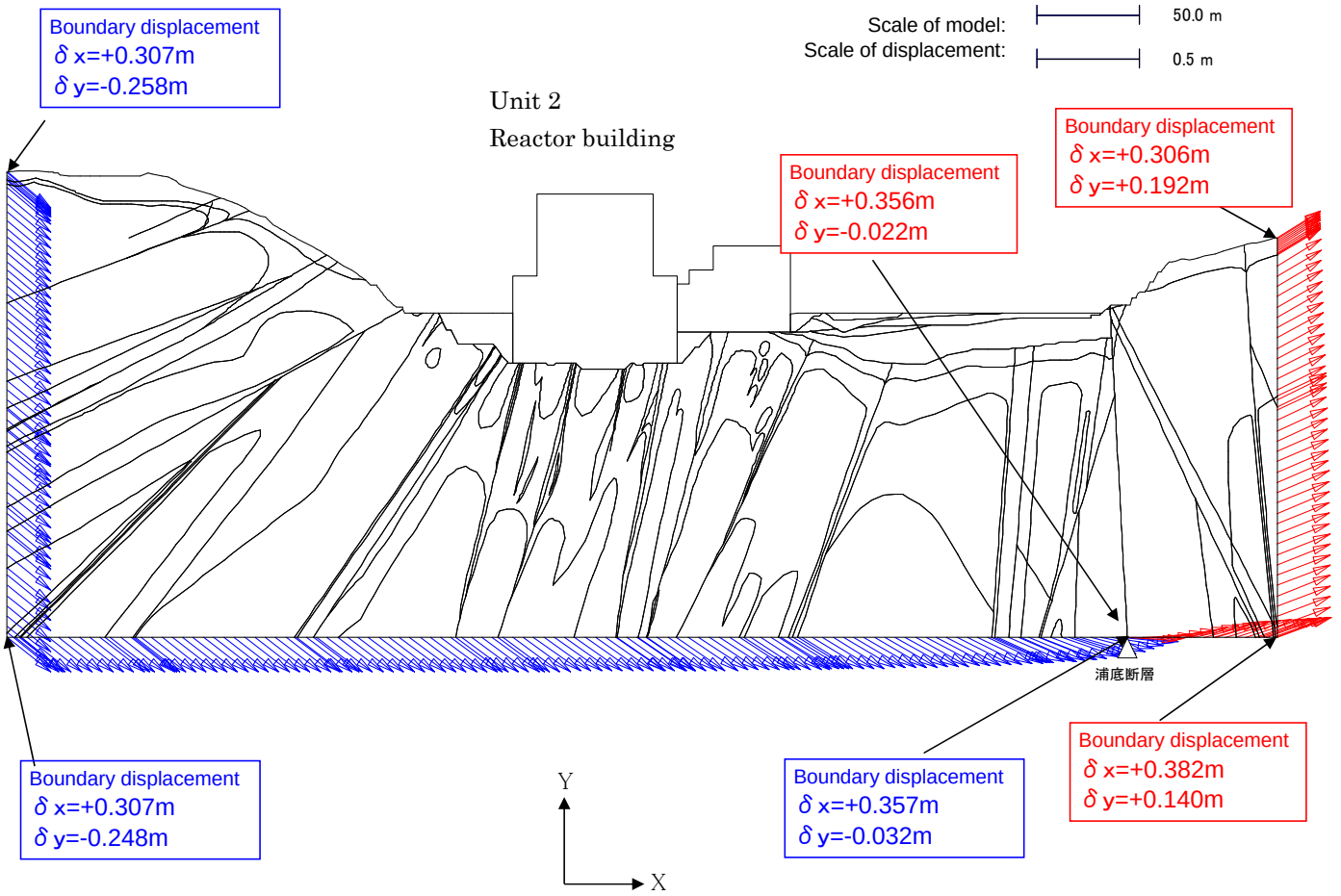

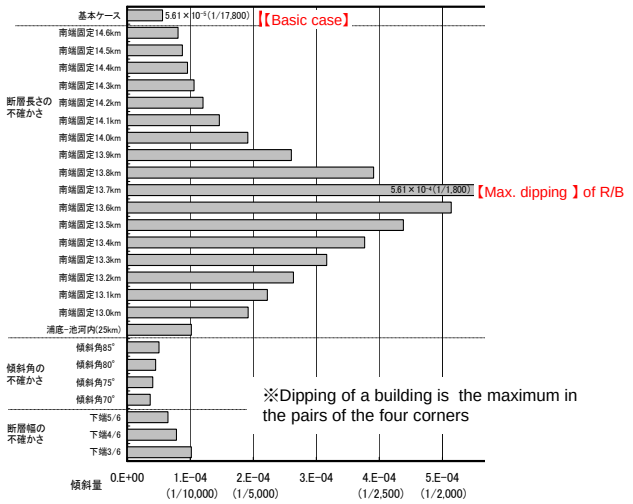

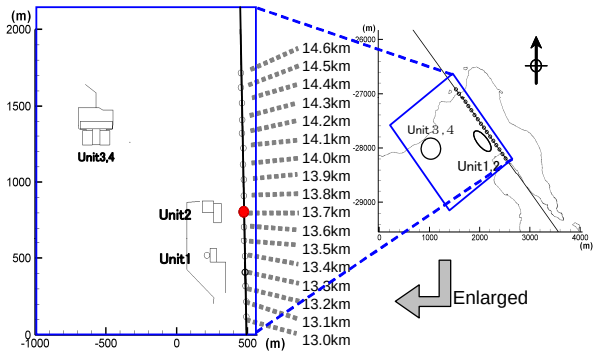

【 Location of northern end of the fault 】

Fig. Input of displacement (Unit 2 cross section)

6. Vertical two-dimensional FEM analysis, (5) Analysis result
① Dipping of reactor building (Cross section at Unit 1)

・Maximum dipping at reactor building calculated by two-dimensional FEM is about 1/4,400.
・Dipping at reactor building calculated by two-dimensional FEM and that calculated by elasticity theory of dislocation are almost the same.

Table. Dipping at reactor building (Unit 1)

【Max. dipping case at Unit 1 reactor building】
P-axis: 90 degrees, Fault length: 13.3 km

Analytical method	Vertical relative displacement $\delta = \delta_A - \delta_B$ (cm)	Dipping
Two-dimensional FEM	0.956	1/4,400
Elasticity theory of dislocation	0.726※	1/5,800※

※ The value at A-A' cross section of FEM analysis

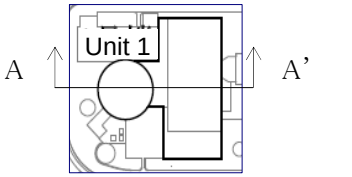

【Location of cross section】

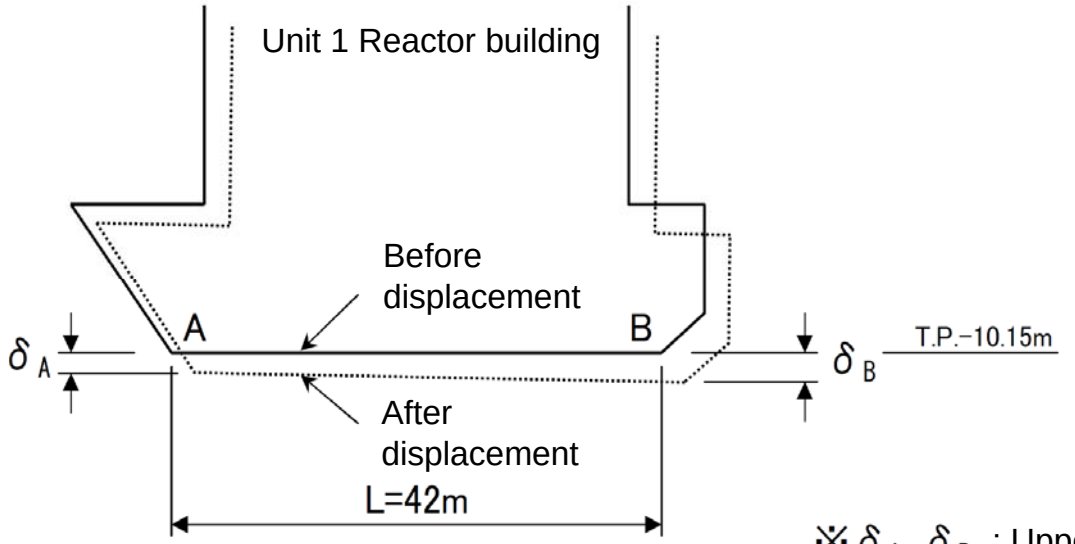

※ δ_A, δ_B : Upper direction is positive

6. Vertical two-dimensional FEM analysis, (5) Analysis result
① Dipping of reactor building (Cross section at Unit 2)

・Maximum dipping at reactor building calculated by two-dimensional FEM is about 1/10,800.
・Dipping at reactor building calculated by two-dimensional FEM and that calculated by elasticity theory of dislocation are almost the same.

Table. Dipping at reactor building (Unit 2)

【Max. dipping case at Unit 2 reactor building】
P-axis: 90 degrees, Fault length: 13.7 km

Analytical method	Vertical relative displacement $\delta = \delta_A - \delta_B$ (cm)	Dipping
Two-dimensional FEM	0.739	1/10,800
Elasticity theory of dislocation	0.786※	1/10,200※

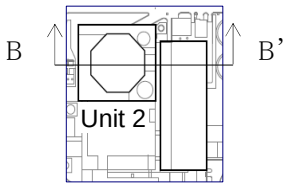

【Location of cross section】

※ The value at B-B' cross section of FEM analysis

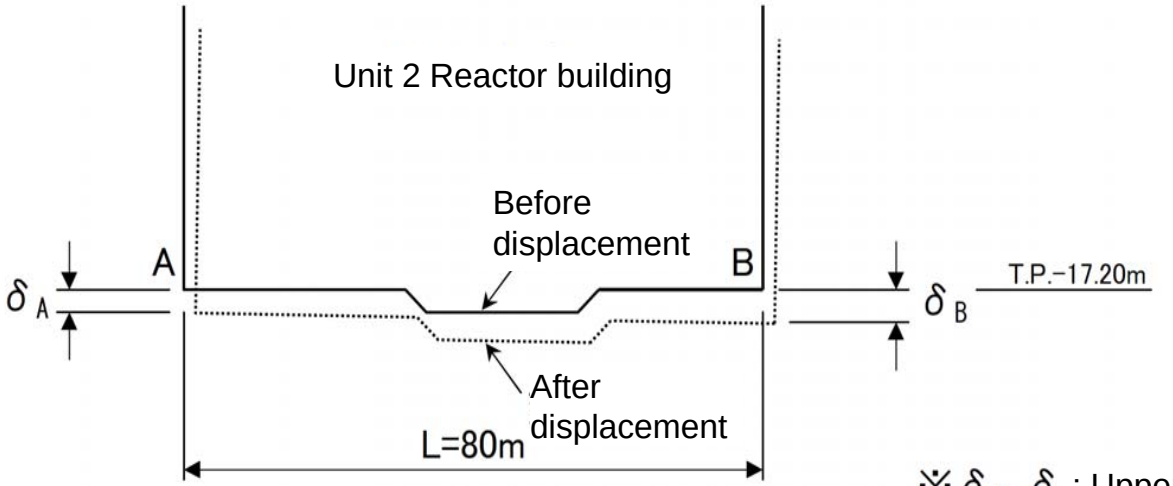

※ δ_A, δ_B : Upper direction is positive

6. Vertical two-dimensional FEM analysis, (5) Analysis result
③ Local safety factor of shatter zones (cross section at Unit 1)

Shatter zones except for Urasoko fault do not have shear failure. Tensile ruptures are limited to the earth's surface. The local safety factors near the building show enough margin.

Distribution of local safety factor of shatter zones

Location of cross section

【Max. dipping case at Unit 1 reactor building】
P-axis: 90 degrees, Fault length: 13.3 km

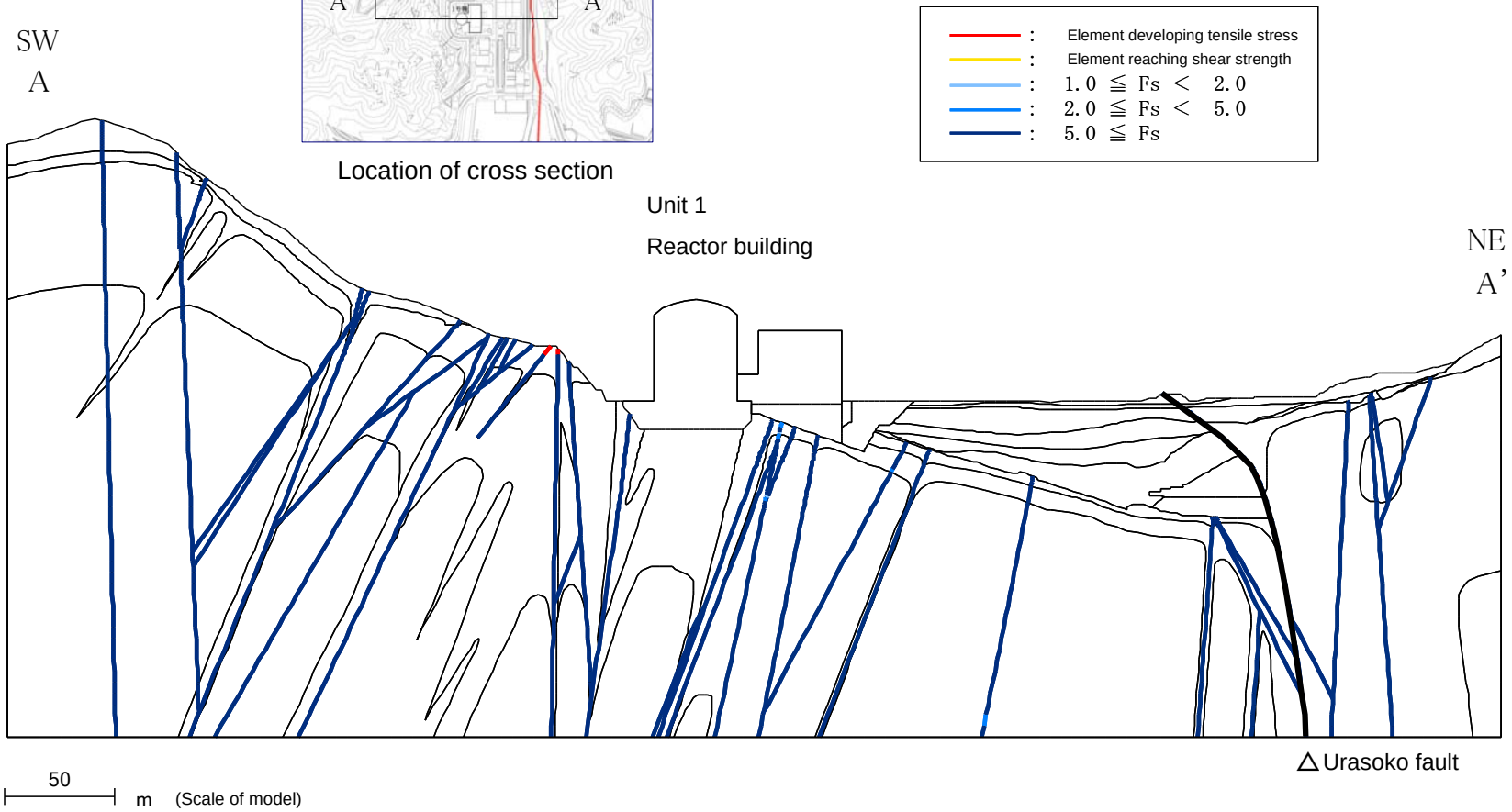

Fig. Distribution of local safety factor of shatter zones (cross section at Unit 1)

6. Vertical two-dimensional FEM analysis, (5) Analysis result
③ Local safety factor of shatter zones (cross section at Unit 2)

Shatter zones except for Urasoko fault do not have shear failure. Tensile ruptures are limited to the earth's surface. The local safety factors near the building show enough margin.

Distribution of local safety factor of shatter zones

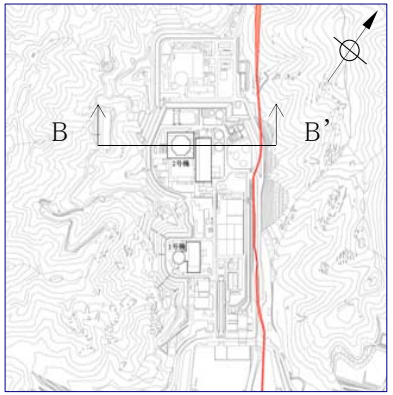

【Max. dipping case at Unit 2 reactor building】
P-axis: 90 degrees, Fault length: 13.7 km

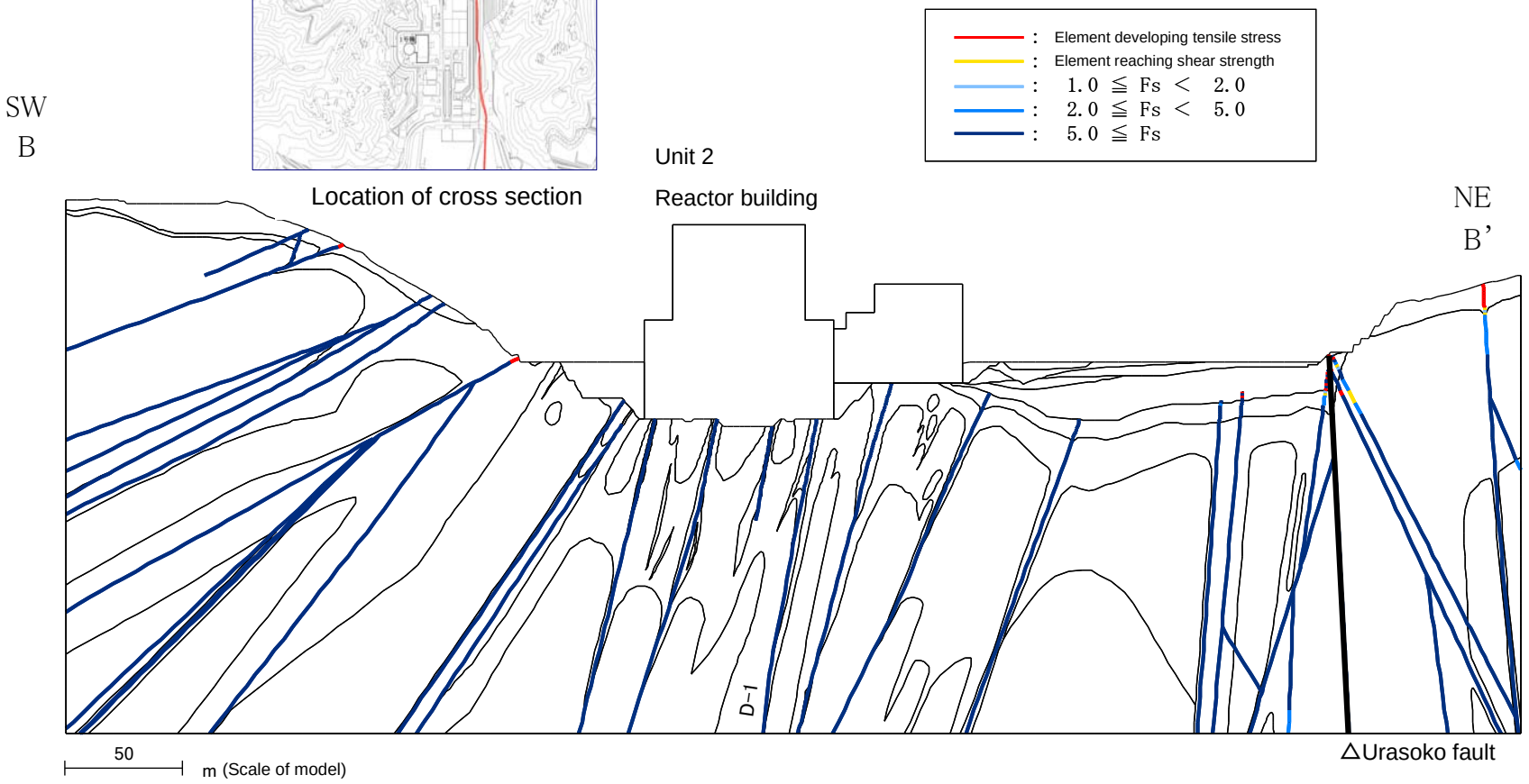

Fig. Distribution of local safety factor of shatter zones (cross section at Unit 2)

7. Horizontal two-dimensional FEM analysis, (1) Flow of the study

【Details of study】

For the detail study on horizontal displacement, horizontal two-dimensional FEM was carried out on the case that maximize horizontal shearing strain at a reactor building.

【Flow of the study】

1. Creating an analytical model
   - ・Horizontal two-dimensional model
2. FEM analysis
   - ・Primly stress analysis (simple three-dimensional model)
   - ・Maximum horizontal shearing strain case at a reactor building
3. Result

Fig. Flow of the study

【Horizontal shearing strain taking account of uncertainty (Unit 2 rector building)】

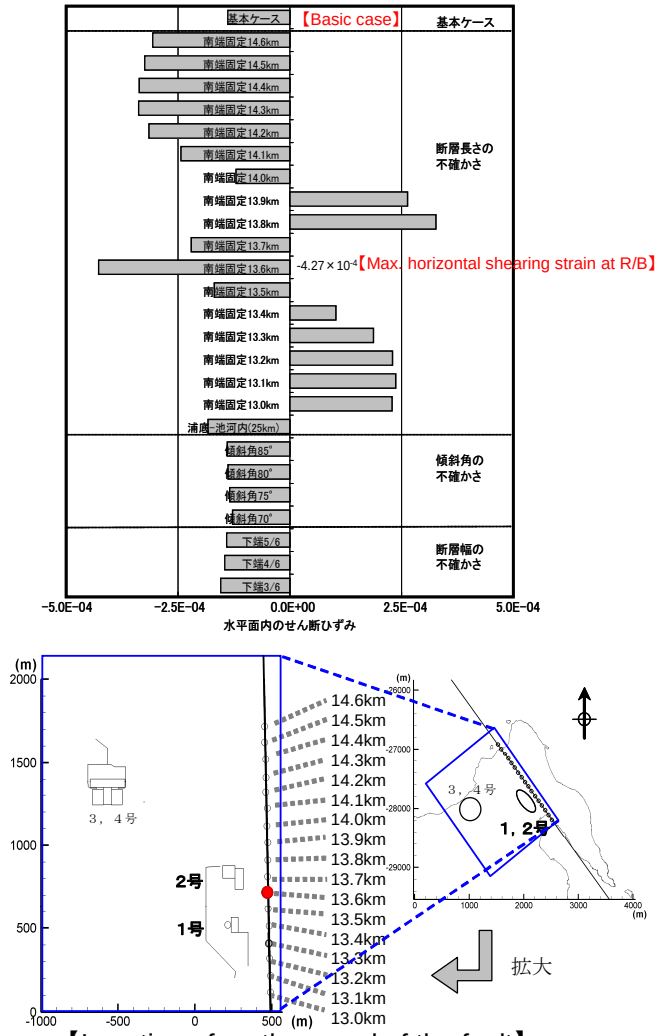

Fig. Horizontal shearing strain at a reactor building taking account of uncertainty

7. Horizontal two-dimensional FEM analysis, (2) Rock distribution

・Physical properties of rocks are classified with CH, CM, CL, and D-class. CM-class is widely distributed around Unit 2.
・Direction of N-S to NE-SW is the dominant direction for shatter zones.
・In the NE side of power station, Quaternary is distributed.

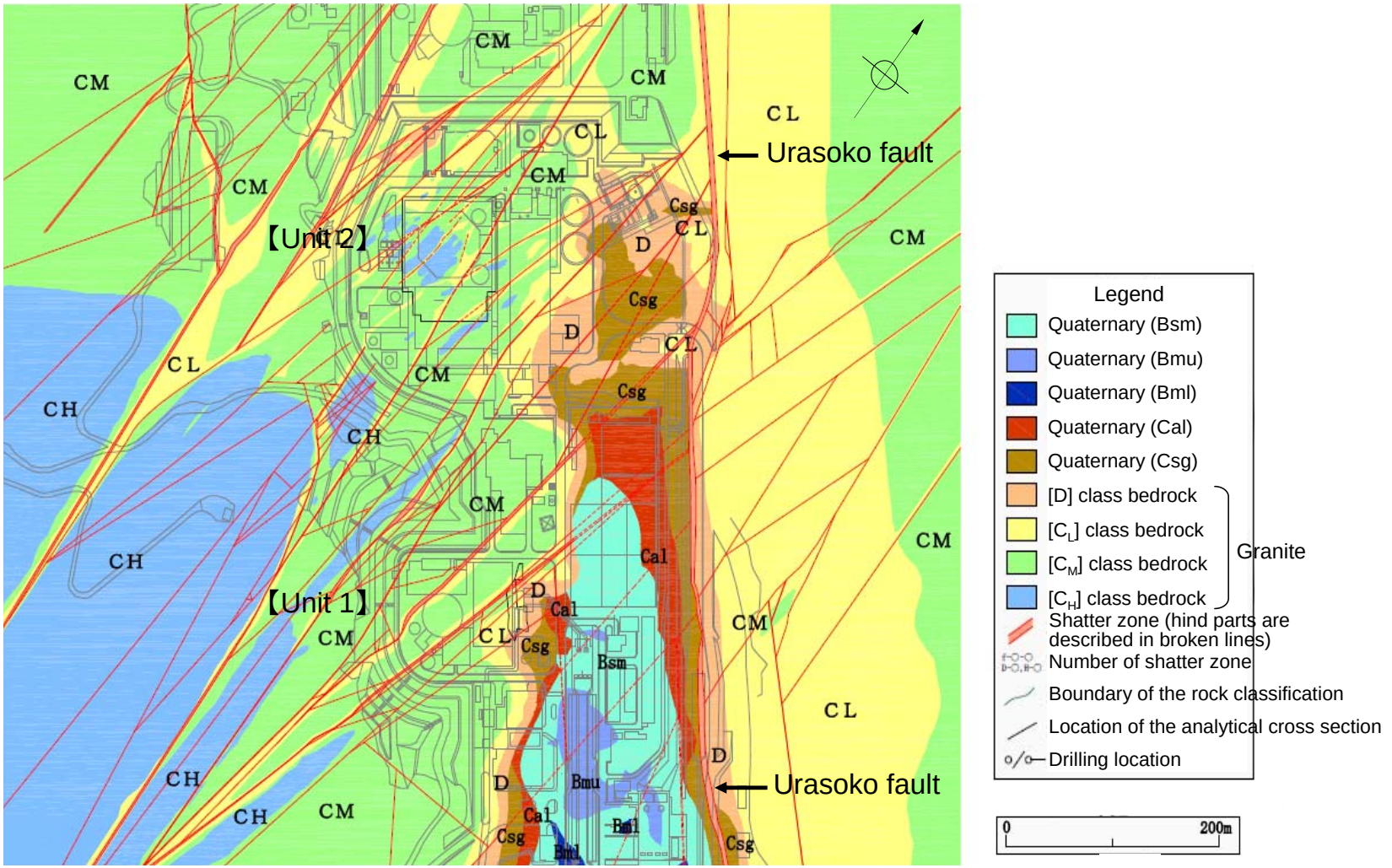

Fig. Figure of rock distribution (T.P. -15m)

7. Horizontal two-dimensional FEM analysis, (3) Analytical model

・Footwall is simulated. In order to consider the effect of rock classification and shatter zones around a reactor building, broad area is simulated.
・Same as the vertical two-dimensional FEM model, the distribution of shatter zones is simulated from the geologic map.
・Physical properties are same as that of vertical two-dimensional FEM model
・Physical properties are set according to the rock classifications (Distribution of Quaternary is limited to the depth direction, therefore quaternary is conservatively simulated as bedrock of CL-class).

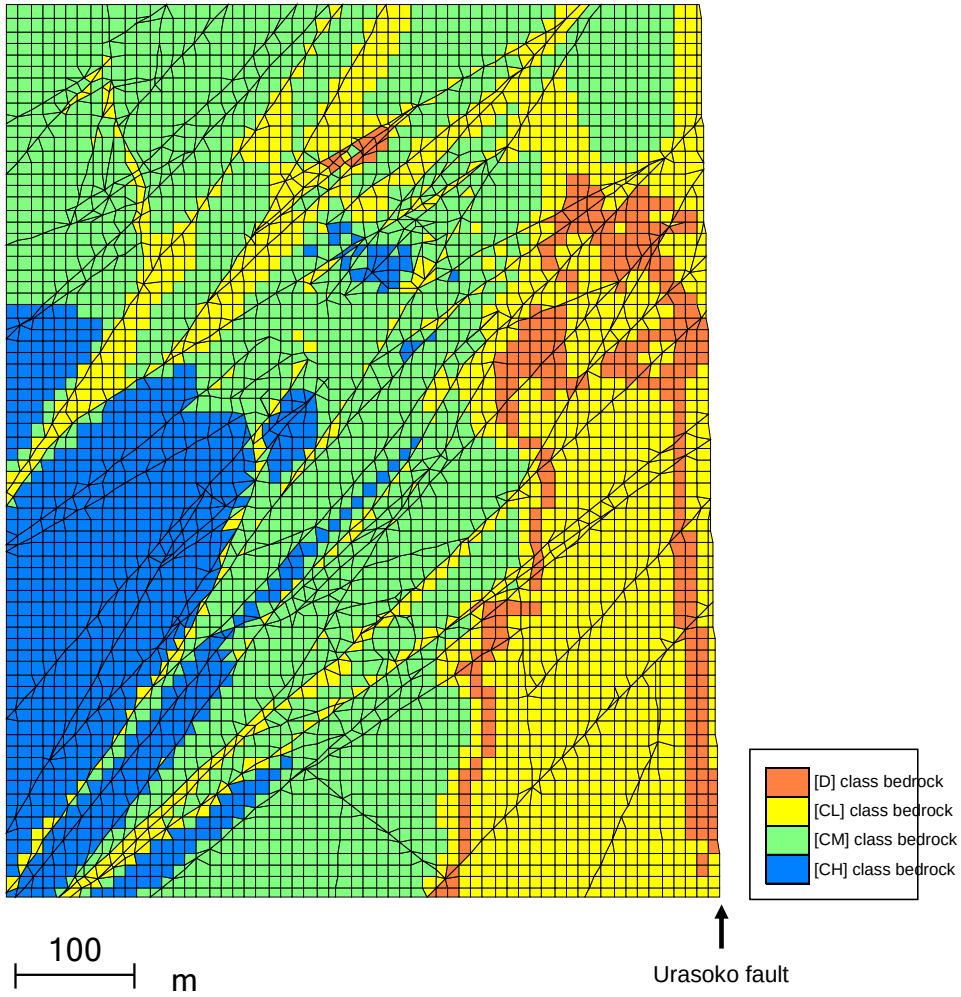

Fig. Analytical model

7. Horizontal two-dimensional FEM analysis, (5) Input of displacement

・FEM analysis is conducted on the case that maximize horizontal shearing strain of the ground at a reactor building in the elasticity theory of dislocation.
・Displacements at boundary of the analytical model is calculated by the elasticity theory of dislocation, and that displacement data is used as enforced displacements of the boundary condition of FEM model.
・Local displacement is developed around the northern end of fault, in the case that maximize horizontal shearing strain.

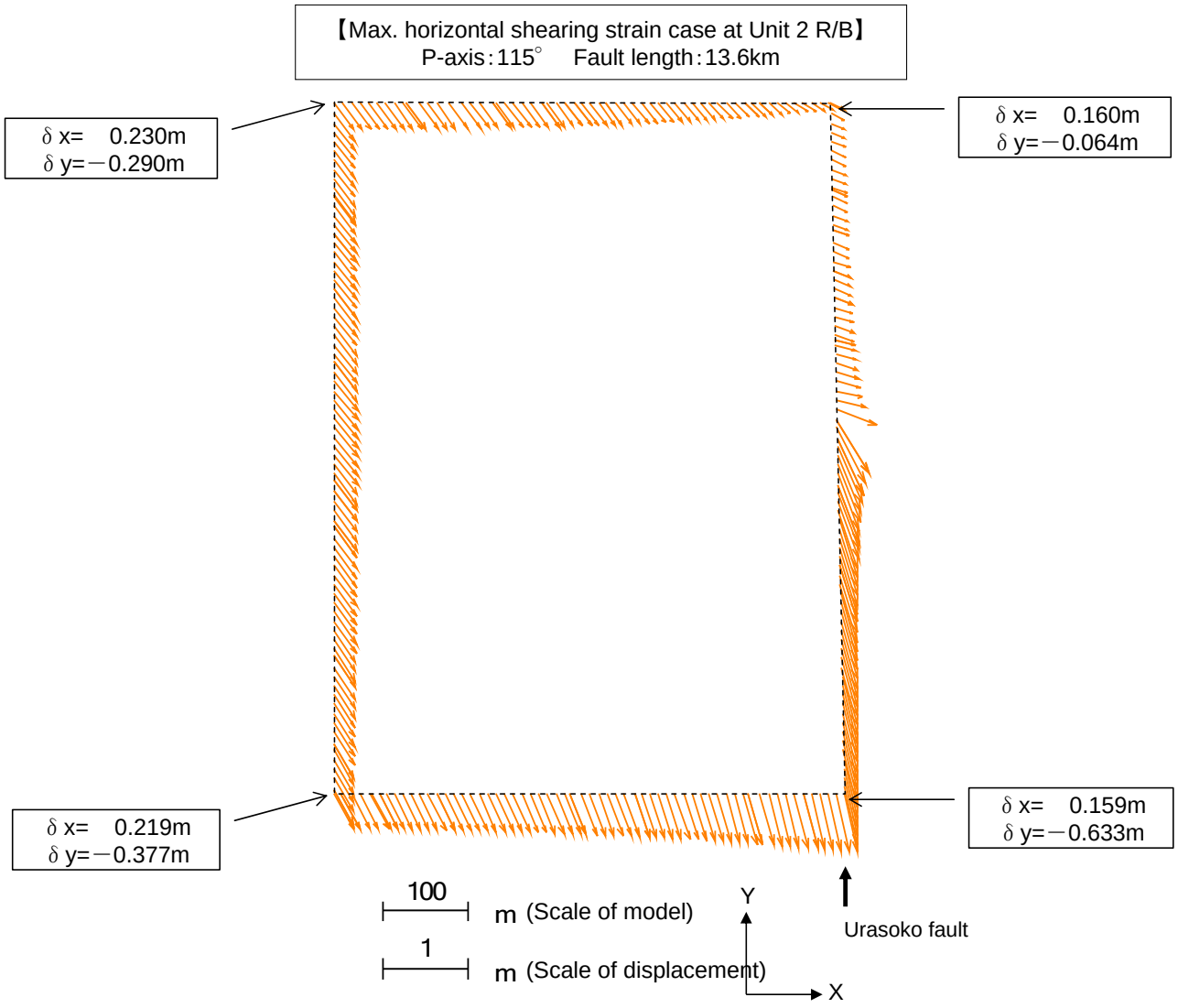

Fig. Input of displacement

【Horizontal shearing strain taking account of uncertainty (Unit 2 reactor building)】

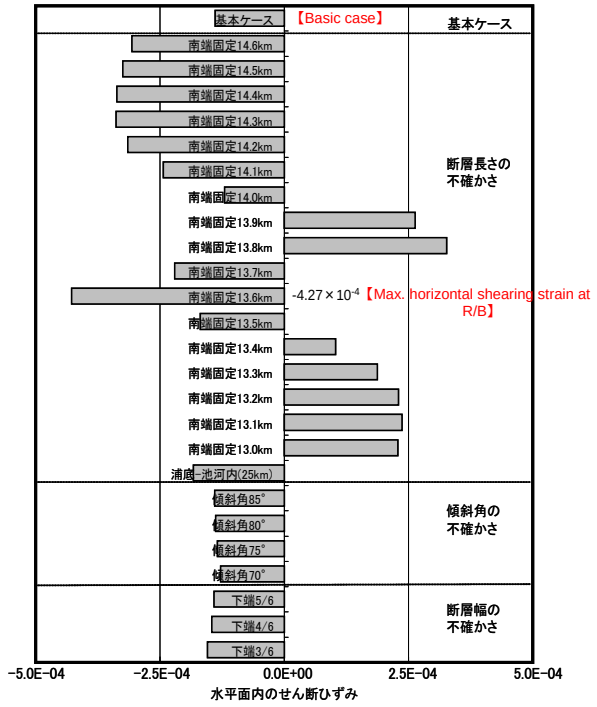

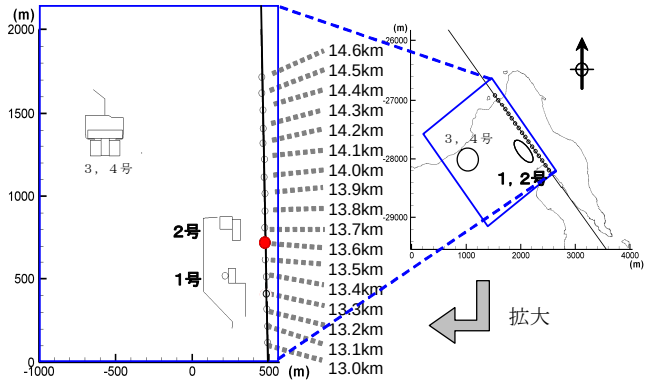

【Location of northern end of the fault】

Fig. Horizontal shearing strain at a reactor building taking account of uncertainty

7. Horizontal two-dimensional FEM analysis, (6) Analysis result
① Relative displacement of reactor buildings and important facilities

・Relative displacement between a reactor building and an important facility is small (for example, relative displacement between centers of Unit 2 reactor building and auxiliary building is about 15mm)

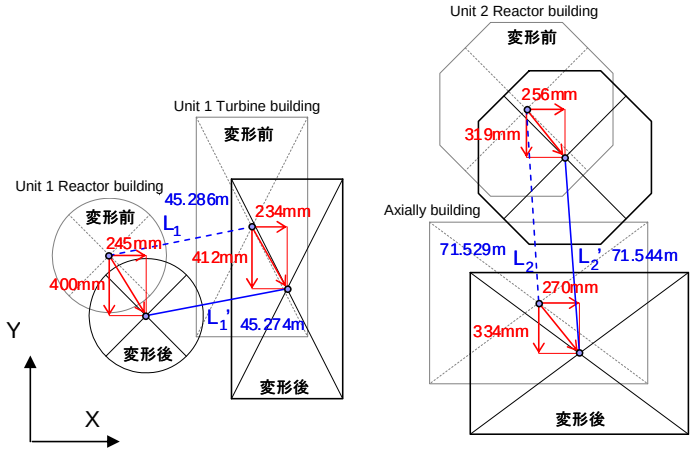

Image of relative displacement

Table. Relative displacement between the centers of a reactor building and an important building

Buildings	Relative displacement
Unit 1 reactor building – Turbine building	-12mm（L_1'-L_1）
Unit 2 reactor building – Auxiliary building	15mm（L_2'-L_2）

※ Direction away from each other is positive.

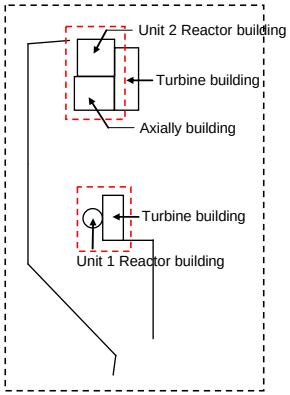

7. Horizontal two-dimensional FEM analysis, (6) Analysis result
③ Local safety factor of shatter zones

Because of local displacement at the northern end of Urasoko fault, partial rapture and decrease of safety factor is developed nearby Urasoko fault. However that area is limited and safety factors near the buildings show enough margin.

Distribution of local safety factor of shatter zone

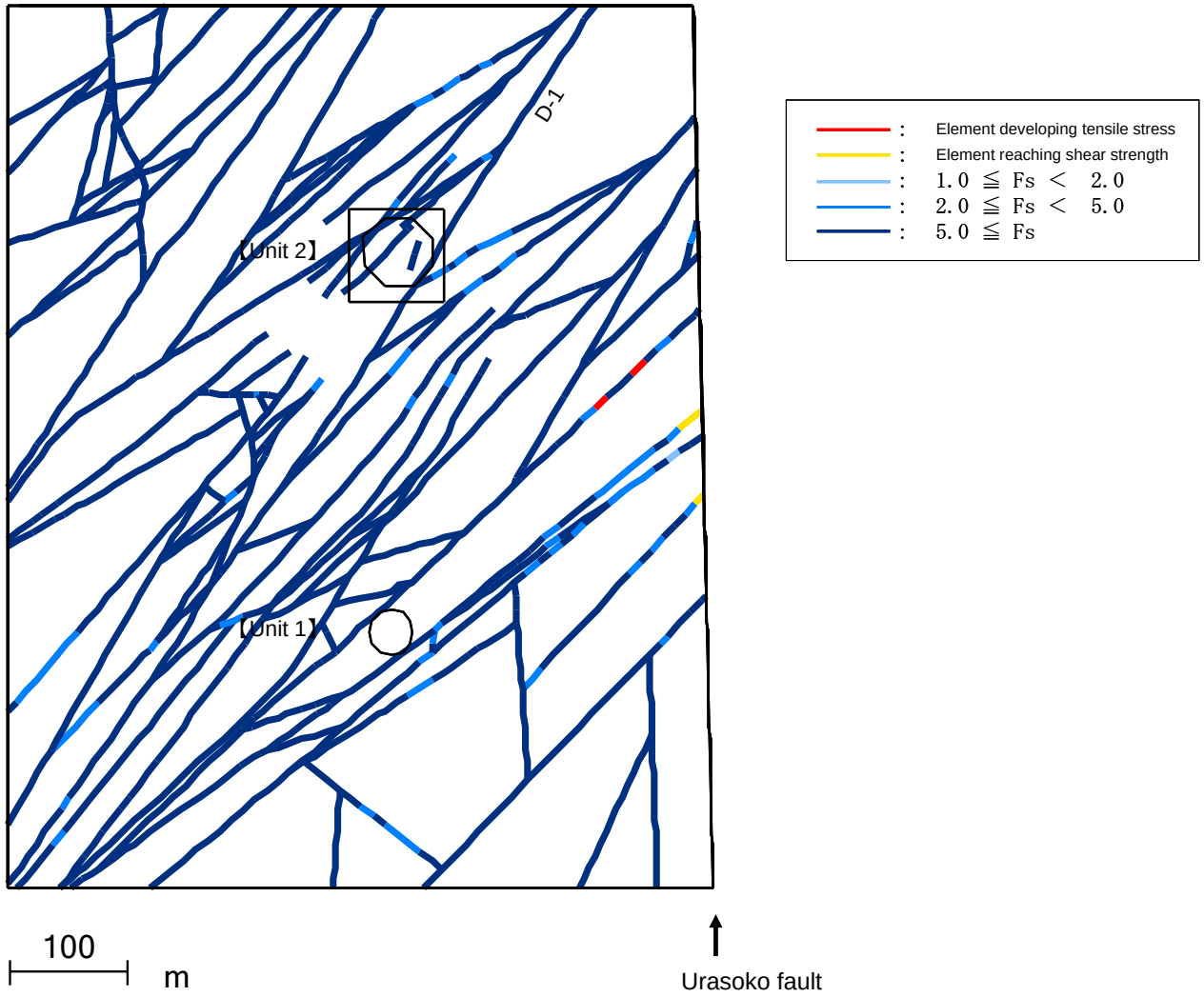

Fig. Distribution of local safety factor of shatter zones

<Reference> Vertical displacement of ground associated with the activity of Urasoko-Uchiikemi fault, (1) Basic case: P-axis 90°

Vertical displacement of ground associated with the activity of Urasoko-Uchiikemi fault is calculated by superimposing vertical displacement calculated from vertical component of the slip and vertical displacement calculated from horizontal component of the slip.

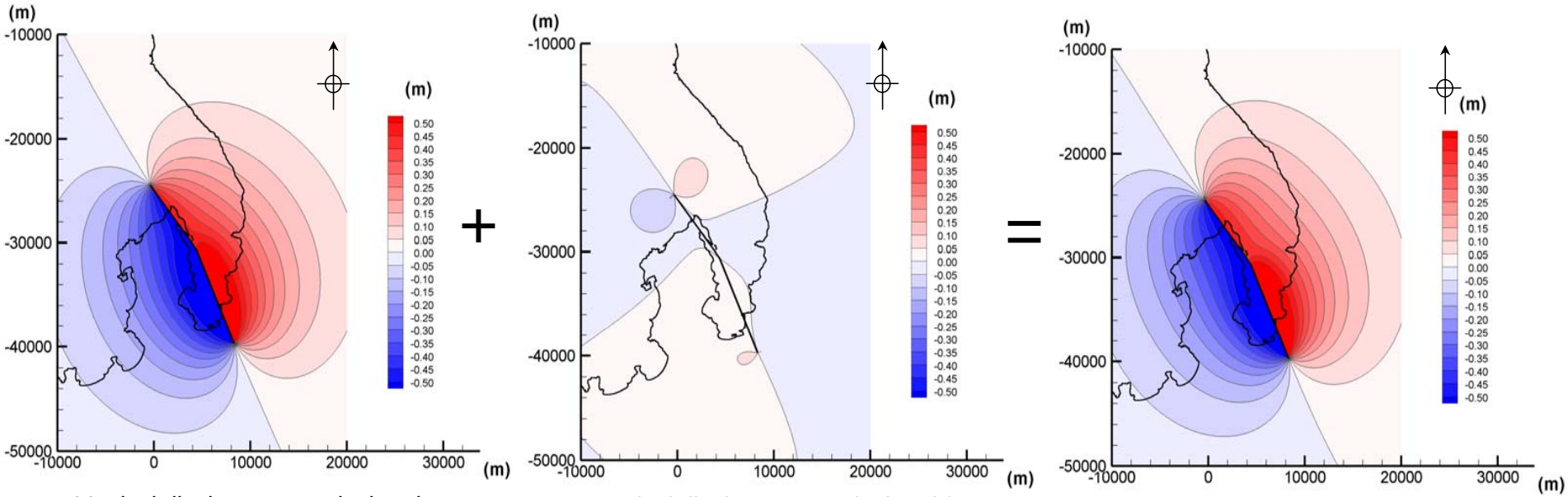

Vertical displacement calculated from vertical component of the slip

Vertical displacement calculated from horizontal component of the slip

Vertical displacement adding both of the displacements

Slip angle (P-axis 90°)	
Northern part of Urasoko-Uchiikemi fault	39°
Southern part of Urasoko-Uchiikemi fault	64°

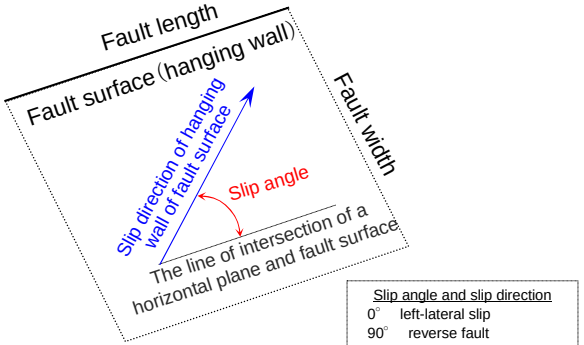

Fig. 【Reference】 Vertical displacement of ground associated with the activity of Urasoko-Uchiikemi fault (basic case: P-axis 90°)

<Reference> Vertical displacement of ground associated with the activity of Urasoko-Uchiikemi fault, (2) Basic case: P-axis 95°

Vertical displacement of ground associated with the activity of Urasoko-Uchiikemi fault is calculated by superimposing vertical displacement calculated from vertical component of the slip and vertical displacement calculated from horizontal component of the slip.

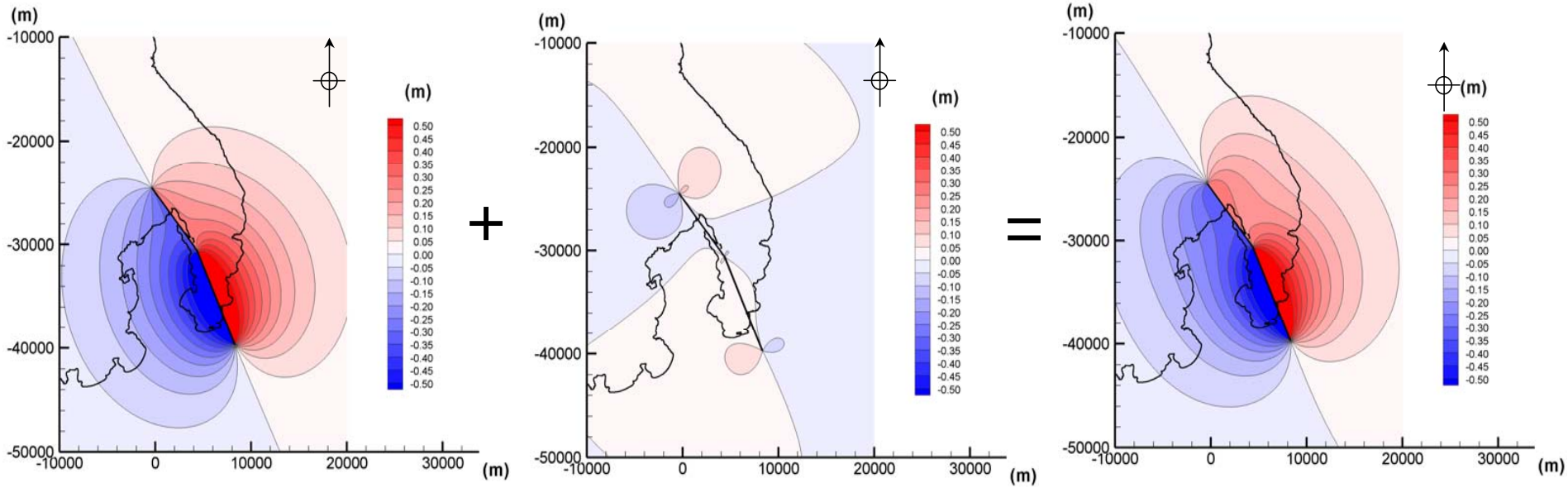

Vertical displacement calculated from vertical component of the slip

Vertical displacement calculated from horizontal component of the slip

Vertical displacement adding both of the displacements

Slip angle (P-axis 95°)	
Northern part of Urasoko-Uchiikemi fault	21°
Southern part of Urasoko-Uchiikemi fault	57°

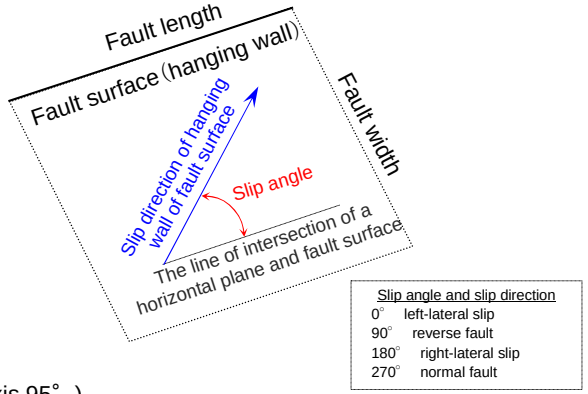

Fig. 【Reference】 Vertical displacement of ground associated with the activity of Urasoko-Uchiikemi fault (basic case: P-axis 95°)

<Reference> Vertical displacement of ground associated with the activity of Urasoko-Uchiikemi fault, (3) Basic case: P-axis 100°

Vertical displacement of ground associated with the activity of Urasoko-Uchiikemi fault is calculated by superimposing vertical displacement calculated from vertical component of the slip and vertical displacement calculated from horizontal component of the slip.

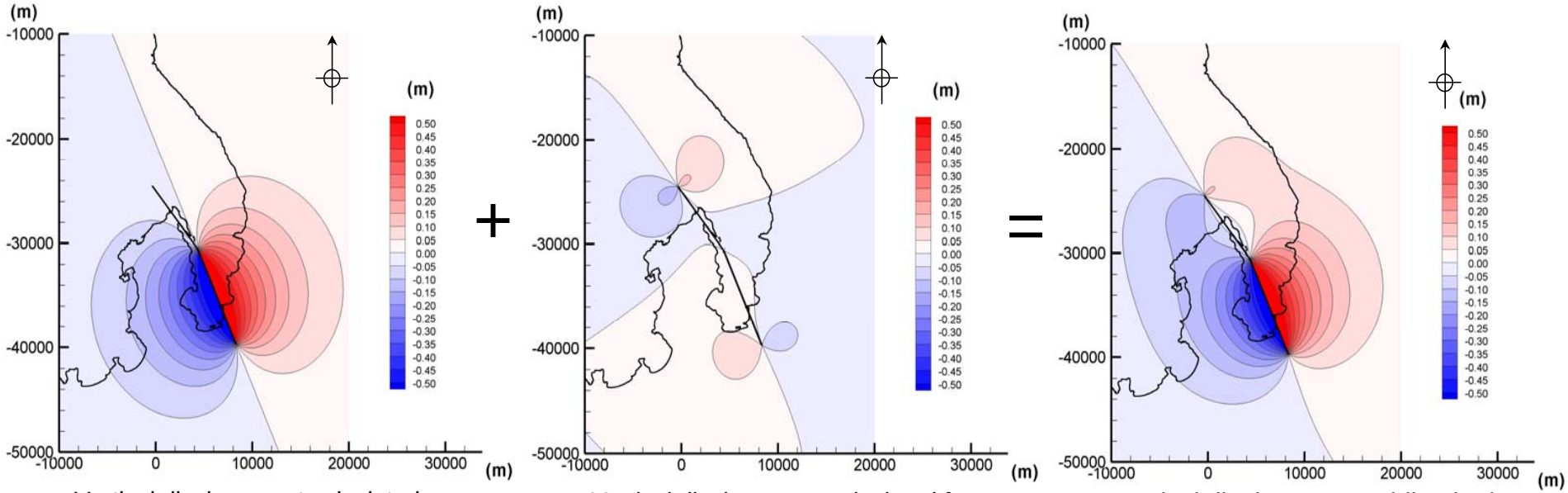

Vertical displacement calculated from vertical component of the slip

Vertical displacement calculated from horizontal component of the slip

Vertical displacement adding both of the displacements

Slip angle (P-axis 100°)	
Northern part of Urasoko-Uchiikemi fault	0°
Southern part of Urasoko-Uchiikemi fault	49°

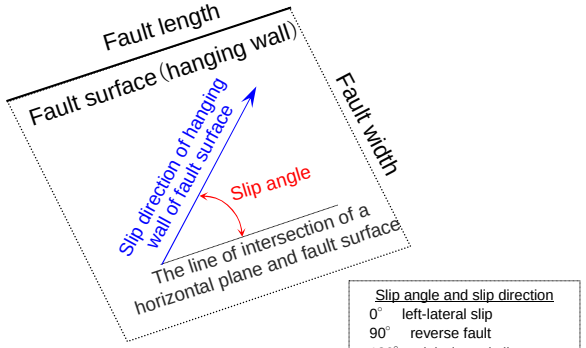

Fig. 【Reference】 Vertical displacement of ground associated with the activity of Urasoko-Uchiikemi fault (basic case: P-axis 100°)

<Reference> Vertical displacement of ground associated with the activity of Urasoko-Uchiikemi fault, (4) Basic case: P-axis 105°

Vertical displacement of ground associated with the activity of Urasoko-Uchiikemi fault is calculated by superimposing vertical displacement calculated from vertical component of the slip and vertical displacement calculated from horizontal component of the slip.

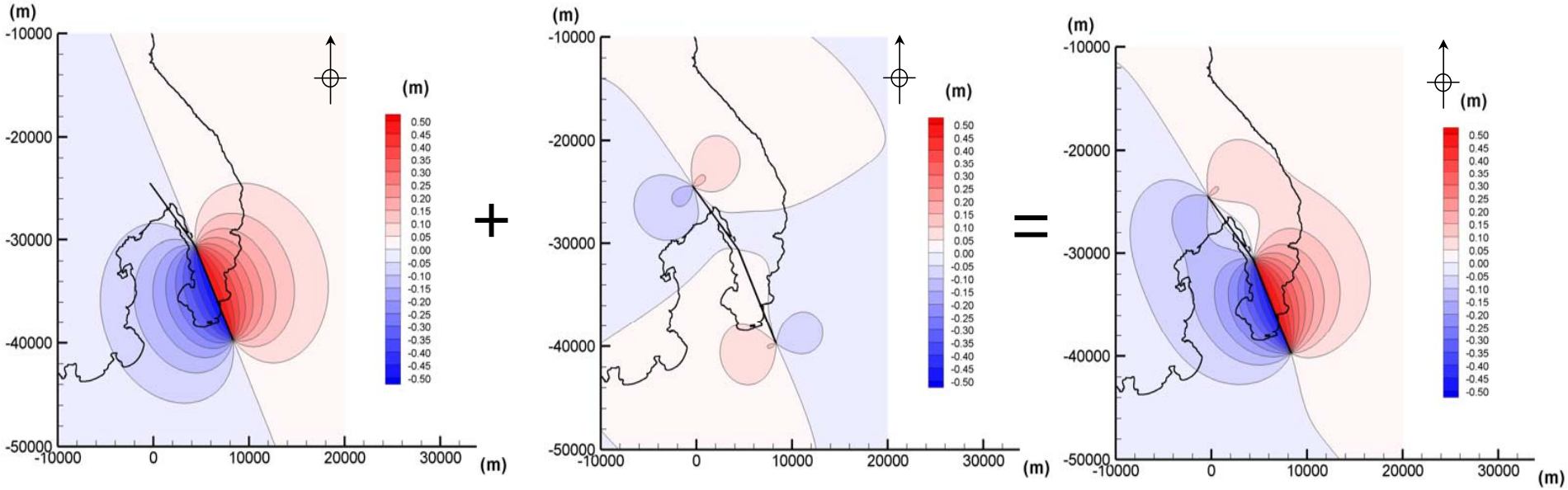

Vertical displacement calculated from vertical component of the slip

Vertical displacement calculated from horizontal component of the slip

Vertical displacement adding both of the displacements

Slip angle (P-axis 105°)	
Northern part of Urasoko-Uchiikemi fault	0°
Southern part of Urasoko-Uchiikemi fault	38°

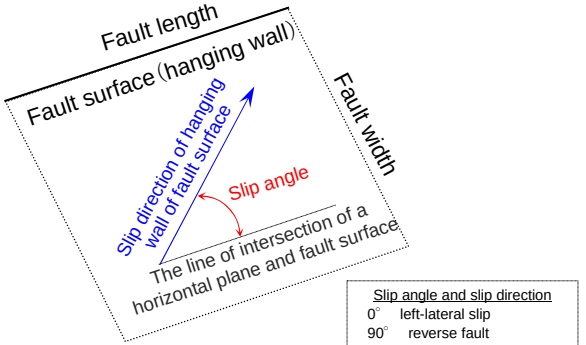

Fig. 【Reference】 Vertical displacement of ground associated with the activity of Urasoko-Uchiikemi fault (basic case: P-axis 105°)

<Reference> Vertical displacement of ground associated with the activity of Urasoko-Uchiikemi fault, (5) Basic case: P-axis 110°

Vertical displacement of ground associated with the activity of Urasoko-Uchiikemi fault is calculated by superimposing vertical displacement calculated from vertical component of the slip and vertical displacement calculated from horizontal component of the slip.

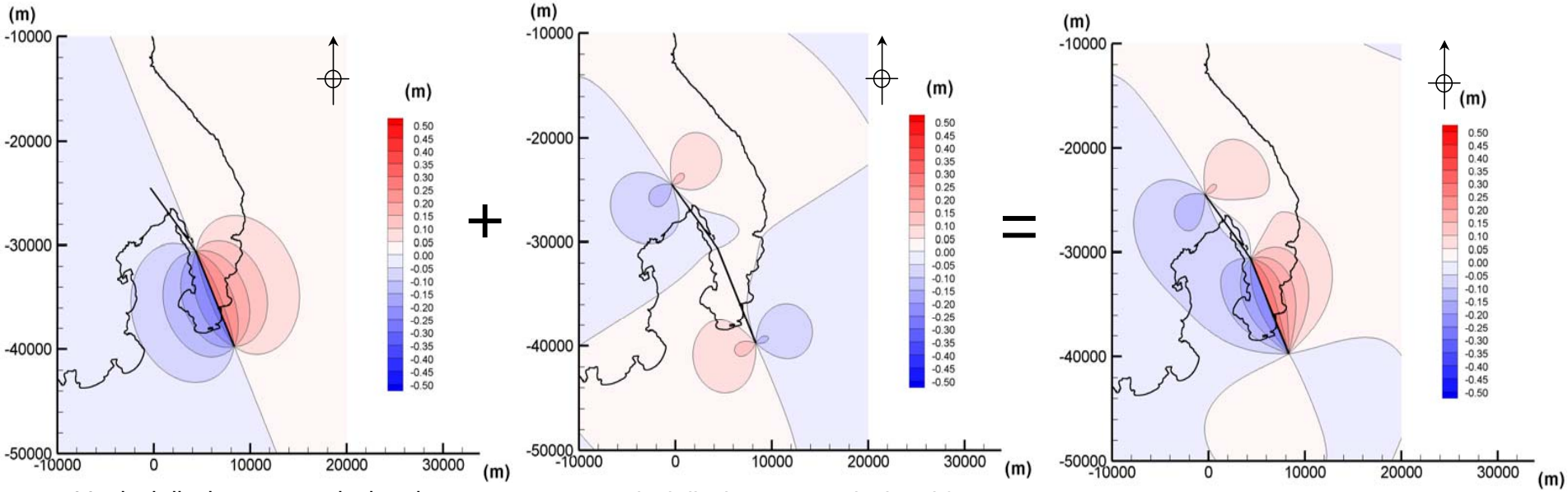

Vertical displacement calculated from vertical component of the slip

Vertical displacement calculated from horizontal component of the slip

Vertical displacement adding both of the displacements

Slip angle (P-axis 110°)	
Northern part of Urasoko-Uchiikemi fault	0°
Southern part of Urasoko-Uchiikemi fault	19°

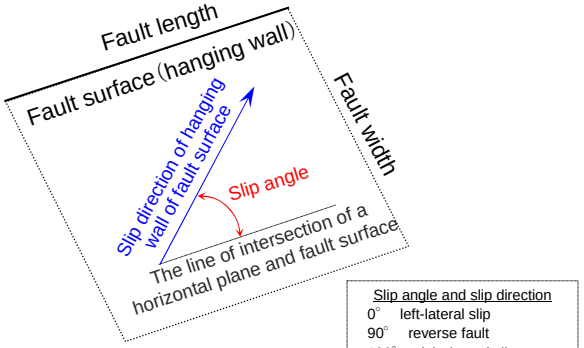

Fig. 【Reference】 Vertical displacement of ground associated with the activity of Urasoko-Uchiikemi fault (basic case: P-axis 110°)

<Reference> Vertical displacement of ground associated with the activity of Urasoko-Uchiikemi fault, (6) Basic case: P-axis 120°

Vertical displacement of ground associated with the activity of Urasoko-Uchiikemi fault is calculated by superimposing vertical displacement calculated from vertical component of the slip and vertical displacement calculated from horizontal component of the slip.

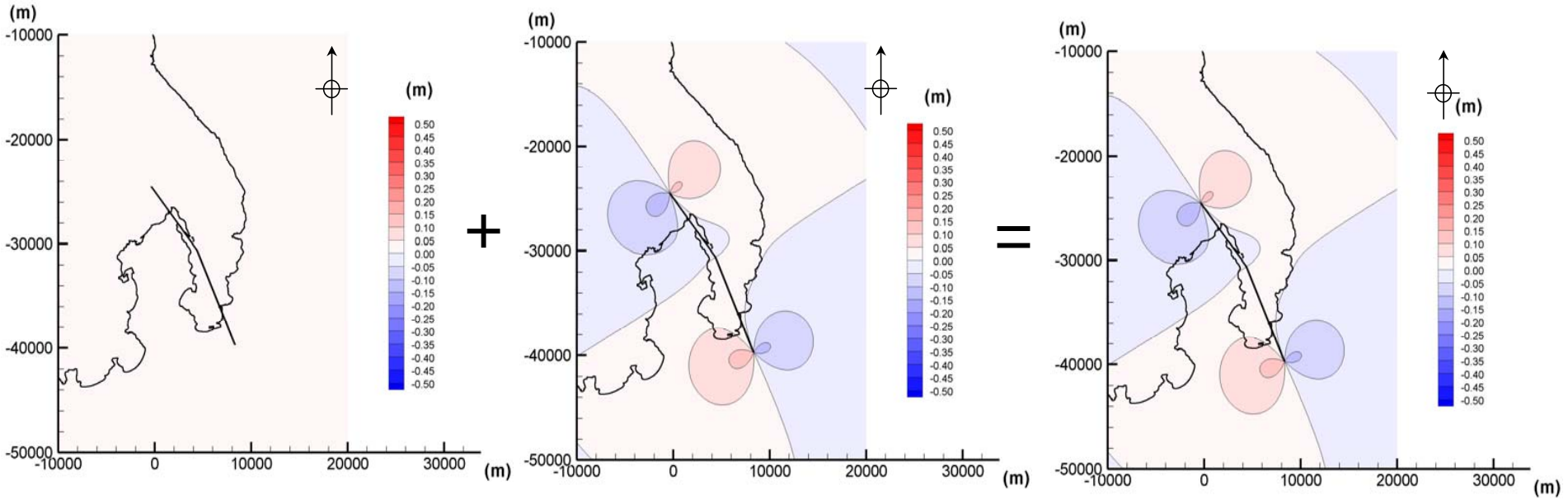

Vertical displacement calculated from vertical component of the slip

Vertical displacement calculated from horizontal component of the slip

Vertical displacement adding both of the displacements

Slip angle (P-axis115°)	
Northern part of Urasoko-Uchiikemi fault	0°
Southern part of Urasoko-Uchiikemi fault	0°

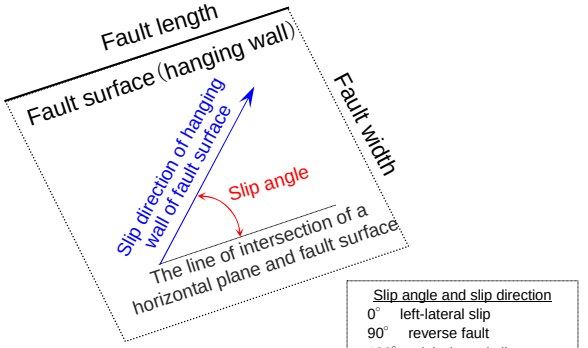

Fig. 【Reference】 Vertical displacement of ground associated with the activity of Urasoko-Uchiikemi fault (basic case: P-axis 120°)

Our opinions on ‘views against JAPC’s claim’

(Draft) EMS’s views against JAPC’s claim concerning the fault evaluations of Tsuruga PS site		JAPC’s opinion	Reference No.
Main texts	Arguments		
【EMS views to Claim 5】 The current seismic design policies stipulate that an active fault given consideration in the seismic design is a “fault with signs of activity after the Late Pleistocene that cannot be denied.” It is not stipulated that an active fault is a “fault, of which signs of activity are recognized.” So, to be of concern here is a case with no data relevant to activity available (with no data available proving no activity is found whatsoever). On the occasion that the operator does not present a data accurate enough, like this time, a fault in question is to be judged as an “active fault given consideration in the seismic design.” EMS also considers that <u>the operator is primarily held accountable for proving that a fault is not an active fault</u>. Thus, the operator, which conducted surveys, has a responsibility to present data relevant to fault activity (showing there is no activity whatsoever). In case a new fact emerges, this evaluation might be reviewed, if necessary. Even on that occasion, though, the operator needs to present a set of “objective data” denying any possibility that a fault under survey is not active through further surveys etc.	・Whether the operator is primarily held accountable for having the burden of proof?	From the legal point of view, we consider as inappropriate that the operator is primarily held for having the burden of proof. Generally speaking, under the regulation laws, it is authorities, as an administrator of regulations, that are accountable for proving whether a subject matter in case makes up regulatory requirements. To that end, authorities are entitled to the right of collection of reports and the right to make on-site inspections. Pursuant to new backfitting rules under the Nuclear Reactor Regulation Law, the Nuclear Regulation Authority (or EMS) is authorities found relevant to the case in question and is responsible for having the burden of proof and making final explanations. We already presented to EMS highly accurate and objective facts and data based on surveys to prove that there are “no signs of activity.” If the NRA (or EMS) tries to overturn our position, it will be held accountable for having the burden of proof, or verifying its position, and making explanations on the given data.	136−138

Relevant rules on “accountability” of administrative agencies

〈 Article 23-2 (1) Administrative Case Litigation Act〉

The court, when it finds it necessary in order to clarify the matters related to the action, may make the following dispositions:

(i) request any administrative agency affiliated with the State or the public entity that stands as a defendant, or the administrative agency that stands as a defendant, to submit the whole or part of materials that clarify the content of the original administrative disposition or administrative disposition on appeal, the provisions of the laws and regulations which give a basis for the original administrative disposition or administrative disposition on appeal, the facts constituting the cause of the original administrative disposition or administrative disposition on appeal and other grounds for the original administrative disposition or administrative disposition on appeal (excluding the records of a case of request for an administrative review prescribed in the following paragraph,) which are held by the administrative agency;

（Expert commentaries）

- ”The purpose of the law is to stipulate that administrative agencies shall be held accountable for clarifying the legality of disposition” (extracted from a book on the administrative law authored by Yoshikazau Shibaike).
- ”If any administrative disposition encroaches on the interests of the people, administrative bodies shall be held accountable for explaining legality of their action” (extracted from the book above).
- To support what is stipulated in Article 23-2, administrative bodies shall be primarily held accountable for explaining disposition (extracted from a book on the administrative law co-authored by Keiko Sakurai and Hiroyuki Hashimoto (third edition)).

＜Administrative Procedure Act＞

Article 1（Purpose etc.） **“to advance a guarantee of fairness and progress towards transparency...”**

Article 8 (1) (Showing of Grounds) “Administrative agencies shall, in cases where they render Dispositions refusing the permission etc. sought by Applications, concurrently show the grounds for the subject Disposition.

(Expert commentary)

The stipulation helps the subject parties bring up motion for complaint etc. (“function of accommodating judicial action”) to inhibit arbitrariness of administrative agencies by guaranteeing fairness of administrative judgment (“function of inhibiting arbitrariness”). Any dispositions without grounds shall be invalid and dispositions with flaws in presenting grounds should be nullified (extracted from a book on the administrative law co-authored by Keiko Sakurai and Hiroyuki Hashimoto (third edition)).

Act 14 (1) (Showing of Grounds for Adverse Dispositions)

“Administrative agencies, in cases where they render Adverse Dispositions, shall concurrently show the ground for the Adverse Disposition to the subject parties.”

The stipulation above is intended to inhibit arbitrariness of administrative agencies by guaranteeing the circumspection and rationality of administrative dispositions in light of predisposition of adverse dispositions, which holds the subject parties directly accountable and refuses their rights (extracted from the 2121st edition of the “Hanrei Jiho” (citation of judicial precedents) published on Jun 7 of 2011).

Comments on the shatter zones in the site of
Tsuruga Power Station owned by The Japan Atomic Power Company
(Translation of original Japanese manuscript into English is performed by JAPC)

April 23, 2013
Koji Okumura
Professor
Graduate School of Letters/Faculty of Letters
Hiroshima University

I visited Tsuruga Power Station (Tsuruga PS) on March 30, 2013 in cooperation of The Japan Atomic Power Company (JAPC) to observe the active fault, shatter zones and related quaternary system in the site of it. I report here the discussion result on the characteristics, continuity and activity of the fault and shatter zones, together with the investigation results summarized as an interim report by JAPC. It is necessary to confirm the results shown below on the structural geological observations including micro structures of the shatter zones through conducting an investigation in detail by tectonic geologists.

1. Structures and continuity of D-1 shatter zone

[Summary] D-1 shatter zone observable on the outcrop just south of Tsuruga PS Unit 2 shows common characteristics with D-1 shatter zone previously described. The comprehensive observation and description of major shear plane with fault gouge and shatter zone structure supports it.

- ✓ Apparent fault plane is single shear plane of N20°E strike and steep westward dip, where white fault gouge with 1—10mm thickness are bordered by black bands with 0—5mm thickness. Joints of NS and N20°E--30°E strike developed with several cm pitches in the cataclasite zones with around 1 m thickness at both sides of the shear plane construct the shatter zone. The shear plane with fault gauge juxtaposes granitic rocks of different color and texture, indicating significant amount of slip. Slip direction was unclear by the outcrop observation.

- ✓ Shear plane described as D-1 shatter zone or considered continuous to it in the investigations to date has closely NS or N20°E--30°E strike. This strike is consistent with that of the shear plane and joints observed in the outcrop mentioned above. It is estimated that the network shear plane system structure of major shear plane with NS strike is connected by N20°E--30°E striking oblique shear planes.

2. G fault characteristics and continuity to D-1 shatter zone

[Summary] The G fault in the North pit of D-1 trench and the D-1 shatter zone on the outcrop just south of Unit 2 are identical for their macroscopic structural characteristics. This indicates the possibility that they had been formed at the same time in the location under a unique geologic environment.

- ✓ G fault on the bottom of the north pit in D-1 trench is a distinctive shear plane of NS strike

dipping steeply to west, and yellowish white fault gauge with 1--10 mm thickness accompanies black bands with 5—10mm thickness on the east side. Joints of NS and N20°E--30°E strike developed with several cm pitches in the cataclasite zones with around 1 m thickness at both sides of the shear plane construct the shatter zone. The shear plane with fault gauge juxtaposes granitic rocks of different color and texture, indicating significant amount of slip. Though the slip direction was unclear by the outcrop observation, displacement of the shear plane had a horizontal component because a dragging structure was observed in the fault gouge on the bottom surface of North pit.

- ✓ Fault gouge and black bands of G fault are very similar to those of D-1 shatter zone on the outcrop south to Unit 2. Here at G fault, major shear plane with NS strike is formed in the system of joints with N20°E--30°E strike and dip identical to those of D-1 shatter zone. This is also common characteristics with D-1 shatter zone observed to date.

- ✓ The fault gouge on the bottom surface of north pit in D-1 trench is distinguished in color from those of the other D-1 shatter zone. It shows the color from yellowish white to orange-white, owing to weathering by dissolved oxygen in ground water. The fault gouge observed here is located just below the plane of unconformity between gravel layers and granite of later Middle Pleistocene. This spot was located on the base of gravel layers about 20m from just below river bed from Middle Pleistocene to Late Pleistocene, and much ground water was flown. It was obvious that the ground water existed because manganese deposited caused by ground water along with the joints of granite. It seemed that weathering of fault gouge and iron oxide deposit were promoted by oxidizing atmosphere.

3. K fault in D-1 trench

[Summary] K fault seemed to be cyclically active in shallower underground with fewer times slip based on configuration and characteristics of the fault plane. K fault has the characteristics different from that of D-1 shatter zone and G fault, and seems not continuous fault acting with D-1 shatter zone and G fault at the same time.

- ✓ K fault cutting the bedrock in 2-1 pit contains a very five material with 1--2 mm size like fault gauge along the shear plane, but there are no joint formation and no brecciation related to the shear plane. Deformation and shatter extent around fault gouge and fault plane is almost negligible compared with D-1 shatter zone, G fault and the other shatter zones near Urasoko fault.

- ✓ Around the specific portion with strike close to NS, cracks are found with strike close to the joint system accompanied by G fault, but the density of those cracks are much lower than that of D-1 shatter zone. Cracks thinly found around the portion with changing strikes from NS to SE, that seem to be the fracture due to the change of strike, are formed independently on the system of joints accompanied by G fault.

- ✓ K fault is bifurcated, gets lower-angle dip in sediment and is covered by the upper layer No.3. Since getting lower-angle of dip is a generally observed phenomenon for reverse fault that

crosses unconsolidated sediment in shallow ground, therefore it was obvious that K fault was active at last while the layer No.3 was deposited.

- ✓ The thickness of sand gravel and silt layers at the upper end of K fault differs across the fault. It means that fault slip contains the strike slip component. However, it is estimated that the strike slip component is smaller than the reverse fault component. The major reason of the estimation is that the sand gravel and silt layer generally corresponds across the fault and the difference of layer thickness is little, though the sand and gravel layer has strong lateral change with channel and point-bar deposit. Also, some little extent of strike slip component is inevitably induced because the strike differs so sharply from SN to NWSE in a small area with 10m and a little more width. It is necessary to examine slip vector components in detail in order to consider strike slip component strictly.

- ✓ The strike change and discontinuity to SW direction implies that a compression stress field distributed locally (in the order of 10m) along Urasoko fault, that might have produced reverse fault and strike slip deformation. Irregular shape of Urasoko fault is considered to be a cause of forming such a local stress field. When a irregular shape such as compressible jog, kink or salient and so on existed on the fault plane of Urasoko fault that had a strike slip component, a local stress field was produced in a local range related to the size of the irregular shape. Some local stress fields change position due to the advance of the strike slip.

- ✓ The observation that a fault without a series of joints or fault breccias had some a little times activation cycle only within the shallow ground, can be reasonably addressed that a compressive stress field was temporally created and disappeared in this position along Urasoko fault. The fact that the displacement by one-time slip observed in the layer No.3 (order of 10cm) was one-order smaller or less than that of Urasoko fault was consistent with the characteristics of collateral derivation fault.

- ✓ The structure of K fault has no relation to that of D-1 shatter zone in the section where the strike tends to the west, tough a part of reverse fault that curves like a bow has identical strike and dip to those of D-1 shatter zone.

4. The latest activation age, slip sense and stress field of fault and shatter zone

[Summary] K fault has no relation to D-1 shatter zone as mentioned above. It is reasonable to consider that D-1 shatter zone had not had any activation histories in the Quaternary, unless the evidence of activation of D-1 shatter zone as the west-side raised reverse fault will be shown at D-1 shatter zone itself.

- ✓ Compressive stress field along east-west direction exists under Tsuruga peninsula and its around based on observations of Urasoko fault and the other faults around.

- ✓ Possible slip that can happen in D-1 shatter zone with SN strike and westward dip should not be any patterns but reverse fault slip. However, the principal component would be reverse fault component and the strike slip component would be a little, though oblique slip could be

generated because the compression axis of stress field is not just aligned to east-west direction.

- ✓ However, only normal fault slip accompanied with right-lateral slip has been observed from the deformation structure of D-1 shatter zone. Any latest slips with reverse fault component should be recorded in superscript. If a right-lateral slip alone occurred in latest, then the motion should be recorded, too. The fact of no such records having been found yet shows that D-1 shatter zone have not had any slips in latest (in late Quaternary).

5. Activation age and activity

- ✓ It is certain that the base of layer No.5 is a irregular shape plane prior to last interglacial from sedimentation rate estimated based on the stratigraphic position of DKP and KTZ with deducing the thickness of wood peat. The existence of amphibole considered originated from Mihama tephra above the base of layer No.5 is harmonic with the estimation based on sedimentation rate. In this case, the formulation age of the irregular shape plane should be MIS 6.

- ✓ It is estimated that Urasoko fault, K fault and D-1 shatter zone have never simultaneously activated, because K fault has no relation to D-1 shatter zone and D-1 shatter zone had not had any activation histories in the Quaternary as mentioned above. Thus, we should consider whether the motion of Urasoko fault in the future will not induce slip of D-1 and the other shatter zones. For this purpose, it is not enough to collect geological evidences in the past. It is necessary to examine the possible fault slip based on dynamic, mechanical simulations. It is an important issue to investigate shear strain, stress concentration, deformation, and so on, based on the distance from elastic analyses and FEM computations, as performed in seismic back check. Also, the influences of Urasoko fault motion on important facilities of Tsuruga PS should be checked by similar evaluation methods. Since such methods developed at first in seismic back check have many challenges to improve, it is desirable to develop more those evaluation methods in the investigation this time.